Macrophages regulate colonic crypt renewal

Sathuwarman Raveenthiraraj

Submitted to the Faculty of Science for the degree of Doctor of Philosophy

School of Pharmacy

June 2021

Word count: 65,291

Abstract

Colonic epithelial cells are constantly insulted by luminal contents. The self-renewing, single epithelial layer conserves its barrier function through Lgr5+ epithelial stem cells located at the base of epithelial invaginations called crypts. Crypt stem cells first proliferate, then differentiate (giving rise to enterocytes, goblet cells; enteroendocrine cells and Tuft cells) and migrate along the crypt-axis where they are shed into the crypt lumen. Skoczek et al. 2014, previously showed that monocytes, (a macrophage precursor) induce colonic crypt proliferation and regulate the number of Lgr5+ stem cells both in vivo and in vitro. During health and inflammation, differential macrophage activity and functions have previously been characterised *in vivo* and *in vitro*, however, the effect of macrophages on crypt renewal and the cellular interactions at the crypt stem cell niche during homeostasis is yet to be fully understood.

The aim of this study was to determine the effect of macrophages on colonic crypt renewal, in particular, its influence on epithelial proliferation and differentiation using a 3D macrophage-crypt co-culture model. This study demonstrates that colonic crypt proliferation significantly increases in the presence of non-activated (Naive), pro-inflammatory (M1) and anti-inflammatory macrophages (M2). Here, Naive and M2 macrophages require crypt-macrophage contact to trigger epithelial proliferation and pro-inflammatory macrophages (M1) can induce crypt proliferation via a physical contact and secretory factor-dependent pathway. Differentiated colonic crypt cell numbers of UEA-1+ goblet cells, DCAMKL1+ tuft cells, Cro-A+ enteroendocrine and Lgr5+ stem cell numbers were maintained in the presence of anti-inflammatory (M2), however a decrease in UEA-1+ goblet cells and DCAMKL1+ tuft cells and an increase in Lgr5+ stem cell numbers was observed in crypts cultured with pro-inflammatory (M1) macrophages that was dependent on M1-crypt contact.

Taken together, this thesis demonstrates that differentially polarised macrophages (Naive, M1 and M2) can regulate colonic crypt growth, differentiation and in particular suggest that the epithelial stem cell fate is influenced by pro-inflammatory (M1) macrophages when in contact with the colonic epithelium *in vitro*.

Declaration

I declare that this thesis represents my own work, except where due acknowledgement is made, and that it has not been previously included in a thesis, dissertation, or report submitted to this University of to any other institution for a degree, diploma or other qualifications.

Sathuwarman Raveenthiraraj

PhD candidate

Acknowledgements

Firstly, I would like to thank the School of Pharmacy who have awarded me with the studentship allowing me to work on this project.

I would like to express my deepest appreciation to my esteemed primary supervisor and Mother of Crypts, Dr. Anastasia Sobolewski. I would like to thank you for taking me on and patiently guiding me through the PhD. You have been a caring mentor; inspiring role model and it was a pleasure to work under your tutelage. I will forever be grateful to you for aiding my personal and professional growth.

I would also like to thank my secondary supervisor, Dr. Mette Mogensen, as well as Prof. Maria O'Connell and Dr. Derek Warren, for your input and support throughout my PhD. Thank you to Dr. Paul Thomas for helping me with the capture of all the fantastic confocal images and to Dr. Ernst Poeschl for allowing me access to your flow cytometer. Thank you also to Dr. Chris Morris for your donation of the Griess assay reagents as well as Dr. Marin and Carla Arnau Del Valle for your donation and help with NO probe experiments.

I am also grateful to Dr. Marcello Chieppa, for giving me an opportunity to be a part of his collaborative project and including me in his recent publications.

A special thank you to all the members of the Disease modelling unit, especially Jon Drury, Rich Croft and Simon Deakin, who have been incredibly accommodating and supporting throughout my PhD, particularly during the pandemic.

I would also like to thank my friends who have accompanied me during my time in Norwich. My thank you goes out to my lab-mate, Griselda Awanis, I will always look back at our humorous conversations with a smile, thank you for your help and livening up the lab. To my two friends, Sultan Ahmed and Vaisakh Puthusseryppady, I thank you for providing the after-hours entertainment and keeping my spirits high in the last couple of years, it has been a pleasure to spend time in your company.

I dedicate this thesis to my parents, who have made countless sacrifices to support and allow me to reach this stage.

Table of Contents

List of Figures

List of Tables

List of abbreviations

5-ASA	5-aminosalicylates
5-HT	5-hydroxytryptamine
AJC	apical juncational complex
AKT	Protein kinase B
AMPS	Anti-Microbial Peptides
APAF1	Apoptotic Protease Activating Factor 1
APC	Adenomatous Polyposis Coli
APO3L	APO3- ligand
ATOH1	Protein atonal homolog 1
BAK	Bcl-2 homologous antagonist killer
BAX	Bcl-2 assocated X protein
BLP	Balloon-like protrusions
BMDC	Bone Marrow-Derived Cells
BMDM	Bone Marrow-Derived Macrophages
BMP	Bone morphogenetic protein
BSA	Bovine Serum Albumin
Ca_2+	Calcium ion
CaCl	Calcium Chloride
CBC	Crypt Base Columnar cells
CCR2	CC-Chemokine receptor 2
CD-	Cluster of Differentiation
CD	Crohn's Disease
CK1	Casein kinase 1

CLP	Common lymphoid progenitor
COX2	Cycloxygenase-2
CpG	5'—C—phosphate—G—3 strand
CREB	cAMP Response Element-binding Protein
CRO-A	Chromogranin A
CSFR1	Colony Stimulating Factor 1 Receptor
CX3CR1	CX3C Chemokine Receptor 1
DAMP	Damage Associated Molecular Pattern
DAPI	4’,6-diamidino-2-phenylindole
DAPT	(2*S*)-*N*-[(3,5-Difluorophenyl)acetyl]-L-alanyl-2-phenyl]glycine 1,1-dimethylethyl ester
DCAMKL	Serine/threonine-protein kinase DCKL1
DISC	Death-inducing signalling complex
Dll-	Delta-like Ligand
DMSO	Dimethyl sulfoxide
DTT	1,4-Dithiothreitol
DVL	Dishevelled
ECM	Extracellular matrix
EDTA	Ethylenediaminetetraacetic acid
EdU	5-ethynyl-2´-deoxyuridine
EEC	Enteroendocrine Cells
EGF	Epidermal Growth Factor
EP-	E-type prostanoid receptor
eQTL	Expression of quantative trait loci
ERK1/2	extracellular signal-regulated protein kinase

DMEM/F12	Dulbecco's Modified Eagle Medium/ Nutirent Mixture F12
F4/80	EGF-like module-containing mucin-like hormone receptor-like 1
FABP-1	Fatty-Acid Binding Protein 1
FZD	Frizzled
GALT	Gut-associated lymphoid tissue
GAP	goblet-cell associated passages
GFP	Green Fluorescent Protein
GI	Gastrointestinal tract
GMP	Granulocyte-macrophage progenitor
GNAT3	Guanine nucleotide-binding protein G(t) subunit α-3
GSK3β	Glycogen Synthase Kinase 3 β
HEPES	4-(2-hydroxyethyl)-1-piperazineethanesulfonic acid
HES1	Hairy and enhancer of split 1
HIF1-α	Hypoxia-inducible factor 1 α
HSP	Heat-Shock Protein
i/NOS	(inducible) Nitric oxide synthase
IBD	Inflammatory Bowel Disease
ICAM-1	Intercellular adhesion molecule 1 precursor
IEL	Intrepithelial lymphocytes
IgG	Immunoglobulin G
IL-	Interleukin-
ILC-2	Group 2 Innate Lymphoid Cells
ISC	Intestinal Stem Cell
JAK	Janus Kinase 1
JNK	c-Jun N-terminal kinase

KCl	Potassium Chloride
KO	Knock-out
LCN-2	Lipocalin-2
LEF1	Lymphoid Enhancer binding Factor 1
LGR5	Leucine-rich G-protein coupled receptor 5
LPS	Lipopolysaccharide
LRP	Lipoprotein Receptor-related Protein
LRP5/6	lipoprotein-receptor related protein 5/6
LY6C	Lymphocyte antigen 6
M-CSF	Macrophage Colony Stimulating Factor
MDP	monocyte-dendritic cell pathway
MgCl	Magensium Chloride
MHC2	Major histocompatibility complex 2
MMP	Matrix Metalloproteinase
MOMP	mitochondrial outer membrane permeabilisation
MST1/2	Mammalian serine/theorine ½
MUC-2	Mucin-2 protein
MYD88	Myeloid differentiation primary response protein 88
NCID	Notch Intracellular Domain
NEAA	Non-Esssential Amino Acid
NF-κB	Nuclear Factor kappa-light chain enhancer of activated B-cells
NLR	nucleotide-binding oligomerisation domain-like receptor
NLRP6	NOD-like receptor family pyrin domain containing 6
NO	Nitric oxide
NOTCH	Notch homolog 1, translocation-associated

OLFM4	Olfactomedin-4
P13K	Phosphatidylinositol 3-Kinases
PAMP	Pathogen Associated Molecular Pattern
PBS	Phosphate Buffered Saline
PCP	Planar cell polarity
PFA	Paraformaldehyde
PGE2	Prostaglandin E2
PIP	Phosphatidylinositol Phosphates
PRR	Pattern Recognition Receptor
PTEN	Phosphatase and tensin homolog
PTPN2	Protein Tyrosine phosphatase non-receptor type 2
RNF43	RING finger protein 43
SAV1	Scaffold proteins Salvador family WW domain containing protein 1
SDS	Sodium Dodecyl Sulfate
SLPI	Serine protease inhibitor
STAT	Signal Transducer and Activator of Transcription
TAZ	Tafazzin
TCF	T-Cell Factor
TEAD	TEA-domain transcription factor
TGF	Transforming Growth Factor
TH1/2	T-helper cell type 1/2
TLR	Toll-like Receptor
TNF	Tumor Necrosis Factor
TRAIL	TNF-Related Apoptosis-Inducing Ligands
TREM2	Triggering Receptor Expressed on Myeloid cells

UC	Ulcerative colitis
UEA-1	Ulex Europaeus Agglutinin 1
WISP-1	WNT1-inducible signalling protein 1
WNT	Wingless-related integration site
WT	Wild-Type
YAP	Yes-associated protein
ZNFR3	ZING and RING finger 3
β-TrCP	B-transducin repeats-containing protein

Chapter 1: General Introduction

1.1 Gastrointestinal tract

The gastrointestinal tract (GI) is part of the digestive system and aids in the digestion of food, absorption of nutrients and defecation of waste. From the upper to the lower ends, the GI tract consists of the oral cavity, pharynx, esophagus, stomach, small intestine, large intestine, rectum and anus. The wall of the GI tract is composed of four distinctive layers, the mucosa, the submucosa, the muscularis externa and the serosa (Liao et al., 2009).

The mucosa is the innermost layers of the gut wall and is comprised of the epithelium, lamina propria and muscularis mucosa. The cellular structure of the mucosal epithelium differs in each region of the GI tract, where stratified squamous epithelial cells may be found in the mouth, esophagus and anal canal and simple columnar or glandular epithelia can be in the stomach, small intestine, and colon (Reed K. and Wickham R., 2009) (**Figure 1.1**). The lamina propria, consists of connective tissue, blood and lymphatic vessels, with a myriad of responsibilities. Most notably, it is home to a collection of lymphocytes and lymph nodes, known as the gut-associated lymphoid tissue (GALT), which protects the GI tract infiltration from bacteria and pathogens. The thinner, underlying layer of the muscularis mucosa consists smooth muscle aiding in gastrointestinal motility (Reed K., Wickham R., 2009). Interestingly, within the gastrointestinal tract the small and large intestine showcase the highest epithelial turnover rate in the human body (Williams et al., 2015).

The large intestine

The large intestine's gross anatomy is composed of the cecum, appendix, colon, rectum and anal canal. Processed foods pass from the small intestine into the cecum and subsequently into the colon. The colon is sectioned into four parts: ascending, transverse, descending and sigmoid colons (Serafini N.Di Santo J., 2016).

Physiologically the colon differs from the small intestine in several aspects, unlike its adjoining counterpart the colon does not possess any protruding villi, instead a flat epithelial surface with mucosal folds lead into invaginations commonly referred to as crypts. The mouse intestine contains approximately 30 million of such crypts (Clevers., 2013).

Whereas digestion and nutrient absorption primarily occurs in the small intestine, the large intestine functions as a fluid and electrolyte absorbent, where water is resorbed leaving solid fecal matter to be defecated. (Pawel and Ghishan., 2016). The colon also hosts the largest community of commensal bacteria in the intestine. Not only does the microbiota aid the fermentation of complex carbohydrates, its communication network with the intestinal epithelium and the GALT is critical in developing a healthy systemic and mucosal immunoregulatory circuitry (Macdonald, 2005).

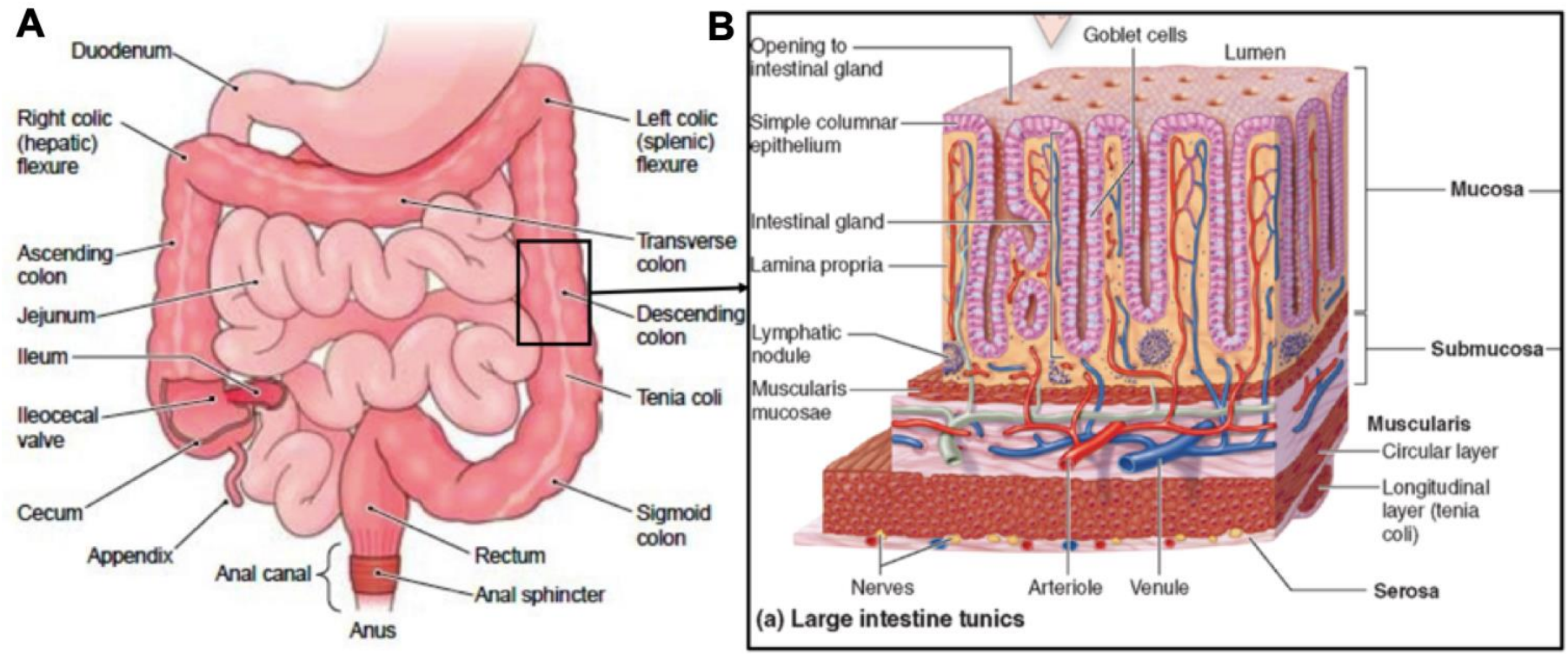

Figure 1.1: **Anatomy of the gastrointestinal tract**

An animated visualisation of the lower gastrointestinal tract and the colonic gut wall. **(A)** Illustration of the lower gastrointestinal tract, digested materials pass through the small intestine to the ascending colon via the ileocecal valve, through the transcending and descending colon, where it then reaches the rectum and waste materials are discarded. **(B)** Illustrated cross-section of the colonic tissue revealing its structure and anatomy. The opening of the intestinal gland lead to the invaginations called crypts consisting of simple columnar cells which are structurally supported by the underlying lamina propria. A thin layer of smooth muscle cells, the muscularis mucosae and the muscalaris, located beneath the lamina propria allows the movement and folding of the tissue to aid nutrient absorption (Adapted from Physiology Plus and Junqueria's Basic Histology).

However, due to the high abundance of commensal microbiota which exists within the colon, it is of upmost importance that the intestinal epithelium maintains its barrier function and integrity (Odenwald and Turner., 2017).

1.2 Intestinal stem cell-driven epithelial renewal

The intestinal epithelium and its colonic crypts are composed of intestinal epithelial cells, form a single-cell thick, simple columnar monolayer, held in shape by tight junction and act as a physical barrier which protects the sub-epithelium from any harmful toxins, antigens and microorganism which may inhabit the lumen (Reed and Wickham., 2009). Due to the continual assault originating from the lumen, the intestinal epithelial cells are continually replaced every 4-5 days (Nibali et al., 2014).

While the epithelial barrier regulates the absorbance of nutrients, water, and the transport of waste products, it must further mediate the crosstalk between luminal contents and the proximal immune system in a non-inflammatory manner. Non-regulated transport or leakage of pathological antigens through the barrier could lead to inadvertent inflammation and escalate towards autoimmune diseases and/or inflammatory bowel disease (Shi and Walker., 2015). The apical junctional complex (AJC) found within the large intestine controlling permeability, consists of tight junctions, adherens junction and desmosomes (**Figure 1.2**). Adherens junctions are often found on the lateral membrane where cadherin-catenin interactions are most frequently encountered. These can influence cell polarity and epithelial migration and the downregulation of E-cadherin has been linked with impeding epithelial proliferation (Groschwitz and Hogan., 2009). Tight junctions such as Occludin, Claudins and junctional adhesion molecules can be found on the apical end of the epithelial cell, these mediate ion movement and impede the transport of luminal molecules (Lee et al., 2018).

The lining of the intestine composed of mucin acts as a secondary defensive barrier. A thick mucus layers lines the epithelia and functions as traps for water molecules. Within the large intestine, two mucus coatings ensure protection from chyme and chemical degradation. Furthermore, the second mucus layer is completely impermeable to bacterial penetration in homeostasis (McGuckin et al., 2011; Johansson et al., 2008). Fascinatingly, to ensure bacterial penetration is further minimised, the intestinal epithelium maintains the highest turnover recorded in the human body (Rees et al., 2020)

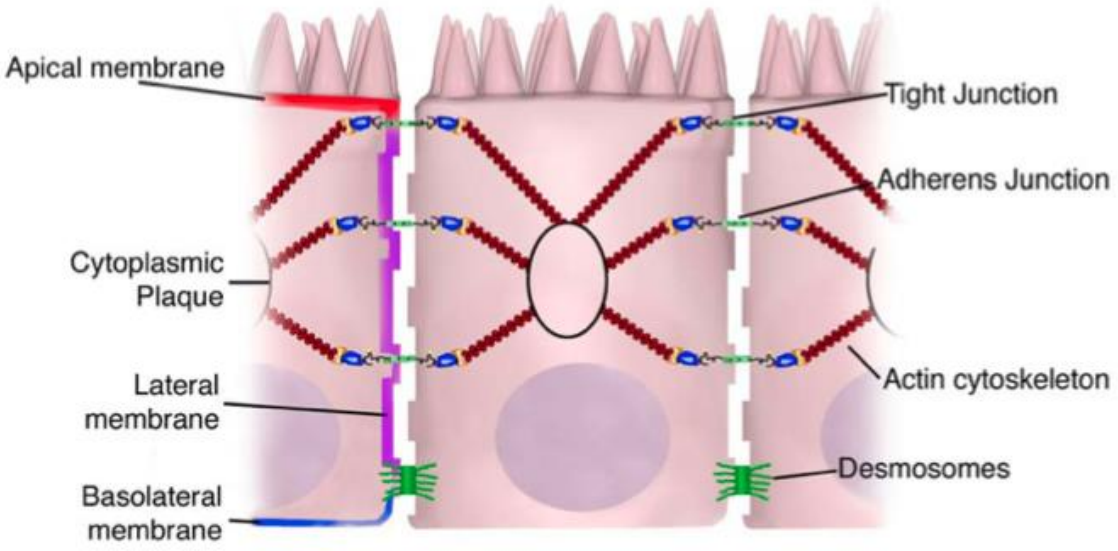

Figure 1.2: Colonic epithelial barrier function

Diagram showing the three main tight junction barrier complexes identified in the intestine: Desmosomes, adherent junctions and tight junctions which play an essential role in regulating intestinal barrier function (Adapted from Groschwitz and Hogan., 2009)

1.2.1 Epithelial renewal

The intestinal epithelium acts as a physical barrier, where its role is to protect the underlying tissue from commensal microbes and invading pathogens. To maintain a high rate of epithelial turnover and to reduce barrier damage-induced inflammation, the epithelial crypts shown in **Figure 1.1** are renewed within 4-5 days in humans and mice (Okamura and Takeda., 2017; Darwich et al, 2014).

Proliferation of such intestinal epithelial crypts, is driven by multipotent adult stem cell population at the base of the crypt where cell division occurs at average of once per day, producing highly proliferative transit-amplifying cells. While migrating upwards, these transit-amplifying cells further differentiate into function-specific epithelial cells and are shed into the lumen towards the end of their life span (Barker et al. 2007).

The crucial driver of epithelial renewal are the intestinal stem cells located at the base of the crypt. With the assistance of electron microscopy, a “slender” cell type was identified by Cheng and Leblond as early as 1974 and decades of further research have led to the identification of two stem cell populations within the crypt: the crypt base columnar (CBC) stem cells and the reserve stem cell population located in the +4 position of the crypt (**Figure 1.3**) (Cheng and Leblond., 1974; Barker et al., 2007; Yan et al., 2012).

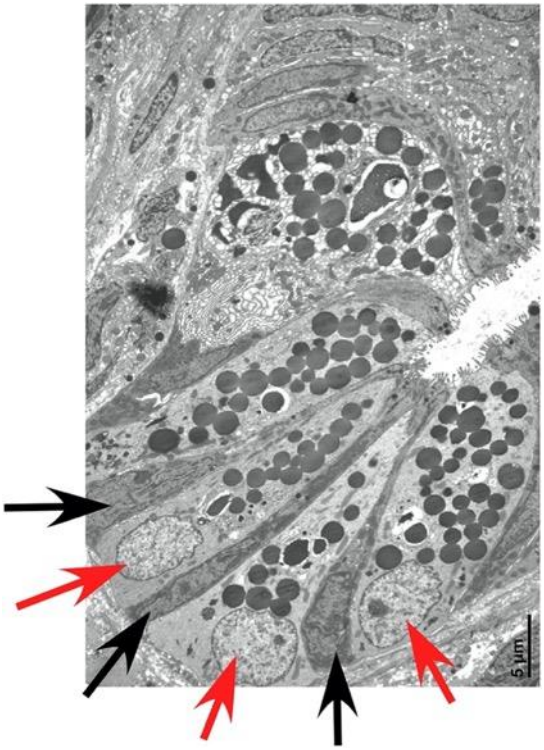

Figure 1.3: Crypt base columnar (CBC) stem cells

Scanning electron microscope image highlighting the presence of ‘slender’ stem cells (black arrows) located between neighbouring Paneth cells (red arrows) at the base of the crypt by Leblond and Cheng (Adapted from Barker et al., 2012).

1.2.2 Crypt base columnar (CBC) stem cells and +4 position stem cells

Based on the the findings in 1974, Cheng and Bjerkness found that CBC cells unlike their reserve stem cell population, were actively proliferating and are susceptible to radiation (Bjerkness and Cheng., 2002). Although a number of stem cell markers such as *Ascl2, Olfm2* and *Smoc2* among others have been identified, Lgr5 (leucine rich G-protein coupled receptor), a Wnt target gene, is considered to be the most robust CBC stem cell marker as

other markers are also prone to labelling early transit-amplifying cells. By insertion of a CreERT2 fusion protein into the Lgr5 locus, the Wnt target gene was localised in fast-cycling cells at the crypt's base in both the small intestine and colon (Barker et al., 2007).

Lgr5+ CBC stem cells symmetrically divide every 24 hours at the base, generating clonal CBC stem cell, one of which can be 'pushed' out of the stem cell niche in a process coined 'neutral competition', where they are then spurred on to differentiation (Snipper HJ, et al., 2010). While only a fraction of Lgr5+ cells are capable of long-term self-renewal, a small population of quiescent, slow-cycling and radiation resistant stem cells are retained at the +4 position which do not express Lgr5. These +4 stem cells are often activated only following epithelial damage at which point they clonally repopulate the crypt domains, suggesting that they may not contribute to homeostatic renewal but are essential in damaged-induced regeneration (Ritsma et al., 2014; Yan et al., 2012). Crucially, intestinal homeostasis was maintained in the colon, despite the depletion of Lgr5+ stem cells *in vivo*, where the stem cell niche was instead repopulated by Lgr5- reserve stem cells, thus highlighting the high level of plasticity within the intestinal epithelium.

Where intestinal stem cells play a crucial role in the regulation of crypt growth, such cells are incapable of executing physiological functions of the intestinal epithelium such as the absorption of water, nutrients, and sustenance of the commensal microbiota, thus stem cell differentiation is essential for maintenance of intestinal homeostasis (Birchenough et al., 2015; Snoeck et al., 2005).

1.2.3 Stem cell differentiation

To fulfil the many functional roles of the colon, stem cells and their progenitors must differentiate into fully functional cell types. Within the large intestine, non-committed cells can be converted into secretory cells such as goblet, enteroendocrine or tuft cells and absorptive enterocytes, depending on the biochemical influences of the mucosa (**Figure 1.4**) (van Flier and Clevers., 2009).

Interestingly, Toth et al., have identified that colonic crypts undergo "early commitment" differentiation where the cell's fate is determined prior to entering the transit-amplifying phase, essentially allowing the colonic cells to mature earlier compared to their small intestinal counterpart, where "late commitment" is preferred. This is important as unlike

epithelial cells in the small intestine where differentiated cells can remain within the crypt-villus formation for a longer time, the lack of villi forces early maturation (Toth et al., 2017).

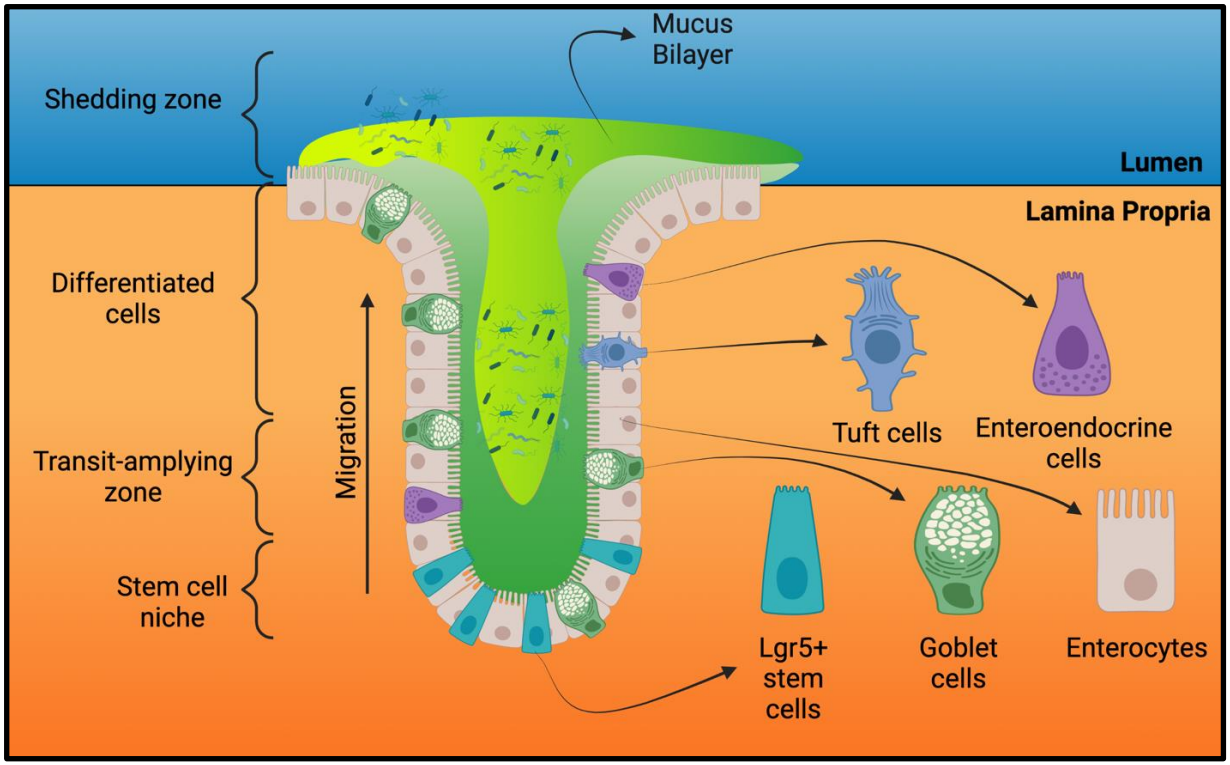

Figure 1.4: Colonic crypt renewal

Diagram highlighting the cycle of epithelial renewal. Lgr5+ cells at the base of the crypt divide and migrate upwards, progenitor cells proliferate in the transit-amplifying zone and differentiate to give rise to enterocyte, tuft, enteroendocrine or goblet cells. At the end of their life-cycle the cells are then shed into the crypt lumen and the cycle of renewal is repeated. A two-layered mucus coating acts as a semi-permeable membrane restricting commensal microbiota to the outer mucosal layer, thereby preventing microbiome-epithelial contact in homeostasis (Created on Biorender.com, 2021).

Enterocytes:

Enterocytes are columnar epithelial cells containing microvilli on their apical surface, this cell line is the most commonly encountered cell type within the colon, where their prime functions are to absorb nutrients and water. (Cheng and Leblond., 1974; Egberts et al., 1984). However, overtime it was found that enterocytes may also play other roles in intestinal homeostasis. As luminal nutrients are absorbed, enterocytes will inadvertently ingest and degrade luminal epitopes which could potentially cause an unwarranted immune response (Miron and Cristea., 2012).

Enterocytes can also act as a mediator between luminal antigens and dendritic cells in the lamina propria as they also possess MHC1/2(major histocompatibility complex) (Chen et al., 2011). Entercoytes' metabolism can also shape the microbiota *in vivo* where the high epithelial oxygen consumption, leads to mucosal hypoxia only allowing anaerobic bacteria to survive, thus allowing the conversion fibres into beneficial fermented compounds (Litvak et a., 2018). Notably, enterocytes precursor cells also seem to able to dedifferentiate to replace previously ablated Lgr5+ stem cell in the small intestine, however whether a similar phenomenon can be observed in the colon is yet to be determined. (Tetteh et al., 2016). As is the case with many epithelial cells within the crypt domain, the differentiation of stem cells towards the absorptive enterocytes cell lineage relies on the Notch signalling pathway, where the balance between the repression of Math1 and Hes1 can decide between the absorptive and secretory cell fate. The deletion of Math1, a downstream Notch transcription factor, led to a change of fate within the intestine prompting cells to differentiate into absorptive enterocytes (Shroyer et al., 2007). Furthermore, increased expression of HES1 can also directly repress Math1 expression and subsequently incite enterocyte differentiation (Jensen et al., 2000; Zheng et al., 2011).

Goblet cells:

In the large intestine, mucus production plays a vital role in acting as a semi-physical barrier which ensures luminal microbes remain out of touching distance to the underlying epithelium. To fulfil this function, goblet cells within the epithelium ensure sufficient mucus is generated (Birchenough et al., 2015). The mucus of the intestinal epithelium is largely

composed of a variety of mucin proteins. Mucins are glycoproteins with a high number of O-linked oligosaccharides. The gel-forming mucin subtypes have been identified as MUC2/5/5B/6 where MUC2 is the most commonly encountered mucin within the intestine (Andrianifahanana et al., 2006).

Uniquely, a two layered mucus structure (illustrated in **Figure 1.4**) can be observed in the colon compared to the small intestine. The mucus was shown to gradually thicken from the duodenum towards the rectum (Matsuo et al., 1997). Here the inner mucus layer separates the bacteria for the epithelium, preventing direct contact whereas the less dense outer mucus layer provides an ideal microenvironment for the commensal microbiota (Johansson et al., 2008). A loss of the inner mucus layer has also shown to be a contributing factor of the formation of spontaneous colitis in mice (Johansson et al., 2014). Goblet cells can be morphologically distinguished by their nucleus at the base and the mucus filled cytoplasm facing the apical side of the crypt. Within the large intestine especially goblet cells can be found scattered across the entire crypt, in order to ensure the even distribution and secretion of mucus (Sancho et al., 2015).

Recent studies have also shown that small intestinal goblet cells are capable of importing antigen to CD103+ dendritic cells in the lamina propria. This is achieved by the formation of GAP (goblet cell associated passages) which deliver soluble antigens to immune cell. Further research revealed that GAP formation is regulated by acetylcholine, which is suppressed in the colon in comparison to the small intestine due to the presence of luminal microbes inhibiting the secretion of acetylcholine, where only a disruption of the microbiota could lead to the activation of the acetylcholine pathway (Knoop et al., 2015). Further evidence also suggest that goblet cells can be coerced into hyperplasia and mucus hypersecretion via Th-2 mediated secretion of IL-13 and IL-4 during parasitic helminth infections (Finkalmann et al., 2004; McKenzie et al., 1998). In 2017, Birchenough identified specialised ‘sentinel’ goblet cells within the colonic crypt entrance which can trigger the secretion of MUC2 via a NLRP6-MyD88 signalling pathways in a Ca2+ independent manner. Goblet cells adjacent to such sentinel cells are also induced into MUC2 secretion via a gap junction signalling pathway. This mechanism described above essentially allows bacteria to be flushed away from crypt openings in order to prevent bacteria-epithelial contact during inflammation (Birchenough et al., 2017).

Enteroendocrine cells:

EECs in the large intestine can be identified by the basal processes which are extended towards the neighbouring epithelial cell (Rindi et al, 2004).

Cristina et al. have found early on that EEC numbers can vary from duodenum and rectum (Cristina et al., 1978). Similarly, to all secretory cell lines within the colon, EEC differentiation also relies on the transcription factors Math1/Atoh1, which is further discussed in this chapter (**Section 1.3.2**). Additionally, Neurogenin 3 is required for its differentiation and is highly dependent on Notch signalling, where Hes1 knockout in mice led to enteroendocrine cell hyperplasia (Jensen et al., 2000). In contrast, disruptions to Wnt signalling via the KO of β-catenin did not affect EEC numbers (Wang et al., 2007).

One of the major roles of EECs is its capability to secrete hormones such as serotonin (5-HT), histamine, somatostatin, gastrin and cholecystokinin (CCK) in order to contribute to the regulation of homeostasis. (Hagborn et al., 2011; Egerod et a., 2012). EECs are able to detect changes in nutrient concentration and adjust the secretion of such peptides accordingly (Gribbe et al., 2016). Interestingly, in IBD patients, chromogranin A levels are highly upregulated in IBD patients (Zissimopoulos et al., 2014). Due to EECs unique affinity to chromium salts, chromogranin A can be used as stable marker for the identification of intestinal EECs (Ahlmann and Nilsson., 2003).

Studies also indicate that EECs are able to regulate macrophage activity via the secretion of GLP-2 which has been shown to reduce iNOS, COX2, TNF-α and IL-6 expression in LPS-activated macrophages (Xie et al., 2014). Similar observations were made by Saia et al., where CCK was also found to reduce NO production in peritoneal macrophages (Saia et al., 2014).

Tuft cells:

Tuft cells are the least commonly occurring epithelial cell type of the intestine making up only 0.5% of the epithelial population. (Bannerjee et al. 2018). Tuft cells can be identified by their apical bristles and a cell body which narrows towards both the apical and basal end (Sato A., 2007). Initially, DCAMKL-1+ cells within the crypts were postulated to be stem cell markers, however Gerbe et al. has demonstrated that DCAMKL-1 can in fact be utilised as a robust tuft cell marker (Gerbe et al., 2011).

It should also be noted that the process of tuft cell differentiation was shown to differ between the small intestine and colon. Herring et al, demonstrated that ablation of tuft cells in the colon resulted in tuft cell depletion whereas Atoh1-deficiency led to tuft cell hyperplasia in the small intestine (Herring et al., 2018).

The exact function of this particular epithelial cell line has not been fully understood. In 2016, Howitt et al. have shown that tuft cells can acts a chemosensory "taster" in the intestine. To do so tuft cells rely on Gnat3 (taste-related G-protein subunit) and TRPM5 (cation channel) both which are utilised in the detection of *Pseudomonas aeruginosa*. Interestingly, the small intestinal epithelium of both Gnat3$^{-/-}$ and TRPM5$^{-/-}$ knockout mice were found to show depleted numbers of DCAMKL1+ tuft cells. Furthermore, the tuft cells response to the parasite *Tritrichomonas muris* was also impaired, thus alluding to the chemosensory role of intestinal tuft cells within the epithelium (Howitt et al., 2016). Tuft cells expansion was also observed germ-free mice following exposure to bacteria (McKinley et al., 2017). Tuft cells also play a distinct role in during parasitic infections. As allergens and helminths can induce a type 2 immune response, this often leads to the recruitment of ILC2-cells (type 2 helper T-cells) which rely on IL-33 and IL-25 secretion to be activated. However, until recently the source of IL-25 within lamina propria was unknown and it has since become apparent that tuft cells constitutively express IL-25 to maintain ILC2 activation. As a result, the positive feedback loop allows ILC2 cells to produce IL-13 in order to continuously promote goblet and tuft cell differentiation (Moltke et al., 2016).

1.3 Regulation of epithelial renewal

The intestinal stem cells rate of self-renewal and differentiation towards the functional epithelial cells mentioned above is finely regulated by a myriad of paracrine and autocrine factors and over time a number of signalling pathways such as BMP, Hedgehog, Notch, Wnt and Eph-ephrin signalling have been shown to contribute to the ISCs homeostasis (Spit et al., 2018).

1.3.1 The Intestinal Wnt signalling pathway

A major contributor to proliferation and intestinal stem cell niche maintenance is the Wnt signalling pathway, where the activity of Wnt is highest towards the base of the crypt and decreases towards the top of the crypt (Nusse and Clevers, 2017; Scoville et al., 2008). The canonical Wnt pathway is initially triggered by binding to the lipoprotein-receptor related protein 5/6 (LRP5/6) and its co-receptor frizzled (FZD), subsequently the protein Dishevelled (DVL) is recruited and the degradation of β-catenin via the destruction complex is blocked. The destruction complex consists of a number of protein component such as adenomatous polyposis coli (APC), casein kinase 1 (CK1) and glycogen synthase kinase 3β (GSK3β) (Mah et al., 2016). The consequent stabilisation of β-catenin allows the protein to translocate to the nucleus and binds to the TCF/LEF transcription factor ultimately activating Wnt target genes such as Myc, COX-2, Cyclin-D1, TCF1 among others (Lecarpentier et al., 2019; (Nusse and Clevers, 2017). In contrast, in the absence of Wnt, DVL is phosphorylated and does not engage the destruction complex. The casein kinase I (CKI) can then phosophorylate the N-terminus of β-catenin, which is then recognised by the β-TrCP which marks β-catenin for ubiquitination and proteosomal degradation. As β-catenin is not translocated to the the nucleus and TCF-LEF remains bound to its co-repressor Groucho inhibiting Wnt target gene transcription (Gregorieff and Clevers., 2005; Flanagan et al., 2018). A summary of activation and inactivation of the Wnt signalling pathway is shown in **Figure 1.5.**

Wnt signalling can be regulated by a number of factors. For example, the membrane-bound RNF43 (RING finger protein 43) and ZNFR3 (zing and RING finger 3) promote the endoytosis and lysosomal degradation of the FZD receptor, thereby reducing the binding of Wnt ligands to the FZD-LRP5/6 complex. The degradation of FZD can be prevented by the secretory protein, R-spondin, which when bound to the LGR4/5/6, inhibits lysosomal degradation and accumulates on the membrane surface, thus amplifying the binding of Wnt ligands such as

Wnt3a, Wnt6, Wnt8 and Wnt9B which are all commonly expressed in the intestinal epithelium (**Figure 1.6**). (de Lau et al., 2014; Zebisch et al., 2013; Flanagan et al., 2018).

Wnt target genes can also be activated in a β-catenin independent manner, however the mechanisms of the non-canonical Wnt signalling pathway has been less well characterised. Here, the a select number of Wnt ligands, such as Wnt5a are able to activate the Wnt-PCP (planar-cell polarity) and Wnt-Ca2+ pathway. Activation of Wnt-PCP results in the activation of the GTPases RAC1 and Rho, which then initiates JNK-mediated signalling which is postulated to regulate cell polarity and microtubule stabilisation. Alternatively, stimulation of the Wnt-Ca2+ pathway activates the phospholipase C (PLC), resulting in the secretion of internal Ca2+, activation of protein kinase C (PKC) and NFAT (transcriptional regulator nuclear factor-associated with T-cells) where it is likely involved in the regulation of actin polymerization (Berwick and Harvey., 2013; Niehrs et al., 2012; Komiya and Habas., 2008) (**Figure 1.5B/C**).

The importance of Wnt signalling in crypt homeostasis have been highlighted by several studies over the years, where, as demonstrated by Korinek et al in 1998, the ablation of TCF4, a downstream Wnt target, led to a decrease in epithelial proliferation and stem cell maintenance (Korinek et al., 1998). Deletion of β-catenin led to the constitutive differentiation of epithelial cells and subsequent loss in crypt function in vivo (Fevr et al., 2007). Overexpression of the Wnt antagonist, Dickkopf-1 resulted in the complete ablation of crypts in vivo, whereas overexpression of R-spondin resulted in human crypt hyperproliferation (Kuhnert et al., 2004; Kim et al., 2005). Similarly, alterations in Wnt activity have also been identified in inflammatory disease such as CD and UC (Serafino et al., 2014). For example, the upregulation of TNF-α, observed in IBD, is able to activate β-catenin expression, by inhibiting the engagement of GSK3β in an AKT dependent manner, thus initiating an increase in cell proliferation (Bradford et al., 2017). Richmond et al's work has shown that IFN-γ, a Th1-cell secretory product, induced the expansion of quiescent stem cell in the small intestine, while the inhibition of Wnt also induced a decrease in IL-6 mediated epithelial proliferation (Richmond et al., 2018). Moparthi and Koch have reviewed the cooperative effects of the NF-κB, MAPK, AKT and STAT signalling pathway have on Wnt target gene activation during inflammation in their review (Moparthi and Koch., 2019)

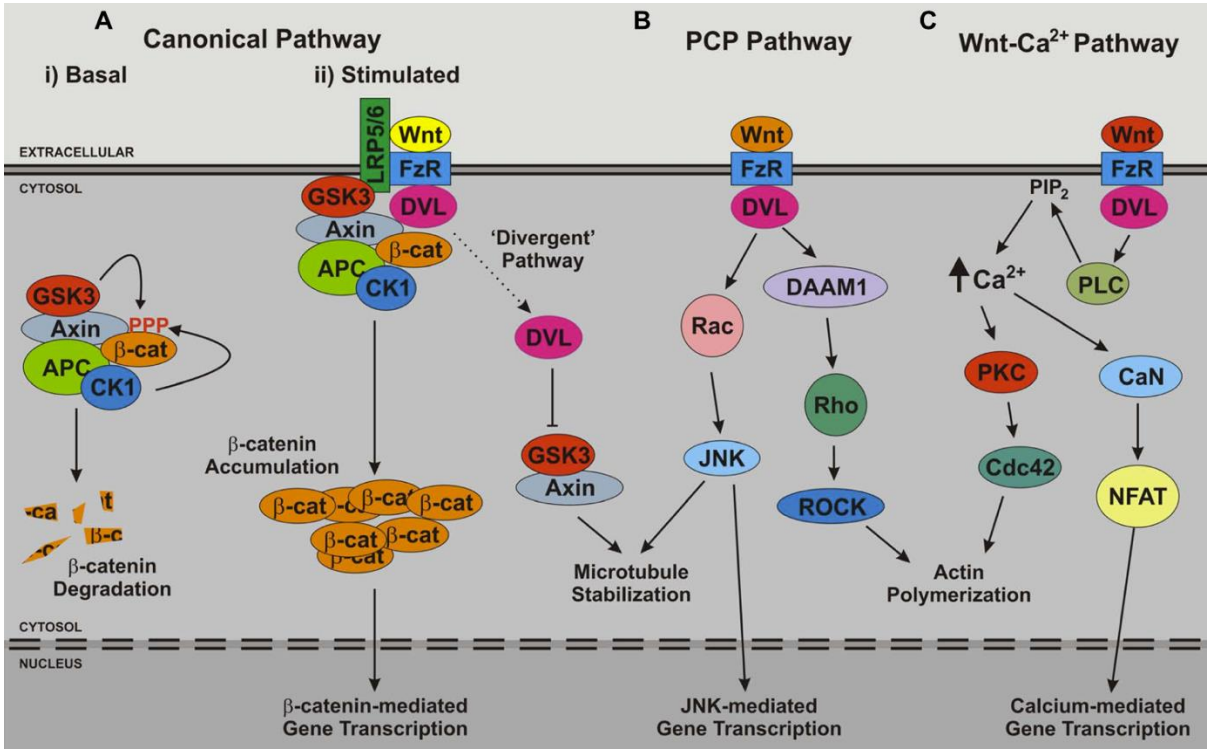

Figure 1.5: The canonical and non-canonical Wnt signalling pathway

Diagram showing the differential activation of the **A)** canonical Wnt signalling pathway **Ai)** in the absence of Wnt ligand stimulation, the GSK3β-Axin complex remains intact leading to the degradation of β-catenin and preventing its nuclear localisation **Aii)** following Wnt ligand stimulation, β-catenin is phosphorylated and translocated to the nucleus where it activates β-catenin mediated transcription factors **B)** planar-cell-polarity (PCP) Wnt pathway mediated via JNK or Rho signalling cascade **C)** non-canonical calcium-dependent Wnt signalling pathways via the PKC or NFAT mediated signalling cascade (Adapted from Berwick and Harvey., 2013).

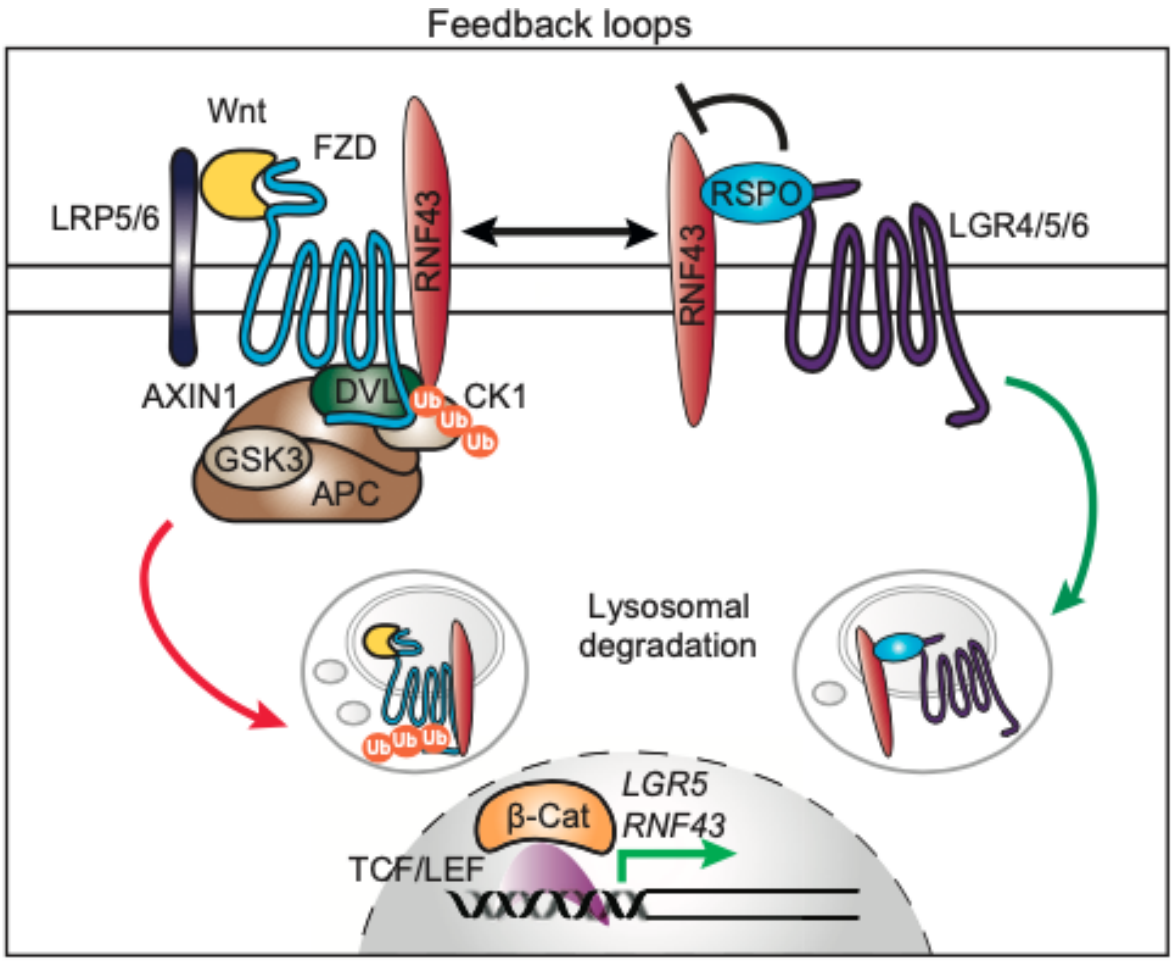

Figure 1.6: The Wnt signalling and R-spondin feedback loop

Diagram showing the regulation of canonical Wnt signalling via a positive feedback loop. Activation of Wnt target genes Lgr5 and RNF43, leads to an increase in RNF43 and LGR4/5/6 complexes which remain on the membrane surface due to the stimulation of R-spondin inhibiting the lysosomal degrdation of the complex, allowing it to engage with the FZD to upregulate Wnt signalling further (Adapted from Merenda et al., 2020).

1.3.2 The intestinal Notch signalling pathway:

The Notch signalling pathway also plays a vital role in intestinal homeostasis. Unlike the other pathways involved, Notch relies on direct cell-to-cell contact (Fre et al., 2005). A number of Notch ligands, Jagged 1,2 (Jag) and Delta-like 1,3 and 4 (Dll) are able to bind to the four Notch receptors (Notch 1-4). The binding of the ligand to the receptor results in the cleavage by ADAM10 and y-secretase (S2 cleavage), after which the Notch intracellular domain (NCID) is further cleaved (S3 cleavage) and translocates to the nucleus, where it then interacts with the DNA-binding protein CSL and MAML-1 to activate the required target gene such as Hes-1,5,6,7 (hairy enhancer of split-1) and Math1/Atoh1 (atonal protein homolog 1). (**Figure 1.7**) (Demitrack and Samuelson., 2016).

In the human colonic epithelium, expression of Notch 1,2 is highly expressed in the basal region of the crypt, specifically the stem cell niche, where Notch signalling was highly active in cycling CBC cells. Similarly, murine small intestinal work showed that Notch 1 and expression as well as the transcription factors Hes-1 and Olfm4 were mostly expressed in intestinal stem cells (Van Dussen et al., 2012; Pellegrinet et al., 2011). In the colonic epithelium, expression of the Notch ligand, Jagged 1 found predominantly at the mid-region of the crypt, whereas Jagged 2 is expressed along the entire crypt-axis. Novel work from Shimizu et al, reported significant differences in the expression of Delta-like ligands 1 and 4 between the small intestine and colon, where Dll1 was primarily localised in at the lower region of the crypt and Dll4 along the entire colonic crypt-axis, Dll4 was only reported to be active in the villus of the small intestine (Shimizu et al., 2014).

The Notch signalling pathways is regulated via a unique negative feedback loop, which is crucial for the maintenance of the stem cell niche. In the intestine, the epithelial cell fate is dependent on the Notch activity within the individual cells, where the mechanism of lateral inhibition ensures the even distribution of both absorptive and secretory cell lineages (Collier et al.,1996; Stamataki et al., 2011). When Notch signalling is initiated by a Delta-like ligand from the signal-sending cell, the signal-receiving cell, translocated the cleaved NCID

into the nucleus which then allows the transcription of Hes-1 to occur, however the expression of Hes-1 antagonises the transcription of Atoh1 and therefore, signal-receiving cell does not express Delta-like ligands itself, where this cycle of crosstalk between the signal-sending and receiving cell maintains the positive feedback loop. As Hes-1 is predominantly expressed in the absorptive cell lineage and Atoh1 is required for the differentiation of the secretory cell fate, in homeostasis this mechanism generates a balanced expression of either cell lineages (**Figure 1.8**) (Sancho et al., 2015).

Using a similar mechanism of negative regulation, small intestinal Paneth cells which express high levels of Dll1 and Dll4 ensure that neighbouring Lgr5+ stem cells remain in their undifferentiated state by maintaining high Notch activity within the intestinal stem cells which is crucial for stem cell proliferation (Sancho et al., 2015; Pellegrinet 2011). As the colon lacks Paneth cells, it is currently postulated that nearby stromal and immune cells or Reg4+ deep secretory cells maintain the stem cell niche via a similar mechanism instead (Demitrack and Samuelson., 2016; Sasaki et al.,2016).

Notch signalling also plays a crucial role in the even distribution of absorptive and secretory cells along the crypt axis, where lineage tracing experiments performed by Toth et al., have revealed that the lateral inhibition within the colon is only operative in the commitment zone, located two rows above the +4 stem cell position and is thereby responsible for the 1:3 goblet cell to enterocyte proportion within the colonic epithelium (Toth et al., 2017).

Dysregulation of Notch signalling can severely affect intestinal homeostasis and an increase in Notch signalling is commonly associated with an increased susceptibility to inflammatory bowel diseases and colorectal cancer (Hsu et al., 2012; Piazzi et al., 2011). For example, the depletion of Hes-1 induced an increase in secretory cell fate in the intestinal epithelium and completely abrogated absorptive cell lineages (Jensen et al., 2000). Furthermore, Hes-1 deficient mice treated with a γ-secretase inhibitor also resulted in an increase of secretory cell lineages (Van Es et al., 2005). Crucially, the mRNA expression of Notch1 and Hes-1 was significantly higher in UC patients compared to healthy individuals, suggesting that regulation of Notch is crucial to avoid inflammatory bowel disease progression (Ghorbaninejad et al. 2019). Corresponding with these findings, earlier work from Zheng et al, also revealed that increasing Hes-1 expression correlated with a decrease in Atoh1 and subsequent goblet cell depletion in UC patients (Zheng et al., 2012).In contrast, an increase

in Atoh1 was reported in CD and gastric cancers samples (Gersemann et al., 2009; Mutoh et al., 2006).

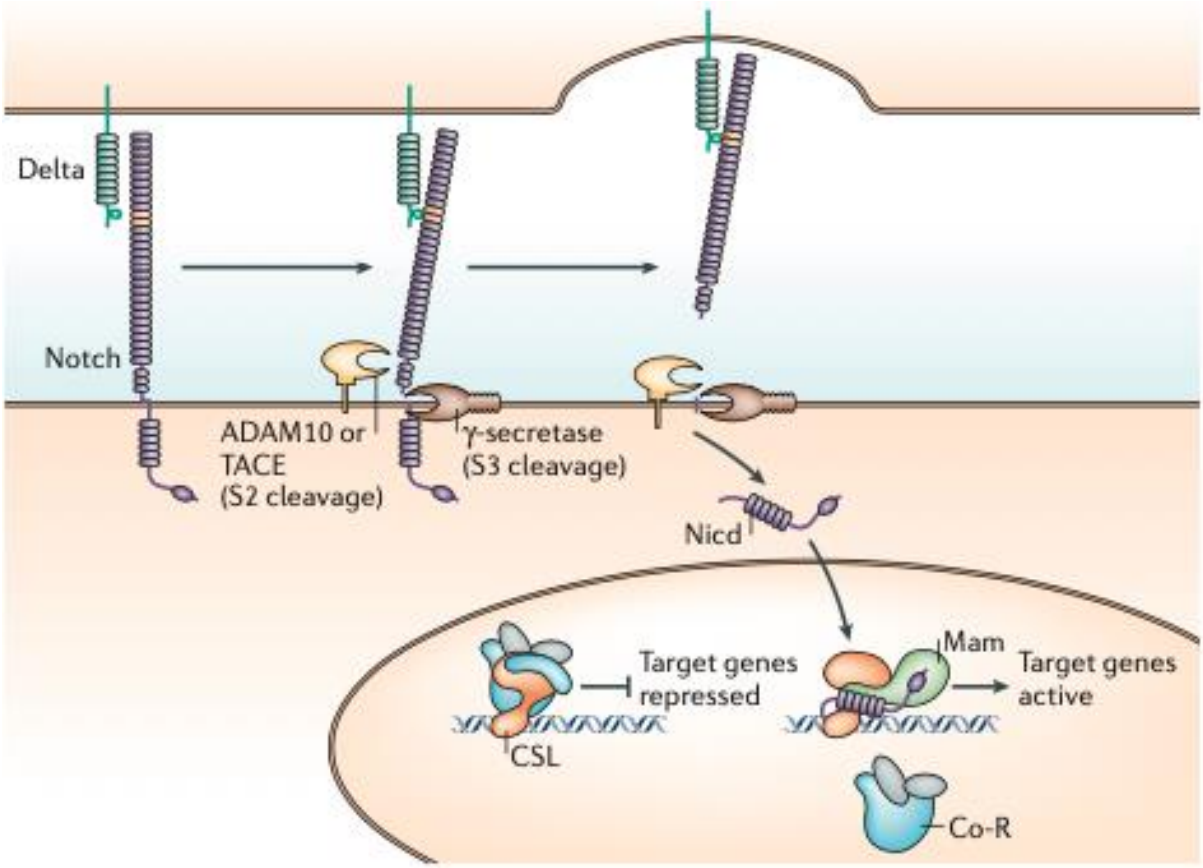

Figure 1.7: **The Notch signalling cascade**

Diagram showing the activation of the Notch pathway via direct cell-cell adhesion. Here, the Delta-like ligand initiates the proteolytic cleavage of its receptor by γ-secretase resulting in the release of NCID, which is translocated and binds to the DNA-binding protein CSL and co-activator Mam (Mastermind) to transcribe the necessary target genes (Adapted from Bray et al., 2006)

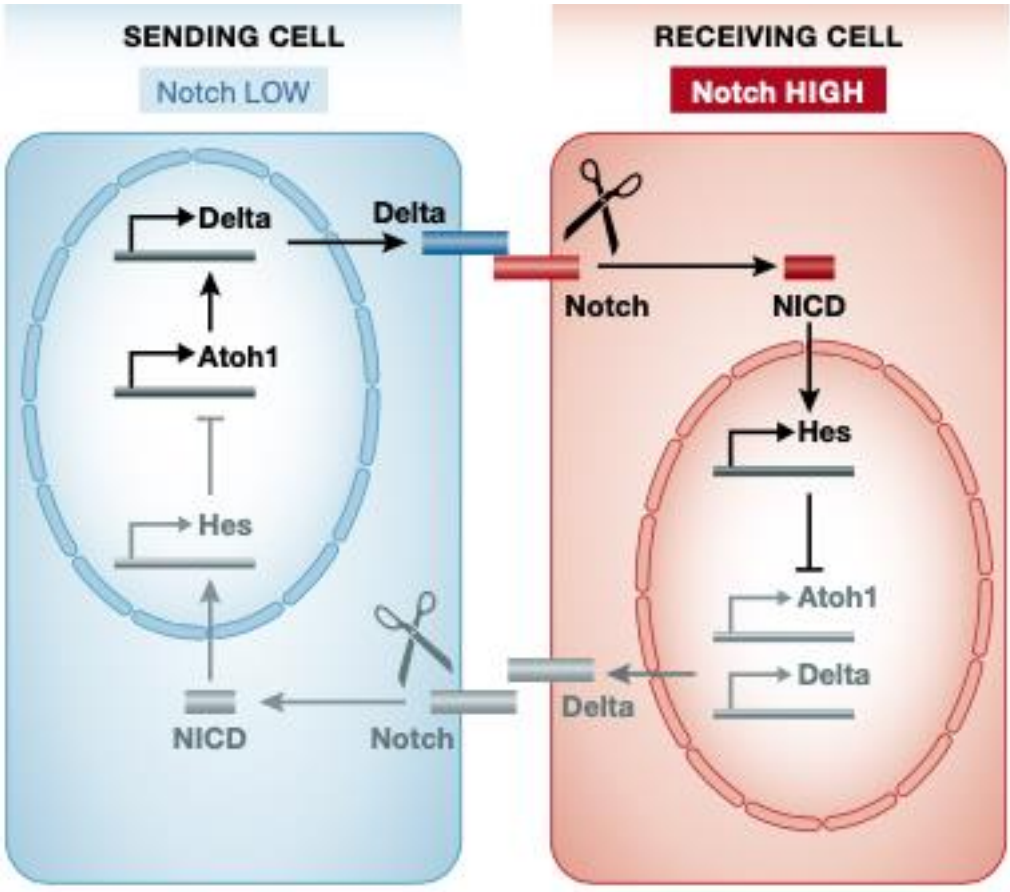

Figure 1.8: Lateral inhibition and the positive feedback loop of Notch signalling

Diagram showing the positive feedback regulation of the Notch in neighbouring cells. The signal sending cell shown in blue, activates Notch signalling in the signal-receiving cells shown in red via the Delta-like ligand, resulting in the downstream transcription of Hes1, which in turn inhibits Atoh1, thus the signal-receiving cell remains Notch-HIGH and DLL-LOW, whereas the signal-sending cell remains Notch-LOW and DLL-HIGH (Adapted from Sancho et al., 2015).

1.3.3 Intestinal BMP, EGF, Hippo signalling pathways:

Bone morphogenetic protein (BMP) signalling pathway, is a Smad-dependent pathway which drives differentiation in a reverse gradient compared to Wnt signalling. BMP can also directly repress Lgr5+ stem cell expansion to maintain homeostasis. The signalling is initiated by BMPS binding to the extracellular receptors Bmpr1-2, following transphosprylation, Smad 1/5/8 form a complex with Smad4, which is translocated to the nucleus to regulate gene expression via target genes such as Msx and JunB (Wang et al., 2014). BMP antagonists such as Noggin, chordin and gremlin 1/2 are present at the at the base of the crypt's stem cell niche where they can regulate BMP activity (Kosinksi et al, 2007). Noggin can also further promote Wnt signalling, by increasing the expression levels of P-PTEN and P-Akt leading to the increased translocation of β-catenin to the nucleus (He et al., 2004). Recent findings have also shown that Lgr5+ proliferation is decreased following the absence of Noggin, highlighting the importance, the BMP signalling pathway plays in intestinal homeostasis and inhibition of stem cell niche expansion (**Figure 1.9**) (Qi et al., 2017)

The epidermal growth factor (EGF) also plays a pivotal role in activating proliferation and inhibiting apoptosis of intestinal stem cells as well as regulating intestinal barrier function (Tang et al., 2016). The binding of the EGF ligand to the transmembrane EGF receptor, leads to the phosphorylation RTK (receptor tyrosine kinase), activation of Ras/MAPK and P13K/AKT (Bran et al., 2011). In human and mouse models, EGF is capable of activating P13K/Akt within the MAP kinase cascade which leads to the phosphorylation of β-catenin thus activating the canonical Wnt pathway (Suzuki et al., 2010). Furthermore, EGF also encourages the secretion of mucins within the intestine (Damiano et al., 2014). Whereas Paneth cells provide the necessary supply of EGF in the small intestine, Sasaki et al postulate that deep secretory cell lineages within the crypt are potentially able to secrete EGF instead (Sato et al., 2013; Sasaki et al., 2016).

The Hippo signalling pathway can be triggered by a number of inhibitory factors, such as cell-cell contact, binding of growth factors such as EGF and cell polarity, however, to date a Hippo-specific ligand-receptor has not been found (Seo et al., 2020). Here, Hippo activation relies on the translocation of the proteins, Yes-associated protein (YAP1) and tafazzin (TAZ) (Konsavage et al., 2013). The mammalian serine/theorine 1/2(MST1/2) protein is activated

its forms a complex with SAV1 (scaffold proteins salvador family WW domain containing protein 1), which then activates LATS1 (large tumour suppressor kinase 1/2). LATS 1/2 then phosphorylates the YAP1 and TAZ, thus inhibiting their localisation to the nulceus and are subsequently degraded in the cytoplasm. When Hippo activation is ceased, YAP1 and TAZ are able to translocate to the nucleus, where they are able to bind to the DNA-binding protein TEAD (TEA domain transcription factor) and activate the required target genes (**Figure 1.10**) (Ma and Shah., 2018; You et al., 2015).

Current evidence suggest that the Hippo pathway plays a significant role in the maintenance of crypt homeostasis. For example, YAP expression was found to be predominantly the highest at the at the base of the crypt, where lower expression was reported at in the small intestinal villi (Liu-Chittenden et al., 2012; Can et al., 2010). Increased YAP1 activation resulted in the increase in undifferentiated progenitor cells while Paneth and goblet cell numbers decreased. Mice depleted of SAV1 and LATS1/2, which are are required to sequester YAP1, were also found to result in increased crypt growth (Camargo et al., 2007; Pan et al., 2019). Other studies have found that the Hippo pathway may be cross-linked with other pathways such as BMP,Notch and Wnt signalling. Byun et al., has demonstrated that Wnt ligands such as Wnt3a and Wnt5a/b promote YAP1/TAZ activity by increasing its nuclear localisation. (Gregorieff et al., 2015). Furthermore, knockout of Axin 1/2 was shown to increase cytoplasmic YAP/TAZ accumulation in vivo. (Cong et al., 2004) Vice versa, the YAP1/TAZ complex was also shown to aid the stabilisation of β-catenin, thus allowing it to enter the nucleus, while in contrast, another study concluded that cytoplasmic YAP1 and TAZ can restrict Wnt signalling activity by reducing the availability of DVL (Dishevelled)(Li et al., 2019; Varelas et al., 2010). The YAP/TAZ complex was also reported to be in contact with the Notch component, NCID, which plays a vital part in the activation of Notch signalling, where the over-expression of NCID also led to an increase in YAP/TAZ and TEAD expression (Yimlamai et al., 2014; Moroishi et al., 2015). In mice with DSS-induced colitis, an increased presence of YAP1 was reported, where it likely plays a crucial role epithelial repair, as its depletion led to a reduction in cellular proliferation (Taniguchi et al., 2015; Can et al., 2010). Furthermore, YAP1 over-expression in mice also induced intestinal hyperplasia where an expansion of progenitor cells was reported. Interestingly, work from Kim et al, has shown that PGE_2 binding to the EP4 receptor can increase the transcription of YAP and CREB

pathway in order to increase epithelial regeneration following injury (Kim et al., 2017). Taken together, the studies highlight the importance of the Hippo signalling pathway in the regulation of intestinal homeostasis (Camargo et al., 2007).

The signalling pathways mentioned previously all play an essential role in regulating the rate of proliferation and differentiation of the intestinal epithelium. However, as such differentiated epithelial cells age there are shed into the lumen in a highly controlled fashion (Bullen et al., 2006).

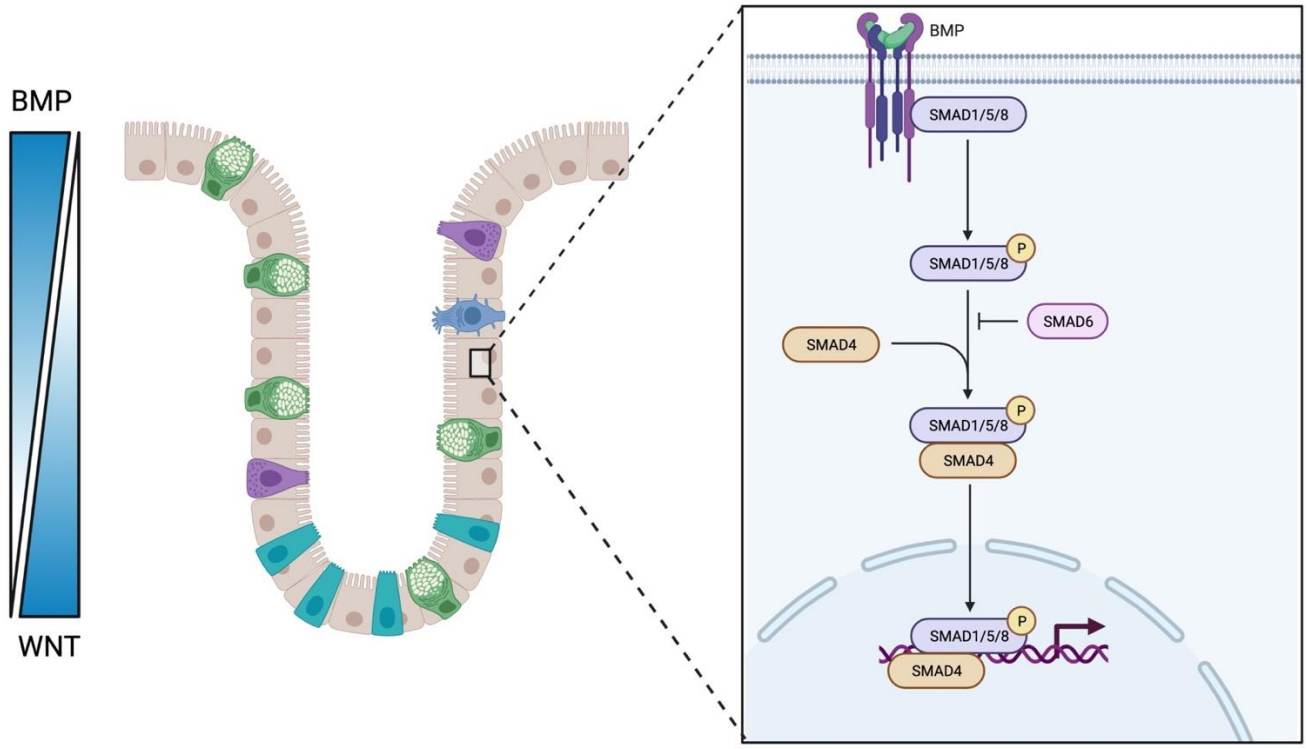

Figure 1.9: The BMP signalling cascade

Diagram summarising the activation of the downstream BMP signalling pathway. The binding of BMP induces the phosphorylation of BMPR1/2, Smad 1/5/8, which then form a Smad4-Smad1/5/8 complex to translocate into the nucleus where it can activate its target genes. BMP expression gradually increases towards the top of the crypt, while Wnt signalling activity is highest at the base of the crypt. (Adapted from Wang and Chen, 2018, created on Biorender., 2021).

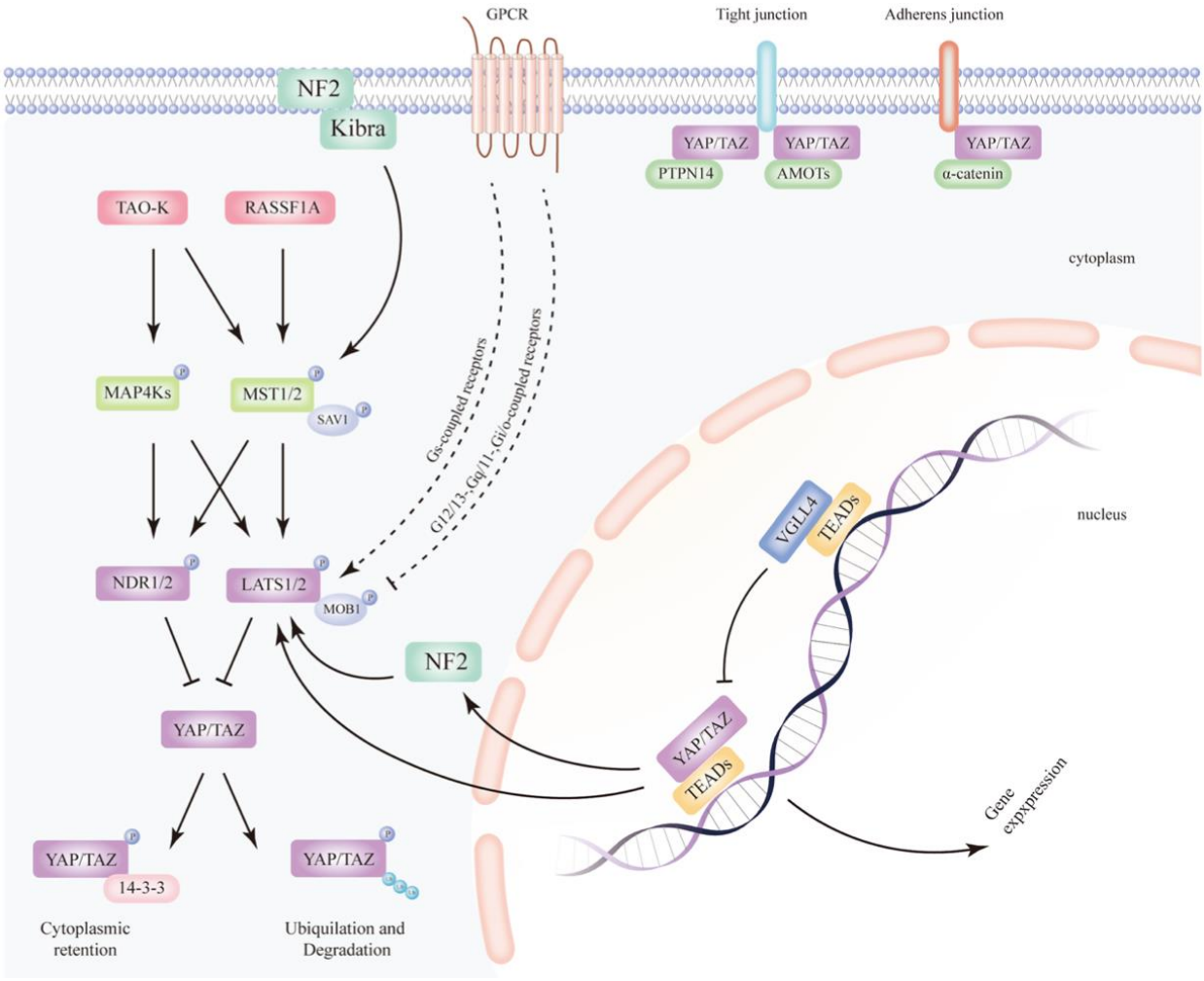

Figure 1.10: The Hippo signalling pathway

Diagram summarising the activation of the downstream Hippo signalling pathway. Hippo activation, MST1/2 forms a complex with SAV1 resulting in the phosphorylation of LATS 1/2 complex, which in turn phosphorylates and sequesters YAP1 for cytoplasmic degradation. In the Hippo signalling OFF state, YAP and TAZ is instead translocated into the nucleus to engage TEAD and activate the appropriate Hippo target genes (Xie et al., 2021).

1.3.4 Epithelial cell shedding

Following the proliferation and differentiation, the epithelial cell migrates progressively upwards until they are then shed into the lumen and the end of their life cycle. However, uniquely to the intestinal epithelium, the apoptotic cell is released from the epithelium while maintaining epithelial integrity. As epithelial integrity is maintained by a single-cell thick epithelium, it is of upmost importance that epithelial cell shedding does not disturb epithelial barrier function (Williams et al., 2014).

In the 1990s, Madara's work demonstrated that epithelial cells at the top of the small intestinal villi may utilise a 'zipper' like motion to detach itself from the epithelium (Madara JL., 1990). Here, the apoptotic cells, lose E-cadherin expression and redistributes the positioning of ZO-1, a tight junction protein towards the baso-lateral region of the crypt, while the neighbouring cells form tight junctions bonds underneath the shedding cell and proceeds to eject the shed cell out of the epithelial barrier, where the entire process was shown to take place within 5-10 minutes in the human small intestine (**Figure 1.11A**) (Fouquet et al., 2004; Bullen et al., 2006; Wiliams et al., 2015).

Prior to the event of cell shedding, the mechanism of cell death, apoptosis, must be triggered, where apoptosis can either be triggered via an extrinsic or an intrinsic pathway (Jan and Chaudhry., 2019). The intrinsic pathway is commonly triggered by stress, hypoxia or DNA damage and other factors, which results in the activation of Bcl-2 family proteins BAX/BAK and permeabilisation of the outer mitochondrial membrane (MOMP) and subsequent release of cytochrome c. The combination of cytochrome c with Apaf-1 leads to the formation of apoptomsome and triggers the secretion of procaspase-9 and caspase 3 signalling cascade. In contrast the extrinsic pathway utilises the activation of the death receptor, which can be triggered by external stimuli such as TNF-α, APO3L and other TRAILs (TNF-related apoptosis-inducing ligands), in turn the intracellular domain, also known as the death-inducing signalling complex (DISC) is cleaved, releasing one of its partial components procaspase-8 which can then trigger the capsase-3 signalling pathway while also activating the MOMP-dependent pathway (**Figure 1.11B**) (Negroni et al., 2015; Blander JM., 2018).

More recently another form of programmed cell death, namely, necroptosis has been identified. Here, the tumor necrosis factor (TNF) superfamily was demonstrated to activate

the formation of intracellular necrosomes leading to the phosphorylation of PIP (phosphatidylinositol phosphates), which induce membrane permeabilisation and release AMPS, HSPs (heat shock proteins among other proteins to trigger a pro-inflammatory response while also leading to self-destruction (Berghe et al., 2014; Dagenais et al., 2014).

Endomicroscopy performed in patients with inflammatory bowel disease demonstrated that excessive epithelial shedding is likely a contributing factor in disease progression (Kiesslich et al., 2012; Nenci et al., 2007). In mice, the administration of TNF-α resulted in an increase in epithelial permeability and barrier function, where mice deficient in IL-10, a residential macrophage secreted cytokine, also resulted in increased permeability and occurrence of spontaneous colitis, which could be alleviated by blocking of the zonulin receptor, thereby reducing epithelial cell shedding (Kiesslich et al., 2007; Arrieta et al., 2009). Crucially, a lack of epithelial barrier function in the steady state may lead to “leaking” of luminal contents into the lamina propria, which then triggers the activation of the intestinal innate immune system (Montalban-Arques et al., 2018).

A

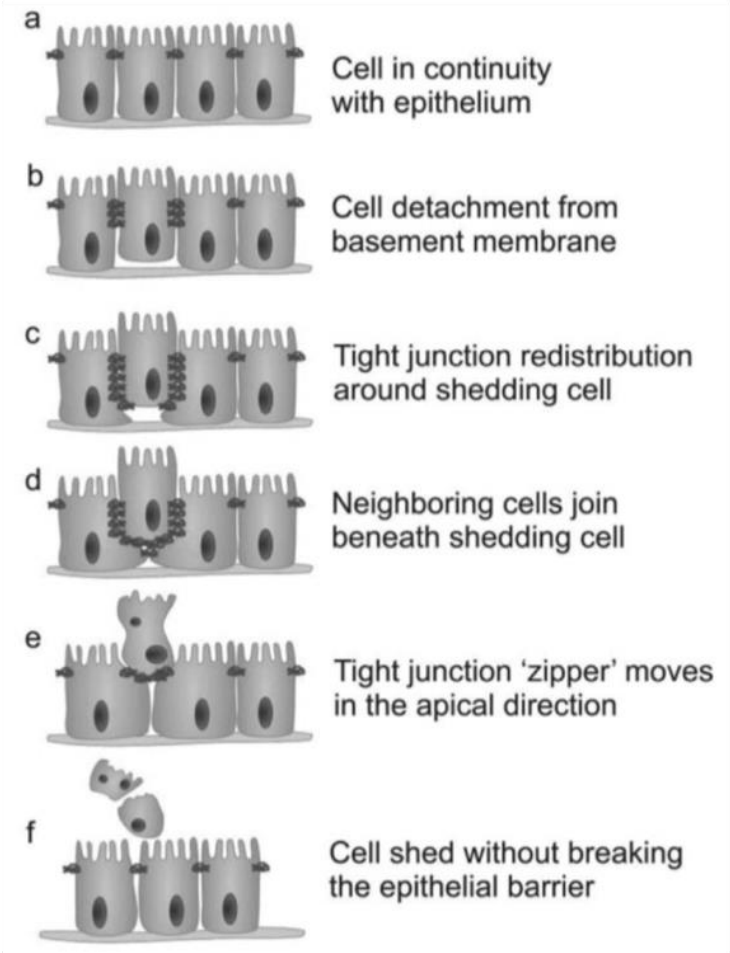
a
Cell in continuity with epithelium
b
Cell detachment from basement membrane
c
Tight junction redistribution around shedding cell
d
Neighboring cells join beneath shedding cell
e
Tight junction 'zipper' moves in the apical direction
f
Cell shed without breaking the epithelial barrier

B

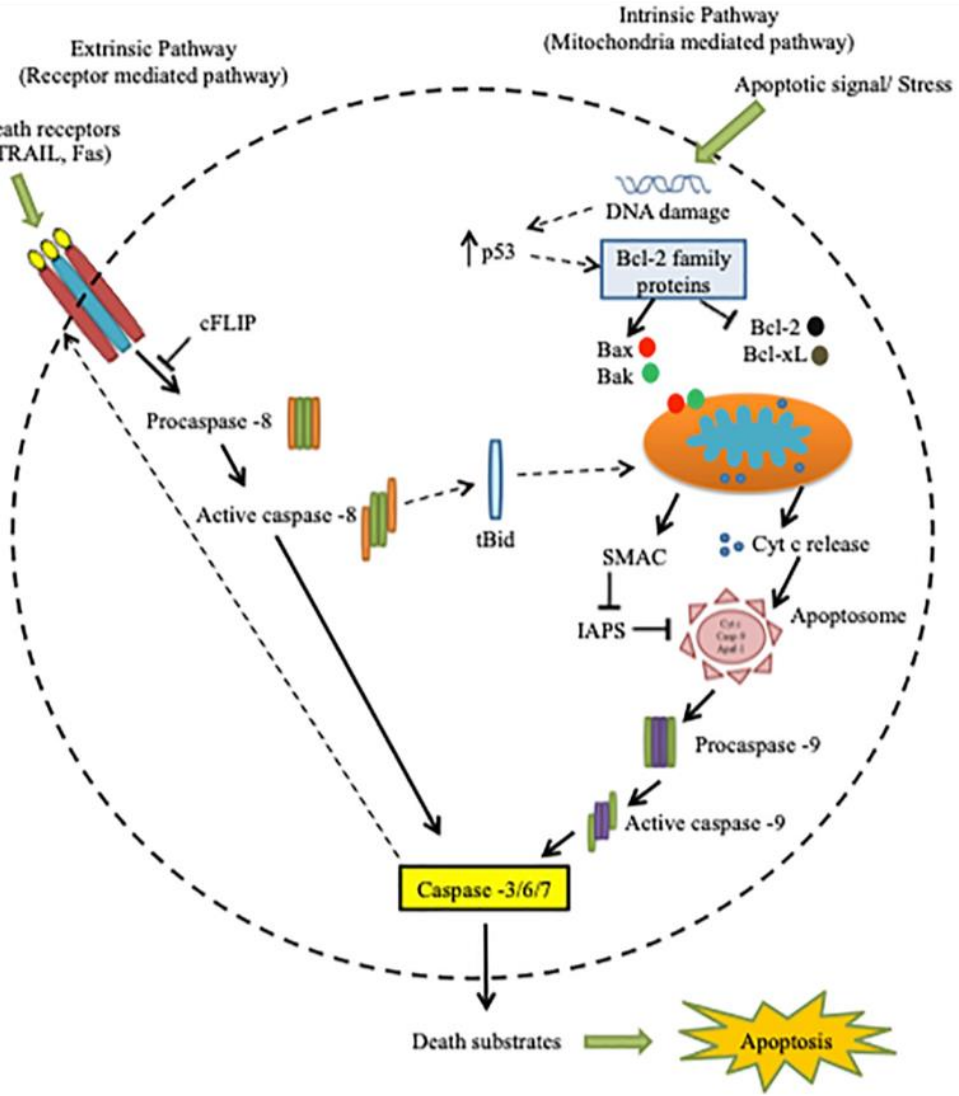
Intrinsic Pathway
(Mitochondria mediated pathway)
Extrinsic Pathway
(Receptor mediated pathway)
Apoptotic signal/ Stress
Death receptors
(TRAIL, Fas)
DNA damage
p53
Bcl-2 family proteins
cFLIP
Bcl-2
Bcl-xL
Bax
Bak
Procaspase -8
Active caspase -8
tBid
SMAC
Cyt c release
IAPS
Apoptosome
Procaspase -9
Active caspase -9
Caspase -3/6/7
Death substrates
Apoptosis

Figure 11: Intestinal epithelial shedding and the extrinsic/intrinsic pathway of apoptosis

A) Diagram summarising the process of epithelial cell shedding. **a)** The epithelial tight junctions are aligned and intact **b)** Basal adhesion proteins are disjoined while cell-cell tight junction proteins remain intact. **c)** Tight junction proteins are redistributed and **d)** neighbouring cells are linked beneath the shedding zone **e)** Tight junction proteins manoeuvre and direct the shedding zone out towards the lumen where **f)** the cell is shed into the lumen, while neighbouring cells of the epithelium maintain their barrier function (Adapted from Williams et al., 2015). **B)** Diagram summarising the process of both extrinsic and intrinsic apoptosis. The intrinsic pathway is commonly stimulated via stress, hypoxia or DNA damage which subsequently triggers the release of procaspase-9 and caspase3. The extrinsic pathway is triggered by external stimuli, leading to the release of procaspase-8 and subsequent activation of caspase-3 (Adapted from Jan and Chaudhry., 2019).

1.4 The intestinal innate immune system:

The intestinal epithelium and pathogen recognition:

The large intestine is home to the largest microbiota population within the gastrointestinal tract (Guarner and Malagelada., 2003). Here commensal bacteria aid the metabolism of food and waste products. As only a single epithelial barrier offers protection to underlying lamina propria, the epithelial cells are naturally in contact bacteria and foreign pathogens which regularly breach the physical barrier leading to inflammation. For this reason, the intestinal epithelium has evolved and developed protective mechanism to efficiently deal with luminal insults within the steady-state and inflammation (Dietrich et al., 2018).

Following a breach and malfunctioning epithelial barrier function, several innate immune cells including dendritic cells, macrophages and NK cells acts as the first responders and are activated by luminal insults and damage associated molecular patterns (DAMPS). These are detected by pattern recognition receptor patterns (PAMPS) on the immune cell surface, consequently leading to the downstream activation of the adaptive immune response (Magrone et al., 2013). The recognition of microorganism is mediated via a highly conserved pattern recognition receptors (PRR) on the surface of the epithelium and immune cells, which are able to recognise a number of bacterial signatures. Here ligand binding to the PRR initiates a downstream signalling cascade and subsequent upregulation of pro-inflammatory transcription genes. Such pathogen associated molecular patterns can also be recognised by underlying antigen presenting cells such as macrophages and dendritic cells, where both act as the first responders of the innate immune response (Wang et al., 2019).

Among the PRR family, twelve Toll-like receptors (TLR) have been identified where each is able to respond to varying pathogenic ligands (Bilack B., 2006). Here, a TLRs such as TLR1,2,4,5 and 6 can all recognise a number of microbial components on the cell surface such as LPS, flagellin and di/tri-acyl tripeptides, whereas TLR3,7 and 9 recognise single, double and CpG DNA strands (Takeda and Akira., 2005). During inflammatory bowel diseases such as CD and UC, the innate immune response becomes dysfunctional and an excessive immune response is triggered, subsequently leading to the influx of macrophages commonly localised beneath the intestinal crypts. Due to the macrophage's malleable

nature, its exact functional role in both homeostasis and inflammatory conditions has not been extensively studied. Intestinal tissue-resident macrophages have evolved and adapted to the intestine's microenvironment in order to cope with the increasing stimuli arising from the commensal microbiota of the host (Mantovani et al., 2012).

Like its namesake suggests macrophages (Greek: macro=large, phage=eat), the recognition of microbial antigen leads to the phagocytosis of the threat while simultaneously inducing a pro-inflammatory and highly bactericidal response where homeostasis can be rapidly re-established, however this response has been dampened in intestinal macrophages in order to prevent an excessive immune response which could potentially cause chronic inflammation (Hadis et al., 2011; PV Chang et al., 2014).

Similarly, to a select few intestinal epithelial cells, the intestinal innate immune system relies on pathogen associated pattern receptors such as Toll-like receptors and NOD like receptor in order to recognise commensal and pathogenic microbes (Allaire et al., 2018). Intestinal macrophages in particular were shown to express Toll-like receptor 3-9 and TREM2 among others, however expression of Myd88 and NOD2 were shown to be downregulated, allowing tissue-resident macrophages to carry out phagocytic tasks in in a hyporesponsive manner (Smythies et al., 2005; Roberts et al., 2001).

The Toll-like receptor 4 is predominantly active in macrophages and is essential for the recognition of LPS and can utilise both the TRIF and Myd88 signalling cascade (Butcher et al., 2018). Intracellularly, the stimulation of TLRs, leads to the activation of the canonical adaptor protein MyD88, which leads to the downstream upregulation of the transcription factor NF-kβ and the induction of pro-inflammatory cytokines such as TNF-α and IL1-β among others (Hooper et al. 2014). Myd88 dependent TLR recognition can also severely affect mechanisms of phagocytosis in macrophages, where the ablation of TLR2 and 4 caused an impairment in the effective removal of *Escherichia coli and Salmonella typhimurim* (Blander et al., 2014). Another PRR family are nucleotide-binding oligomerisation domain-like receptor (NLR), where NOD1 and NOD2 are localised within the cytoplasm. Interestingly, the stimulation of both TLR and NOD enhances the phagocytic activity of macrophages *in vitro,* while studies have shown that polymorphism in NOD2 protein expression are heavily linked with a high risk of Crohn's disease (Hedl et al., 2007; (Zhou et al., 2019).

To understand how the function of the innate immune system in the large intestine may differ during homeostasis versus injury, it is important to understand the ontogeny of innate immune cells, specifically, the role of the most abundant colonic immune cell population, the macrophage (Jones et al., 2018).

1.4.1 Monocyte education:

The origins of intestine-resident macrophages have long been debated. In the liver, heart and lung, tissue-resident macrophages have been confirmed to migrate from the yolk-sac at the embryonic stages and are maintained throughout adulthood in both mice and humans.

Initial studies have affirmed that haematopoietic stem cells, initially present within the bone-marrow can differentiate into either common myeloid or common lymphoid progenitors depending on the presence of various cytokines such as M-CSF,IL-6, IL-6 or IL-2, IL-7 or IL-12, respectively (Seita and Weissmann., 2010). . Such myeloid progenitors are then further differentiated into either erythrocytes, thrombocytes and crucially via the aid of GM-CSF myeloblasts, where myeloblasts are finally capable of differentiating into basophils, neutrophils, eosinophils or monocytes, where the presence of M-CSF is crucial for the development of the monocyte phenotype (Lim et al., 2013). This process of differentiation is summarised in **Figure 1.12**.

Elegant fate-mapping techniques applied by De Schepper et al, have identified a sub-population of self-maintaining macrophages (gMac) which are derived from embryonic precursors and are then placed in the underlying intestinal lamina propria. Interestingly however following the depletion of such gMacs with diptheria-toxin the residential population was re-established by bone-marrow derived macrophages instead (De Schepper et al., 2018). Uniquely to the intestine, Bain et al's studies have demonstrated that circulating monocytes constitutively migrate into the intestinal mucosa where they are then educated towards a mature macrophage phenotype (Bain et al., 2014). Indeed, Shaw et al confirmed that both yolk-sac derived, and bone-marrow derived macrophages co-exist within the lamina propria, however whether either sub-population's functions differ *in vivo* is yet to be determined (Shaw et al., 2018).

A study from Wolf et al, recently revealed the existence of two independent pathways of monopoiesis in homeostasis. Monocytes can be derived from GMPs (granulocyte-macrophage progenitor) where they give rise to pre-dominantly Ly6C+ and MHC2-

monocytes or alternatively give rise to MHC+Ly6C+ monocyte via the MDP (monocyte-dendritic cells) pathway, as shown in (**Figure 1.12B**) (Wolf et al., 2019).

The Ly6C is a cell surface marker has been acknowledged as a robust marker for circulatory monocytes and MHC-2 were usually associated with antigen-presenting cells such as macrophages and dendritic cells where their role was to bind to pathogenic antigen in order to display them on the surface of the immune cells, later to be identified by T-cells, subsequently initiating an appropriate immune response (Janeway et al., 2001; Desalegn et al., 2019).

As mentioned above, the intestinal macrophage population is continuously replenished by an influx of monocyte in homeostasis and a high abundance of intestinal macrophages resides in the underlying lamina propria of the colonic epithelium where the play a number of key roles required for the regulation of intestinal homeostasis (Bain et al., 2017).

Following 2-3 weeks after birth an influx of Ly6C+, CCR2+ monocytes cause a significant increase in residential macrophage numbers (Wolf et al., 2019; Geismann et al., 2003). In order for Ly6C+ blood circulating monocytes to enter the intestinal lamina propria, the expression of the chemokine receptor, CCR2 is crucial for entry into the tissue. In CCR2 deficient mice, where monocytes were unable to enter the lamina propria (Serbina and Palmer., 2006). Unlike other tissues in adult mice, it was noted that monocytes are not only recruited to the intestinal mucosa during inflammation but are also constitutively migrating towards the lamina propria, under homeostatic conditions (Bain et al., 2014).

The gradual education of monocytes towards a macrophage phenotype has been coined the 'monocyte-waterfall' pathway. Here $CCR2^{high}$, $Ly6C^{high}$, $MHCII^{low}$, $CX3CR1^{low}$ monocytes gradually gain the cell surface marker MHCII and finally morph into $F4/80^{high}$, $CD64^{high}$, $MHCII^{high}$, $CX3CR1^{high}$ and $Ly6C^{low}$ macrophages (Tamoutounour et al., 2012). Due to the high plasticity of macrophages, studies over the past two decades have demonstrated that only a combination of cell surface markers allows the positive identification of murine macrophages (**Figure 1.14**).

The expression of F4/80 was initially established to be a unique murine macrophage marker, where studies have suggested that such cells were capable of TNF-α, IL-12 and IFN-γ production in response to microbial insults, however Mowatt's work later also confirmed

that mucosal eosinophils also express Cd11+ and F4/80 markers *in vivo* thus requiring further cell surface marker characterisation. (Warschkau and Kiderlen., 1999; Mowatt and Bain., 2011).

As both dendritic cells and macrophages are considered antigen presenting cells (APC) where they may share similar functional roles, studies needed to distinguish between either population. Work from Tamoutonour et al, has shown that the Fcγ receptor CD64 is only expressed in intestinal macrophages but not dendritic cells (Tamoutonour et al., 2012; Bain et al., 2013). Another commonly expressed macrophage marker is the fractalkine receptor, CX3CR1. As reviewed by Regoli et al., CX3CR1 expressing macrophages are involved in functions ranging from gut antigen sampling to wound repair and were most importantly shown to be highly phagocytic (Regoli et al., 2017; Burgess et al., 2019). Surprisingly it was found that CX3CR1 positive cells have a short half-life of 3 weeks after which they'll need to be replenished by blood monocytes (Jaensson et al., 2008).

Conclusively, the combination of the aforementioned markers can then be used to positively identify a macrophage population both *in vivo* and *in vitro*. (Zigmond et al.2012; Bogunovic et al. 2009; Bain et al., 2018).

The differentiation from a haematopoietic stem cell towards a monocyte and subsequent macrophage phenotype in a steady state heavily depends on the environmental presence of the macrophage colony stimulating factor (M-CSF) (**Figure 1.12A**) (Pixley J., 2012). Very early research has shown that macrophages are able to form colonies in the presence of CSF-1/M-CSF (Stanley et al., 1978; Guilbert ≥and Stanley., 1980). Although HSC (hamatopoietic stem cells) express low levels of M-CSF, increased levels are found in both monocytes and macrophages. Here M-CSF, a myeloid cytokine can directly up-regulate the PU.1 transcription factor and initiate a myeloid cell development within HSCs (Mossadegh-Keller et al., 2013). M-CSF stimulation leads to the phosphorylation of tyrosine residues and activation of the MAPK pathway which subsequently activate the p38 pathway, commonly associated with the production of pro-inflammatory cytokines such as IL-1β, TNF-α and IL-6 (Zarubin et al., 2005; Lloberas et al., 2016; Gobert-Gosse et al., 2005).

The central role of M-CSF in macrophage differentiation was highlighted by a number of studies in which the depletion of the csfr1 gene in mice led to a deficiency in macrophage numbers. Similarly, direct blocking of anti-CSF1R also led to the complete ablation of tissue-

resident macrophages *in vivo (*Dai et al., 2002; MacDonald et al., 2010). Intriguingly, further research by Sehgal et al, has shown that M-CSF null mice and anti-CSFR antibody showed a reduction in macrophage numbers but also reduced Paneth and Lgr5+ intestinal stem cell numbers (Sehgal et al., 2018; Na et al., 2019).

While monocyte to macrophage differentiation relies on the presence of various cytokines and chemokines, the macrophage phenotype and function can also be significantly altered by lamina-propria derived cells and their secretory products as revealed in the upcoming section (Mills et al., 2000; Italiani and Boraschi., 2014).

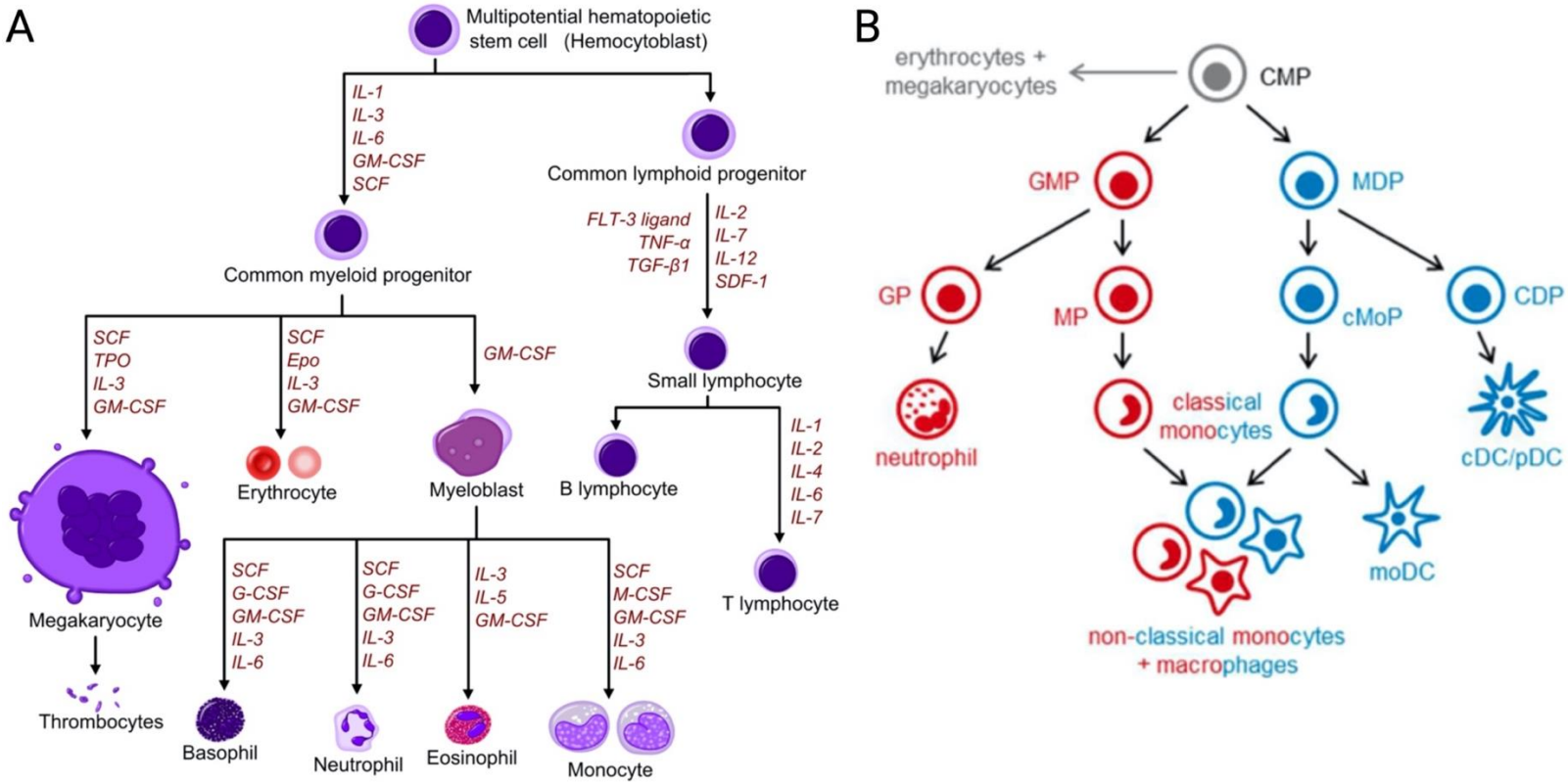

Figure 1.12: The process of monocyte differentiation in the bone-marrow

Diagram showing **A)** various differentiation pathways of haematopoietic stem cell, where a monocytic phenotype can be derived in the continuous presence of GM-CSF (granulocyte/macrophage- colony stimulating factor) and **B)** the independent pathways of myeloid differentiation, where they can be derived from granulocyte-macrophage progenitors (GMPS) shown in red or via the monocyte-dendritic cell (MDP) pathway, shown in blue (Adapted from Wolf et al., *2019).*

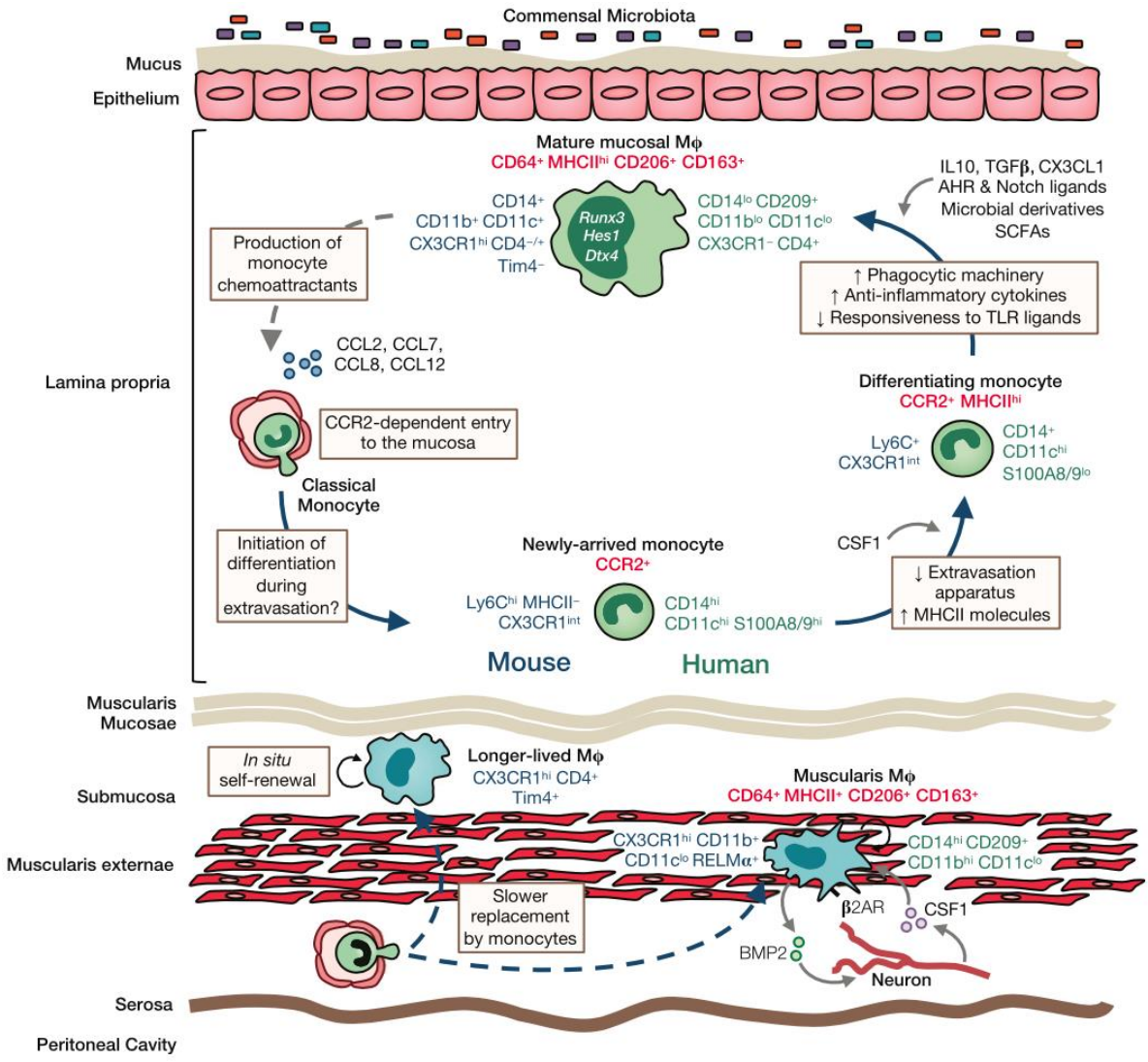

Figure 1.13:The monocyte-waterfall differentiation pathway

Diagram highlighting the process of intestinal monocyte differentiation towards a macture macrophage phenotype. In vivo, Ly6C+, MHC2-, CX3CR1-low monocytes arrive in the lamina propria where they gradually gain the macrophage markers MHC2+, CX3CR1, CD64 while losing CCR2 and LY6C expression in mice (Bain and Schridde., 2018).

	Newly extravasated monocytes	Mature macrophages
CD11b	+	+
CD11c	–	++
CD14	+	++
CD64	Low	+++
CD103	–	–
CD172a	+	+
F4/80	Low	+++
MHCII	–	+++
Ly6C	+++	–
CX3CR1	++	+++

Figure 14:Phenotypic cell surface marker expression of tissue-resident monocytes and macrophages

Figure highlighting the differential markers expressed in intestinal tissue-resident monocytes and macrophages, where expression of Ly6C is increasingly downregulated, while marker expression of F4/80, MHC2, CX3CR1, CD14 and CD11c is increased (Adapted from Bain et al., 2012).

1.4.2 Macrophage activation and the M1 and M2 paradigm

In 2000, Mills et al, have made the observation that macrophages respond differentially to stimuli from either Th1 or Th2 cells (Mills et al., 2000). Whereas Th1 cells stimulated a pro-inflammatory cytokine response in which production of IFN-γ, TNF-α is upregulated, the Th2 cells induce the upregulated secretion of IL-4 and Il-13 (Berger A., 2000). Mill's work demonstrated that mice with a Th1 cytokine profile were more likely to produce macrophages producing nitric oxide (NO) in comparison to Th2 strains, where arginine was metabolised to produce ornithine instead. These two differing macrophage subtypes have been coined as inflammatory M1 and homeostatic M2 macrophages (Mills et al., 2000). Furthermore, following its activation, both M1 and M2 macrophages were also shown to respond differentially to LPS stimulation, where M2 macrophages continually produce ornithine while M1 macrophages do not (**Figure 1.15**) (Mills et al., 1991).

The functions of both M1 and M2 macrophages have been shown to differ significantly (Orecchioni et al., 2019). Following activation via Th1 derived secretory factors (IFN-γ), M1 macrophages produce inflammatory cytokines such as TNF-α, IL-1β, IL-6 and nitric oxide in a bid to rapidly alleviate acute inflammation (**Figure 1.16**). (Martinez et al., 2006). IFN-γ the main cytokine associated with M1 activation as it is recognised as the major Th1 cytokine product (Mantovani et al., 2004). Expression of IFN-g then triggers the downstream activation of Jak1/2 which activate STAT1 leading to an increase of cell adhesion molecules and upregulation of cytokine receptor expression of IL6R, IL2RA among others in human (Martinez et al., 2006).

The Toll-like receptor 4 (TLR4) was shown to recognise LPS stimulation, leading to the activation of Myd88 and consequently upregulating production of TNF-α, IL-6 and IL-1β and MHC2. (Takeda and Akira., 2004). Notably by way of upregulated *Traf2* and *Tnfaip3I* expression, M1 activated macrophages and can also induce the release of inflammatory cytokines via the activation of transcription factor Nf-kb in response to LPS and IFN to regulate the innate immune response (Jin et al., 2015). In contrast M2 macrophages driven by Th2-derived secretory factors trough STAT6 activation (IL-13, IL-4), exhibit anti-inflammatory properties, thus producing IL-10 and TGF-β.

The cytokines, IL-4 and IL-13 are the main secretory products of Th2 cells, binding to IL-4 leads to the activation of the Jak1 and Jak3 further causing the activation of STAT6

(Martinez et al., 2013; Lian et al., 2012). Although IL-4 knockout mice did not show any macrophage depletion, tissue-resident macrophages were unable to respond and apprehend parasitic infections effectively (Van Dyken et al., 2013).

The C-type Mannose receptor (CD206) was shown to be upregulated in M2 macrophages and tissue resident macrophage where it's postulated to increase the phagocytic capacity *in vivo* (P.J Murray et al, 2014). The phagocytosis of apoptotic cells and cell debris can then enhance the anti-inflammatory functions of the M2 macrophages by inducing increased IL-10 production (Piraghai et al., 2018). Although M1 macrophages mediate the early inflammatory response, they can undergo phenotypical changes over time to assist wound healing, these macrophages closely resemble the M2 macrophage characteristics (Das et al., 2015).

Over the years, several studies have attempted to understand the functional roles both M1 and M2 macrophages play in an *in vivo* environment where they have revealed some of their differential effects in the steady state versus inflammation (Ginhoux & Jung., 2014; Mantovani et al., 2013).

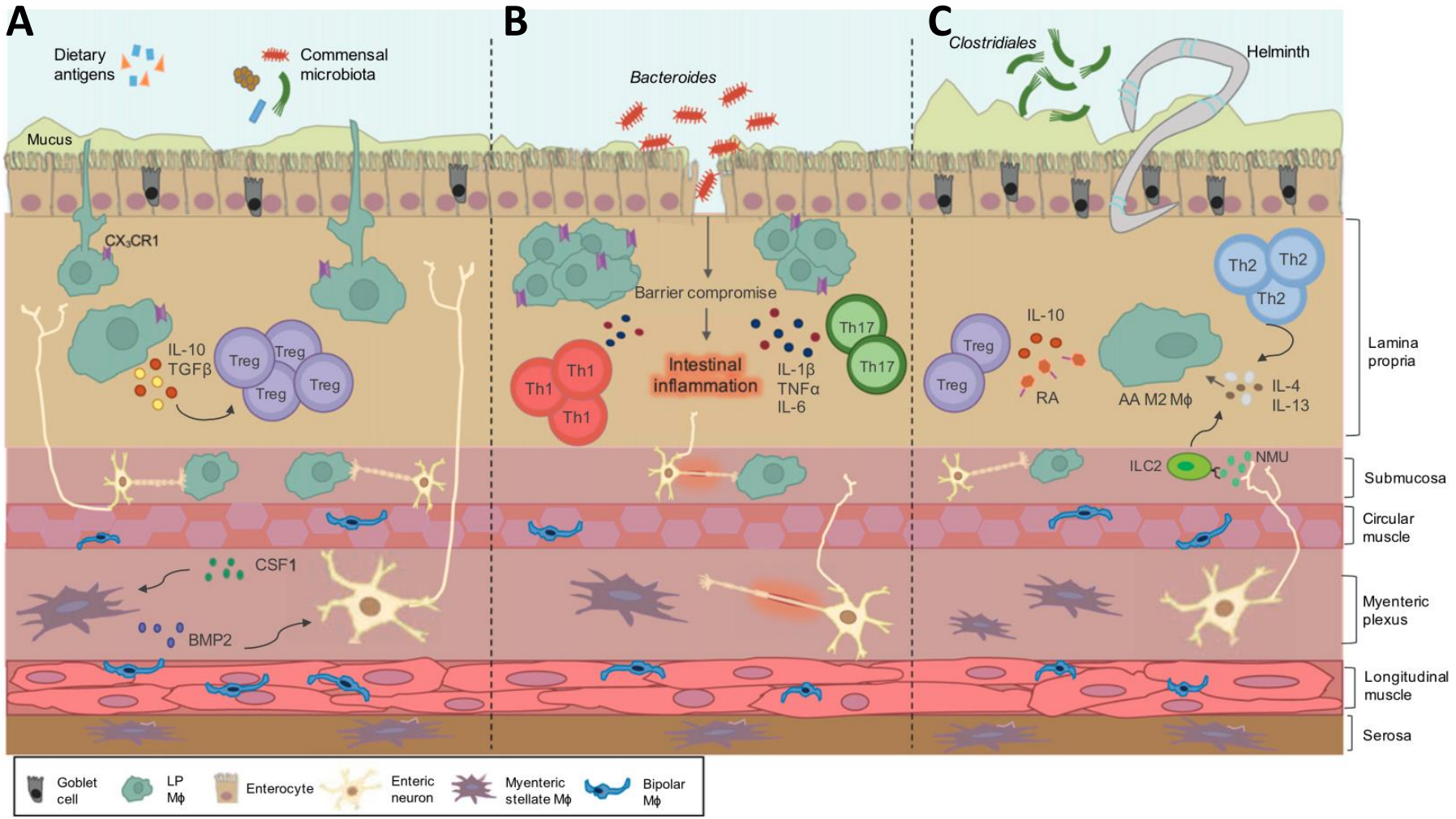
A
Dietary antigens
Commensal microbiota
Mucus
CX3CR1
IL-10
TGFβ
Treg
Treg
Treg
Treg
CSF1
BMP2
B
Bacteroides
Barrier compromise
Th1
Th1
Th1
Intestinal inflammation
IL-1β
TNFα
IL-6
Th17
Th17
C
Clostridiales
Helminth
Th2
Th2
Th2
IL-10
Treg
Treg
RA
AA M2 Mϕ
IL-4
IL-13
ILC2
NMU
Lamina propria
Submucosa
Circular muscle
Myenteric plexus
Longitudinal muscle
Serosa
Goblet cell
LP Mϕ
Enterocyte
Enteric neuron
Myenteric stellate Mϕ
Bipolar Mϕ

Figure 1.15:Immune-cell response in intestinal tissue homeostasis and inflammation

Diagram showing the presence of intestinal macrophages in in **A)** intestinal homeostasis **B)** bacteria-induced inflammation and **C)** parasite-induced inflammation, here CX3CR1+ macrophages are present during homeostasis, M1 macrophages are activated by the presence of Th1-mediated secretion of IFN-γ and the presence of Th-2 cells during parasitic infections results in the recruitment of M2 macrophages.

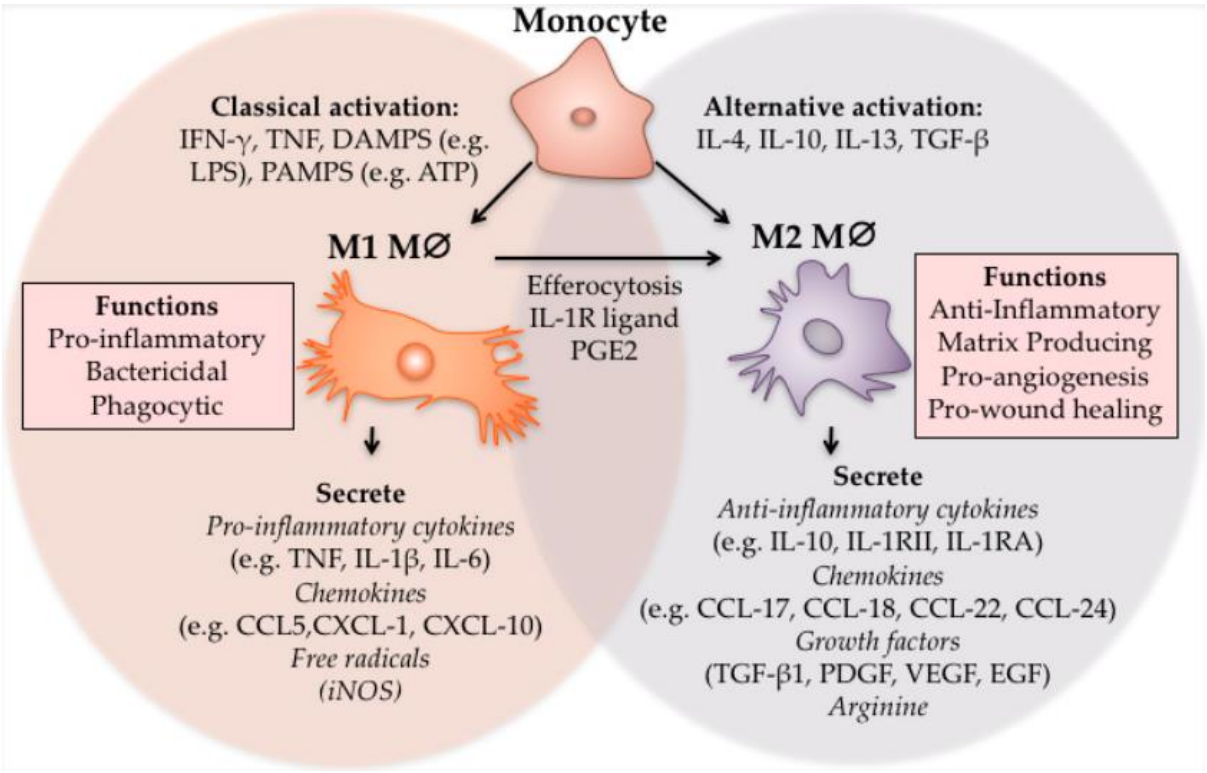

Figure 1.16: The 'pro-inflammatory' M1 and 'anti-inflammatory' M2 macrophage phenotype

Summary diagram highlighting the differences in secretory products and functions of both M1 and M2 macrophages (Adapted from Hesketh et al., 2017).

1.4.3 Macrophages in intestinal inflammation and disease

Intestinal homeostasis heavily relies on the presence of intestinal macrophages; thus its dysregulation can result in the loss of tolerance towards commensal bacteria, consequently causing inflammation in the underlying mucosa. The cause of chronic inflammation is commonly initiated by the failure to resolve acute inflammation within the tissue, likely due to a dysregulated mechanism within the innate and adaptative immune response. During inflammatory bowel diseases such as Crohn's disease and ulcerative colitis an aberrant influx of macrophages is found within the intestinal mucosa and increased lesion severity in patients is linked to an increasing macrophage presence (Cammarota et al., 2010).

As previously mentioned, macrophages can be easily influenced by the environmental cues within the lamina propria. Naturally, the injury induced dysregulation of the lamina propria also affects the function of residential and newly recruited macrophages. Initially, inflammation causes an influx of monocytes towards the site of injury. Similarly, to the steady state, the chemoattractant CCR2 plays an essential role in the recruitment of monocytes into the tissue and is also upregulated during inflammation. Failure to enter the lamina propria exacerbates the effects of colitis in CCR2 depleted mice *in vivo* (Platt et al., 2010). Whereas CX3CR1+ macrophages maintain their tolerance for microbial pathogens and continually produce anti-inflammatory cytokines such as IL-10, newly extravasated monocytes were shown induce the secretion of pro-inflammatory cytokines such as IL-1β and TNF-α as well as iNOS. Furthermore, the 'inflammatory' CX3CR1^{int} monocytes outnumber residential CX3CR1 macrophages by 10:1. Due to its bactericidal and inflammatory nature, these CCR2+, CX3CR1^{int} are also thought to drive inflammation. Microarray analysis of the CX3CR1^{int}Ly6C^{high} macrophages have shown that the PRR signalling pathways NOD1,2 and TLR2 were upregulated in response to LPS stimulation resulting in the production of the inflammatory cytokine IL-6 *in vivo* With time, such pro-inflammatory monocytes differentiate into MHC2^{high}, CD11c^{high} cells with the ability to induce a naïve T-cell response (Zigmond et al., 2012).

A number of studies have delineated some of the environmental cues that can affect the macrophage function and phenotype over the years. The anti-inflammatory cytokine plays an important role in regulating the intestinal immune response and are essential in

macrophage regulation. This was demonstrated by Zigmond et al in 2014, where the knockout of IL-10 in *in vivo* mice induced spontaneous colitis (Zigmond et al., 2014). Later work also showed that the absence of IL-10 led to decreased mitochondrial damage and dysregulation of PRR recognition, subsequently leading to the increased expression of the inflammatory cytokine IL-1β, which is also upregulated in IBD (Ip et al., 2017).

Similarly, TGF-β is another anti-inflammatory cytokine which is pre-dominantly produced by residential M2-like macrophages and is considered to be an immunosuppressant (Zizzo et al., 2012). Furthermore, Schridde et al work also suggests can regulate macrophage numbers by dampening the expression of monocytes via the inhibition of CCL8 in colonic macrophages and depletion of the TGF-β receptor reduces the production of both TNF and IL-10 (Schridde et al., 2017).

1.4.4 Macrophages role in tissue repair

The macrophage localised early on in inflammation are functionally distinct compared to those present during tissue resolution. Initial injury to the tissue is often resolved by the influx of granulocytes such as neutrophils and mononuclear phagocytes. The mechanism of granulocyte recruitment relies on the release of chemoattractant by platelets. Incoming neutrophils then produce reactive oxygen species and proteases. Crucially, following the end of its assignment, the neutrophils then apoptose and release 'find-me' and 'eat-me' signals which are recognised by the newly arrived macrophages. As an inflammatory setting generates a M1 macrophage phenotype, the efferocytosis of apoptotic neutrophils results in switch towards the M2-like phenotype which can then aid epithelial wound repair (Martinez and Gordon, 2014). However, in chronic inflammation, this process is impaired and M1 macrophages remain in their pro-inflammatory state, where consequently inflammatory cytokine expression such as TNF, IL-1β and iNOS remain further damaging the tissue (Hesketh et al., 2017).

A number of mediating factors have been recognised, which can influence the tissue repair *in vivo*. Whereas more M1 macrophages are present in the early inflammatory phase, M2 macrophages are predominantly present in the latter stages of wound repair (Daley et al., 2009).

In the colon, IL-1 expression was shown to play a role in mediating inflammation. Here the IL-1 precursor mainly expressed by intestinal epithelial cells expressed in the steady state and is translocated to the nucleus following inflammatory stimuli, the secretion of which then leads to the recruitment of neutrophils. Juxtaposing this, the myeloid-cell derived IL-1β expression was observed in the latter stages of wound repair, where it is able to promote vascularisation, IL-1β deficiency can lead to impaired repair, increased colon permeability and crypt proliferation in DSS induced mice *in vivo* (Bersudsky et al., 2013; McEntee et al., 2019). As Wilkinson et al have highlighted, iron may also play a regulatory role in the polarisation of M1 macrophages towards a homeostatic M2 macrophage state, which are able to aid the latter stages of wound healing. This was also confirmed in another study where, iron loading led to an increase in pro-inflammatory M1-like expression *in vitro.* (Wilkinson et al. 2019).

The metabolism of iron also differs in M1 macrophages compared to its M2 counterpart. M1 macrophage store iron intracellularly via ferritin, whereas M2 macrophage release iron extracellularly via ferroportin. This correlates with findings in chronically inflamed intestinal tissue where iron loaded M1 macrophages were present (Sindrilaru et al., 2011). Recently, the collagen triple helix repeat containing 1 protein (CTHRC1) was also shown to aid wound repair in the epidermis of mice. The presence of CTHRC1 resulted in an increase of M2 macrophages and was shown to involve the Notch pathway, where the inhibition of Notch led to the decreased M2 macrophage presence in epidermal cell lines *in vitro (*Qin et al., 2019; Xia et al., 2021).

Several studies have identified TGF-β as another factor required for progressive wound repair. This was shown previously where germ-free mice deficient in TGF-β1 a number of inflammatory colonic lesions were found (Shull et al., 1992). In skin wound experiments, where macrophages were depleted, a decreased in TGF-β and VEGF was also found (Lucas et al., 2010). TGF-β expression was also high in IBD patients, likely in order to counteract inflammation within the tissue (Ihara et al., 2017). Notably, in CX3CR1 knockout wound

healing was also impaired and resulted in a decrease in TGF-β, thus indicating macrophage derived TGF-β play a role in aiding tissue repair (Ishida et al. 2008).

In a tumorigenic environment, tumour associated macrophages produce large amounts of TGF-β in order to support tumour growth and metastasis. Zhang et al, later revealed that TGF-β is also essential for the polarisation of M2 macrophages via the transcription SNAIL while suppressing the M1 phenotype in vitro (Zhang et al., 2016).

1.4.5 Luminal sampling of macrophages

Seminal work in 2004, has shown that CX3CR1+ macrophages are able to sample luminal antigens by extending processes between epithelial cells (Chieppa et al., 2006; Rescigno et al., 2008). The presence of such mucosal-sampling macrophages is heavily CX3CR1 dependent as its removal can lead to decrease in mucosal macrophages (Medina-Contreras et al., 2011). Within the steady-state of the mucosa, macrophages can be exposed to a number of stimuli, which cause the release of cytokines such as TNF-α, IL-6 and IL-10 among others. (Duque et al., 2014). Intestinal macrophages also play a role in the differentiation of CD4+ T cells into FoxP3+ regulatory T-cells, where the number of intestinal macrophages were proportional to Treg numbers (Denning et al., 2007; Denning et al., 2011). Here, macrophage mediated IL-10 secretion is essential for the maintenance of FoxP3+ T-cell expression where IL-10 knockout in mice led to spontaneous inflammation (Murai et al., 2009). As mentioned previously, dendritic cells were able to process IgGA samples from the luminal side via goblet cells, in a similar fashion CX3CR1+ macrophages have also been shown to send out protrusion into the lumen in order to capture antigen samples (Chieppa et al., 2006), highlighting the important role of APC's within the intestinal tissue.

1.4.6 Intestinal epithelial pathogen recognition:

Like immune cells, intestinal epithelial cells are also able to sense microbial pattern via the help of TLRs and NLRs (Ronald and Beutler., 2010). Among those, TLR4 was shown to play a particularly essential role in mediating an epithelial-derived immune response.

Bacterial components such as LPS and flagellin can bind to TLR4, which then induces the expression of CXCL1, a chemoattracts subsequently recruiting antigen-presenting macrophages and dendritic cells towards the crypt base (Brandl et al., 2010). Furthermore, TLR4 was also shwown to induce proliferation within human intestinal cells via EGF ligand (Hsu et al., 2010, Brand et al., 2010).

The nucleotide-binding oligomerisation domain-like receptor (NLR) is another PAMP which activates downstream signalling of NF-kB via NOD1 and NOD2 and activates an inflammatory signalling pathway (Alam et al., 2013). The importance of NOD1 and NOD2 in regulating the intestinal immune response was evident in depletion experiments where an increased susceptibility to TNBS-induced colitis was found due to the increasing build-up of bacterial burden *in vivo* (Sidiq et al., 2016). Furthermore, nod-like receptors (NLRs) also participate in the clearance of parasites via the secretion of IL-25 which promotes the adaptive immune response by activating Th2 cells (Burgueno and Abreu., 2020).

The role MyD88 plays in regulating an innate immune response was widely studied. Interestingly, Skoczek et al's work with MyD88 deficient mice showed that unlike wild-type mice, exposure to LPS showed no increases in epithelial proliferation. Similarly, other studies have highlighted the importance of Myd88 in which its deficiency impaired epithelial repair (Pull et al., 2005; Rakoff-Nahdum et al., 2004).

While the innate immune system is considered the first responder to acute inflammatory infection and damage, the intestine also relies on a secondary immune response, the adaptive immune system, to ensure that repetitive threats from a reoccurring pathogen are rapidly and efficiently eliminated (Spencer and Solid., 2016).

1.5 Adaptive immunity:

The intestinal innate immune system works in close association with the adaptive immune system which mounts a rapid and more pathogen-specific secondary immune response upon recognition of previously encountered pathogens. Here, the two major players of the adaptive immune system are T-cell and B-cell lymphocyte cell lineages (Choy et al., 2017).

The adaptive immune system is initiated by nearby antigen-presenting cells (APC), including macrophages and dendritic cells, which present the previously engulfed and processed foreign antigen towards the T cells. In some instances, CX3CR1+ macrophages are also able to transfer to dendritic cells which due to their ability to translocate to the interfollicular zone can prime T-cells (Mazzini et al., 2014).

T-helper cells play an essential role in activating other cells within the immune system and thereby indirectly regulate B-cell specific antibody secretion. Early work from Boom and colleagues in 1988, have identified the presence of distinct CD4+ T-cell lineages, where a Th1 cell response was induced by the presence of pathogenic bacteria and Th2 cells were present during parasitic infections (Boom et al., 1988). Later studies then also confirmed the presence of IL-17-producing Th17 cells. (Ivanov et al., 2008). Both, Th1 and Th2, subsets could also be differentiated via their secretory products, were Th1 cells produced IFN-γ and IL-2 whereas Th2 cells largely produced anti-inflammatory cytokines such as IL-4 and IL-13 and IL-10 (Szabo et al., 2000; Bonechhi et al., 1998). Dysregulation in the T-cell response can lead to chronic inflammatory bowel disease. Early work from Neurath et al, suggested that IFN-γ deficient mice, alleviated the symptoms of CD in vivo, possibly highlighting the role Th1-cells play in disease progression (Neurath et al., 2002). However, this is in stark contrast to UC patients, where Th2 cells were present and IFN-γ expression was not elevated (Romagnani S.,1999). In the presence of such activated T cells, naive B-cells differentiate into IgGA+ B-cells, where the production of IgGA aids as a protective barrier between the commensal bacteria and the epithelium (Cerutti A., 2008 Gutzeit et al., 2014).

During intestinal homeostasis, regulatory T cells are commonly presented in the lamina propria, where they can suppress inflammation and maintain tolerance against commensal bacteria via the production of IL-10 and TGF-β (Cosovanu and Neuman., 2020). In the steady state, CD11b+ macrophages ensure FoxP3+ T-reg cells are persisent in the mucosa via the secretion of IL-10 (Murai et al., 2009). This in turn prompts FoxP3+ T-reg cells to inhibit the

production of pro-inflammatory cytokines (Tiemessen et al., 2007; Okeke and Uzonna., 2019). Additionally. FoxP3+ Treg cells also contribute to bacterial clearance where its secretion of IL-13, triggers an increase in phagocytic activity in macrophages (Proto et al., 2018).

Overall, in *vivo* studies highlighted in the previous sections have shown that intestinal macrophages can significantly affect intestinal tissue repair and the resolution of inflammation during homeostasis and inflammation, however it is currently not known whether differential macrophage phenotypes such as the M1 or M2 macrophage population contribute towards the pathogenesis of inflammatory bowel disease (Lissner et al., 2015).

1.6 Inflammatory bowel disease and Intestinal Inflammation

Chronic inflammation is defined as the inability for a tissue to resolve acute inflammation. Inflammatory bowel disease (IBD) is the chronic inflammatory disorder of the gastrointestinal tract, where Crohn's disease (CD) and ulcerative colitis (UC) are the two most prevalent form of the disease (Zhang and Li., 2014).

In the UK, over 250,000 people are diagnosed with IBD each year, while over 1.5 million incidences have been reported in North America alone and although prevalence is generally high in western countries, its occurrence has also significantly increased in Asia and Africa, possibly due to an increase in urbanisation (Pasvol et al., 2020; Ahuja et al., 2010). The prevalence of UC is higher in the general population, regardless of geography, whereas CD is more common in children (Kugathasan and Cohen et al., 2008).

Although Crohn's disease shares some pathogenic features with ulcerative colitis some distinct differences exist. Whereas inflammation in CD can affect any region of the bowel including the colon, UC is restricted to the colorectum, where it most commonly affects the rectal mucosa and spreads towards the proximal regions of the colon. Crucially, UC only affect the innermost layers of the colon, while CD can affect all regions of the bowel (Dignass et al., 2012; Mehdizadeh et al., 2008).

Currently, only smoking cigarettes and appendectomies are clearly linked to an increased susceptibility to IBD. However, over time, a combination of factors have shown to increase the patients susceptibility to UC and CD including alterations in the patients microbiome, genetic factors, alteration in epithelial barrier function and immune response (Ramos and

Papadkis., 2020). For example, 5-10% of all IBD patients have affected family members, while genetic linkage and association studies have identified several mutations and risk loci which can contribute to disease progression (Binder et al., 1998; Liu et al., 2015). In total, 53 gene loci have been identified, in which 23 and 30 loci are specific to UC and CD, respectively. Early research has found that the mutations in the *NOD2* gene are crucial for the regulation of the T-cell response. *NOD2* is an intracellular sensor of MDPs and defects in *NOD2* expression can severely affect microbial sensing and defective processing of bacteria (Nabhani et al., 2017). Triggering *NOD2* results in the activation of the downstream target NF-κB, thereby inducing the secretion of TNF-α and IL-1β, which directly contribute to epithelial injury. The gene loci's *NOD2* and *PTPN2* are both strongly linked with Crohn's disease, however the opposite was true for UC, where both genes exhibit a protective function (Sabbah et al., 2009; Franke et al., 2010). Furthermore, IBD was also associated with *IL23R, JAK2* and *STAT3* gene, where genetic mutations could directly affect the recruitment of pro-inflammatory Th17 cells (Anderson et al.,2011; Brand et al., 2009). Interestingly, such susceptibility loci have also been shown to be linked with the regulation of macrophage differentiation (Baille et al., 2017). Other risk loci such as *ECM1, HNF4A, CDH1* and *LAMB1* have also been associated with an impaired epithelial barrier function, which is often compromised in IBD (Jostins et al., 2012; Beaudoin et al., 2013*).*

As the intestine is colonised by a microbiome which co-exist in a symbiotic relationship, changes in the microbiome diversity can also contribute to IBD pathogenesis (Khosravi et al., 2014). Significantly, in the small intestine, the diversity of *Bacteriodetes* and *Firmicutes* phyla was reduced where such abnormalities could reportedly be mended by the administration of biological agents, (Vanderploeg et al., 2010; Swidsinski et al., 2002).

In homeostasis, the mucous layer is around 700µm thick, largely composed of Muc-2, on the surface of the epithelium and can undergo hydration, mix with IgG and other antimicrobial peptides to reduces the likelihood of microbe-epithelial contact (Johansson et al., 2014; Johansson and Hanson., 2013).However in chronic inflammatory diseases, the inner mucosal layers are often defective in patients with IBD, partly caused by the reduced presence of goblet cells within the epithelia, which in turn further irritates the colonic tissue (Gersemann et al., 2009).

In the steady state, following acute injury commonly initiated by a breach in the epithelium, neutrophils are recruited to the site of inflammation and are later removed by incoming macrophages via phagocytosis in a hyporesponsive manner, however under chronic conditions, neutrophils survival is upregulated and exacerbate inflammation through the release of various pro-inflammatory cytokines, causing further tissue damage as phagocytosis by macrophages of the neutrophil population is prevented (Park et al., 2016).

In the inflamed colon of patients with IBD, CD14+ monocyte migration to the lamina propria is increased, consequently lading to the differentiation and accumulation of CD11c+ pro-inflammatory macrophages (Kamada et al., 2008; Ogino et al., 2013). Furthermore, macrophages in IBD patients also displayed the ability to induce an abnormally high expansion of inflammatory Th17 cells, where their production of pro-inflammatory cytokines such as IL-17, TNF-α among others, escalate inflammation, indirectly causing further tissue damage (Ogino et al., 2013; Tesmer et al., 2008). When CD68+ (a phagocytic marker) macrophage numbers in IBD patients were analysed, it was found that large segments within the inflamed tissue contained lower or no CD68+ macrophages, the lack of macrophage presence within the inflamed tissue thereby highlighting the importance this cell population plays in the resolution of inflammation (Rubio and Schmidt., 2018).

Interestingly, Chapuy et al., showed that the frequency of immature inflammatory macrophages present in the colonic mucosa of IBD patients is significantly higher compared to the steady state while GM-CSF, a crucial factor required for the differentiation and maturation of macrophages is also unregulated during IBD (Lacey et al., 2012). A few studies have established that macrophage numbers are increased in the lamina propria in IBD patients, where an upregulation in human cell surface markers CD40, CD14 and TREM1 was recognised (Steinbach and Plevy., 2014). Furthermore, secretory cytokine production of IL-12, IL-6, IL-8 and TNF-α were also observed when compared to healthy tissue, highlighting the inflammatory role macrophages play in IBD pathogenesis (Dinarello et al., 2009; Hart et al., 2005; Baumgart et al., 2009).

In vivo studies have also shown the differential effects cytokines can play in UC and CD. For example, UC lesions produced increased amount of IL-5 and normal amounts of IFN-γ, while normal amounts of IFN-γ were produced in CD (Fuss et al., 1996). Interestingly, the Th2 cell

response was not increased in CD, however, an increase in both Th2 and Th17 was noted in UC. Furthermore, increased levels of IL-13 were also noted in UC models (Heller et al.,2002).

For patients with mild or ulcerative colitis, 5-aminosalicyclic acid is commonly utilised treatment method (Lim et al., 2016). If the patient is unresponsive to oral or rectal 5-aminosalicyclic acid treatment, corticosteroids such as hydrocortisone and budesonide (Scholmerich et al., 2004). Patients with severe ulcerative colitis can be treated with anti-TNFα (tumor necrosis factor α) monoclonal antibody treatment (Rutgeerts et al., 2005; Seyedian et al., 2018). Following 5 weeks of Anti-TNF therapy in IBD patients, Dige and colleagues noted a significant reduction in immature "inflammatory' macrophage numbers in IBD patients, while work from Vos et al, confirmed that mature "homeostatic" macrophage numbers increased after 4 weeks of anti-TNF therapy (Dige et al., 2016; Vos et al., 2012).Although, anti-TNF therapies have improved patient outcomes over the last decade, a significant number of patients are non-responsive or intolerant to the drugs described above and the need for more effective therapeutic targets remains (Chudy-Onwugaje et al., 2018).

To understand how the molecular mechanisms and signalling pathways may differ in inflammatory bowel disease compared to homeostasis, researchers have utilised *in vitro* experimental models for almost a decade, where the models are constantly evolving to mimic the in vivo setting more closely (Lyapun et al., 2019).

1.7 Intestinal organoid culture models

The current multi-hit IBD model suggests that several causative factors highlighted above can accrue to contribute towards the disease progression of IBD patients and as a number of variables are present within an *in vivo* model, it becomes difficult to study the molecular signalling interactions between individual cell populations within the colonic tissue. For this reason, *in vitro* models have and are currently being utilised to further understand crosstalk between lamina propria-resident cells and the intestinal epithelium (Ihara et al., 2018; Brazil et al., 2019).

Since more than two decades, 2D cell culture has been utilised to understand a cells basic physiological function in health and disease, where immortal cell lines are commonly grown as a monolayer onto a culture dish/flask (Kapalczynska et al., 2016). As it inexpensive and requires relatively low maintenance it allows for easily accessible gene manipulation, a technique which remains relevant to this day (Almeqdadi et al., 2019). For example, work from Al-Ghadban and colleagues were able to study interactions between macrophages and the intestinal epithelium within a 2D co-culture model however such culture models often only vaguely mimic the in vivo environment (Jensen and Teng., 2020; Al-Ghadban et al., 2015). However, there are some limitations to such culture systems, as the cell morphology and metabolism, of cell's cultured onto a 2D monolayer do not accurately mimic the function observed *in vitro* (Duval et al., 2017). To counter this, over the last decade, the development and utilisation of 3D culture models has increased exponentially and have allowed researchers to better understand a cell's morphology, cell migration, drug delivery and epithelial-immune cell crosstalk in vitro (Jensen and Teng., 2020). In particular, to study interactions in complex tissues such as the colonic mucosa, new models are being developed in order to study intestinal epithelial renewal while more closely resembling the mucosal environment (Sachs et al., 2017).

In 2009, seminal work from Sato and colleagues were able to utilise Lg5+ stem cells to culture self-renewing human small intestinal and colonic organoids (Sato et al., 2009; Sato et al., 2011). Previous attempts to culture organoids to study Lgr5+ stem cells using a 2D monolayer were unsuccessful, thus scaffolding-based organoid models were developed (Sugimoto and Sato et al., 2017).

Scaffolds are synthetic 3D structures commonly composed of several materials which offer cells in culture the structural support which resemble the in vivo microenvironment. Both synthetic and biological scaffolding have been utilised in 3D culture (Duval et al., 2017). Here the structural integrity of a synthetic manufactured, polymer-based hydrogels can be optimised and tailored to suit a specific experimental model, while biological scaffolds such as Matrigel provide a physiologically more accurate environment for the culture of intestinal organoids due to the presence of hormones and other molecules required for cell-ECM interaction (Fang and Eglen., 2017). **Table 1,** highlights the differences between 2D and 3D cell cultures. New emerging and advances in organoid culture are further discussed later in this study in **Chapter 7**.

In 2014, Skoczek and colleagues have established an isolation method, in which intact, fully functioning and heterogenous colonic crypt populations were liberated from the colonic tissue and co-cultured with inflammatory monocytes to extensively study epithelial-immune cell crosstalk in vitro (Skoczek et al., 2014). This model was adapted for this study to include to study the renewal of colonic crypts when cultured with macrophages in an 3D *in vitro* organoid culture model.

Type of culture	2D	3D
Time of culture formation	Within minutes to a few hours	From a few hours to a few days
Culture quality	High performance, reproducibility, long-term culture, easy to interpret, simplicity of culture	Worse performance and reproducibility, difficult to interpret, cultures more difficult to carry out
In vivo imitation	Do not mimic the natural structure of the tissue or tumour mass	*In vivo* tissues and organs are in 3D form
Cells interactions	Deprived of cell-cell and cell-extracellular environment interactions, no *in vivo*-like microenvironment and no "niches"	Proper interactions of cell-cell and cell-extracellular environment, environmental "niches" are created
Characteristics of cells	Changed morphology and way of divisions; loss of diverse phenotype and polarity	Preserved morphology and way of divisions, diverse phenotype and polarity
Access to essential compounds	Unlimited access to oxygen, nutrients, metabolites and signalling molecules (in contrast to *in vivo*)	Variable access to oxygen, nutrients, metabolites and signalling molecules (same as *in vivo*)
Molecular mechanisms	Changes in gene expression, mRNA splicing, topology and biochemistry of cells	Expression of genes, splicing, topology and biochemistry of cells as *in vivo*
Cost of maintaining a culture	Cheap, commercially available tests and the media	More expensive, more time-consuming, fewer commercially available tests

Figure 1.17: 2D vs 3D in vitro cell culture model

Summary diagram highlighting the distinct differences of 2D and 3D *in vitro* cell culture (Adapted from Kapalczynska et al., 2016).

1.8 Rationale

Previously, Skoczek et al. has shown that immune cells of monocyte-macrophage lineage work in concert with gut epithelial stem cells to maintain gut homeostasis. Furthermore, unpublished work from the Sobolewski lab has demonstrated that inflammatory monocytes are able to cause a significant increase in crypt cell proliferation and increase in the number of stem cells, when compared to the homeostatic setting. The molecular and cellular mechanisms by which the epithelial stem cell niche is modulated by monocyte-macrophage cells during inflammation is largely unknown.

Monocytes and macrophages arise from a common precursor in the bone marrow and are recruited to the lamina propria where they undergo a four-step differentiation process to become tissue resident homeostatic macrophages; a process called the Monocyte Waterfall Pathway. During inflammation, this differentiation pathway cannot be completed, and the phenotype of monocytes becomes halted at an early 'inflammatory' stage.

Hallmarks of inflammatory bowel disease (IBD) include increase in the number of these monocyte-macrophage lineage cells in the gut mucosa; compromised epithelial barrier function, which results in direct contact of microbes with mucosal immune cells and the basal surface of the crypt epithelial stem cell niche; and an increase in crypt cell proliferation. Notably, patients with IBD have an increased risk of colon cancer, which is likely due to an altered inflammatory microenvironment that increases epithelial proliferation and the risk of acquiring mutations. Taken together previous findings suggest that the epithelial stem cell response to inflammation could be critical to whether, remission/resolution or chronic inflammation (or tumour progression) ensues.

A reductionist in vitro co-culture system was developed to help determine how macrophages affect the crypt epithelial renewal during inflammation, particularly the proliferation and differentiation of cells contained within the epithelium such a stem, goblet, tuft, enteroendocrine cells and enterocytes.

1.9 Hypothesis

Naïve, inflammatory (M1) and homeostatic (M2) macrophages differentially regulate colonic crypt renewal *in vitro*

1.10 Aims

1. To develop and characterise an *in vitro* macrophage-crypt co-culture model to compare pro and anti-inflammatory macrophages on crypt cell growth and differentiation
2. To determine whether Naïve, M1 or M2 macrophages regulate colonic crypt cell proliferation
3. To determine whether Naïve, M1 or M2 macrophages regulate colonic crypt cell differentiation
4. Characterise the physical interactions between the colonic crypt epithelium and Naïve, M1 and M2 macrophage *in vitro* co-culture

Chapter 2: Materials and Methods

2.1 Laboratory Consumables

2.1.1 Chemicals and reagents

Chemical and reagent	Source
100% Methanol	Fisher-Scientific
Advanced DMEM/F12	Thermo-Fisher, Gibco
Ammonium Chloride (NH_4Cl_2)	Fisher-scientific
B27- supplement	Thermo-Fisher, Gibco
Bovine Serum Albumin	Sigma-Aldrich
Cytocentrifuge filter paper	Thermo Shandon
D-glucose	Fisher-Scientific
DAPT, γ-secretase inhibtor	TOCRIS
Dimethyl sulfoxide (DMSO)	Sigma-Aldrich
Disodium phosphate (Na2HPO4)	Fisher-Scientific
Donkey Serum	Sigma-Aldrich
DTT 1,4-Dithriothreitol	Formedium
EDTA	Fisher-Scientific
EdU Click-iT Reaction kit	Thermo-Fisher
Ethanol	Honeywell, VWR
Gluta-Max	Thermo-Fisher, Gibco
Growth-Factor Reduced Matrigel	VWR
Heat-Inactivated Fetal Bovine Serum	Thermo-Fisher, Gibco

HEPES	Thermo-Fisher, Gibco
HEPES	Fisher-Scientific
Hoechst-33342	Thermo-Fisher
Human Wnt3a	RnD Systems, Bio-Techne
Interferon-γ (IFN-γ)	Sigma-Aldrich
Interleukin-13 (IL-13)	Sigma-Aldrich
Interleukin-4 (IL-4)	Sigma-Aldrich
Lipopolysacharide (LPS)	RnD systems
Murine EGF	Peprotech
Murine Noggin	Peprotech
Murine R-Spondin	RnD Systems, Bio-Techne
Murine RM-CSF	Peprotech
Murine Wnt3a	Peprotech
N-acetyl-L-cysteine	Sigma-Aldrich
N2-supplement	Thermo-Fisher, Gibco
Non-essential amino acid	Thermo-Fisher, Gibco
PAP Pen	Abcam
Paraformaldehyde (PFA)	Sigma-Aldrich
Penicillin-Streptomycin	Gibco
Phosphate buffered saline	Sigma-Aldrich
Phosphate buffered saline (-$CaCl_2$,-$MgCl_2$)	Gibco
Potassium Chloride (KCl)	Fisher-Scientific
Propidium Iodide	Sigma-Aldrich
Reastain Quick-Diff Kit	Reagena

Rhodamine-conjugated *Ulex europaeus Agglutin I* (UEA-1)	Vectorlabs
RPMI 1640	Thermo-Fisher, Gibco
Sodium bi-carbonate ($NaHCo_30$)	Fisher-Scientific
Sodium chloride (NaCl)	Fisher-Scientific
Sodium Dodecyl Sulfate (SDS)	Melford
Triton-X	Roche
Vectashield Anti-fading mount	Vectorlab

Table 1: Chemicals and reagents

2.1.2 Primary and secondary antibodies

Antibody	Species Origin	Clonality	Dilution	Source/Cat. Number
B-catenin	Rabbit	Monoclonal	1:100	Abcam/Ab242226
CCR2	Rabbit	Monoclonal	1:100	Abcam/ab203128
CD11b	Rabbit	Monoclonal	1:100	Abcam/ab52478
CD11c	Armenian Hamster	Polyclonal	0.5mg/ml	Abcam/Ab33483
CD206	Mouse	Monoclonal	0.3 mg/ml	Abcam/ab8918
CD64	Rabbit	Monoclonal	1:100	SinoBiological/50086-R0272
CD68	Rat	Monoclonal	1:100	Abcam/ab53444
CD69	Armenian hamster		1:100	Biolegend/104502
Cleaved caspase 3	Rabbit	Monoclonal	Assay dependent	Cell signalling/(5A1E)
CX3CR1	Rabbit	Polyclonal	1:100	Abcam/ab8021
CX3CR1	Ultra-lead purified		1:100	Biolegend/149011

Cyclin-D1	Rabbit	Monoclonal	1:100	Abcam/Ab242226
DCAMKL1	Rabbit	Polyclonal	1:50	Abcam/Ab37994
E-cadherin	Rabbit	Monoclonal	1:200	Cell signalling/(24e10)
F4/80	Rabbit	Polyclonal	1:100	Abcam/ab100790
F4/80	Rat	Monoclonal	1:100	Bio-rad/MCA497GA
GSK3-β	Rabbit	Monoclonal	1:100	Abcam/Ab242226
h/m E-cadherin	Goat	Polyclonal	1:50	RND Systems/AF648
IgG Isotype Control	Rabbit	Monoclonal	1:100	Abcam/ab172730
IgG2b Isotype Control	Rat	Monoclonal	1:100	Bio-rad/MCA6006GA
LEF-1	Rabbit	Monoclonal	1:100	Abcam/Ab242226
Lgr5	Mouse	Monoclonal	1:100	Oregene/TA503316
MHCII	Rat	Monoclonal	1:100	Abcam/ab25333
Occludin	Mouse	Monoclonal	1:100	Santa-Cruz/SC-271842
ZO-1	Rat	Monoclonal	1:100	Santa-Cruz/Sc-33725

Table 2: Primary antibodies

Conjugate	Reactivity	Species Origin	Dilution	Source/Cat. Number
Alexa Fluor 488	Anti-mouse	Donkey	1:200	Invitrogen/A-21202
Alexa Fluor 488	Anti-rat	Donkey	1:200	Invitrogen/A-21208
Alexa Fluor 488	Anti-rabbit	Donkey	1:200	Invitrogen/A-21206
Alexa Fluor 568	Anti-mouse	Goat	1:200	Invitrogen/A-11004
Alexa Fluor 568	Anti-rabbit	Donkey	1:200	Invitrogen/A-10042
Alexa Fluor 568	Anti-rat	Goat	1:200	Invitrogen/A-11077
Alexa Fluor 647	Anti-rabbit	Donkey	1:200	Invitrogen/A-3157
Alexa Fluor 647	Anti-rat	Goat	1:200	Invitrogen/A-21247
Alexa Fluor 647	Anti-mouse	Donkey	1:200	Invitrogen/A-31571

Table 3: Secondary antibodies

2.1.3 Preparation of 4% formaldehyde

As a fixative, a 4% formaldehyde solution was prepared. Paraformaldehyde (0.04g/ml) (Sigma), was added to a beaker containing PBS. Using a hotplate/stirrer (Stuart U152), the solution was heated between 60-70^{o}C until the powder was dissolved. The solution was then left to cool, and the pH was adjusted to 7.4 using 0.1M sodium hydroxide and 0.1M hydrochloric acid. PFA was stored in the fridge and used within 24 hours of making or stored in the freezer at -20'C for long-term storage (up to 1 month).

2.1.4 Preparation of SDS (Sodium dodecyl sulfate)

To prepare a 1% working solution, SDS (Melford) was added to a beaker of PBS (pH 7.4) and stirred for at least 24 hours prior until the powder is fully dissolved. The working solution is stable for one month at room temperature.

2.1.5 Preparation of Ammonium Chloride (NH_4Cl_2)

To prepare a 100mM working solution of Ammonium Chloride (Fisher-Scientific) was added to a beaker of PBS (pH 7.4) and stirred until the powder is fully dissolved. The working solution is stable for one month at room temperature.

2.2 *In Vitro* Experiments

All animal experiments were conducted in accordance with the Home Office Animals (Scientific procedures) Act of 1986, with approval of the University of East Anglia Ethical Review Committee, Norwich, U.K. Female C57BL/6 (UEA-Disease Modelling Unit) aged between 8-12 weeks, were euthanized by CO_2 asphyxiation and subsequent cervical dislocation in accordance with Schedule 1 of the Act.

2.2.1 Isolation and culture of bone marrow-derived macrophages

Following the isolation of the femur/tibia and the removal of residual connective tissue, the bone's epiphyses were severed, and the bone marrow was flushed in a sterile environment using a 28-gauge syringe and cold RPMI 1640 (+10% FBS, +1% Pen/Strep). The flushed bone marrow contents were then then filtered through a 70µm nylon cell strainer (Falcon) and collected in a 50ml Centrifuge tube (Falcon). Following centrifugation at 600g for 10 minutes the cell suspension was re-suspended in warm RPMI1640. A bone-marrow yield was established (**Figure 2.1),** and the cells were appropriately seeded onto 6-well ultra-low attachment plates (Corning) at a cell density of 1 x 10^6 cells/ml. To drive BMDM differentiation towards macrophages, supplementary murine RM-CSF (Peprotech) at a concentration of 0.2µg/ml was added on day 0 and 3. The schematic in **Figure 2.3** summarises the protocol described above.

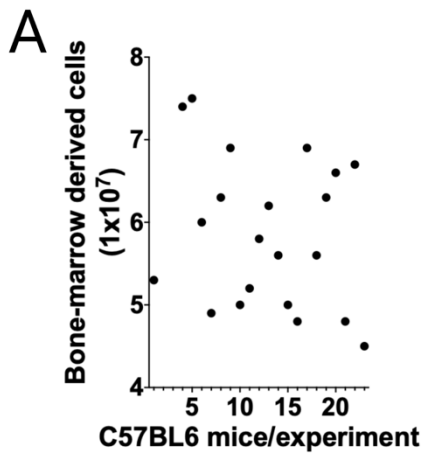

Figure 2.1: Bone-marrow derived cell isolation and culture

A) Scatter plot showing the bone-marrow cell yield, averaging 5.9x10^7 ± 0.2 (Mean ± SEM) from each subject (C57BL6) (n=20).

2.2.2 Polarisation of macrophage population

Macrophages were polarized based on methods previously described by Wei Ying et al in 2013 (Ying et al., 2013). BMDM cells were cultured in RPMI 1640 media up to day 7. On day 7, the floating cell population was removed, and the media was replaced by new fresh media. For M1 activation, supplementary LPS (100ng/ml) and IFN- γ (50ng/ml) were added to the media solution. To reach M2 activation, IL-4 (10ng/ml) and IL-13 (10ng/ml) were added instead.

2.2.3 Liberation of adherent macrophage population *in vitro*

To isolate the monocyte population on day 4, the floating cell population was collected, centrifuged at 600g for 10 minutes and re-suspended in fresh RPMI-1640 media (Gibco). To segregate the macrophage population on day 7, the supernatant of each well was removed, the wells washed in PBS (pH 7.4, Gibco) and Versene (Gibco) (1ml) was added to each well and incubated for 37^{o}C for 10 minutes until the macrophages fully detached themselves from the well bottom. The cell suspension was then centrifuged at 600g for 10 minutes and re-suspended in fresh media accordingly.

2.2.4 Cytospinning of bone marrow isolates

Cells were isolated and re-suspended at 1x10^{6} cells/ml as previously described. To ensure an equal distribution of cells onto the slide, a filter card (Thermo-Fisher) was placed between the microscope slide (VWR) and the cyto-funnel allowing the absorption of excess media. Following the cytospin (Thermo Shandon), the cell suspension (120µl) was transferred to the cytofunnel and centrifuged at 450g for 5 minutes.

2.2.5 Histological staining of BMDC

To histologically stain and record phenotypical changes, bone marrow-derived cells were isolated during different time points of their development. Initially, an appropriate cell number (1 x 10^{5} cells/ml) was collected, and the cells were cyto-centrifuged at 450g for 5 minutes using the Cytospin (Thermo-Shandon). The microscope slides (VWR) were air-dried overnight and fixed in the RESTAIN QUICK-DIFF solution for 3 minutes to allow permeabilisation. The cytoplasm and the nucleus were stained using Reastain Quick Diff Red

and Reastain Quick Diff Blue for 4 minutes, respectively. The slides were then rinsed in water, air-dried overnight and mounted with DPX (Sigma) using size 0, 16mm coverslips (VWR) the following day. The histological stains were then captured on a bright-field microscope.

2.2.6 Immunofluorescent labelling of BMDCs

For immunolabelling of a monocyte and macrophage population, the BMDM were cultured for 5 & 7 days, respectively. In brief, the bone marrow isolates were then cytocentrifuged at 450g for 5 minutes. The slides were fixed with in 4% PFA. Following fixation, the slides were washed with PBS and 0.1% Triton-X (Roche Diagnostics) was added for 20 minutes. The cells were later washed in ice-cold PBS and primary antibody (Table 1.2) was added and left to incubate overnight at 4^{o}C. The following day, cells were washed in PBS and a secondary antibody (Table 1.3) was added. Following a 2-hour incubation at 4^{o}C, the slides were finally mounted with Vectashield/Hoechst (Vector Labs) before being imaged on an epifluorescence or confocal microscope.

2.2.7 Flow cytometry

For the characterisation of the *in vitro* macrophage population, a flow cytometer (Beckmann Coulter Cytoflex) was utilised. Its versatility allows its user to measure various morphometric properties of individual cells, as well as identify fluorescently tagged cells within a cell population.

To analyse the individual properties of a cell, the fluidics system initially injects sheath fluid (usually a form of PBS) into the flow chamber. A second stream introduces the suspended cells into the flow chamber via a pressurised airline. As the pressure of the sample stream is greater than that of the sheath fluid, the cells align themselves into a single line while passing through a laser beam positioned adjacent to the stream. (**Figure 2.2A**)

As the laser strikes each single cell with varying excitation wavelengths, the fluorescence light emitted by the cells can then be measured by the photodetector and are translated onto a computer (**Figure 2.2C**). Following the laser strike, some of the light is often deflected off the cell, such scattered light can be defined into two categories, forward scatter (FSC)

and side-scatter (SSC) where each can provide the user with further information regarding the cell's phenotypic properties. The forward scatter is proportional to the cell size and shape, whereas the side-scatter is proportional to cell granularity (**Figure 2.2B**).

In this study, the instrument was used in order to characterise the phenotype of *in vitro* bone marrow-derived cells (BMDC) via an indirect immunolabelling protocol.

The following protocol was implemented to fluorescently label bone marrow-derived cells using a primary and a conjugated secondary antibody:

On Day 4-9, BMDC's were collected from each ultra-low attachment well. To liberate the adherent population, 1ml of Versene (Gibco) was added. The collected cell suspension was then centrifuged at 600g for 10 minutes and re-suspended in PBS/FBS (10%) at a cell density of $1x10^6$ cells/ml. 100µl of the cell suspension was then transferred to a 12-75 mm polypropylene tube (BD Falcon) and primary antibodies (diluted in 3% BSA) listed in **Table 1.2** were added. Following a 30-minute incubation on ice, the cells were washed with 3% BSA and centrifuged at 400g for 5 minutes and Alexa-fluor conjugated secondary antibodies (diluted in 1% BSA) listed in **Table 1.3** were added to each tube. After another incubation time of 30 minutes on ice, a washing step and final centrifugation, the samples were then analysed using a flow cytometer (Beckman Coulter Cytoflex). A minimum of 30,000 events were recorded for each condition, where more than 2,000,000 events were recorded to measure the FSC and SSC of both BMDM-M1 and BMDM-M2 phenotypes. Additionally, to measure cell viability, un-treated cells were stained with Propidium Iodide (10µg/ml).

The data obtained was analysed using Beckman Cytoflex-Flow Cytometry Analysis software, to measure cell surface marker expression of bone-marrow derived cells, at least $3x10^5$ events were measured and then gated to exclude cell debris (events of SSC and FSC of <20). On a histogram overlay, the area expressed by the antigen-specific primary antibody marker was then measured and deducted from the area expressed by the IgG antibody to reveal the true cell surface marker value displayed as the percentage.

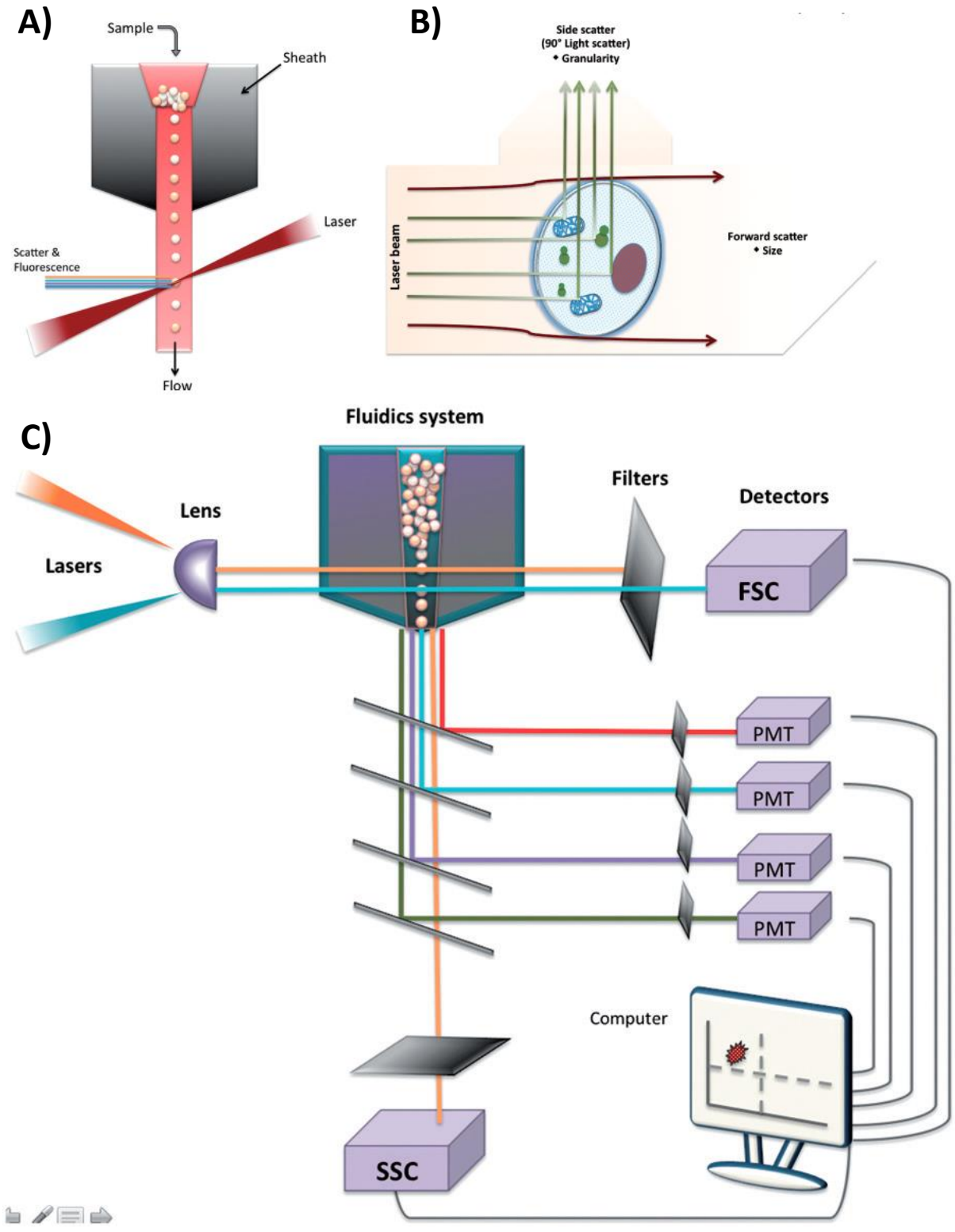

Figure 2.2: The principle of flow cytometry

Setup of flow cytometry system showing **A)** the fluidics system **B)** FSC and SSC detection of a cell within a flow cytometer **C)** the general method of detection and processing of data (Adapted from Adan et al., 2017).

2.2.8 Isolation and culture of murine colonic crypts

Colonic crypts were isolated from the distal colon of C57BL6 mice, as previously described by Skoczek et al.

Briefly, following the culling of the mouse, the colon was removed and washed with ice-cold PBS to remove excess faecal matter; the colon was then cut longitudinally and excess mucus within the tissue was gently dissociated. 0.5mm tissue pieces were placed in a saline solution [50ml dH_2O with NaCl (140mM), KCl (5mM), HEPES (10mM),d-glucose (5.5mM), Na_2HPO_4 (1mM), MgCl (0.5mM), CaCl (1mM), EDTA (1mM), DTT (0.153µg/ml), L-glutamine (200mM), Pen/Strep (200U/ml) and NEAA (2%)] for 1 hour. To liberate the crypts, the solution containing the tissue was shaken to aid gentle dissociation and then collected following crypt sedimentation. The single crypts were embedded in growth factor-reduced matrix matrigel (VWR) and seeded onto No.0 coverslips (0.08-0.13mm) contained within 12-well plates (Starlab). Following polymerization of the matrigel after 8 minutes at 37°C, the coverslips were flooded with 0.1ml of colonic crypt culture media (Advanced DMEM/F12, containing B27 (20µl/ml), N2 (10µl/ml), N-acetyl-L-cysteine (0.163µg/ml).HEPES (10mM), Pencillin/Streptomycin (100U/ml), GlutaMAX (2mM), EGF (50ng/ml), Noggin (100ng/ml) (all from Peprotech), Wnt-3A (200ng/ml) and R-spondin-1 (1mg/ml) (BioTechne).

2.2.9 Co-culture of macrophages and colonic crypts

To isolate the monocytes and macrophages population, the cells were harvested on day 4 and day 7, respectively. On day 4, the supernatant was removed, and the adherent population was liberated using 1ml of Versene (0.48mM). The cells were centrifuged, and macrophages at a cell density of $3x10^5$ was then added to the colonic crypt/Matrigel solution (prepared as previously described in **Section 2.2.1**) the mixture was then seeded onto a No.0 coverslip with. Following polymerization at 37°C for 8 minutes, the Matrigel was then flooded with 100µl of murine colonic crypt culture medium (prepared as described in Section **2.2.8**). The isolation and culture of bone-marrow derived macrophages and colonic crypts is summarised in **Figure 2.3.**

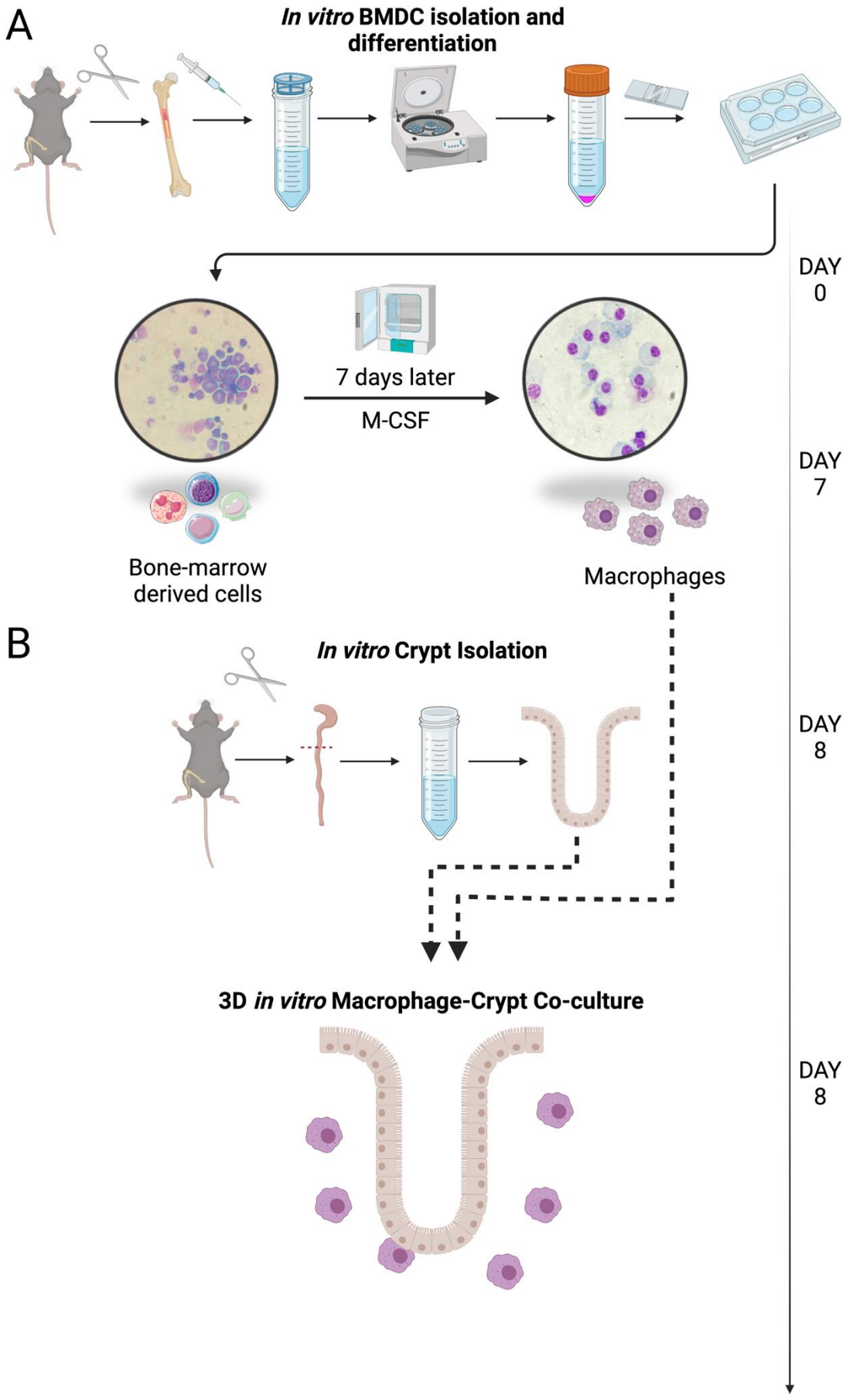
A
In vitro BMDC isolation and differentiation
DAY 0
7 days later
M-CSF
DAY 7
Bone-marrow derived cells
Macrophages
B
In vitro Crypt Isolation
DAY 8
3D *in vitro* Macrophage-Crypt Co-culture
DAY 8

Figure 2.3: Summary of the 3D in vitro macrophage-crypt co-culture protocol

Summary diagram showing the **A)** The *in vitro* isolation and culture of bone-marrow derived cells and their differentiation towards a bone-marrow derived macrophage phenotype following 7 days in culture with M-CSF. The progressive changes in morphology have been tracked using cytospun cells and Diff-Quick staining. **B)** The *in vitro* isolation of murine colonic crypts and their co-culture along with differentiated bone-marrow derived macrophages. Created in Biorender (2021).

2.2.10 Culture of macrophages and colonic crypts in the 'conditioned media' and 'M1 only' model

Macrophages and crypts were isolated and cultured as previously described. In **Figure 2.3**, macrophage-crypt co-culture are seeded on part of the coverslip, while crypts alone were seeded on the other part of the same coverslip. Figure A shows an example of a two-dotted 3D matrigel co-culture model with homogenous macrophages and crypts suspended in media (M1-crypt co-culture). **Figure 2.4C** and **2.4B** show the experimental setup of the 'M1-conditioned media' crypts and 'M1 only' crypt model.

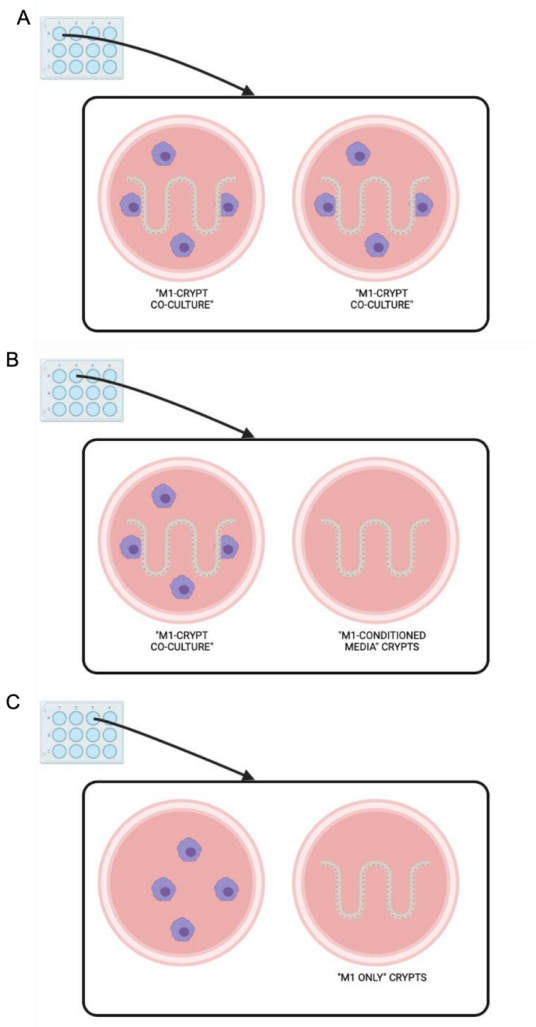

Figure 2.4: Conditioned media experimental setup

Diagram showing the **A)** Two-dotted Matrigel culture of crypts in the presence of M1-macrophages. **B)** Two-dotted Matrigel cultured with crypts in w/o M1 macrophages and **C)** Two-dotted Matrigel with crypts cultured alone but in vicinity to M1 macrophages. Created in Biorender (2021).

2.2.11 Culture of macrophages and colonic crypts with DAPT

Macrophages and crypts were isolated and co-cultured as previously described, however for treatment with the γ-secretase inhibitor, DAPT (TOCRIS), the Matrigel was previously spiked with DAPT (25µM) and then cultured with M1 macrophages which have also been pre-incubated in DAPT (25µM) shortly before their introduction to the colonic crypts. The concentration of 25µM was previously utilised within a 3D crypt culture model by Van Dussen and colleagues. Here small intestinal crypts were isolated, cultured and 24 hours following their culture, the crypts were treated daily with a vehicle control (DMSO) and DAPT (25um) to determine the effects of Notch inhibition on the intestinal stem cell

expression, proliferation, and apoptosis *in vitro*. During the treatment, the organoid budding efficiency and Lgr5-GFP+ cell numbers were then monitored over the course of 5 days (Van Dussen et al., 2012).

2.2.12 Immunofluorescent labelling of crypt-macrophage co-cultures

For characterising cells within the co-culture system, epithelial and macrophage marker-specific antibodies were used. Following the co-culture, the coverslips were fixed with 4% PFA (1ml/well) for 1 hour on ice. Washing steps were carried following each step.

Ammonium chloride (100mM in PBS (pH7.4), prepared as previously described in **Section 2.1.5** was added to each coverslip for 13 minutes, washed with PBS, followed by further incubation with 10% SDS in PBS (pH 7.4) for 5 minutes. 1% Triton-X was added for 30 minutes to permeabilise the organoids. Non-specific binding was inhibited using 10% Donkey or Goat serum (Gibco) (depending on antigen retrieval) for 20 minutes. A primary antibody (Table 1.2) was added for overnight incubation at 4^{o}C. The following day, a compatible secondary antibody (Table 1.3) added for 2 hours at 4^{o}C. Finally, the slides were washed and mounted with Hoechst/Vectashield. the slides were later visualised using an epifluorescence or confocal microscope.

2.2.13 EdU incorporation experiments

Colonic crypts were cultured as previously described. Following 24 hours post-culture, a 100µM EdU solution, diluted in crypt culture medium (1ml), was added to each coverslip (10µl) to obtain a final concentration of 10µM. By repeatedly pipetting the EdU solution up and down ten times, it was ensured that a homogenized solution was attained. The crypts were then left to incubate at 37^{o}C/5% CO_2 overnight. On day 2, the crypts were fixed in and further exposed to NH_4CL_2 for 13 minutes, washed in 1% SDS for 5 minutes and permeabilised in Triton-X for another 30 minutes. The crypts were subjected to the Click-iT reaction cocktail (ThermoFisher) for 35 minutes as per manufacturer's instructions.

2.3 Image Analysis

All fluorescent images were captured on the equatorial plane, (the plane which passes through the equator of the cell/crypt) using either a Nikon TI with a x20 0.4 NA (numerical aperture), Zeiss Axiovert 200 with a x20 NA or Zeiss LSM-510-META with a x63 1.4NA 0.75mm WD oil immersion objective was used. All images were analysed with Fiji (Image J) software.

2.3.1 Epifluorescence and confocal microscopy

Fluorescent molecules tagged to antibodies or dyes, emit light after being excited by shortwave-length light source. Simply put, a photon excites the molecules from a ground state, where a loss of vibrational energy leads to the emission of a photon, which can be captured by an epifluorescence (Nikon TI, Zeiss Axiovert 200M) or confocal microscope (Zeiss LSM-510-META).

In an epifluorescence microscope, light excited from above the sample, passes through an objective lens which is directed onto the sample. The light emitted from the specimen is then focused towards a detector such as a CCD Camera (Hamamatsu ORCAII). A dichroic mirror acts as a colour filter allowing some wavelengths to pass through while others are reflected. It also filters out excited light from emitted light thereby reducing background fluorescence (**Figure 2.5A**).

In confocal microscopy, following the excitation of the specimen, emitted light converges onto a second objective lens towards a narrow pinhole. Sitting behind the pinhole is a detector quantifying the emission of light. The sample is scanned several times to obtain an image (**Figure 2.5B**). Overall, this results in high resolution with lower background fluorescence in comparison to a traditional epifluorescence microscope (Bretschneider and Weile., 2019).

For thick tissue samples such as a colonic crypt, optical sectioning (z-stacks) will be required to obtain clearer images, this can be achieved by simply varying the focal plane of the sample while capturing consecutive images. Unless otherwise stated, optical sections (z-stacks) were captured at 1µm intervals, 5µm above and below the equatorial plane.

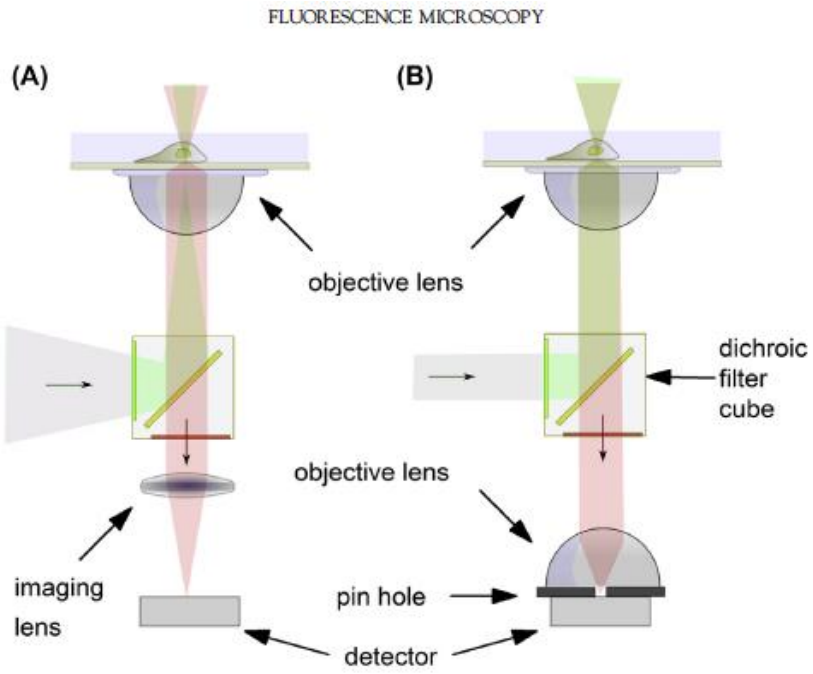

Figure 2.5: The principle of epi-fluorescent and confocal microscopy

Diagram showing **A)** epifluorescence microscope setup, where light is excited from above the sample and passes through the objective lens, meeting the dichroic filter cube, where the emitted wavelength is filtered and detected by the imaging lens. **B)** Confocal microscope setup, where excited light passes through the objective lens, onto the dichroic mirror and a second objective lens in which light emission is restricted by the pinhole prior to reaching the detector or camera. Excitation beams are shown in green and emitted fluorescence shown in red (Adapted from Bretschneider and Weile, 2019).

2.3.2 Quantification of EdU-labelled crypt cells

All fluorescent crypt images were captured at a x20 or x64 magnification Zeiss Axiovert 200M or Zeiss LSM-510-META. To identify newly synthesised a. The total number of DAPI+

positive cells were counted and compared to the number of EdU-nuclei double-positive cells, the percentage of total nuclei number expressing EdU was then expressed.

2.3.3 Quantification of Enteroendocrine, Tuft cells, Goblet and Stem cells

To identify enteroendocrine cells (Cro-A+) (Abcam), tuft cells (DCAMKL1+)(Abcam), goblet cells (UEA-1+) (Vectorlabs) and stem cells (Lgr5+)(Origene), z-stacks were taken at a 1µm intervals for 5µm above and below the equatorial plane.

Goblet cells were identified by following the UEA-1 + present within the cytoplasm of the individual cells throughout the equatorial plane. E-cadherin was used to aid the visualisation of the cytoplasm within the goblet cell (**Figure 2.6**). The location of each marker positive cell was recorded and separated into three crypt regions, base (cells within the +4 position of the crypt), mid and top region.

To identify the stem cells within a crypt, the basal Lgr5 expression of each cell across the z-stack (optical slices), 5µm above and below, the equatorial plane was counted (**Figure 2.7Ai**). The average Lgr5 fluorescence intensity within each crypt region was measured by recording the overall fluorescent measurements of each cell's basal region along the crypt-axis as shown in **Figure 2.7Aii**. Here, the overall fluorescent per cell was measured in each crypt region (Base, Mid and TOP). To accurately measure the average basal expression of each cell in the equatorial plane was determined, by taking three separate (2x2 pixels) measurements across the basal region of each crypt cell.

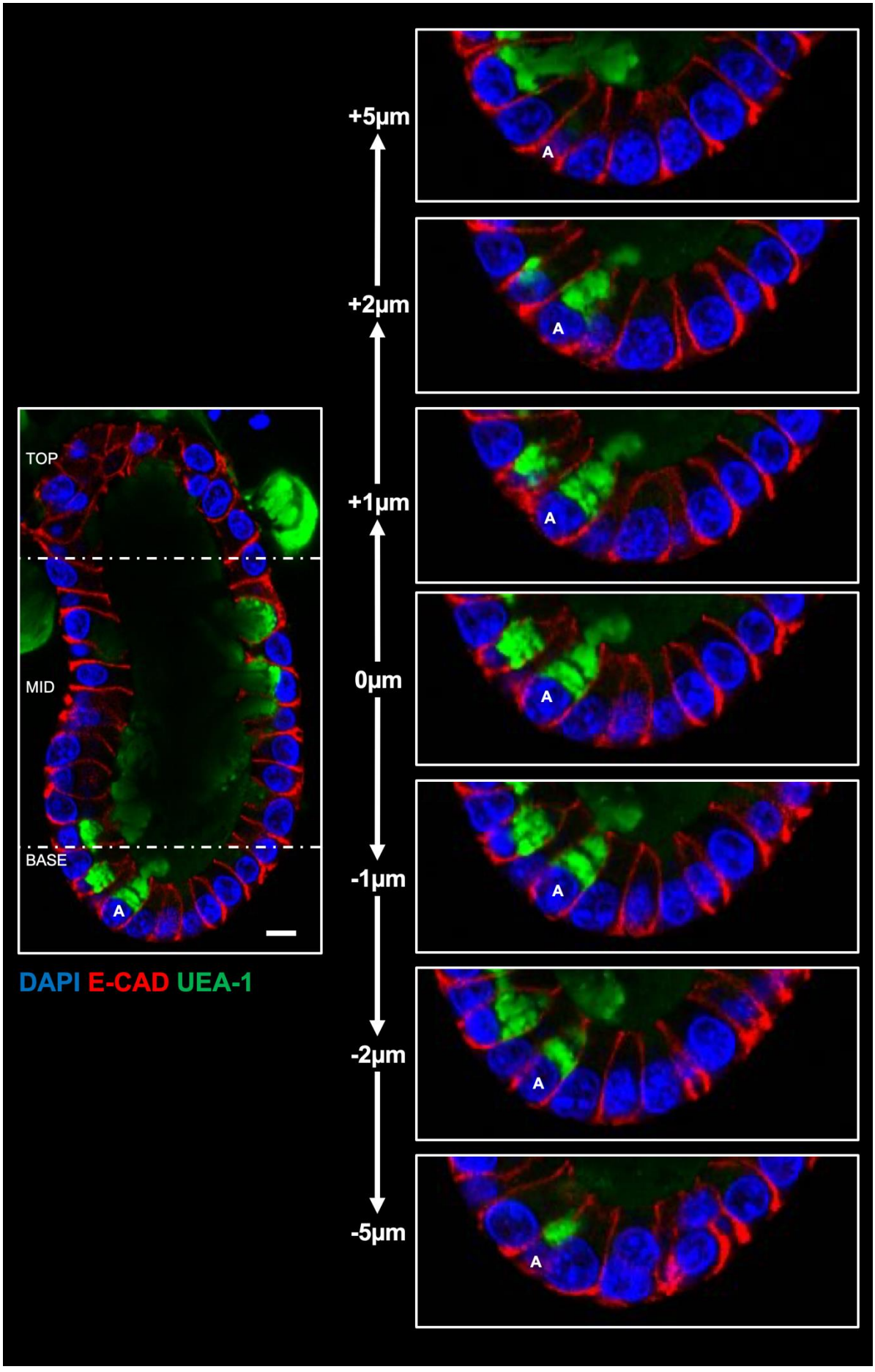
+5µm
+2µm
+1µm
0µm
-1µm
-2µm
-5µm
TOP
MID
BASE
A
DAPI E-CAD UEA-1

Figure 2.6: Identification and analysis of UEA-1+ goblet cells

Analysis of goblet cells numbers using UEA-1 (green) staining. DAPI+ and UEA-1+ cells (A) at the equatorial plane were counted. To confirm UEA-1 staining originates from the cell (A), staining was followed 5µm above and below the equatorial plane.

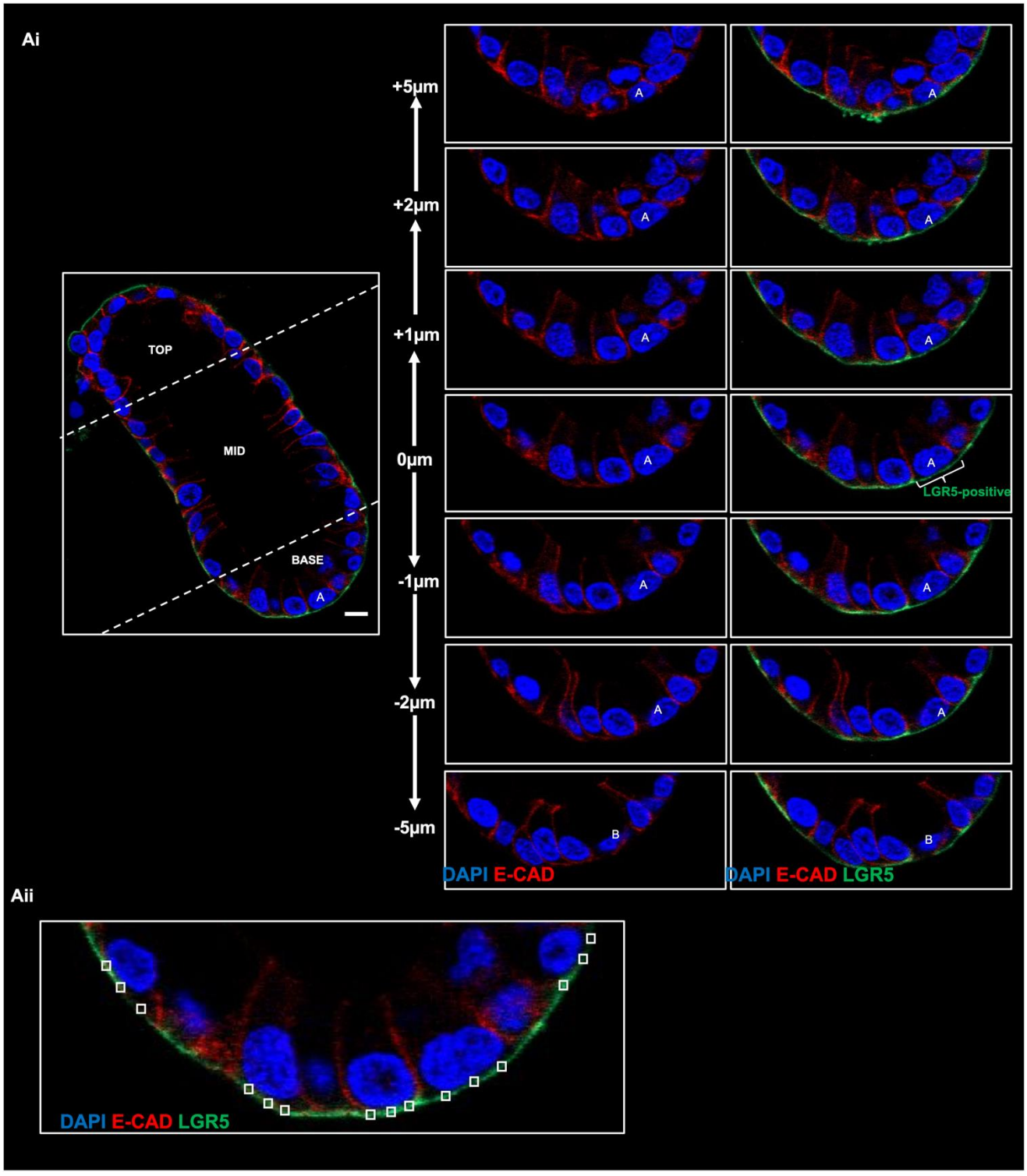
Ai
+5µm
+2µm
+1µm
0µm
-1µm
-2µm
-5µm
TOP
MID
BASE
A
B
LGR5-positive
DAPI E-CAD
DAPI E-CAD LGR5
Aii
DAPI E-CAD LGR5

Figure 2.7: Identification and analysis of Lgr5+ stem cells

Ai) Analysis of Lgr5+ stem cell numbers in each crypt and crypt region (Base,Mid,Top). Basal expression of Lgr5 is shown in green. DAPI+ cells (shown in blue) were identified at the equatorial plane and Lgr5+ stem cells (A) were identified by their continuous basal expression of Lgr5 across all planes of the cell (5µm above and below the equatorial plane). Note that cell B is located above the equatorial plane and was not included in the data. E-cadherin (shown in red) was utilised to aid the identify each cell's boundaries. **Aii)** Individual DAPI+ cells (shown in blue) were identified, and three separate fluorescence measurements (2x2 pixels) were taken and the fluorescence value of each cell within a crypt region was averaged and presented.

2.3.4 Quantification of nuclear fluorescence intensity

Images were captured using the confocal microscope (LSM-510-META) with a x63oil a x63 1.4NA 0.75mm WD oil immersion objective. To quantify the expression of Cyclin-D1 and LEF1 within the nucleus, first the TIFF images were converted to 8-bit and the average fluorescence value of every nucleus present at the equatorial plane was then measured. Using Fiji- Image J's polygon tool, the nuclear area was identified by following the perimeter of each individual DAPI+ nuclei in the equatorial plane. The arbitrary fluorescent value of the channels occupied by Cyclin-D1 and LEF1 were then measured as shown in **Figure 2.8**.

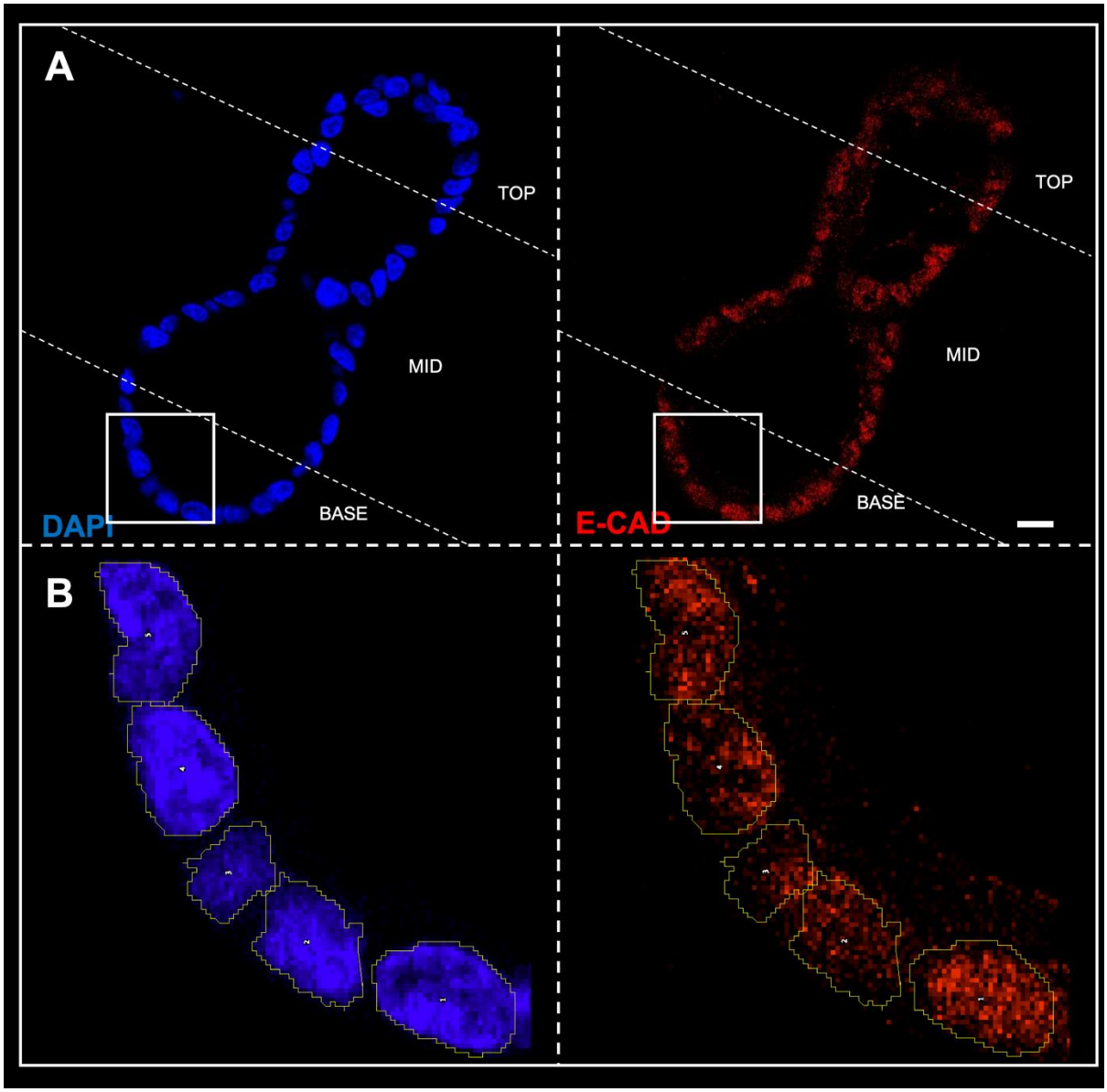

Figure 2.8: Identification and analysis of nuclear LEF1 localisation

Analysis of nuclear fluorescence intensity per crypt **A)** DAPI+ and LEF1 expression in a crypt **B)** The nuclear area was highlighted using DAPI and the channel was switched to LEF1, where the average fluorescence intensity of the area was measured. This analytic approach was also mirrored with analysis of Cyclin-D1. Scale bar at 15µm.

2.3.5 Quantification of macrophage localisation, vesicle localisation and epithelial protrusions along the crypt-axis

To measure macrophage localisation along the crypt-axis, live crypt images were first captured on a brightfield microscope at x10 magnification using a GXCAM3EY-5. The number of macrophages in contact with each crypt region (Base, Mid and Top) were recorded and presented as the percentage and average number of macrophage-crypt contact point per total crypt number.

Epithelial vesicles were defined as small (less than 5µm in diameter), rounded droplets found in the vicinity (>10µm) of the colonic epithelium, where the presence such vesicles within our macrophage-crypt co-culture model, were analysed in a binary manner, where one or more vesicles present near the crypt was quantified as 1 and the absence of vesicles near the crypt was quantified as 0 (**Figure 2.9E**).

Epithelial processes were defined as slender, sharp protrusions which measure less than >20µm in length and in contact with the colonic epithelium's base (+4 position and below). Such processes were quantified, analysed, and presented as the percentage and average number of epithelial processes per total crypt number (**Figure 2.9F**). 'Shedding' processes were defined as long (<20µm), processes exclusively present in the mid and upper region of the crypt, where unlike epithelial processes the distal end of the "shedding" process was globular in shape. "Shedding" processes were quantified and presented as the percentage and average number of processes per total crypt number (**Figure 2.9G**).

2.3.6 Morphological analysis of colonic crypts

The morphological characteristics of colonic crypts *in vivo* were analysed by first capturing brightfield images using a GXCAM3EY-5 at x10 magnification. The length of the crypt was measured using Fiji Image J's linear tool, where the distance between the base and the beginning of the shedding zone was measured (**Figure 2.9D**). The epithelial area was measured by following the perimeter of the polarised crypts (excluding the lumen) (**Figure 2.9A,B,C**).

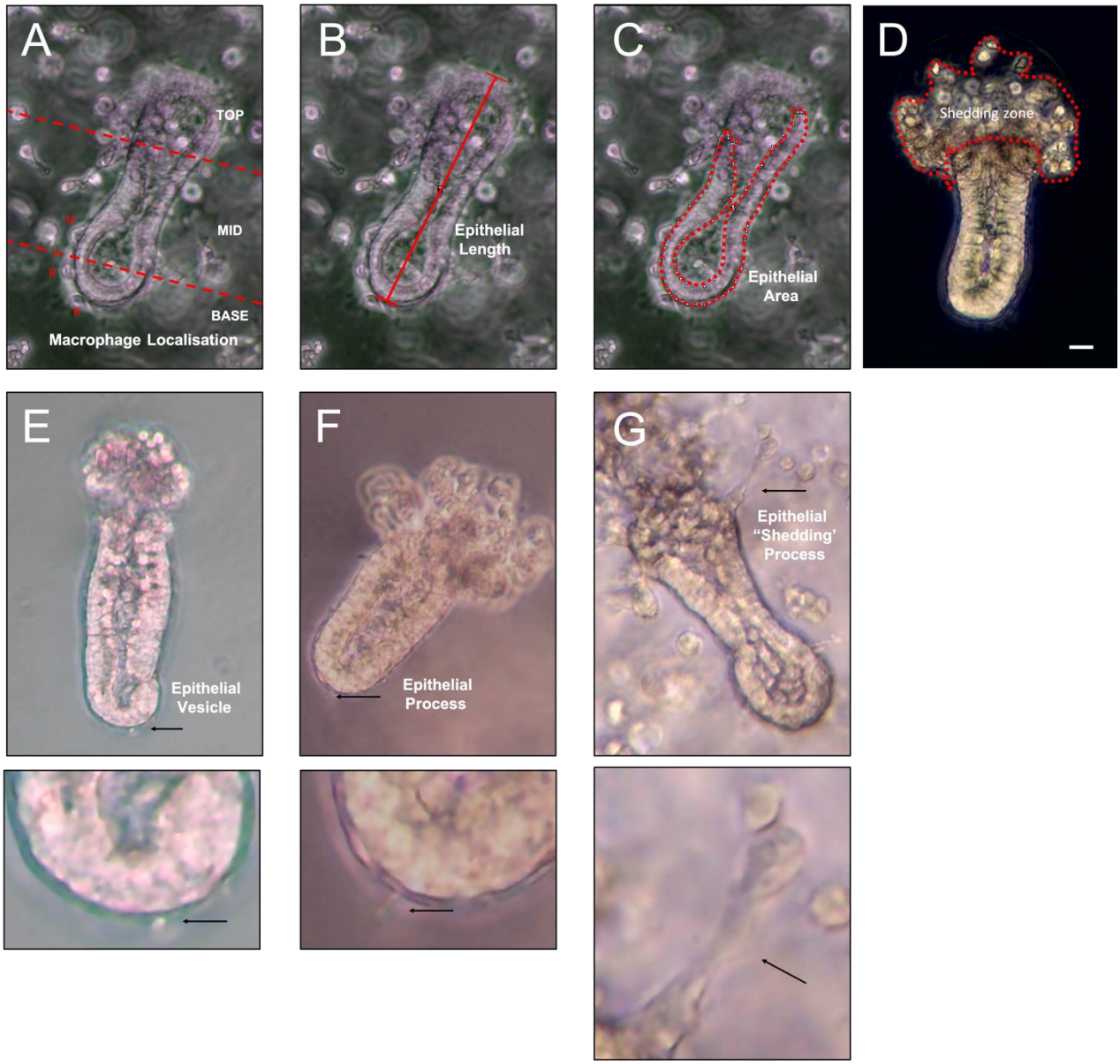

Figure 2.9: Morphological analysis of in vitro macrophage-crypt co-culture

Panel showing **A)** Quantification of macrophage-crypt localisation in each crypt region (B-Base, M-Mid, T-Top). **B)** Measuring crypt length, the distance between the base and the start of the shedding was measured. **C)** Measuring crypt area, the perimeter around the polarised epithelium at its equatorial plane was highlighted and measured **D)** The perimeter around the shedding zone (highlighted in red) was measured using Image J's freehand tool. Scale bar at 20µm. **E)** Example of an epithelial vesicle present at the base of crypt, which was quantified in a binary manner **F)** Example of an epithelial process which was analysed and presented as the average number of epithelial process per crypt **G)** Example of epithelial "shedding" process present near the upper region of the crypt which was quantified and presented as the average number of "shedding" processes per crypt.

2.3.8 Measuring nitrite concentration within a culture system

To measure nitric oxide formation, the nitrite concentration (a stable by-product of nitric oxide) within the tissue culture media was determined via a Griess reagent assay. This assay was performed at room temperature. To measure the nitrite concentration of the macrophage subtypes, the supernatant media (100µl) was removed from a 12-well plate in which cells were seeded at a density of $1x10^6$/ml and centrifuged at 600g for 5 minutes to ensure the media is void of all cells. As a control group, RPMI-1640 media was used to compare to BMDM-derived media. Similarly, to measure nitrite concentration within the co-culture's media, the supernatant (100µl) was removed from each crypt-macrophage co-culture condition and also centrifuged at 600g for 5 minutes to ensure the media is void of all cells. As a control group, conditioned media from crypts cultured alone were used. The supernatants (0.1ml) were then mixed with 0.05 ml of sulphanilamide (1% w/v in 1% v/v HCl) (Sigma). Following 15-minute incubation, further 0.05ml of *N*-1-napthylethylenediamine dihydrochloride (0.1 % w/v in 1% HCl) (Sigma) was added, after which the solution was transferred into a 96 well plate and the absorbance of measured at 550nm using a BMG Labtech Clariostar plate reader. A nitrite standard curve was prepared using 100µM of sodium nitrite and the nitrite concentration of each sample was determined via interpolation of their respective absorbance values against the standard curve (**Figure 2.10**).

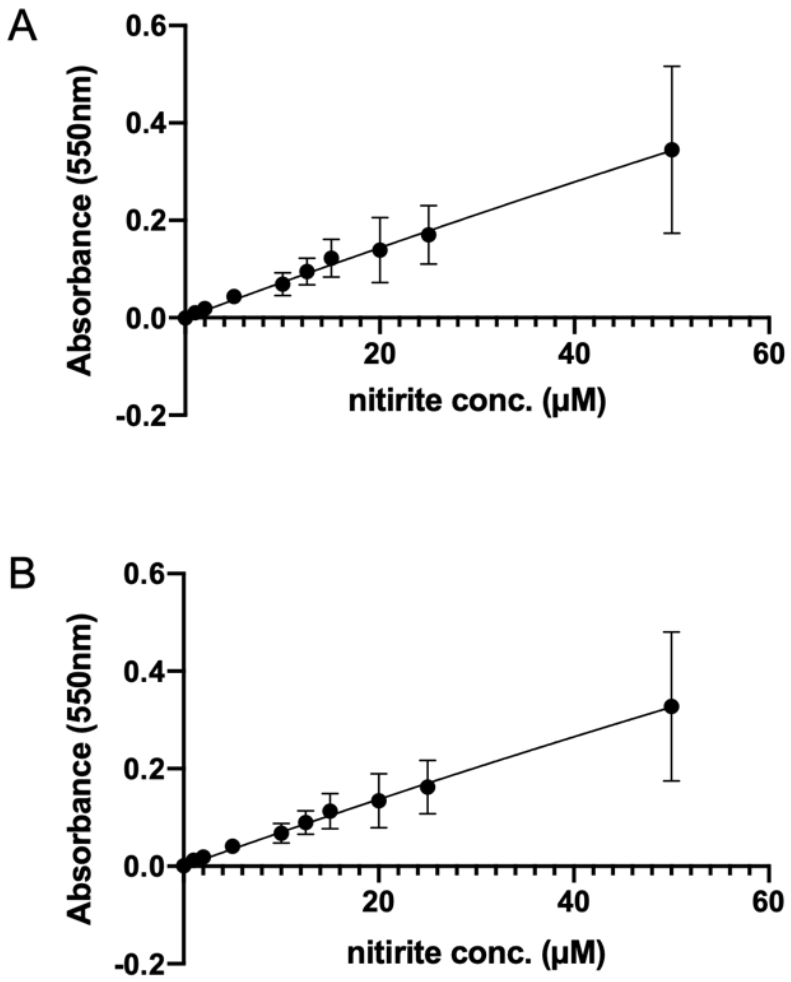

Figure 2.10: Nitrite standard curve

Absorbance readings of the nitrite standard curve following a Griess assay **A)** in BMDM-derived media and **B)** in crypt-macrophage co-cultured derived media (n=3).

2.3.9 Measuring nitric oxide expression in BMDM using the MODEL probe

A nitric acid probe (MODEL-DNC) kindly donated by Dr.Marin's lab and experiments performed in collaboration with Carla Arnau Del Valle. BMDMs were isolated and cultured onto No.0, 19mm coverslips within 12-well plates. On Day 7, the nitric acid probe was added and simultaneously activated towards an M1 phenotype, or the media was replaced to maintain the Naïve phenotype. Cells were incubated in the presence or absence of the NO-

probe for at 24 hours and then fixed the following day with 4% paraformaldehyde and the images were captured on a confocal microscope (Zeiss LSM-980).

2.4 Statistical Analysis

All experiments were repeated at least three times unless stated otherwise. Data are expressed as mean ± standard error of mean (SEM), n= number of independent experiments, N= minimum total number of crypts and a minimum of 20+ crypts per experiment were counted. Statistical analysis was carried out using the Graphpad Prism 8 software. Comparisons between two or more groups were measured using one-way ANOVA with post-hoc Tukey analysis and a paired t-test was utilised to compare differences between two groups. P-value of less than 0.05 was considered statistically significant. For the analysis of nitrite absorbance in each culture condition, the individual nitrite concentration was interpolated from a plotted nitrite standard concentration curve **(Figure 2.10)**

Chapter 3: Development and Characterisation Of 3D *In Vitro* Crypt-Macrophage Co-culture Model

3.1 Introduction

The colonic epithelium is continually exposed to luminal insults such as commensal microbiota, foreign pathogens and chemical degradation and is therefore required to renew itself every 4-5 days (Darwich et al., 2014). The large intestine is home to the largest macrophage population in the body, which commonly reside in the underlying lamina propria (Gordon and Plueddemann., 2017).

Although the macrophages' ability to clear foreign pathogens and threats has been recognised for more than a century, in the intestine their role has seemingly expanded and are now considered to be crucial regulators of T-cell expansion and wound repair (Murai et al., 2009; Hesketh et al., 2017; Wang et al., 2019). In the steady state, monocytes constitutively enter the lamina propria, where the gradually differentiate into mature macrophages during a process coined the 'monocyte-waterfall' pathway (Bain et al., 2018; Tamoutounour et al., 2012). Due to the high presence of commensal microbiota in the colonic mucosa, intestinal macrophages have evolved and are able to discriminate commensal microbes from foreign pathogens via PAMPS (pathogen associated molecular patterns). Should epithelial barrier function be compromised in homeostasis, residential macrophages are able to antagonise the pathogen via phagocytosis while also secreting several anti-inflammatory cytokines which ensure the mucosa is not further perturbed (Smythies et al. 2005).

In stark contrast to homeostasis, chronic inflammation or inflammatory bowel disease is often caused by the inability of the gastrointestinal tract to resolve acute inflammation (Lissner et al., 2015). Aberrant accumulation of macrophages present in the lamina propria in patients suffering from IBD have since been identified as one of the hallmarks of the disease and more interestingly, the macrophage phenotype within the tissue is significantly altered compared to the steady state (Thiesen et al., 2014; Bernardo et al., 2018). While residential macrophages remain hypo-responsive and produce IL-10, TGF-β among others to repress the immune response in the steady state, TNF-a, IL-6 and high nitric oxide production are secreted by macrophages in inflammatory disease further exacerbating

tissue damage (Duque and Descoteaux., 2014; Novak and Koch., 2013). In 2000, Mill's et al's work defined two macrophage subtypes based on their response to either Th1 or Th2 regulatory cells, here M1 'inflammatory' macrophages were found to produce higher levels of nitric oxide than M2 'anti-inflammatory' macrophages from Th2 strains which produced ornithine instead (Mills et al., 2000). These two unique phenotypes have since been studied more extensively in an attempt to understand their effects on IBD and disease progression (Italiani et al., 2014; Mills and Ley., 2014).

Among other key causative factors which can determine the patient's disease progression such as genetics, microbiotics and environmental factors, macrophages and the adaptive immune cells are postulated to play a key role in the exacerbation of chronic inflammation in the colon (Ramos and Papadkis., 2020). However, in most patients, the amalgamation of environmental and host factors described above can contribute to IBD and affect epithelial renewal, therefore it becomes more challenging to study the interactions and effects of the macrophage population on colonic crypt renewal (Maloy and Powrie., 2011). We have therefore developed and characterised a 3D in vitro macrophage-crypt co-culture model, which will allow us to mimic the conditions of health and inflammation as it may occur in vivo, to study the effects of pro and anti-inflammatory macrophage-crypt crosstalk on colonic crypt renewal.

Previous in vivo studies have showcased the plasticity of intestinal macrophages in an inflammatory and steady state, while also highlighting the differential role of M1 and M2 macrophages in the maintenance of intestinal homeostasis, however, the understanding of the molecular mechanism involved in the crosstalk between macrophages and the colonic epithelium in an in vivo model are limited (Shapouri-Mohgadam et al. 2018).

In colonic crypts, the functional cells residing within the epithelium are responsible for maintaining the intestinal steady state, these include secretory cells such as goblet cells, tuft cells and enteroendocrine cells and the absorptive enterocyte cell lineage, while stem cells located at the base of the crypt divide and proliferate to maintain the high epithelial turnover rate required for intestinal homeostasis (Barbara et al., 2003; Meran et al., 2017). Over the last decade the culture of 3D *in vitro* intestinal crypts has made it possible to track and quantify differentiated cell lineages and stem cells to study their rate of proliferation,

differentiation, and shedding (Johansson et al., 2011; Gerbe et al., 2009; Clevers and Nusse., 2012; Sugimoto and Sato., 2017).

In this study, we have developed and characterised an *in vitro* 3D macrophage-crypt co-culture model, allowing the study of the spatiotemporal relationship and determine the macrophage population's effect on colonic crypt renewal, including crypt proliferation and differentiation.

3.2 Results:

To investigate the role macrophages, play in *in vitro* crypt homeostasis, bone-marrow derived cells from C57Bl6 mice were cultured and differentiated towards macrophage-like phenotype via the supplementation of M-CSF as per **Section 2.2.1**. This chapter aims to characterise the differential phenotypic changes observed during the BMDC's process of differentiation by use of histological staining, flow cytometry and immunofluorescent labelling, while also determining the presence of epithelial differentiated cells within our 3D *in vitro* model.

3.2.1 M-CSF drives differentiation of heterogenous BMDC towards a homogenous macrophage-like population

To harvest macrophages, bone-marrow derived cells were initially isolated and cultured as per **Section 2.1.1** and supplemented with M-CSF (0.2µg/ml), a factor required for the differentiation of monocyte precursors towards a macrophage phenotype (Francke et al., 2011). The morphological changes *in vitro* were documented in **Figure 1A and Figure 1B.**

White light images of *in vitro* BMDC were captured from Day 1 to Day 8 in **Figure 3.1A.**

On Day 1 following the culture of BMDC, a largely spheroidal cell population and a number of smaller cells (<5µm) were most commonly observed. On Day 2, an adherent sub-population forming small filopodia can be observed with the number of adherent cells (**a**) increasing over time. The number of non-adherent floating cells within the cell culture population is also steadily decreasing from Day 4 to Day 7 with adherent cells, largely dominating the landscape (**Figure 3.1A).** Following the removal of non-adherent cells and cell debris on Day 7, the adherent population was classically and alternatively activated towards an M1 and M2 phenotype (**Section 2.2.2).** A significant morphological difference between either activated phenotypes was not found.

To further determine the phenotypic changes observed above, Cytospins were taken of the bone-marrow derived cell population and stained with Diff-Quick s in order to track the M-CSF driven differentiation of individual haematopoietic cells over the course of eight days (**Figure 3.1B**). On Day 1 of, a highly heterogenous population including lymphocytes (**a**) and neutrophil (**b**) were identified. Day 4 Cytospins show an increase of kidney-bean shaped monocytes (**d**) which are gradually replaced by macrophages (**c**) with a larger cytoplasm

(**Figure 3.1B)**. The cytospun, Quick-Diff staining did not show a definitive difference between the M1 and M2 phenotypes.

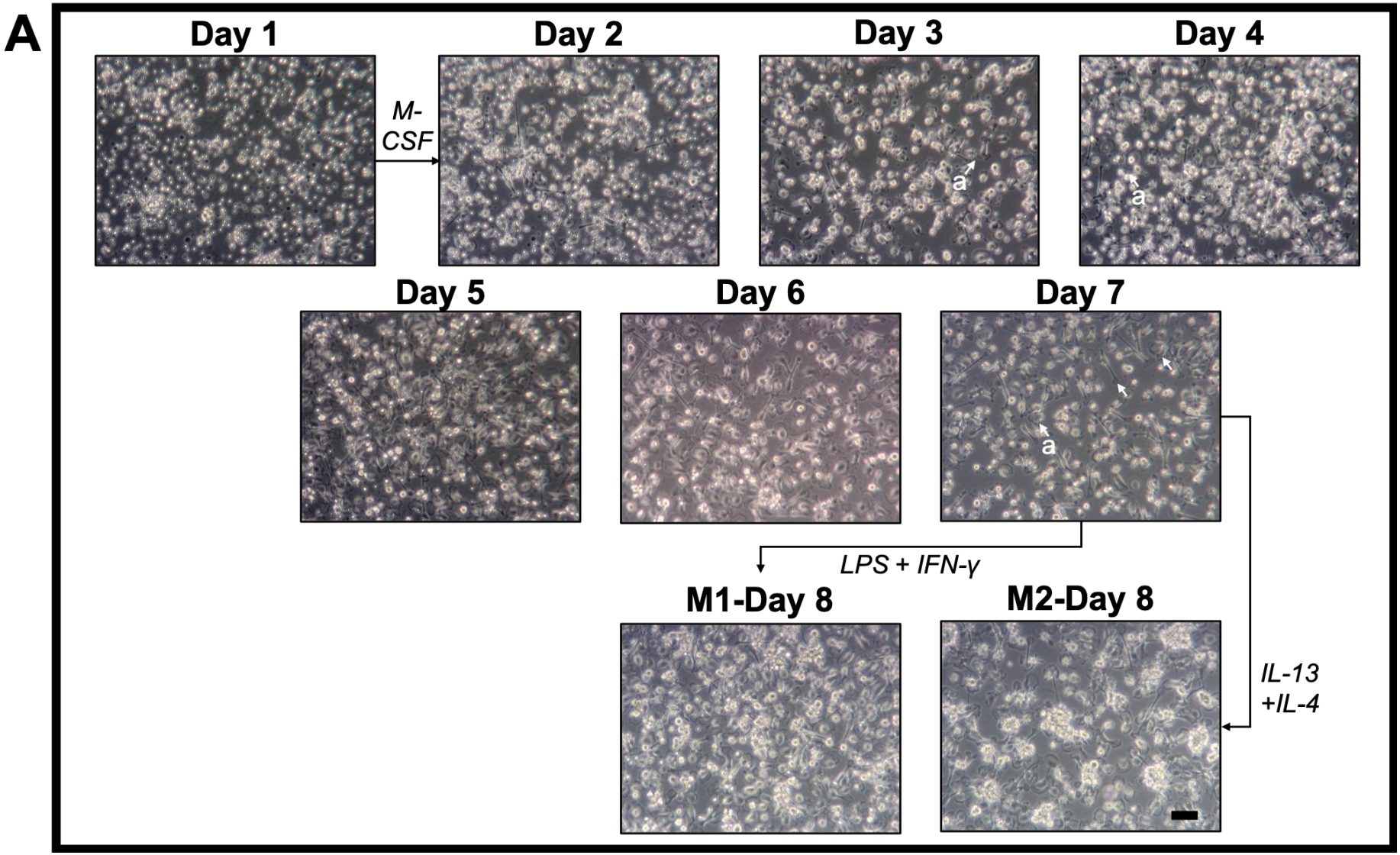
A
Day 1
Day 2
Day 3
Day 4
M-CSF
a
a
Day 5
Day 6
Day 7
a
LPS + IFN-γ
M1-Day 8
M2-Day 8
IL-13
+IL-4

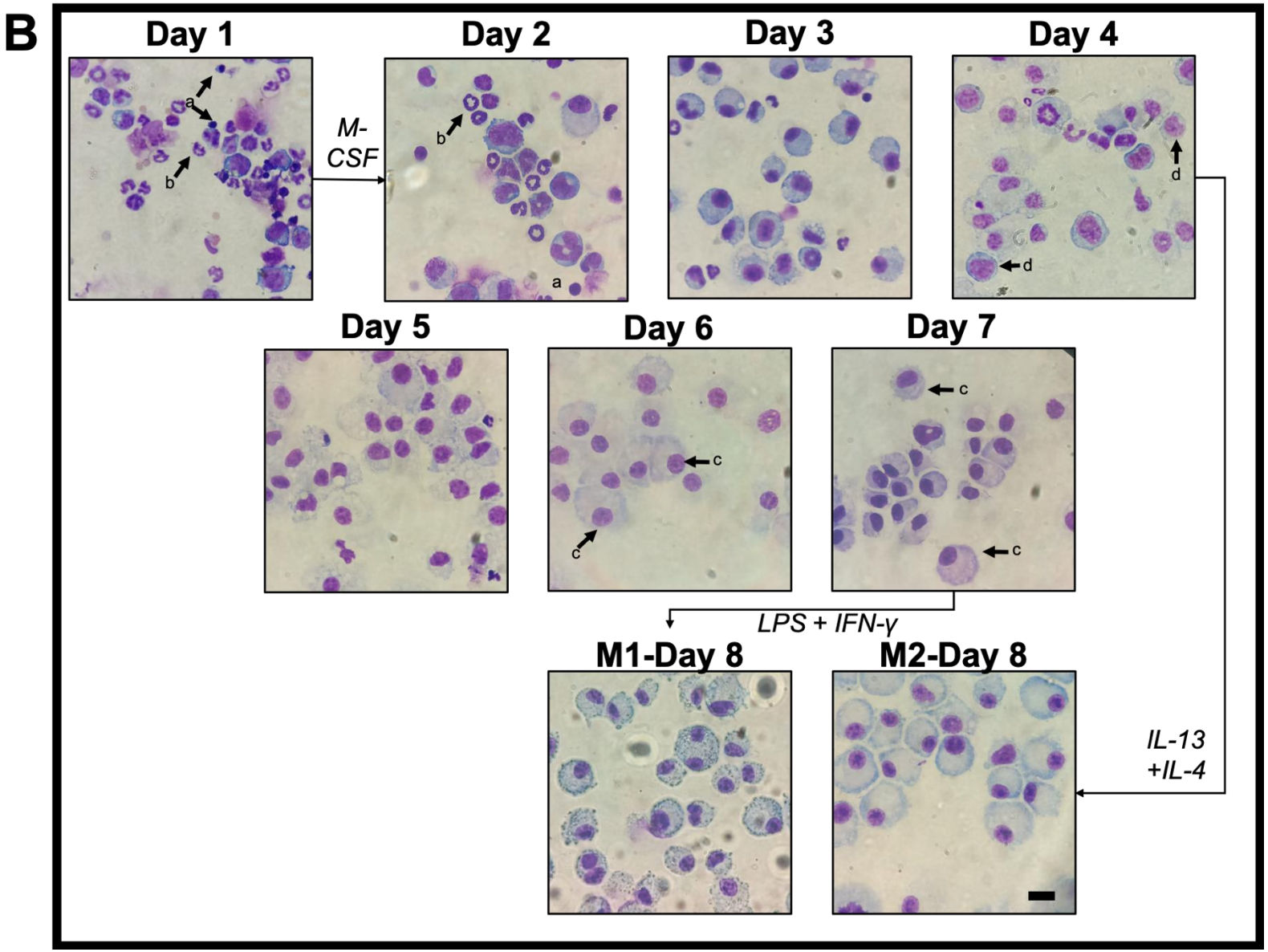
B
Day 1
Day 2
Day 3
Day 4
M-CSF
a
b
b
a
d
d
Day 5
Day 6
Day 7
c
c
c
c
LPS + IFN-γ
M1-Day 8
M2-Day 8
IL-13
+IL-4

Figure 3.1: **Morphological and histological characterisation of bone-marrow derived cells differentiation following 8 days *in vitro* culture**

A) Representative white light images (x10 magnification) of in vitro bone-marrow derived cells and their gradual morphological differentiation towards a homogenous macrophage-like phenotype in the presence of M-CSF over 7 days. On the 7th day, bone-marrow derived macrophages were polarised with IL-13 (10ng/ml) and IL-4 (10ng/ml) or LPS (100ng/ml) and IFN-y (50ng/ml) to activate M2 and M1 subtypes, respectively. Scale bar 40µm. **B)** Representative Diff-Quick images (x100 oil magnification) of bone-marrow derived cells and their gradual differentiation towards a homogenous macrophages-like phenotype in the presence of M-CSF over 7 days. IL-13 and IL-4 or LPS and IFN-y was supplemented on the 7th day to polarise cells towards and M2 and M1 phenotype, respectively. Scale bar 15µm.

3.2.2 M-CSF drives differentiation of bone-marrow derived monocytes towards an adherent macrophage-like phenotype *in vitro*

To further assess the phenotypes of the bone-marrow derived cell population, leukocyte cell surface markers were utilised to characterise non-adherent BMDC on Day 4 (**Figure 3.2C)** and adherent BMDC on Day 7 (**Figure 3.2D).** Flow cytometry was used to quantify marker expression as per **Section 2.2.7**

Initial forward scatter (FSC-cell size) and side scatter (SSC-cell granularity) (**Figure 3.2A)** analysis of the non-adherent Day 4-BMDC and adherent Day 7-BMDC was shown. Here the non-adherent BMDC population on Day 4 expressed a low FSC and SSC value, whereas the adherent BMDC population on Day 7 expressed a high FSC and SSC value. In **Figure 3.2Bi**, the average cellular size (FSC) of the non-adherent BMDC population on Day 4 (red) was compared to the adherent BMDC on Day 7 (green), where the adherent population was shown to larger in cell size compared to its non-adherent counterpart. Furthermore, in **Figure 3.2Bii**, the adherent BMDC cell population on Day 7 was also shown to be more granular when compared to non-adherent BMDCs on Day 4.

Succeeding this, monocyte and macrophage cell surface markers were utilised to characterise the non-adherent BMDC population from Day 4 and the adherent BMDC population from Day 7 in **Figure 3.2C and D.**

Here marker expression of a known macrophage precursor and common monocyte marker Ly6C, revealed a higher expression in non-adherent Day 4- BMDC (67% ± 11.4) compared to its Day 7-BMDC (8% ±4.5). counterpart. A significantly lower expression of CX3CR1 was recorded in Day 4-BMDC (29%±1.03), compared to adherent Day7-BMDC (82%±13.6).

Similarly, CD64 expression, was also found to be high in Day7-BMDC (88%±9.4) but not in Day 4-BMDC ((23%±8.4). The membrane protein, F4/80 is was also highly expressed in Day 7-BMDC (F4/80 (81%±7.8) where a significantly lower expression was found in the Day 4-BMDC (26%± 6.2) population. Expression of the major histocompatibility complex 2 (MHC2) was observed to be significantly higher in Day 7-BMDC (63%± 13.2) compared to Day 4-BMDC (MHC II (15%±7.1).

Labelling for the chemokine receptor CCR2 revealed a 22%±6.3 expression in Day 4-BMDCs compared to the 76±7.8 in adherent-Day 7-BMDC population.

Although CD11b expression was observed to be marginally higher in Day 7-BMDC (44%±14.7) than in Day 4-BMDC (15%±5.5), the changes observed did not differ significantly.

Both populations were also labelled for CD11c and CD206, where Day4-BMDC lack the expression of either CD11c (13%±12.2) and CD206 (0%±0.9), whereas Day7-BMDC's expression of CD11c (76% ±11.8) and CD206 (75 ±8.8) was significantly higher (**Figure 3.2C and 3.2D)**.

Overall, cell surface expression of CX3CR1, MHC2, F4/80, CD64, CD11c, CD206 and CCR2 was significantly higher in the adherent BMDC population compared to the non-adherent BMDC population on Day 4 of *in vitro* C567BL6 BMDC (**Table 4**).

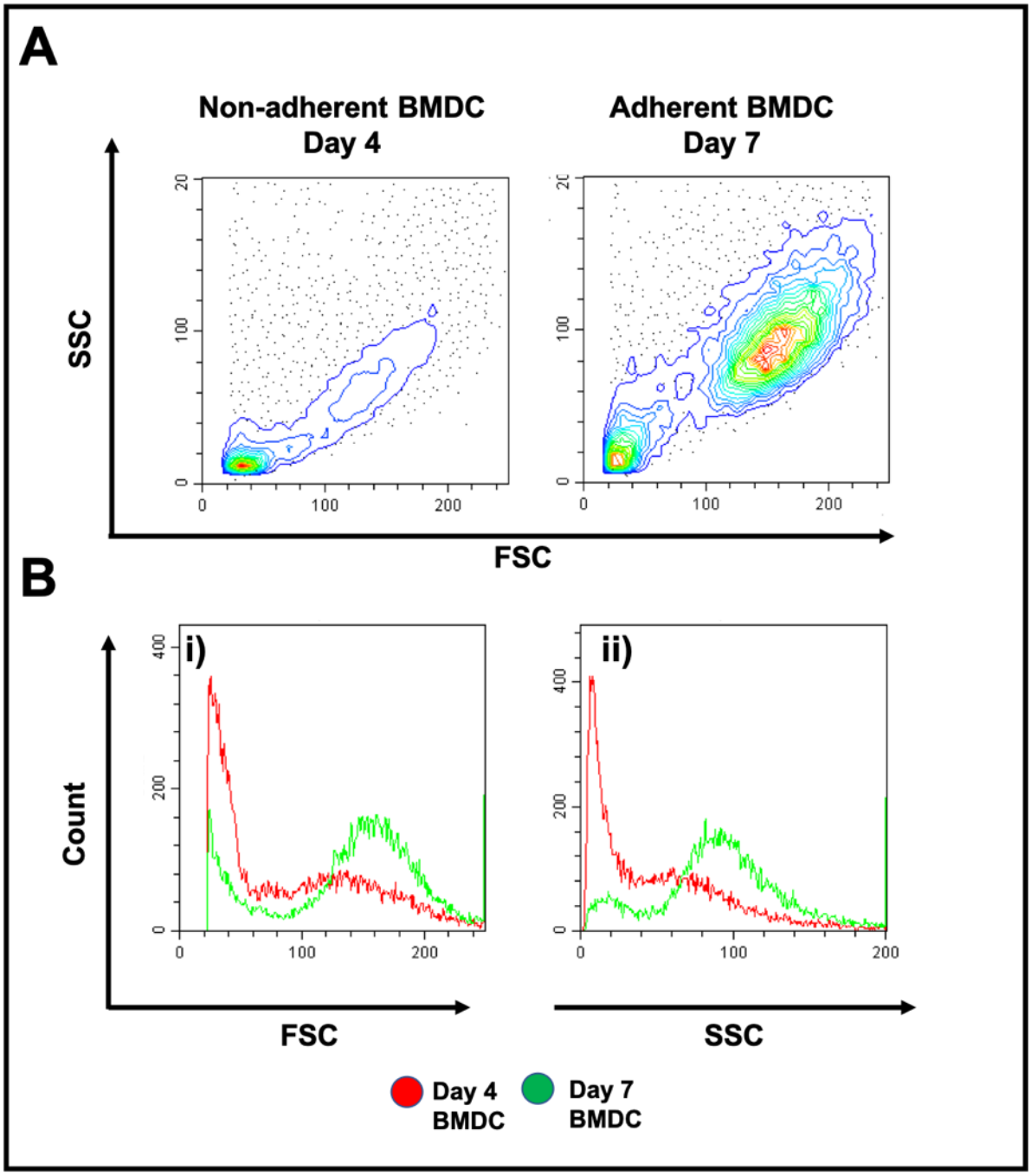
A
Non-adherent BMDC
Day 4
Adherent BMDC
Day 7
SSC
FSC
0
100
200
B
i)
ii)
Count
FSC
SSC
400
Day 4
BMDC
Day 7
BMDC

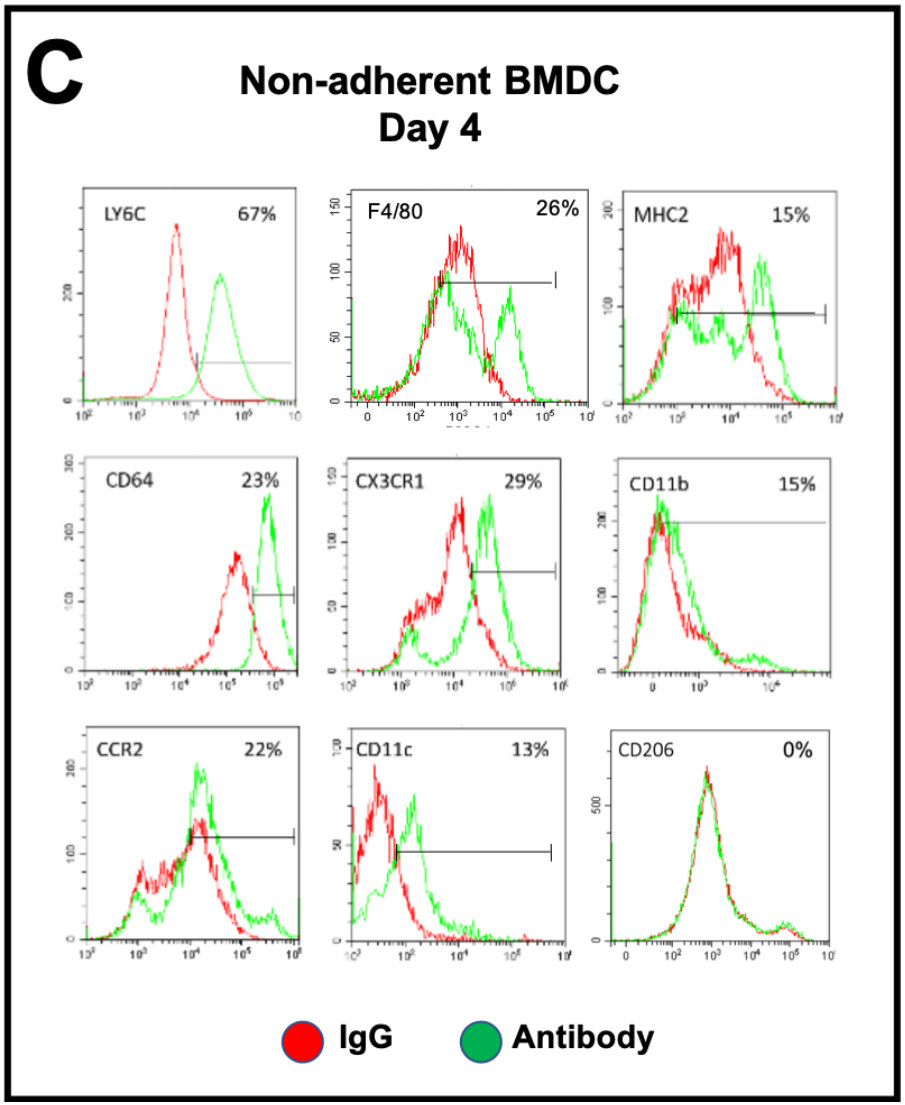
C
Non-adherent BMDC
Day 4
LY6C 67%
F4/80 26%
MHC2 15%
CD64 23%
CX3CR1 29%
CD11b 15%
CCR2 22%
CD11c 13%
CD206 0%
IgG
Antibody

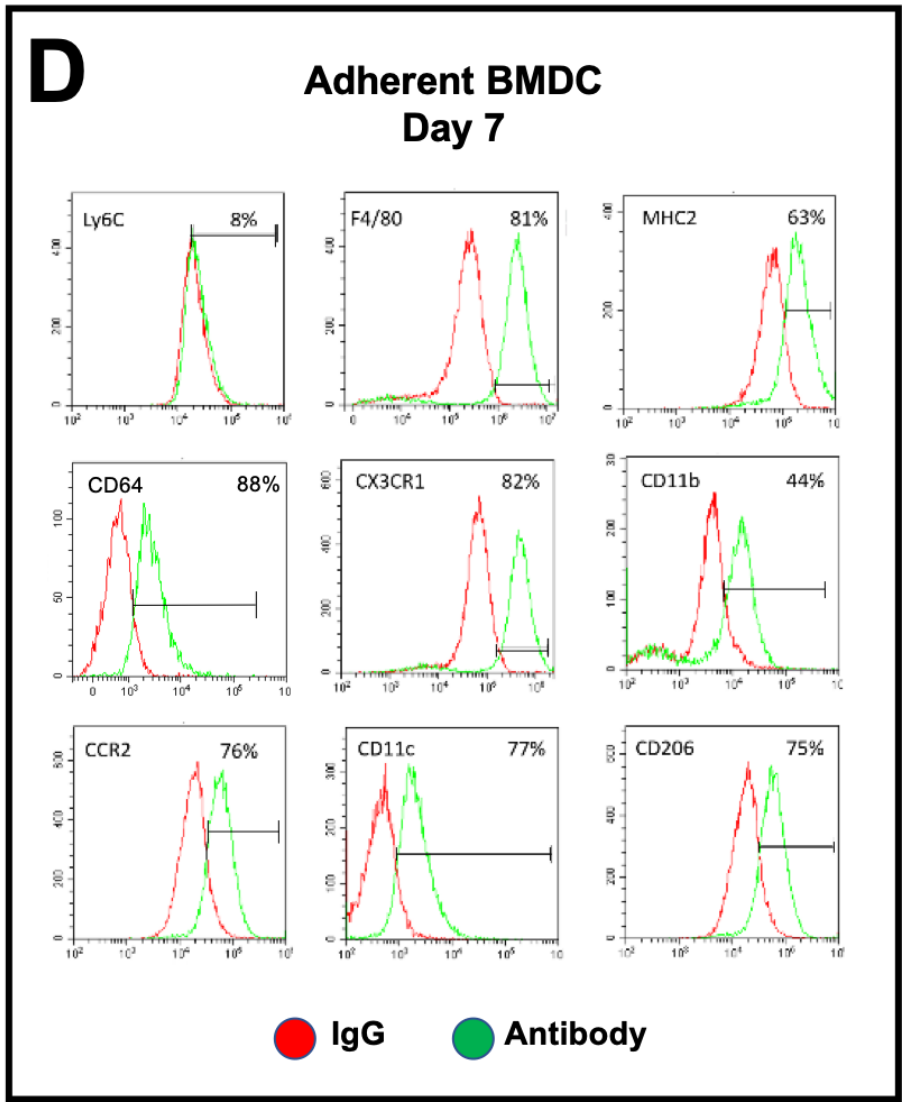
D
Adherent BMDC
Day 7
Ly6C 8%
F4/80 81%
MHC2 63%
CD64 88%
CX3CR1 82%
CD11b 44%
CCR2 76%
CD11c 77%
CD206 75%
IgG
Antibody

Figure 3.2: Characterisation of the non-adherent Day 4-BMDM and adherent Day 7-BMDM phenotypes using leukocyte cell surface marker expression

Flow cytometry phenotyping of bone-marrow derived cells in culture supplemented with RM-CSF. Cells were analysed for lymphocyte markers (green). The indicated bar represents the positive population and gating was performed in comparison to isotype marker (red).
A) Countor plot showing the SSC (granularity) and FSC (cell size) in the non-adherent BMDC population on Day 4 and adherent BMDC population on Day 7 of culture **B)** Histogram showing the the FSC **(Bi)** and SSC **(Bii)** of the non-adherent BMDC on Day 4 and adherent BMDC population on Day 7 of culture.
C) Histograms showing various expression of commonly found lymphocyte cell surface markers in the non-adherent *in vitro* BMDC population on Day 4 of culture (n=3). **D)** Histogram showing various expression of commonly found myeloid cell surface markers in the adherent *in vitro* BMDMC population on Day 7 of culture. IgG (red) and antibody (n=3).

Cell surface expression	Day 4- non adherent BMDC	Day 7- adherent BMDM	P<0.05* P<0.001**
CX3CR1	29 (±1 0.3)	82 (± 13.6)	*
MHC2	15 (± 7.1)	63 (± 13.2)	*
F4/80	26 (± 6.2)	81 (± 7.8)	**
CD64	23 (± 8.4)	88 (± 9.8)	**
CD11b	15 (± 5.5)	44 (± 14.7)	ns
Ly6C	67 (± 11.4)	8 (± 4.5)	**
CD11c	13 (± 12.2)	76 (± 11.8)	*
CD206	0 (± 0.9)	75 (± 8.8)	**
CCR2	22 (± 6.3)	76 (± 7.8)	**

Table 4: Comparison of leukocyte marker expression in Day 4 and Day 7 BMDC

Leukocyte marker expression (mean± SEM), compared between non-adherent BMDC population and adherent BMDC population on Day 4 and Day 7, respectively. (n=3, *P<0.05; **P<0.001 Day 4 BMDM compared to Day 7 BMDM).

3.2.3 Classical and alternative activation of BMDM leads to differentiation of distinctive M1 and M2 phenotypes *in vitro*

Following the characterisation of Day 7-BMDC, the adherent population was then polarised towards an M1 and M2 phenotype as per **Section 2.2.2** and leukocyte cell surface marker expression was determined via flow cytometric analysis (**Section 2.2.7**).

Analysis of cell size (FSC) and granularity (SSC) within the M1 and M2 phenotype (**Figure 3.3 A**) has shown M2-BMDM to be marginally more diverse in size and granularity compared to M1-BMDM. In **Figure 3.3Bi**, M2-BMDM (green), shown to express a smaller FSC (cell size) compared to M1-BMDM (red). Furthermore, the SSC (cell granularity) also shows that a distinctively less granular population is visualised in M2-BMDM (green) compared to M1-BMDM (red) in **Figure 3.3Bii.**

Levels of CX3CR1 expression were observed to be similar, in both the M1 (92% ± 8.3) and M2 population (91%±6.4). M1-BMDM also highly expressed markers MHC2 (74%± 6.4), F4/80 (90%±6.0), CD64 (81% ± 14.6), CD11b (79% ±15.5) and CCR2 (80%±18.7).

M2-BMDM also express high levels of MHC2 (72% ±12.2), F4/80 (91.5% ±4.9), CD64 (58% ±10.8), CD11b (54% ±12.7) and CCR2 (67% ±12.8). Notably, M1-BMDM show a slight reduction in CD206 (16.5±23.3) compared to M2 (60% ±42%) (non-significant).

The expression of CD11c differed significantly between either subtype, where high expression was recorded in M1-BMDM (77%± 7) compared to M2-BMDM (7.5% ±10.6).

Overall, similar cell surface expression levels of CX3CR1, MHC2, F4/80, CD64, CD11b, Ly6C, CD206 and CCR2 were found in both M1-BMDM and M2-BMDM whereas only the expression of CD11c differed between either BMDM-subtypes (**Table 5**).

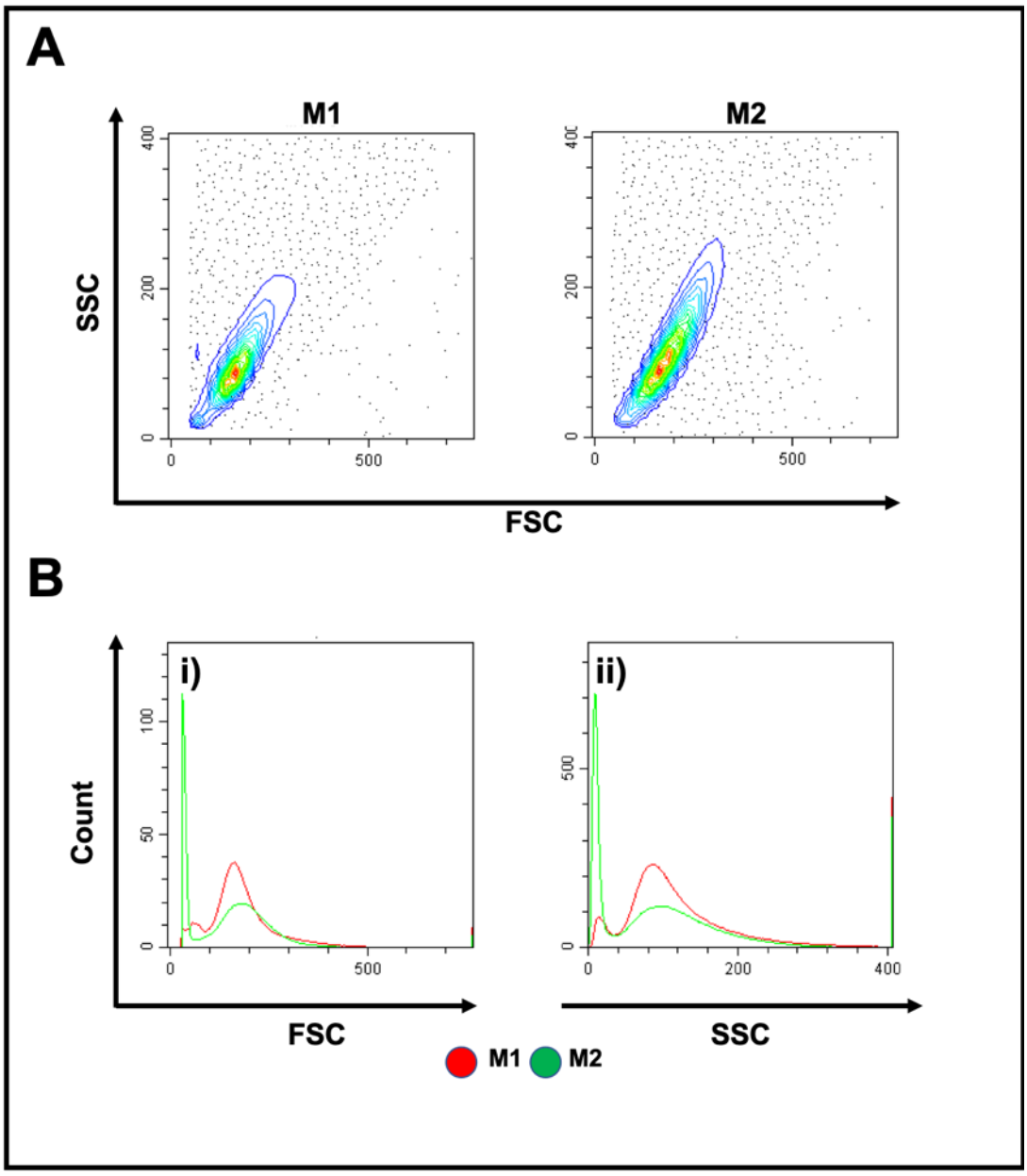
A
M1
M2
SSC
FSC
400
200
0
500
B
i)
ii)
Count
100
50
FSC
SSC
M1
M2

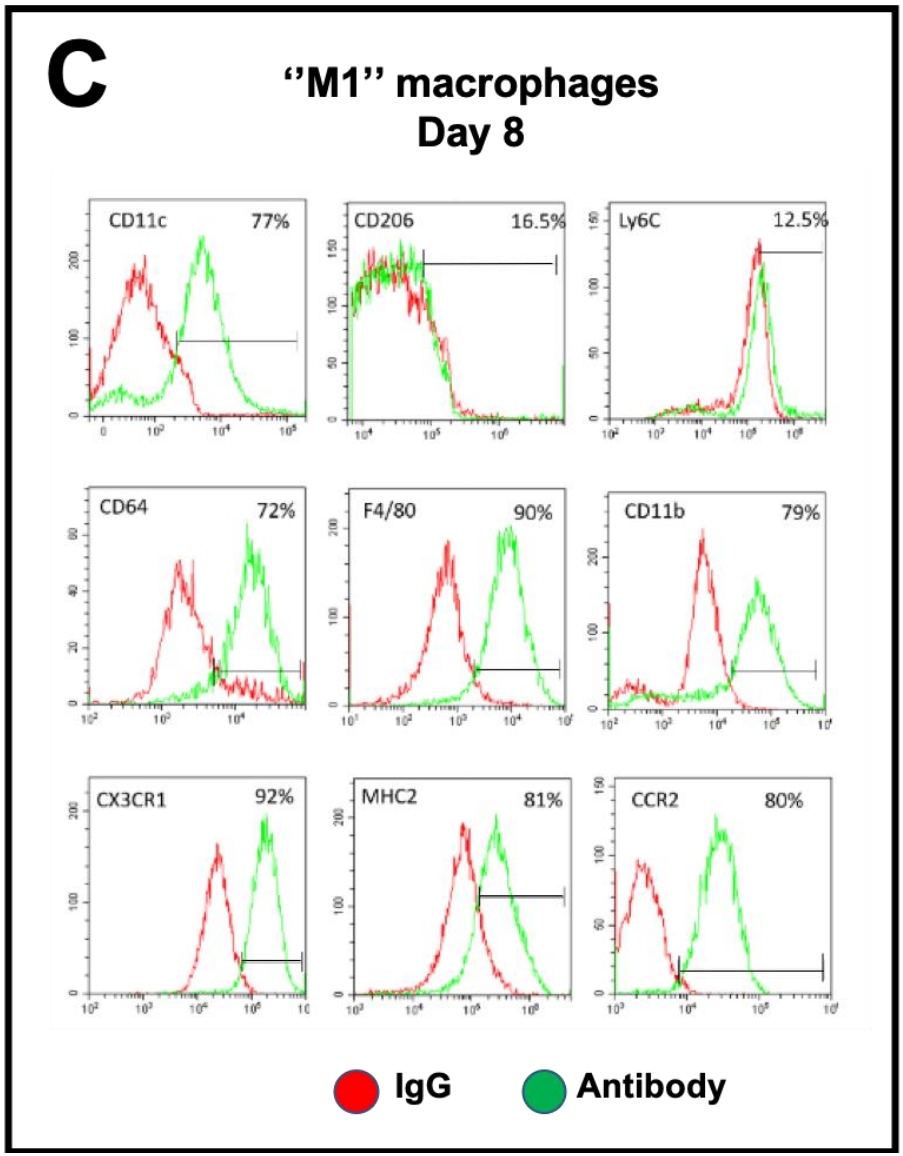
C
''M1'' macrophages
Day 8
CD11c 77%
CD206 16.5%
Ly6C 12.5%
CD64 72%
F4/80 90%
CD11b 79%
CX3CR1 92%
MHC2 81%
CCR2 80%
IgG
Antibody

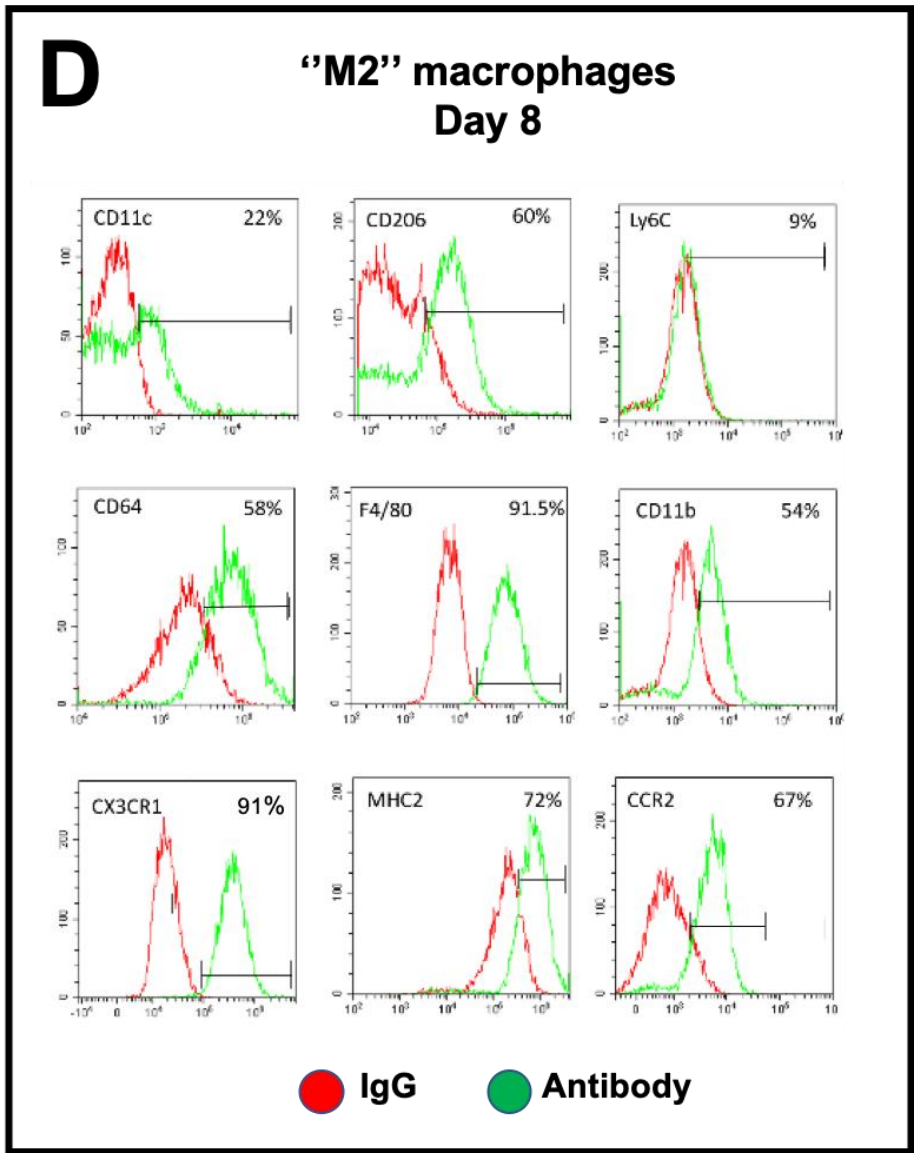
D
''M2'' macrophages
Day 8
CD11c 22%
CD206 60%
Ly6C 9%
CD64 58%
F4/80 91.5%
CD11b 54%
CX3CR1 91%
MHC2 72%
CCR2 67%
IgG
Antibody

Figure 3.3 Characterisation of classically activated M1-BMDM and alternatively activated M2-BMDM phenotypes leukocyte cell surface marker expression

Flow cytometry phenotyping of bone-marrow derived cells in culture supplemented with RM-CSF. Cells were analysed for macrophage markers (green). The indicated bar represents the positive population and gating was performed in comparison to isotype marker (red).
A) Countor plot showing the SSC (granularity) and FSC (cell size) in the adherent M1-BMDC population following a 24-hour activation with LPS (100ng/ml) and IFN-γ (50ng/ml) and M2-BMDC following 24-hour activation with IL-13 (10ng/ml) and IL-4 (10ng/ml)(n=3). **Bi)** Histogram showing the FSC (size) cell count of both M1-BMDC (red) and M2-BMDC (green). **Bii)** Histogram showing the SSC (granularity) of both M1-BMDC (red) and M2-BMDC (green)
C) Histograms showing various expression of commonly found macrophage cell surface markers in the adherent M1-BMDC population following a 24 hours activation with LPS (100ng/ml) and IFN-γ (50ng/ml) (n=3). **D)** Histograms showing various expression of commonly found macrophage cell surface markers in the adherent M1-BMDC population following a 24 hours activation with IL-13 (10ng/ml) and IL-4 (10 ng/ml) (n=3).

Cell surface expression	BMDM- M1	BMDM-M2	P<0.05* P<0.001**
CX3CR1	92% (± 8.3)	91% (±6.4)	ns
MHC2	74% (± 6.4)	72% (± 12.2)	ns
F4/80	90% (± 6.0)	91.5% (± 4.9)	ns
CD64	81% (± 14.6)	58% (± 10.8)	ns
CD11b	79% (± 7)	54% (± 12.7)	ns
Ly6C	12.5% (± 5.5)	9% (± 5.3)	ns
CD11c	77% (± 15.5)	7.5% (± 10.6)	*
CD206	16.5% (± 23.3)	60% (± 42%)	Ns
CCR2	80% (± 18.7)	(67% ± 12.8)	Ns

Table 5: Comparison of leukocyte marker expression in M1 and M2 BMDM

Summary of leukocyte marker expression (mean± SEM**)** compared between in adherent M1-BMDC population and adherent M2- BMDC population following overnight incubation with LPS, IFN-γ and IL-13, IL-4 respectively. (n=3, *P<0.05 M1 compared to M2).

3.2.4 Expression of cell-death is maintained in Naïve, M1 and M2 macrophage *in vitro*

To determine cell death within a live cell population, propidium iodide expression was measured using a flow cytometer (**Section 2.2.7**) Here, propidium iodide is able to bind to DNA in cells with defect plasma membrane allowing the quantification of cell death within a live-cell population (Crowley et al., 2016). Similar levels of propidium iodide expression were recorded in all adherent Day 8 subtypes, Naïve (2.6%±1.3), M1(3.6% ±8.9) and M2 (1.3%± 0.67) (**Figure 3.4**).

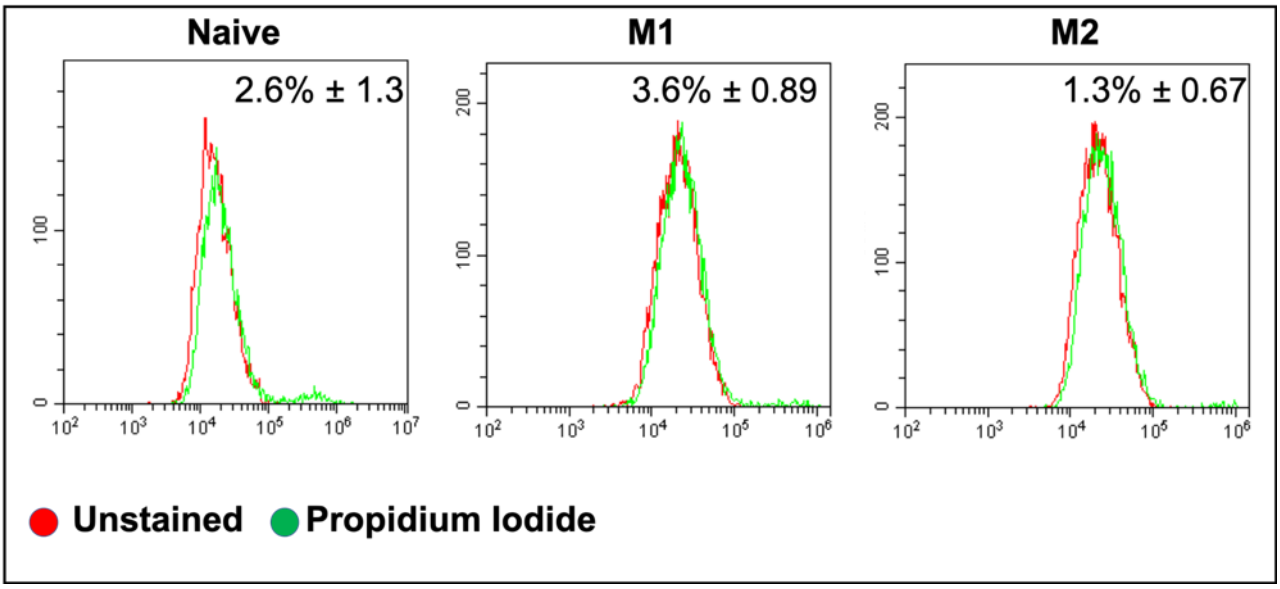

Figure 3.4: Expression of Propidium Iodide) expression remains unchanged in BMDM macrophage phenotypes

Histogram showing the absorbance of propidium iodide (cell death) in all Naïve, M1 and M2 macrophage subtypes on Day 8 of culture (n=3) (ns).

3.2.5 M1 macrophages increase nitrite accumulation and nitric oxide expression

An identified hallmark of the M1-macrophage phenotype is its capability to produce nitric oxide following the activation with LPS and IFN-γ (Mills et al., 2000*)*. To further determine whether bone-marrow derived M1 macrophages preserved this function *in vitro,* Naïve and M1 BMDC cultures were spiked with a nitric oxide (NO) probe on Day 7 of culture for 24 hours and immunofluorescently labelled according to **Section 2.1.1. Figure 3.5A** shows representative white light and fluorescent nitric oxide probe in both Naïve and M1 macrophages, where a higher fluorescence intensity can be observed in the M1 phenotype.

Similarly, the nitrite concentration within *in vitro* BMDM culture was measured using the Griess Assay as per **Section 2.3.8,** 24 hours following polarisation of the N, M1 and M2 macrophages, the absorbance (550nm) was read and compared to a nitrite standard curve (**Figure 3.5B and 3.5D)**.

Interpolation of each condition showed a significant increase of nitrite in M1 (20.1µM) compared to both Naïve (0.09µM) and M2 (0.362µM) (**Figure 3.5C).** The Griess assay was also performed 24 hours following a co-culture of crypts along with Naïve, M1 or M2 macrophages, in which the conditioned media was removed and analysed with high nitrite accumulation recorded in M1 co-cultures (13µM) in comparison to Naïve (0.25µM) and M2 (1.4µM) (**Figure 3.5E**).

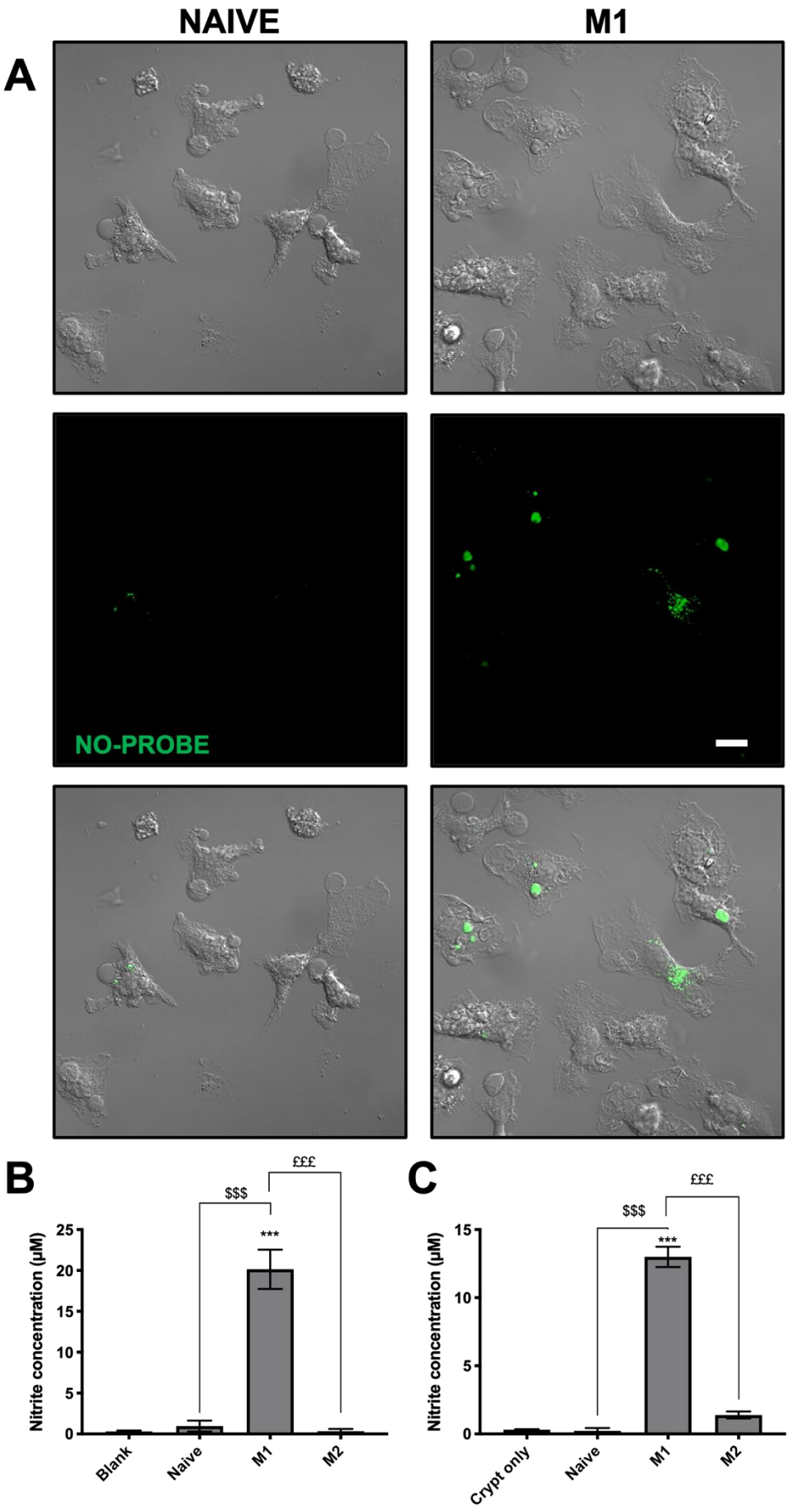
NAIVE
M1
A
NO-PROBE
B
Nitrite concentration (μM)
25
20
15
10
5
0
$$$
£££
***
Blank
Naive
M1
M2
C
Nitrite concentration (μM)
15
10
5
0
$$$
£££
***
Crypt only
Naive
M1
M2

Figure 3.5: M1 macrophage induce nitrite expression and nitric oxide expression within *in vitro* culture and *in vitro* crypt-macrophage co-culture

A) Confocal images showing expression of NO-probe (green) *in vitro* adherent BMDM Naïve and M1 macrophages 24 hours following activation. Scale bar 15µm.
B) Histogram showing the mean nitrite concentration (µM), in *in vitro* culture of Naïve, M1 and M2 macrophages, 24 hours following activation (n=3, N=31; Control vs M1,***P<0.0001; Naïve vs M1 $$$ P<0.0001; M2 vs M1, £££ P<0.0001).
C) Histogram showing the mean nitrite concentration (µM) 24 hours following an *in vitro* macrophage-crypt co-culture with Naïve, M1 and M2 macrophages. (n=3, N=23; Control vs M1, ***P<0.0001; Naïve vs M1 $$$ P<0.0001; M2 vs M1, £££ P<0.0001).

Having determined that M-CSF is required for the differentiation of bone-marrow derived cell towards a macrophage phenotype and while also characterising the cell surface marker expression of Naïve, M1 and M2 macrophages *in vitro*. We next set out to determine whether macrophages maintained their surface marker expression in co-culture with colonic crypts.

3.2.6 Classical and alternatively activated BMDM maintain macrophage cell surface marker expression *in vitro*

To confirm whether macrophages maintain leukocytic cell surface marker expression within the co-culture model, immunofluorescent labelling was performed as per **2.2.10.**

Figure 3.6A, confirmed that both M1 and M2 macrophages were observed to be CCR2 (green), F4/80 (red) and CX3CR1(magenta) positive. Examples of triple (F4/80, CX3CR1, CCR2) positive cells are highlighted below (white arrow). The antibody-specific IgG controls in **Figure 3.6B** confirm that the labelling is antigen-specific.

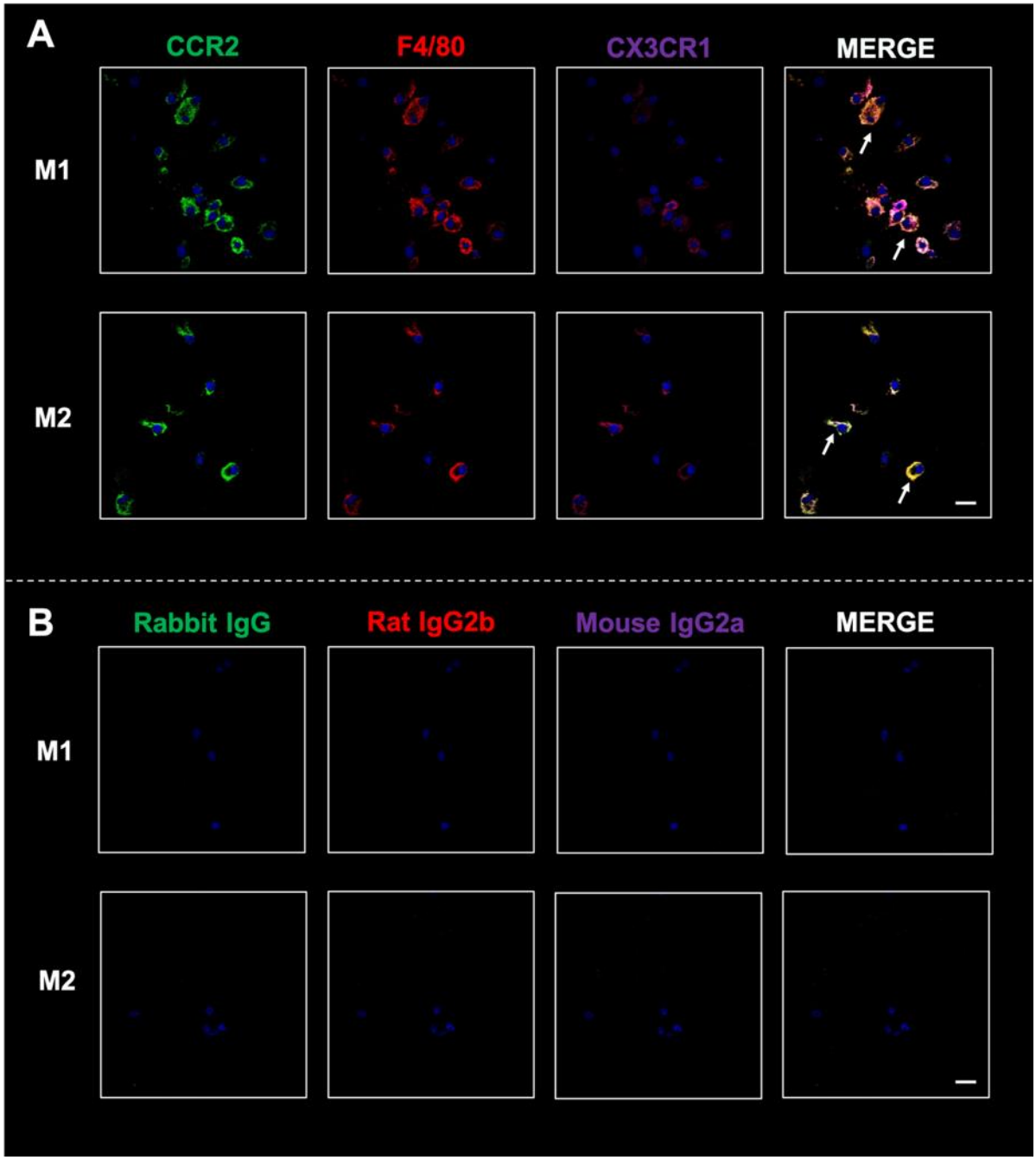

Figure 3.6: BMDM macrophages express CX3CR1, F4/80 and CCR2 leukocyte cell surface markers within the in vitro co-culture model

A) Confocal images (x64 oil) of M1 and M2 BMDMs in 24 hours following a macrophage-crypt co-culture, showing positive expression of CCR2 (green), F4/80 (red), CX3CR1 (magenta) and nuclei (blue). Scale bar at 25µm. **B)** Confocal Images (x63) of antibody-matched IgG, Rabbit (green), Rat IgG (red) and Mouse IgG (magenta) (n=1) Scale bar at 15µm

As the previous results suggest that the M1 and M2 phenotype was maintained throughout its co-culture, we next determined the optimal macrophage: crypt seeding density and

further set out to investigate whether colonic crypts are able to maintain their morphology, were able to proliferate in the presence of macrophages, did not undergo apoptosis and maintained their differentiated epithelial cell types within our crypt-macrophage co-culture model.

3.2.7 Cell density dependent increase in crypt cell EdU incorporation in the presence of Naïve macrophages

To determine whether macrophage can affect colonic crypt growth, co-cultures with increasing Naive macrophage densities were seeded (**Figure 3.7A &B**). Crypts cultured in the presence of Naïve macrophages were treated with EdU on Day 1 following the co-culture as per **Section 2.2.13**. In **Figure 3.7C,** Naïve macrophages significantly increased %EdU incorporation only at a density of $3x10^5$ and $6 x10^5$, colonic crypts at a macrophage density of $8x10^5$ (**Ci**) did not survive compared to $3x10^5$ **(Ci).**

Figure 3.7B, crypts were cultured along with Day 4 monocytes at a density of $6x10^5$, although an increase in the percentage of EdU incorporation was observed a statistical significance was not recorded. In parallel, crypts were also cultured along with Naïve macrophages at an increasing density ranging from $0x10^5$ to $6x10^5$, here a significant increase in the percentage of EdU incorporation was recorded only at a density of $3x10^5$.

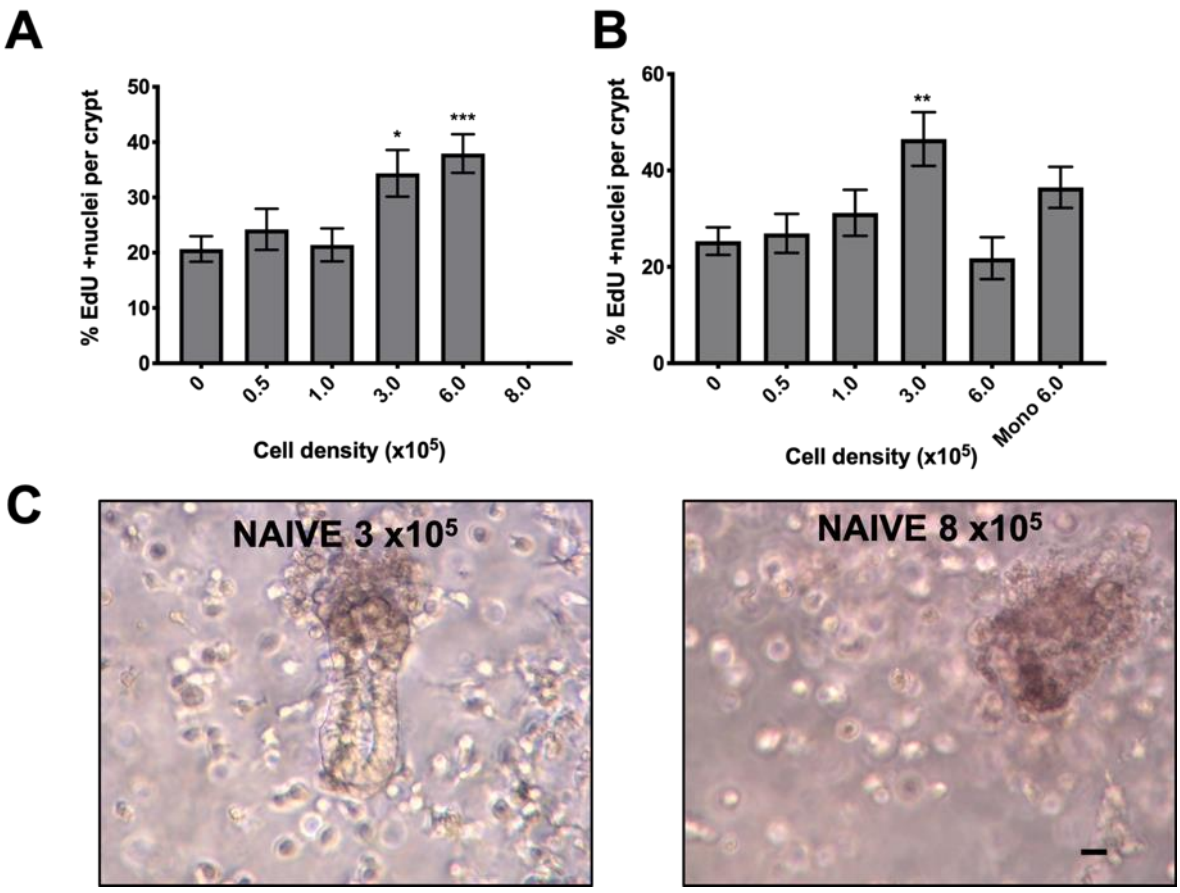

Figure 3.7: **Cell density dependent increase in crypt cell EdU incorporation in the presence of Naïve macrophages**

A) Histogram showing the percentage of EdU positive nuclei under increasing Naïve-macrophage densities (1x10^5). (n=4, N≥73), compared to Control *P<0.05, ***P<0.001). Scale bar at 15µm. **B)** Histogram showing the percentage of EdU positive nuclei under increasing Naïve macrophages (1x10^5) and monocytes (Mono-1x10^5) densities (n=3, N≥46) compared to Control **P<0.01. **C)** Representative images showing *in vitro* crypt-macrophage co-culture under macrophage densities of 3x10^5 and 8x10^5, where colonic crypts disintegrated, and the pH-sensitive culture media developed a yellow tint at the highest density.

As the results suggest that a macrophage seeding density of 3x10^5 is sufficient to initiate a response in colonic crypt cell proliferation while crypt architecture is maintained. To determine whether colonic crypt cell apoptosis is excessively engaged within our crypt-macrophage co-culture model compared to crypts cultured alone, we then sought to identify the differential expression of Caspase-3 within our co-culture model.

3.2.8 Low Caspase-3 expression was observed in all BMDM-crypt co-cultures

To determine whether the BMDM within the *in vitro* macrophage-crypt co-culture cause a change in epithelial cell death, immunofluorescent labelling with an anti-Caspase-3 antibody was performed. **Figure 3.8A** shows an example of a Caspase-3 positive cell within the crypt's base, in which Caspase 3 is expressed within the bounds of the cell's cytoplasm (white arrow). Caspase-3 positive cells identified within the crypt lumen (white arrow-a) or the shedding zone (white arrow-b) were excluded from analysis and not considered to be part of the epithelium. **Figure 3.8B** show representative confocal images of the crypts in macrophage-crypt co-cultures, where macrophages are seeded at a density of $3x10^5$ cells as previously optimised in **Figure 3.7**. There are no significant changes in the number of Caspase3 positive cells in the crypts, when in culture with Naïve, M1 or M2 macrophages (**Figure 3.8C)** however the percentage of Caspase-3 positive cells compared to total number of DAPI-positive cells revealed a significant decrease in Caspase-3 expression in M2-crypt co-cultures (**Figure 3.8D)**.

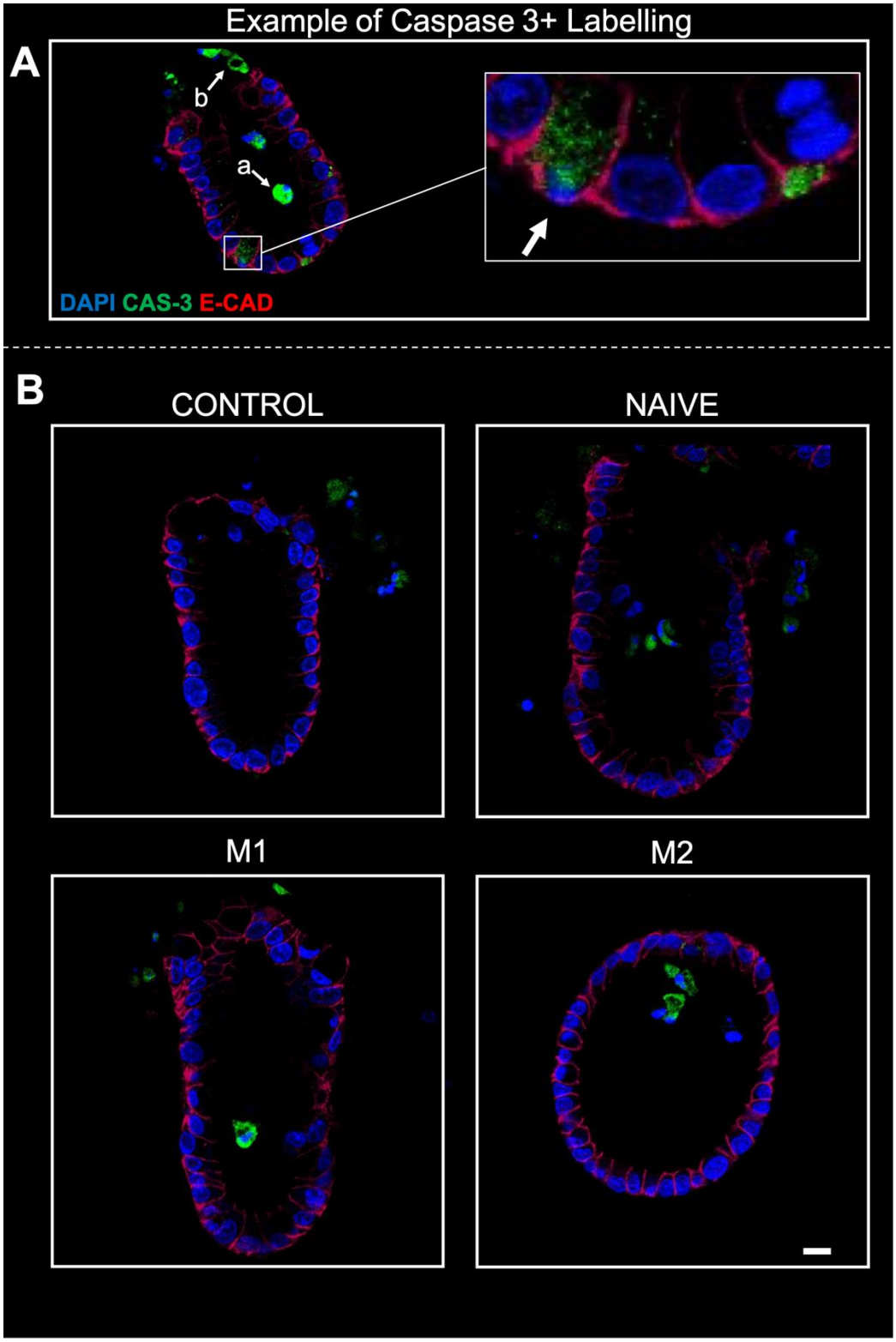
Example of Caspase 3+ Labelling
A
b
a
DAPI CAS-3 E-CAD
B
CONTROL
NAIVE
M1
M2
C
Caspase 3+ cells per crypt
0.5
0.4
0.3
0.2
0.1
0.0
Control
Naive
M1
M2
D
Percentage of Casp3+ cells per crypt
2.0
1.5
1.0
0.5
0.0
*
Control
Naive
M1
M2

Figure 3.8: Expression of Caspase-3 in the colonic epithelium within a 3D macrophage-crypt co-culture.

A) An example of a Caspase-3 positive cell (white arrow) expressed within the crypt epithelium. found within the lumen and crypt surface but are distinctly absent from the colonic epithelium. Positive example shown above (lumen- **a** and shedding area-**b**).
B) Representative confocal images showing Caspase-3 expression (green), nuclei (blue) and E-cadherin (red) in crypt-macrophage subtype co-culture. Caspase-3 expression is found within the lumen and crypt surface but are distinctly absent from the colonic epithelium. Scale bar at 15µm. **C)** Histogram showing the average number of Caspase-3 positive epithelial cells per crypt within each co-culture condition (n=3, N>24) and **D)** Histogram showing the average percentage of Caspase-3 positive epithelial cells per crypt compared to average nuclei count (n=3, N>24, Control vs M2*<P0.05).

Having confirmed that the crypt-macrophage co-culture model is viable and does not induce excessive Caspase-3 expression, we finally determined to confirm whether colonic crypts in *in* vitro culture express the differentiated cell phenotypes commonly present within epithelium.

3.2.9 Colonic epithelial cells express antibody-specific labelling *in vitro* co-culture

To confirm that the colonic epithelium expressed differentiated cell lineages within the epithelium in *in vitro* culture, while IgG controls were utilised to show that immunofluorescent labelling was specific to each of the cell lineages. The immunofluorescent labelling protocol was performed as described in **Section 2.2.12.** It was confirmed that labelling of stem cells (Lgr5+) (**Figure 3.9Ai)**, enteroendocrine cells (Cro-A) (**Figure 3.9Aii)** and tuft cells (DCAMKL1) (**Figure 3.9Aiii)** was antigen-specific. UEA-1 (**Figure 3.9Aiv)** is a fucose-reactive lectin used to stain secretory vacuoles of the epithelial goblet cells and can therefore not be associated with an IgG isotype (**Figure 3.9A**).

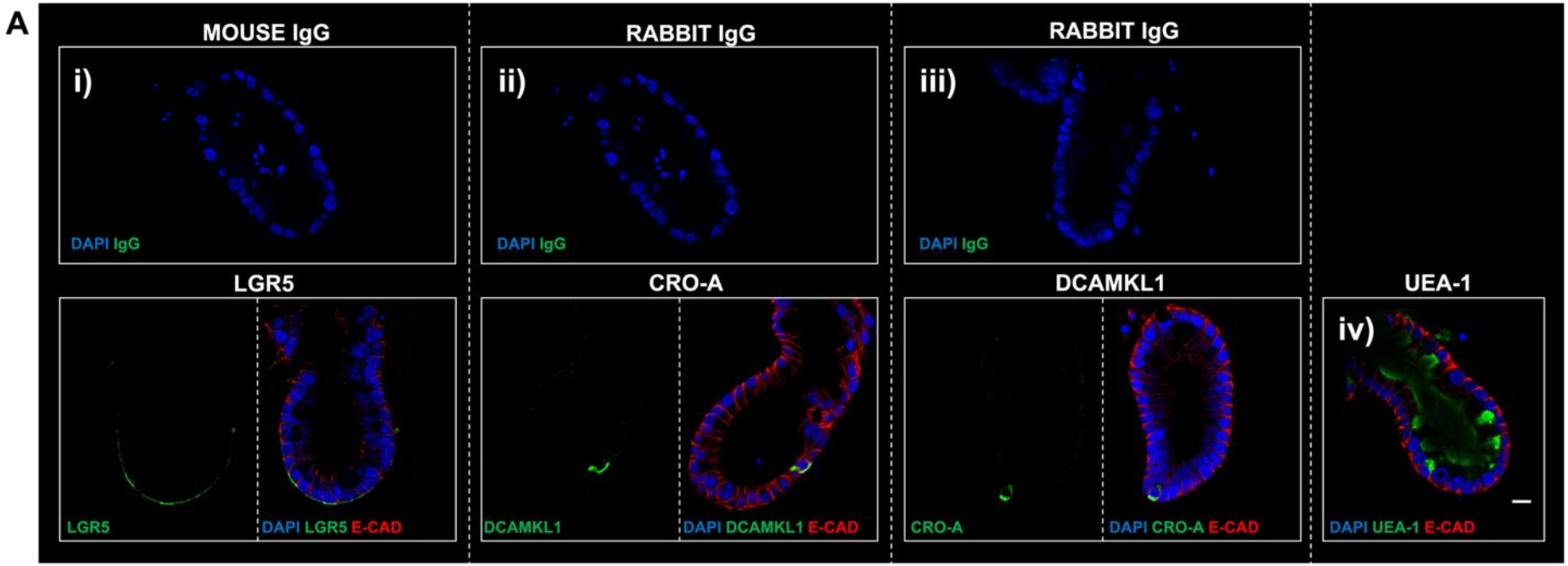

Figure 3.6: Immunofluorescent labelling of Lgr5, Cro-A and DCAMKL1 are antigen-specific to differentiated epithelial cell types

Comparison between the antigen-specific antibody labelling for **Ai)** Lgr5, **Aii)** Cro-A and **Aiii)** DCAMKL1 and its complementary IgG Control and **Aiv)** UEA-1 staining in 3D *in vitro* colonic crypt culture. Scale bar 15µm

In this chapter, the results have characterised, the phenotypes of M-CSF driven differentiation of bone-marrow derived Naïve, M1 and M2 macrophages, the *in vitro* differentiated cell groups of the colonic crypt and the feasible conditions required for the co-culture of macrophages and crypts in order to study its effect on crypt growth and differentiation.

3.3 Discussion

This chapter established the characteristics of *in vitro* bone-marrow derived macrophages following its differentiation in the presence of M-CSF; characterised the phenotypic differences of classically and alternatively activated M1 and M2 macrophages respectively and established the conditions required to conduct the study of colonic crypt growth and differentiation in the presence of bone-marrow derived macrophages within a 3D *in vitro* co-culture model.

Prior to the culture of bone-marrow derived macrophages along with colonic crypts, the phenotype of the macrophage population was first established. Initially, it was confirmed that bone-marrow derived cells cultured in the presence of M-CSF over the course of seven days exhibited macrophage-like characteristics. The effects of CSF on granulocyte differentiation were established in 1987 by Stanley et al, where it was confirmed that hemopoietic progenitor cells within L-cells, can be differentiated into macrophages in the presence of M-CSF (Stanley et al., 1978). Following this further research revealed that the receptor for CSF (CSFR1) is likely expressed on a selective number of cells, specifically, mononuclear phagocytes such as monocytes and macrophages (Guilbert and Stanley et al., 1980), stimulation of CSF-1R causes the downstream activation of the transcription factor PU.1, leading to differentiation towards monocytes and subsequently macrophages (Mossadegh et a., 2013). In 1982, Tushinski et al, also revealed a gradual increase in CSFR1 expression in macrophage when compared to their progenitors and monocytes (Tushinski et al., 1982). Several studies early on have confirmed that cell ruffling, formation of vacuoles and cell spreading are hallmark characteristics of maturing phagocytic macrophages *in vitro* (Tushinki et al., 1982; Boocock et al., 1989, Park et al., 2011). Such characteristics have also been identified within the *in vitro* culture of BMDM in this chapter (**Figure 3.1)**.

Further confirmation of this was observed in the morphological analysis of monocytes and macrophages using flow cytometry, where an increase in cell size and higher granularity was recorded when compared to bone-marrow derived cells on Day 4. Here evidence suggest that the higher granularity is likely caused by the internalisation of CSF-1 within phagocytic macrophages leading to the formation of vacuoles as described by Tushinksi et al, in 1982. To further ensure the differentiation of non-adherent monocytes towards an adherent macrophage population was completed, granulocyte/macrophage-specific cell surface markers were utilised to confirm their phenotypic characteristics.

In the *in vivo* steady state, Ly6C+ 'blood' monocytes were identified to migrate into the colonic mucosa where they undergo differentiation in continuous intermediary stages to form mature macrophages after four to five days (Bain et al., 2013). Differentiation in our *in vitro* culture model also show a high presence of Ly6C+ bone-marrow derived cells on Day 4 in culture and a significant reduction in Ly6C+ cell expression on Day 7 in the presence of M-CSF, thereby suggesting that the 'blood' monocytic characteristics has been lost following the continuous culture of monocytes in M-CSF.

To further characterise the adherent bone-marrow derived cell population, the fractalkine receptor CX3CR1 was identified as a phenotypic mononuclear phagocytic marker and this study confirms that a significant increase in CX3CR1 expression in the adherent BMDM fraction compared to non-adherent monocytes. Regoli et al, have reviewed the multiple functions of CX3CR1+ macrophages including its ability to form transepithelial dendrites to sample luminal antigens, however CX3CR1 expression is commonly present in both macrophages as well as dendritic cells thus further characterisation was needed (Regoli et al., 2013; Chieppa et al., 2006).

As macrophages and dendritic cells are defined as antigen-presenting cells (APC), expression of the major histocompatibility -2 (MHC2) would confirm the presence of such mononuclear phagocytes in culture. Here we show that MHC2 expression was significantly higher in the adherent BMDC fractions compared to non-adherent monocytes, thereby indicated a shift towards a macrophage or dendritic cell phenotype (Shapouri-Moghaddam et al., 2017).

Similarly, the expression of the integrin CD11c, mannose receptor CD206, CD11b were all highly expressed in the adherent BMDC population on Day 7 compared to the non-adherent monocyte fraction confirming that the adherent fraction phenotypically differs from that of

the non-adherent monocyte population. However, according to a number of studies expressions of previously mentioned markers can also be present in dendritic cells, therefore it could not be utilised to differentiate between the bone-marrow derived macrophage and a dendritic cell population (Bain et al., 2013). As F4/80 and the FcγR receptor-CD64 were considered to be definite murine macrophage markers, both non-adherent BMDC on Day 4 and adherent BMDC on Day 7 labelling ultimately confirmed that the adherent fraction shared a macrophage-like rather than dendritic-like phenotype *in vitro* (Hirsch et al, 1981; Tamatounour et al., 2012). Interestingly, macrophages in our *in vitro* are also highly expressed CCR2 within the adherent macrophage compared to the non-adherent monocyte fraction, this contrasts with findings from Bain et al., where CCR2+ Ly6C+ monocytes were shown to be essential for the influx of monocytes into the intestinal tissue *in vivo*. (Bain et al., 2013;). However, our findings do share similarities work from Tsou et al., in which CCR2 knockout mice in the bone-marrow contained an increased number of monocytes (Tsou et al., 2007).

To study the crosstalk of both 'inflammatory' and 'homeostatic' macrophages on colonic crypts, the activation of M1 and M2 macrophages and their respective phenotypic characteristics were also established (Martinez and Gordon., 2014). The now characterised 'Naïve'/non-activated macrophages were polarised with either LPS and IFN-γ or IL-13 and IL-4 towards an M1 or M2 macrophage phenotype, respectively. It should be noted that following polarisation, the macrophages were not further supplemented with M-CSF as this was considered to induce an M2 macrophage phenotype (Zhang et al., 2017).

White light images and histological staining of either sub-type following a 24 hour incubation period did not reveal any discernible morphological differences, however flow cytometric analysis of cell size and granularity, showed that M1 macrophage were marginally more homogenous compared to M2 macrophages a finding which was mirrored in Ying et al's work (Ying et al., 2013).

Cell surface marker analysis of M1 and M2 macrophages within this study were observed to have obtained a similar immuno-phenotype compared to Naïve macrophages previously characterised. To fully differentiate between M1 and M2 macrophages, Lumeng et al, have previously reported that *in vivo* pro-inflammatory cytokines such as IL-6 and TNF-α were predominantly produced by CD11c+ macrophages whereas CD206+ macrophages produced

arginase-1 and IL-10 and thus defining the M1 and M2 macrophages population, respectively (Lumeng et al., 2008). In our study we were able to confirm that M1 macrophages did indeed express high levels of the cell surface marker CD11c compared to M2 macrophages. However, in contrast to both *in vivo* studies from Lumeng and Zhu, we did not observe a significant increase in CD206 expression in M2 macrophages compared to M1. (Zhu et al., 2017). It should also be noted that Jablonski et a's work on immuno-phenotyping of bone-marrow derived M1 and M2 macrophages remarked that the characterisation of M2 macrophages via CD206 is not reliable for flow cytometric detection as M1 macrophages were also found to express arginase-1. Instead CD38 and Egr2 should be used in the future experiments to label distinct M1 and M2 macrophage populations *in vitro.* CD38+ has been recognised to be upregulated macrophages exposed to LPS, where the genetic loss of CD38 resulted in the reduced secretion of IL6, thereby highlighting its likely regulatory role in intestinal inflammation (Amici et al., 2018; Jablonski et al., 2015, Antonios JK, 2013). To define the M2 macrophages, the marker Egr2 was shown to be effective in labelling this sub-population. According to work carried out by Veremeyko and colleagues, they have further revealed that Egr2 appears to be involved in the upregulation of MHC2 and crucially for the differentiation of both M1 and M2 macrophages, it was shown that LPS and IFN-γ treated macrophages such as the M1 macrophages within our cultue system show highly downregulated Egr2 expression, thereby making both CD38 and Egr2 excellent candidates to further differentiate our in vitro BMDM-M1 and M2 macrophage populations (Veremeyko et al., 2018).

An alternatively method of characterising the phenotypic differences between BMDC-derived M1 and M2 macrophages, is to collect and purify the cells RNA for use in quantitative real-time PCR (qPCR), a technique previously utilised to great effect by Jablonski and colleagues, allowing us to represent and compare in vitro CD marker expression levels (Jablonski et al., 2015) more accurately.

One of the hallmarks of M1 and M2 phenotype is shown in its differential capacity to metabolize arginine. In M1 macrophages, iNOS (inducible nitric oxide synthase) aids the oxidation of arginine to nitric oxide (NO) which is then converted to the more stable nitrite and l-citrulline. In contrast M2 macrophages favour the oxidation of arginine via arginase leading to the production of urea instead (Rath et al., 2014). Our study indicates that M1

macrophages accumulate significantly more nitrite *in vitro* culture compared to Naïve and M2 macrophage and as nitrite expression was not elevated in Naïve and M1 phenotypes *in vitro* it can be assumed that the iNOS oxidation pathway was not utilised and can therefore be considered an exclusive M1 macrophage hallmark. Similarly, iNOS expression was also shown to be elevated in colonic tissue *in vivo* in the presence of M1 but not M2 macrophages (Rabbi et al., 2017).

Further analysis of the nitrite expression in colonic crypts cultured with Naïve, M1 and M2 macrophages revealed elevated levels of nitrite only within the M1-crypt co-culture, confirming that M1 macrophages were able to maintain their ability to metabolise arginine to nitrite within the confines of the 3D *in vitro* co-culture model.

Due to the short half-life of nitric oxide, studies were not able to visualise or quantify the presence of nitric oxide in an *in vitro* culture setting until Legett's work identified intracellular nitric oxide in RAW 265.7γ macrophages treated with LPS and IFN-γ (Kelm M, 1998: Legett et al., 2017). Similarly, with the kind aid and donation of a novel fluorescent nitric oxide probe from Dr.Marin's lab at UEA, we were able to visualise the expression of nitric oxide in M1 macrophages but not in Naïve following a 24 hours incubation with the probe, conclusively showing that only M1 macrophage can produce the bactericidal product in our *in vitro* study. Overall, within this study, M1 macrophages can be characterised as CD11c+ and nitrite/NO+ compared to M2 macrophage which are CD11c- and nitrite/NO -.

As macrophages phenotypes in the intestine can be easily influenced by environmental cues within the lamina propria, we next aimed to investigate whether macrophages maintained their antigen-specificity when cultured with colonic crypts, indirect immunofluorescence antibody labelling protocols were established (Bain and Schridde., 2018). The results show that M1 and M2 macrophages both maintained their macrophage-like phenotype when cultured with colonic crypts after 24 hours, as both macrophage sub-types were positively labelled for CCR2, CX3CR1 and F4/80.

Having cultivated and established the phenotypic characteristics of the individual macrophage population, we aimed to validate the feasibility of the culture of colonic crypts with macrophages in a 3D *in vitro* setting, a macrophage-density dependent co-culture model was set up, in which colonic crypt proliferation was quantified. As Skoczek et al, utilised an identical culture system where crypts were cultured with monocytes and

observed an increase in colonic crypt growth, we repeated this experiment in parallel with crypts cultured along with naïve macrophages. The results suggested that a seeding density above $6x10^5$ led to decreased crypt survival while also leading to a loss in crypt architecture. As macrophages are also able to regulate ECM degradation via the secretion of MMP9 which specifically degrades gelatin and type IV collagen, it is likely that the 3D Matrigel was unable to maintain its shape due to increased degradation of collagen IV which makes up 30% of the ECM (Rourke et al., 2019; Corning Matrigel Matrix FAQ, 2021). As a peak EdU incorporation was recorded at a macrophage density of $3x10^5$, this seeding density was utilised in all experiments in the upcoming chapters.

In IBD, elevated levels of apoptosis have been commonly observed and in 2011, Marchiando et al have established that the cleavage of capase-3 is essential for cell shedding to occur in intestinal crypts (Souza et al., 2005, Marchiando et al., 2011). To establish whether the high metabolic activity of Naïve, M1 and M2 macrophages can cause colonic epithelial cell death within our co-culture model, a cleaved capase-3 marker was utilised. Caspase-3 is cleaved through the activation of the apoptotic cascade exposing a unique epitope which can be immunofluorescently labelling, thus allowing the detection of epithelial cell death prior to the occurrence of shedding (West et al., 2009). Injection of LPS into mice, triggered the activation of pro-inflammatory cytokines subsequently initiating an increase in apoptosis in intestinal epithelial cells *in vivo*, whereas a study from Lissner et al., previously reported that caspase-3 expression in HT-29/B6 (colonic adenocarcinoma-cell line) cultured along with M1 or M2 macrophage was not affected (Delgado et al., 2015; Lissner et al., 2015). Within our co-culture model, we report that, Naïve and M1 macrophages did not affect capase-3 expression and instead a reduction in caspase-3 expression was noted in crypts cultured with M2 macrophages. Currently, the mechanisms which have caused the observed reduction in apoptosis have not been studied very well. However, a study in 2018, detected an increase in bcl-2 expression in IL-4 treated M2 macrophages, previously, bcl-2 has been established as a crucial regulator of caspase-3 activated apoptosis, where it is known to inhibit the release of apoptogenic factors such as cytochrome c from the mitochondria. (Tsujimoto et al., 1989; Orrechioni et al., 2018). A study in renal tubular epithelia further observed M2 macrophages inhibited caspase-3 expression via inhibition of ROS-p38 and activation of the P13K/Akt pathway and subsequent upregulation of the target gene bcl-2

(Liu et al., 2019). Furthermore, bcl-2 expression was upregulated at the base of colonic but not small intestinal cells likely limiting apoptosis within the stem cell niche (Merritt et al., 1995). Interestingly, in the latter stages of wound healing in which M2 macrophages are predominantly present, iron accumulation was also increased leading to increased extracellular matrix deposition (ECM), however there is currently no further evidence to support this (Wilkinson et al., 2019). Whether M2 macrophages within this 3D *in vitro* model can inhibit epithelial apoptosis via the aforementioned signalling pathways is yet to be determined. Although caspase-3 was utilised to identify apoptotic cell shedding within the crypt epithelium, the number of necroptotic cells within this study's co-culture cannot be identified as the mechanism of necroptosis functions in a caspase-3 independent manner. To detect necroptosis, we therefore suggest the use of an MLKL phosphorylation antibody, to detect the translocation of MLKL to the necroptotic cell's membrane prior to its destruction (Negroni et al., 2015).

Interestingly, Bhasin et al. have noted genetic variances (eQTLs) in bone-marrow derived macrophages in male and females, while we aimed to isolate BMDM from 8-12-week-old C567BL6 male mice, these were subject to availability and we resorted to isolating BMDMs from female mice on occasions (Bhasin et al., 2008). Furthermore, it should be noted that, although bone-marrow derived macrophages can be isolated and cultured in abundance *in vitro*, macrophage maturation *in vivo* commonly occurs within the intestinal tissue (Bain et al., 2014).

As work from Shaw as well as De Schepper previously highlighted that self-maintaining macrophages are gradually replaced by bone-marrow derived macrophages during adulthood in mice *in vivo*, both tissue-resident macrophages and bone marrow derived macrophages do share some commonalities such as their expression of F4/80, MHC2, CD64 and lack of Ly6C+ (Shaw et al., 2018; De Schepper et al., 2018, Jablonski et al., 2015). However, little is known to which extent the molecular mechanisms and function of the niche-specific tissue-resident macrophage *in vivo* may differ compared to bone-marrow derived macrophages *in vitro* and this will need to be further investigated in the future to allow comparative studies between our BMDM-crypt co-culture model and the *in vivo* environment (Bain et al., 2018; Viola and Boeckxstaens., 2020).

Although it is feasible to culture colonic crypts along with freshly isolated tissue-resident macrophages, there are several disadvantages pertaining such a co-culture model. To isolate and culture tissue-resident macrophages, the mucosa and submucosa must first be enzymatically digested and separated after which the mononuclear phagocytes are then separated via FACS (flow cytometric cell sorting) or MACS (magnetic-activated cell sorting), however this often leads to lower yields (with a typical yield of up to $20x10^5$ macrophages per mouse) while the cells also often undergo more mechanical stress, leading to disrupted cell functionality thereby, reducing the feasibility of a tissue-resident macrophage-crypt co-culture model. Although, tissue-resident macrophages have been described as long lived *in vivo*, comparatively, only around 70% of all human tissue resident macrophages isolated and cultured *in vitro* were viable, whereas 97% of all bone-marrow derived macrophages in our culture remained intact. (Doyle et al., 2021; Bhattacharjee et al., 2018; Andrä et al., 2020; Shaw et al., 2018).

To study epithelial renewal, we were determined to identify the individual differentiated cell populations within the colonic epithelium *in vitro* culture, where the cell lineages were labelled with an antigen-specific marker. As Barker et al., has shown, the actively cycling stem cells within colonic crypts can be labelled with Lgr5, unlike previous markers such as Olfm4, which also labelled for stem cell progenitors (Barker et al., 2007; van der Flier et al., 2009). To label for enteroendocrine cells within the colonic epithelium, the acidic glycoprotein chromogranin-A was utilised as it has been established as a robust marker for enteroendocrine cells (Norlen et al., 2001). Where DCAMKL-1 was previously assumed to be gastrointestinal stem cell marker, work from Gerbe et al, has demonstrated that it exclusively labelled tuft cells in both the small and large intestine, for this reason the anti-DCAMKL1 antibody was utilised to positively identify tuft cells within the co-culture (Gerbe et al., 2009). Unlike the previously used antigen specific labels, UEA-1 staining was utilised to identify goblet cells within the epithelium. Although, UEA-1 staining can label both Paneth cells and goblet cells, the lack of Paneth cells within the colon allows it to be used as solely as goblet cell markers (El-Salhy et al, 2016; Ihara et al., 2018). A crucial marker of the absorptive cell lineage within the colonic epithelium is FABP-1 which was considered to be a definitive marker of epithelial enterocyte cells *in vivo* (Lau et al., 2016). However, we were unable to positively identify colonic enterocytes *in vitro* using a number of

immunofluorescent protocols and to our understanding commercial enterocyte markers specifically for *in vitro* labelling are currently not available.

Conclusion:

The aim of this study was to investigate the effects of macrophages on colonic crypt renewal, to do so, we have developed and characterised, the feasible conditions required for the co-culture model of macrophages and colonic crypts within a 3D *in vitro* environment in this chapter.

The study of the morphological, histological and immuno-phenotypical properties of bone-marrow derived monocytes, Naïve, M1 and M2 macrophages *in vitro* revealed that M-CSF drove the differentiation of bone-marrow derived cells towards a macrophage phenotype following 7 days in culture. We were also able to segregate the M1 and M2 macrophage phenotypes within this study prior to its culture along with colonic crypts. Furthermore, the optimal seeding density ($3x10^5$) required to conduct the co-culture of macrophages and colonic crypts were established and epithelial cell death did not increase in presence of either Naïve, M1 or M2 macrophages. Lastly, immunofluorescence protocols for labelling differentiated epithelial cells and macrophages *in vitro* were established.

Chapter 4: The Effects Of Macrophages On Colonic Crypt Growth And Differentiation

4.1 Introduction:

The intestinal epithelium's rapid rate of regeneration can be largely credited to the highly preserved Lgr5+ stem cell population residing at the base of the intestinal crypt (Barker et al., 2007). This intestinal stem cell niche is regulated via autocrine signalling but can also be influenced by a number of external stimuli, produced by various sub-epithelial cell types (Sailaja et al., 2016). Myofibroblasts, smooth muscle cells, neurons and mononuclear phagocytes such as monocytes, dendritic cells and macrophages and their finely regulated secretion of paracrine signals, such as Wnt, BMP, R-spondin, Notch and Hedgehog can dictate the rate of stem cell division and differentiation and is crucial for maintaining intestinal homeostasis and renewal (Santos., 2018).

Initially, monocytes are recruited and terminally differentiate into residential CX3CR1+ macrophages following environmental conditioning (Regoli et al., 2017). In a steady state, macrophages can take on a CX3CR1+, CD206+ anti-inflammatory (M2) signature (Isidro et al., 2016). Residential macrophages can play a number of important functions which are essential for maintaining intestinal homeostasis (Viola and Boeckxstaens., 2020). Macrophages are perfectly positioned in the sub-epithelial lamina propria in order to sample and clear foreign antigens and microorganisms, where CX3CR1 + macrophages were even able reach through the epithelium to sample luminal contents and the number of bacteria such as *Salmonella* Typhimurium penetrating through the epithelial barrier significantly increased in the absence of such CX3CR1+ cells, highlighting the importance of their presence in the intestine (Niess et al., 2005; Chieppa et al., 2006; Man et al., 2016).

Due to the high concentration of commensal bacteria within the colon, residential macrophages have been homed to be tolerogenic to the microbiota and highly phagocytic in its steady state (Liu et al., 2018). Residential macrophages play a critical role in tissue remodelling following injury, where inflammatory M1 and anti-inflammatory M2 macrophages play differential roles in wound repair (Yi Rang N et al., 2019). M2

macrophages act as the early responders to epithelial damage and remove cell debris and apoptotic cells in a non-inflammatory manner as they are hyporesponsive to toll like receptors (TLR) stimulation (Smythies et al., 2005). Furthermore, this sub-type can secrete a number of anti-inflammatory cytokines/chemokines in order to downplay injury-induced inflammation (Orecchioni et al., 2019). An example of a major player in wound repair is IL-10 which is secreted by M2 macrophages in large quantities and where its downstream target of CREB, leads to the secretion of the WNT1 inducible signalling protein WISP-1 and consequently aids epithelial proliferation and barrier function (Quiros et al., 2017; Morhardt et al., 2019). Epithelial repair is further encouraged by M2 macrophages' cytokine product TGF-β which promotes fibrosis following injury (Wick et al., 2010). In contrast, classically activated M1 macrophages regulate wound repair via the secretion of bactericidal and pro-inflammatory cytokines such as IL-6, IL-1β, TNF-α and iNOS production, aiding the removal of intracellular infections within the lamina propria (Jones et al., 2018). Over the years, *in vitro* studies have utilised a Naïve macrophage population, often referred to as an uncommitted or resting phenotype to compare their characteristics to M1 and M2 macrophages (Jablonski et al., 2015; Zhao et al., 2017; Antonios et al., 2013). However, it is currently unclear to which extent the function of Naïve macrophage differs to its M1 and M2 macrophage counterpart and whether such a phenotype can exist in an *in vivo* setting.

Intestinal macrophages also act as bridge to the adaptive immune system. Both macrophage sub-types and T-cells are grounded in a continuous feedback loop where, M1 and M2 macrophages can both be polarised by Th1 and Th2 mediated cytokines, respectively. Inversely, M2 Macrophages mediated IL-10 and TGF-β secretion can lead to the expansion and induction of regulatory T-cells and M1 secretory cytokines promote the activation and differentiation of Th1 and Th17 cells. (Zigmond and Jung., 2014; Mosser et al., 2008). Recent studies have shown that M1-mediated secretion of IL-1β enhances ILC3-cell mediated IL-22 production, thereby indirectly contributing to the restoration of the epithelial barrier following injury (Yang et al., 2019). In chronic inflammatory diseases however, Th1 and M1 mediated secretion of TNF-α can disrupt the epithelial integrity of the crypt thus leading to further inflammation (Schmitz et al. 1999; Mantovani et al., 2012; Shapouri-Moghaddam et al., 2017). The importance of regulatory T-cells in controlling intestinal homeostasis was also

highlighted in a study in which increased cases of colitis was recorded in T-cell deficient mice (Josefowicz et al, 2012).

While it has been established that M1 and M2 macrophages can influence intestinal homeostasis through T-cell crosstalk, rapid clearance of apoptotic cells and restoration of epithelial barrier function (Henson., 2005; Bain and Mowatt., 2011), increasing evidence suggests that such macrophage may also be major constituent in the regulation of stem-cell driven epithelial renewal (Pull et al., 2005; Sehgal et al., 2018; Yang et al., 2019).

A few studies have hinted at the importance of the physical presence of macrophages near the epithelium and its potential impact on the intestinal stem cell niche. Previously, Pull et al have shown that the macrophage presence near crypt bases increases following DSS (dextran sodium sulfate) treatment, this was followed by the classical activation of M1-like macrophages which made cell-cell contact with the colonic epithelial progenitor cell niche via short cellular processes (Pull et al., 2005).

In addition, a study in the small intestine demonstrated that macrophage depletion via the blocking of CSF1 signalling led to a depletion of Lgr5+ stem cells and reducing Ki67+ progenitor cell numbers thereby impairing homeostasis (Seghal et al., 2018).

The intestinal macrophage's ability to secrete pro and anti-inflammatory cytokines to indirectly influence epithelial regeneration have also been showcased in a number of studies (Duque and Descoteaux., 2014). A recent *in vivo* study highlighted the potency of M1 macrophages secreted factors, in which its ability to secrete IL-1β led to the ILC3-mediated synthesis of IL-22, a cytokine crucially required for the restoration of the epithelial barrier in DSS-induced mice (Yang et al., 2019). In the small intestine, the secretion of the anti-inflammatory cytokine IL-10 by residential macrophages following epithelial injury played a major role in re-epithelisation although the mechanism behind this remains unclear (Mathilde J.H et al., 2015; Morhardt et al., 2018).

Interestingly, macrophages have also proven to be a reliable source of Wnt, a known promoter of cellular proliferation. Macrophage-derived extracellular vesicles (EV) were shown to carry Wnt ligands, inducing β-catenin activity and thereby increasing epithelial proliferation. Saha et al were able to demonstrate that these EVs play a crucial role in inducing regeneration in crypts following radiation injury. Deletion of the *Porcn* gene (a Wnt

gene) specifically within the macrophages led to the removal of the EVs and subsequent depletion of secretory Wnt (Saha et al., 2016).

While previous research has focused on identifying individual elements of the liaison between macrophages and the intestinal epithelium, this chapter takes on a broader perspective by firstly aiming to determine the effects non-activated (Naïve), classical (M1) and alternatively (M2) activated macrophages have on the colonic crypt growth and differentiation. As in an *in vivo* setting intestinal macrophage quickly differentiate based on the environmental cues provided to them in the lamina propria (Hine and Loke., 2019). Our findings in this chapter highlight the differential effects the macrophages sub-populations, can have on colonic crypt proliferation and the crypt differentiated cell lineages in our 3D macrophage-crypt co-culture.

4.2 Results:

To determine whether non-activated (Naïve), inflammatory (M1) or anti-inflammatory (M2) BMDM play a role in regulating stem cell driven renewal within colonic crypts, a novel macrophage-crypt co-culture model was utilised as per **Section 2.2.8**.

4.2.1 Naïve, M1 and M2 macrophages increase colonic EdU incorporation *in vitro* colonic crypt

To determine crypt growth in each of the Naïve, M1 and M2 co-cultures, an EdU click-iT kit was used as per **Section 2.2.13**. Representative epi-fluorescent images of EdU incorporation in colonic crypts in the presence of Naïve, M1 or M2 co-cultures for 48 hours are shown in **Figure 4.1A,** where DAPI positive cells are labelled in red and EdU positive cells are labelled in green. A significant increase in EdU incorporation was found in all macrophage-crypt co-cultures (Naïve, M1 and M2), at a macrophage's density of $3x10^5$. Furthermore, EdU incorporation in crypts when cultured with M1 macrophages was significantly higher compared to crypts co-cultured with Naïve or M2 macrophages (**Figure 4.1B**). Having shown that Naïve, M1 and M2 macrophages are able to induce an increase in colonic crypts cell proliferation when cultured with colonic crypts, we next sought to determine the macrophages sub-population can have on the differentiated crypt cell population within our *in vitro* 3D macrophage-crypt co-culture model.

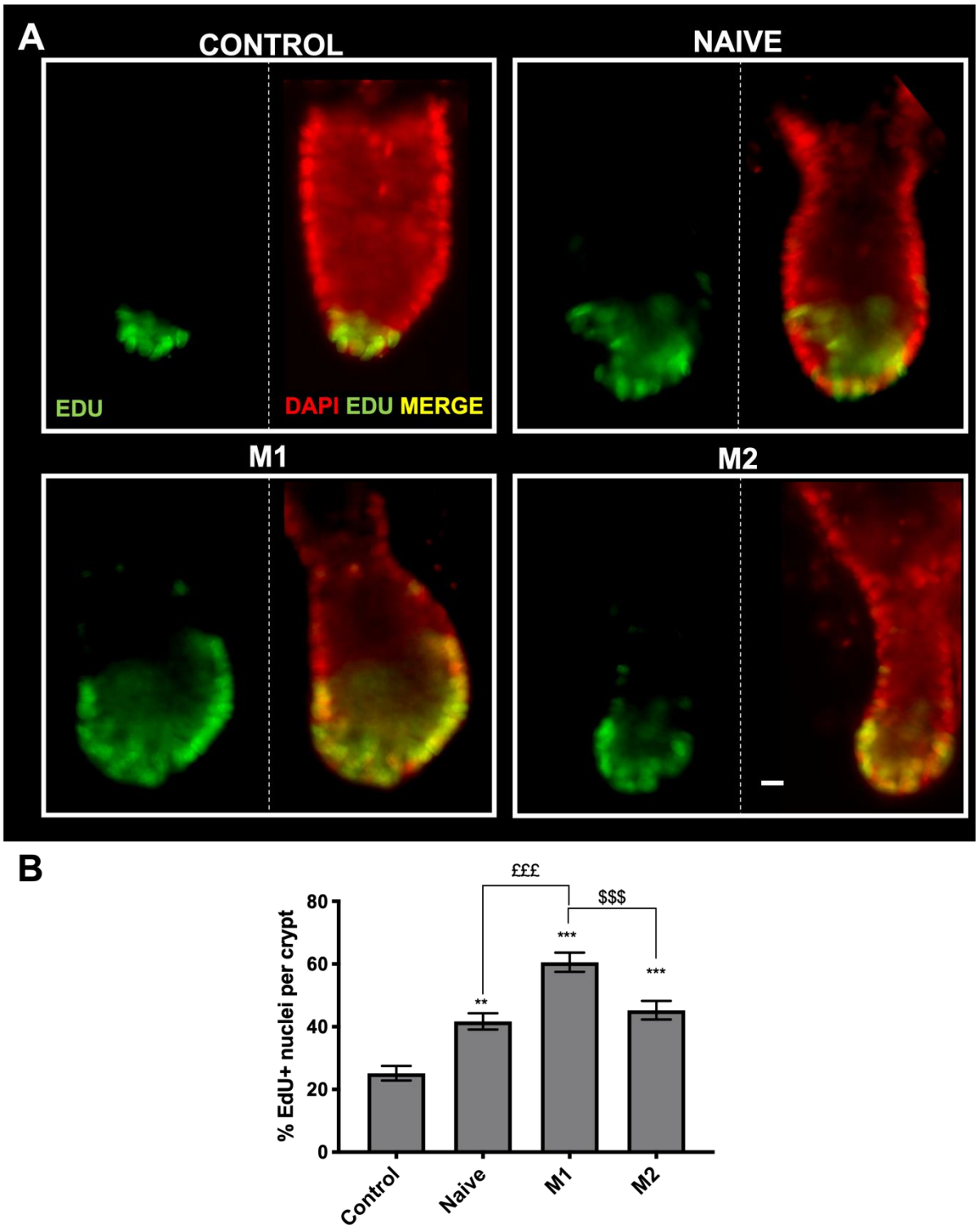

Figure 4.1: Macrophages increase EdU incorporation of colonic crypts in *in vitro* co-culture

A) Representative epi-fluorescent images showing EdU incorporation (green) in the nuclei (red) within colonic crypt-macrophage co-cultures. Co-labelling of nucleus and EdU shown in yellow **B)** Histogram showing the percentage of EdU positive nuclei per crypt within the macrophage subtype

co-culture condition. condition (n=3 N≥107, compared to control **P<0.01, ***P< 0.001; Naïve compared to M1 $$$ P< 0.001; M2 compared to M1 $$$ P< 0.001). Scale bar 20µm

4.2.2 Macrophages maintain Cro-A+ enteroendocrine expression in colonic crypts

To identify enteroendocrine cells within the colonic epithelium, Chromogranin-A (Cro-A), a glycoprotein which specifically binds to monoamine-storing cells within the GI tract was used (Engelstoft et al., 2015). In **Figure 4.2A**, representative confocal images show Cro-A positive in white, where the labelling is predominantly located at the basal side of the crypt and confined by the cell's borders, visualised with labelling of E-cadherin (a cell-cell adhesion molecule) shown in red, while the nucleus is positioned inwards, facing the luminal side of the epithelium.

Comparison of the number of Cro-A positive cells in the crypt when in co-culture with Naïve, M1 and M2 macrophages showed no significant changes in the number of Cro-A positive cells expressed per crypt (**Figure 4.2B**) or percentage of Cro-A positive cells compared to per crypt (**Figure 4.2C**). To further understand the role of macrophages on Cro-A differentiation, the distribution of Cro-A positive cells within the epithelium were analysed. In control crypts, Cro-A distribution was similar at the base, mid or top region of the epithelium. When Naïve, M1 and M2 macrophages were co-cultured along with colonic crypts, Cro-A positive cell numbers were also maintained throughout the base region of the crypt and no significant changes were observed at the mid and top region of crypts (**Figure 4.2D**).

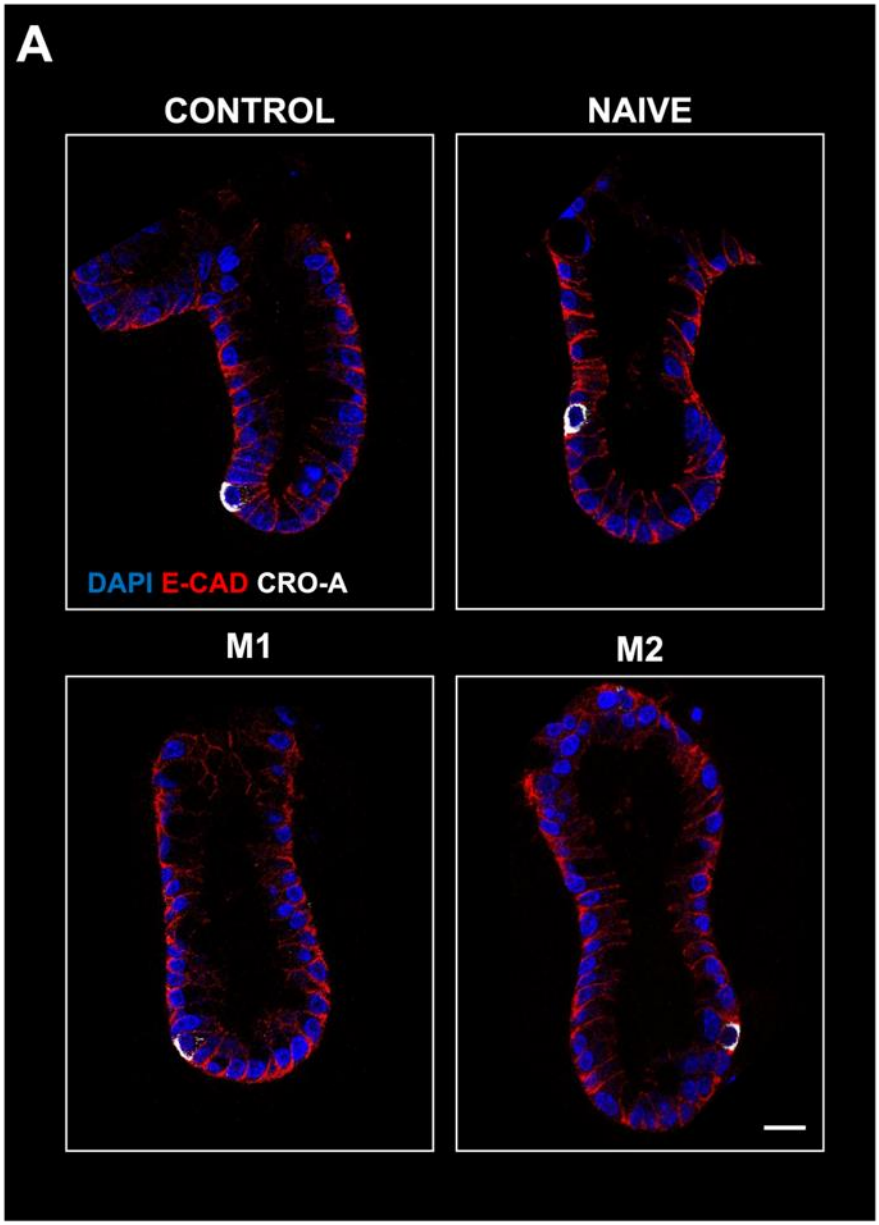
A
CONTROL
NAIVE
DAPI E-CAD CRO-A
M1
M2

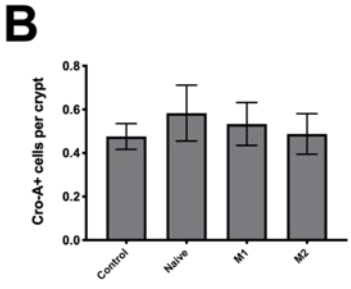
B
Cro-A+ cells per crypt
0.8
0.6
0.4
0.2
0.0
Control
Naive
M1
M2

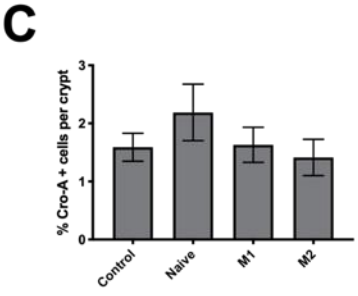
C
% Cro-A + cells per crypt
3
2
1
0
Control
Naive
M1
M2

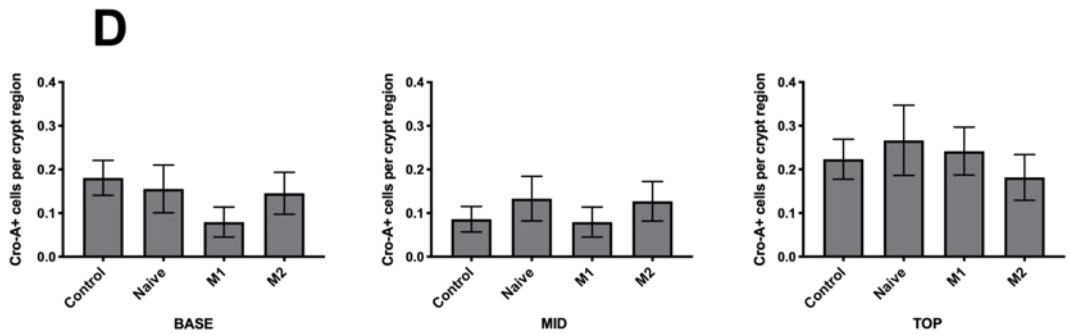
D
Cro-A+ cells per crypt region
0.4
0.3
0.2
0.1
0.0
Control
Naive
M1
M2
BASE
MID
TOP

Figure 4.2: Macrophages maintain *in vitro* Cro-A+ cell expression in colonic crypts in co-culture model

A) Representative confocal images showing Chromogranin-A expression (white), DAPI (blue) and E-cadherin (red) in crypt-macrophage subtype co-culture. Scale bar 20µm **B)** Histogram showing the average number of Cro-A positive cells per crypt within each co-culture condition **C)** Histogram showing the percentage of Cro-A positive cells per crypt within each co-culture condition.). **D)** Histogram showing the position of Cro-A positive cells within each crypt region (base, mid, top). *(n=4, N≥ 36, ns).*

4.2.3 Naïve and M1 macrophages reduce UEA-1+ goblet cell expression in colonic crypts

To determine any differential changes in goblet cell expression within each macrophage subtypes, the lectin *Ulex europaeus agglutinin* (UEA-1) was used. UEA-1 has a high binding affinity to the mucosal product α1,2-fucose, which is primarily produced by colonic goblet cells (Sato et al.,1986; Goto et al., 2016).

Following immunofluorescent labelling with UEA-1, images were captured on confocal microscope. **Figure 4.3A,** show representative images of UEA-1 positive cells within the colonic epithelium in co-culture with Naïve, M1 or M2 macrophages for 24 hours. UEA-1 staining shown in green is displayed throughout the crypt lumen, with E-cadherin (cell-cell adhesion molecule) shown in red and DAPI positive cells shown in blue. UEA-1 positive cells (white arrows) can be identified via the labelling of its intracellular vacuolous space which often where the UEA-1+ mucus extends out from the cell into the lumen. In **Figure 4.3B**, the number of UEA-1 positive cells per crypt were compared to in the presence of Naïve, M1 or M2 macrophages. Notably, the number of UEA-1 positive cells per crypt is significantly reduced in crypts co-cultured with both Naïve and M1 macrophages but not in the presence of M2 macrophages. (**Figure 4.3B**). Similarly, the percentage of UEA-1 positive cells per crypt compared to the total number of DAPI positive cells show a significant decrease in UEA-1 positive cell expression when cultured with Naïve or M1 macrophages. (**Figure 4.3C**).

The position of UEA-1 positive cells within the epithelium were also analysed in **Figure 4.3D**. Control crypts show that most UEA-1 positive cells are found in the mid and base region of the crypt, with the least located at the top region of the crypt. This pattern of distribution is also maintained in crypts in culture with M2 macrophages. In crypts cultured in the presence of Naïve macrophages, the number of UEA-1 positive cells found in the mid region was significantly decreased, where expression at the base and top were maintained compared to control crypts. Within the M1-crypt co-culture model, UEA-1 positive cells were maintained in base region compared to control; however, a significant decrease was recorded at the mid and top region of the crypt (**Figure 4.3D**). Having established that Cro-A+ enteroendocrine cell numbers were unaffected in crypts cultured with Naïve, M1 or M2 macrophages and that the culture of Naïve or M1 macrophages caused a reduction in UEA-1+ goblet cells colonic crypts, we finally aimed to determine whether the differentiated DCAMKL1+ tuft cell lineage is affected by the presence of either Naïve, M1 or M2 macrophages *in vitro.*

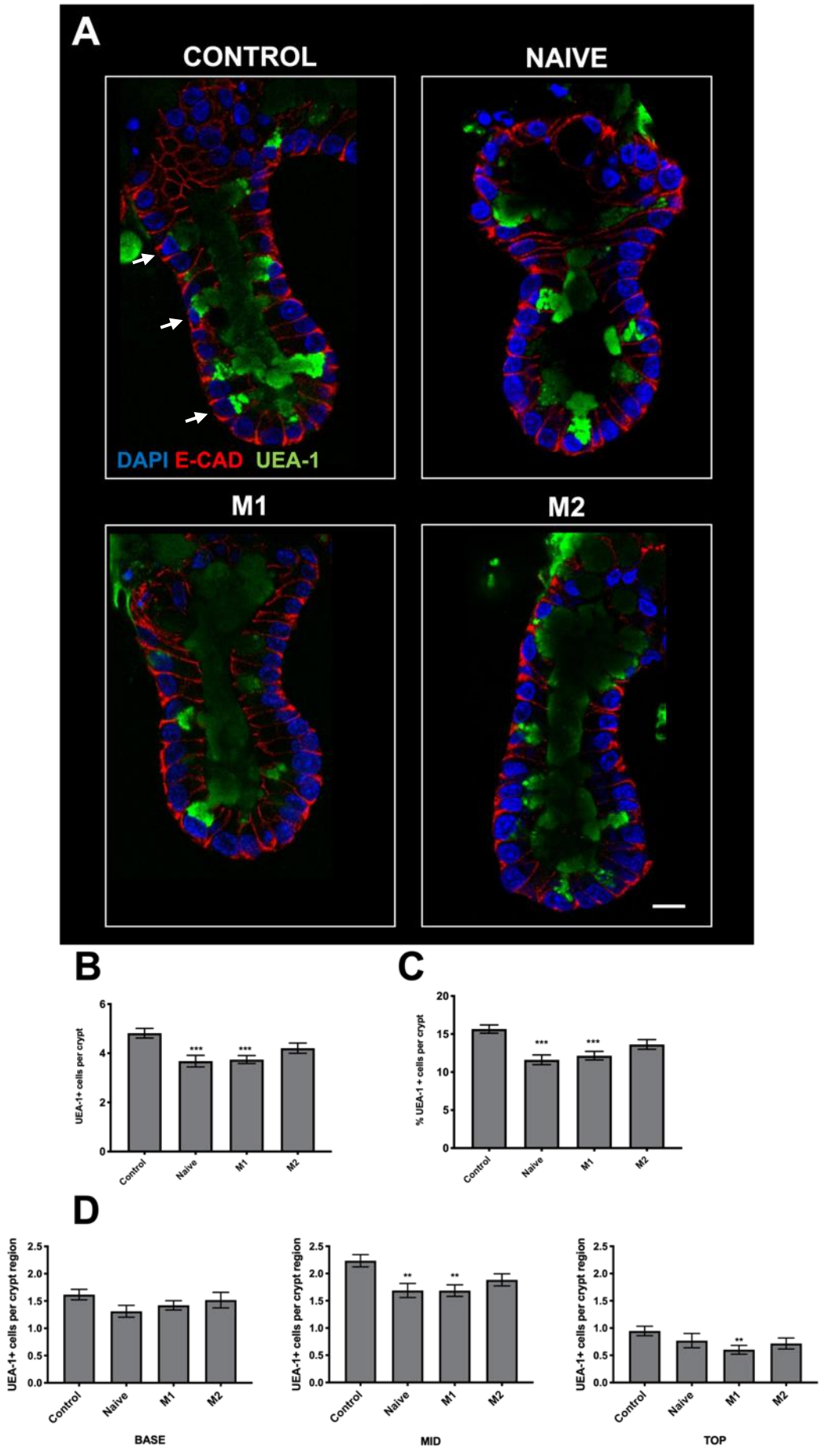
A
CONTROL
NAIVE
DAPI E-CAD UEA-1
M1
M2
B
UEA-1+ cells per crypt
***
***
Control
Naive
M1
M2
C
% UEA-1 + cells per crypt
***
***
Control
Naive
M1
M2
D
UEA-1+ cells per crypt region
Control
Naive
M1
M2
BASE
**
**
MID
**
TOP

Figure 4.3: Naïve and M1 but not M2 macrophages reduce *in vitro* UEA-1+ cell expression in colonic crypts within the co-culture model

A) Representative confocal images showing UEA-1 expression (green), DAPI (blue) and E-cadherin (red) in each crypt-macrophage subtype co-culture **B)** Histogram showing the average number of UEA-1 positive cells per crypt within each co-culture condition **C)** Histogram showing the percentage of UEA-1 positive cells per crypt within each co-culture condition. **D)** Histogram showing the position of UEA-1 positive cells within each crypt region (base, mid,top.) *(n=5, N≥ 63, **P <0.01 ***P<0.0001 compared to Control).* Scale bar 20μm.

4.2.4 M1 macrophages reduce DCAMKL1+ tuft cell expression in colonic crypts

To identify tuft cells within the colonic epithelium, current studies have shown that only labelling for DCAMKL1 (doublecortin and calcium/calmodulin-dependent protein kinase-like 1) is considered to be a robust tuft cell specific marker (Gerbe et al., 2009).

Figure 4.4A shows representative confocal images of DCAMKL1 positive cells in the crypt epithelium when cultured with Naïve, M1 and M2 crypt co-cultures for 24 hours. DCAMKL1 positive cells are visualised by green intracellular labelling enveloping DAPI (blue) positive within the confines of the E-cadherin (cell-cell adhesion molecules) borders.

Analysis of DCAMKL1 positive cell numbers in crypts cultured with Naïve, M1 and M2 macrophages only revealed a significant reduction in crypts when cultured in the presence of M1 macrophages, although a non-significant downward trend was also noted in crypts within the Naïve and M2 co-culture models (**Figure 4.4B**). Further statistical analysis of the datasets revealed that an average of 2.8% (± 0.05) of all crypts contain at least a single DCAMKL1 positive epithelial cell when cultured with M1 macrophages compared to Naive (9.5%± 0.05), M2 (7.7% ± 0.08) and control (16.1% ± 0.06), where these quantifications were made based on DCAMKL1 positive cells present on the equatorial plane.

In **Figure 4.4C**, the percentage of DCAMKL1 positive cells per crypt compared to the total number of DAPI positive cells per crypt are shown, revealing a significant decrease in DCAMKL1 expression in crypts cultured with M1 macrophages, but not with Naïve or M2 macrophages.

Analysis of the average position of each DCAMKL1 positive cells in **Figure 4.4D** revealed no significant differences in the base, mid and top region in crypts when cultured with Naïve, M1 and M2 macrophages compared to control.

As we have now established the differential effects Naïve, M1 or M2 macrophages have on the colonic crypts differentiated cell population, next, we aimed to determine their effect on the Lgr5+ stem cell population in crypts cultured with Naïve, M1 or M2 macrophages *in vitro.*

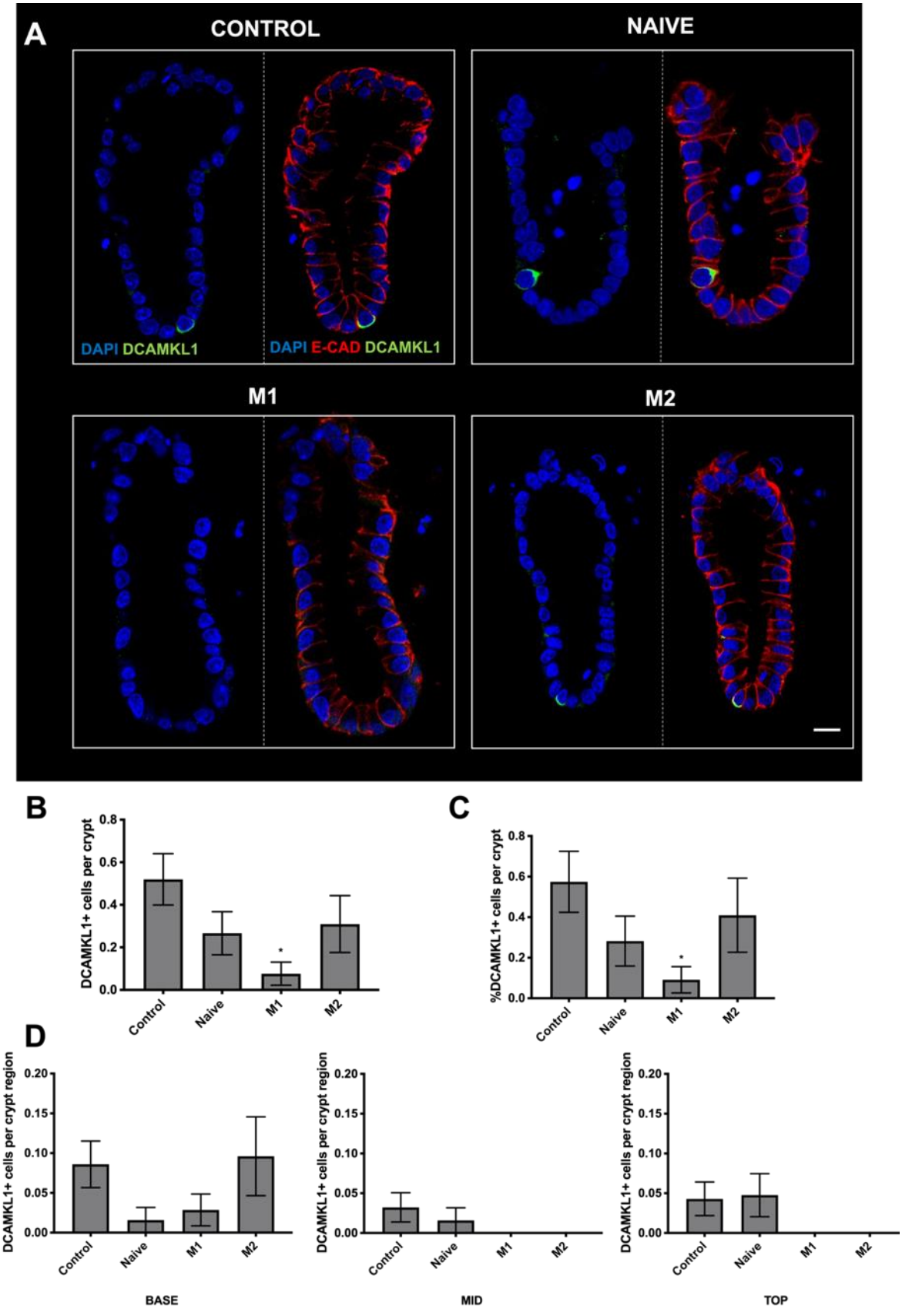
A
CONTROL
NAIVE
M1
M2
DAPI DCAMKL1
DAPI E-CAD DCAMKL1
B
DCAMKL1+ cells per crypt
0.0
0.2
0.4
0.6
0.8
Control
Naive
M1
M2
*
C
%DCAMKL1+ cells per crypt
0.0
0.2
0.4
0.6
0.8
Control
Naive
M1
M2
*
D
DCAMKL1+ cells per crypt region
0.00
0.05
0.10
0.15
0.20
Control
Naive
M1
M2
BASE
MID
TOP

Figure 4.4: M1 macrophages but not Naïve and M2 reduce *in vitro* DCAMKL1+ cell expression in colonic crypts within the co-culture model

A) Representative confocal images showing DCAMKl1 expression (green), DAPI (blue) and E-cadherin (red) in each crypt-macrophage subtype co-culture **B)** Histogram showing the average number of DCAMKL1 positive cells per crypt within each co-culture condition **C)** Histogram showing the percentage of DCAMKL1 positive cells per crypt within each co-culture condition. **D)** Histogram showing the position of DCAMKL1 positive cells within each crypt region (base, mid, top). (*n=5, N≥52, *P<0.05 compared to Control).* Scale bar 20µm.

4.2.5 M1 macrophages increase Lgr5+ stem cell expression in colonic crypts

Stem cell expression within the co-culture model was quantified via the basal epithelial expression of cell surface marker Lgr5 (leucine-rich G protein coupled receptor 5), a Wnt target gene commonly expressed on actively cycling columnar cell within the stem cell niche (Barker et al., 2007).

Representative confocal images expression showing basal expression of Lgr5 on the colonic epithelium in Naïve, M1 or M2 co-cultures cultured for 24 hours are shown **Figure 4.5A**, here a Lgr5 gradient, originating from the base of the crypt and gradually weakening towards the upper regions is visualised in green and Lgr5 positive cells were identified as per **Section 2.3.3.**

Lgr5 positive cell expression is maintained within Naïve and M2 macrophage co-cultures, however a significant increase from 3.6% (± 0.26) to 6.0% (± 0.48) Lgr5+ cells per crypt were recorded in the M1 co-culture compared to control crypts (**Figure 4.5B**).

The histogram in **Figure 4.5C** shows the percentage of the total number of Lgr5 positive cells compared to the total number of DAPI positive cells per crypt revealing a significant increase in Lgr5+ cell expression in crypts in the M1 co-culture model compared to control crypts.

In contrast, the expression of Lgr5 positive cells in crypts cultured in the presence with Naïve or M2 macrophages were maintained compared to control crypts. (**Figure 4.5C**).

The distribution of Lgr5+ cells along the longitudinal crypt-axis in culture with Naïve, M1 and M2 macrophages compared to control are shown in **Figure 4.5D**. In control crypts, the basal and mid region was shown to contain the majority of Lgr5 positive cells with the least

expressed at the top. Crypts cultured in the presence of Naïve and M2 macrophages also share this pattern of expression and no significant changes in Lgr5 positive cell distribution at the base, mid or top of the crypt region was noted when compared to control crypts. In contrast, a significant increase in Lgr5 positive cell expression was found in crypts cultured with M1 macrophages at the base and mid region of the epithelium but not at the top. Here in both, the basal and mid region of the crypt, at least one additional Lgr5 positive cell was found compared to control crypts.

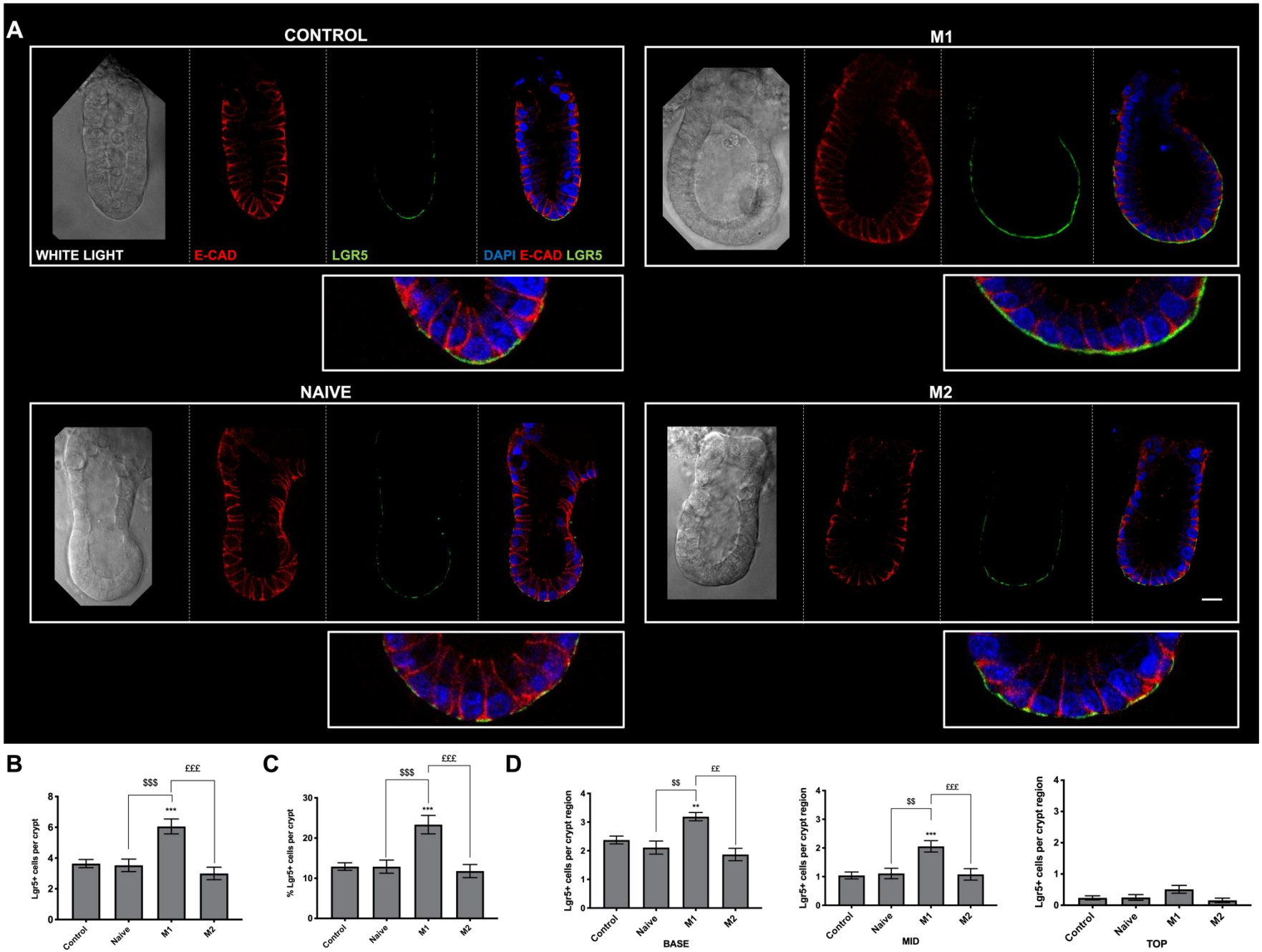
A
CONTROL
M1
NAIVE
M2
WHITE LIGHT
E-CAD
LGR5
DAPI E-CAD LGR5
B
Lgr5+ cells per crypt
C
% Lgr5+ cells per crypt
D
Lgr5+ cells per crypt region
BASE
MID
TOP
Control
Naive
M1
M2

Figure 4.5: M1 but not Naïve or M2 macrophages increase *in vitro* Lgr5+ cell expression in colonic crypts within the co-culture model

A) Representative confocal images showing Lgr5 expression (green), DAPI (blue), E-cadherin (red) and brightfield (white) in each crypt-macrophage subtype co-culture **B)** Histogram showing the average number of LGR5 positive cells per crypt within each co-culture condition **C)** Histogram showing the percentage of Lgr5 positive cells per crypt within each co-culture condition. **D)** Histogram showing the position of Lgr5 positive cells within each crypt region (base, mid, top). *(n=4, N≥36 **P<0.01 compared to control, ***P<0.001; Naïve compared to M1 $^{\$\$}$ P<0.01; M2 compared to M1 $^{£££}$ P<0.001; $^{££}$ P< 0.01).* Scale bar 20µm.

4.2.6 M1 macrophages increase Lgr5 fluorescence intensity in colonic crypts

As Lgr5 is commonly expressed on the basal surface of the colonic crypt, semi-quantative analysis of the fluorescence intensity of Lgr5 expression was performed as per **Section 2.3.4** in order to determine changes in receptor expression in each co-culture condition.

In **Figure 4.6A** the average Lgr5 fluorescence intensity within each crypt co-culture with Naïve, M1 and M2 macrophages are shown. A significant increase in fluorescence intensity was observed at the base and mid regions of crypts cultured with M1 macrophages. Crypts from the M2-macrophage co-culture model however displayed a significant decrease in Lgr5 fluorescence intensity in all regions of the crypt (base, mid and top). When crypts were cultured alongside Naïve macrophages, a significant decrease in fluorescence intensity was only observed in the mid region of the crypt (**Figure 4.6B**).

Overall investigation into the effects of Naïve, M1 and M2 macrophages on colonic crypt growth and differentiation have been summarised in **Table 6.**

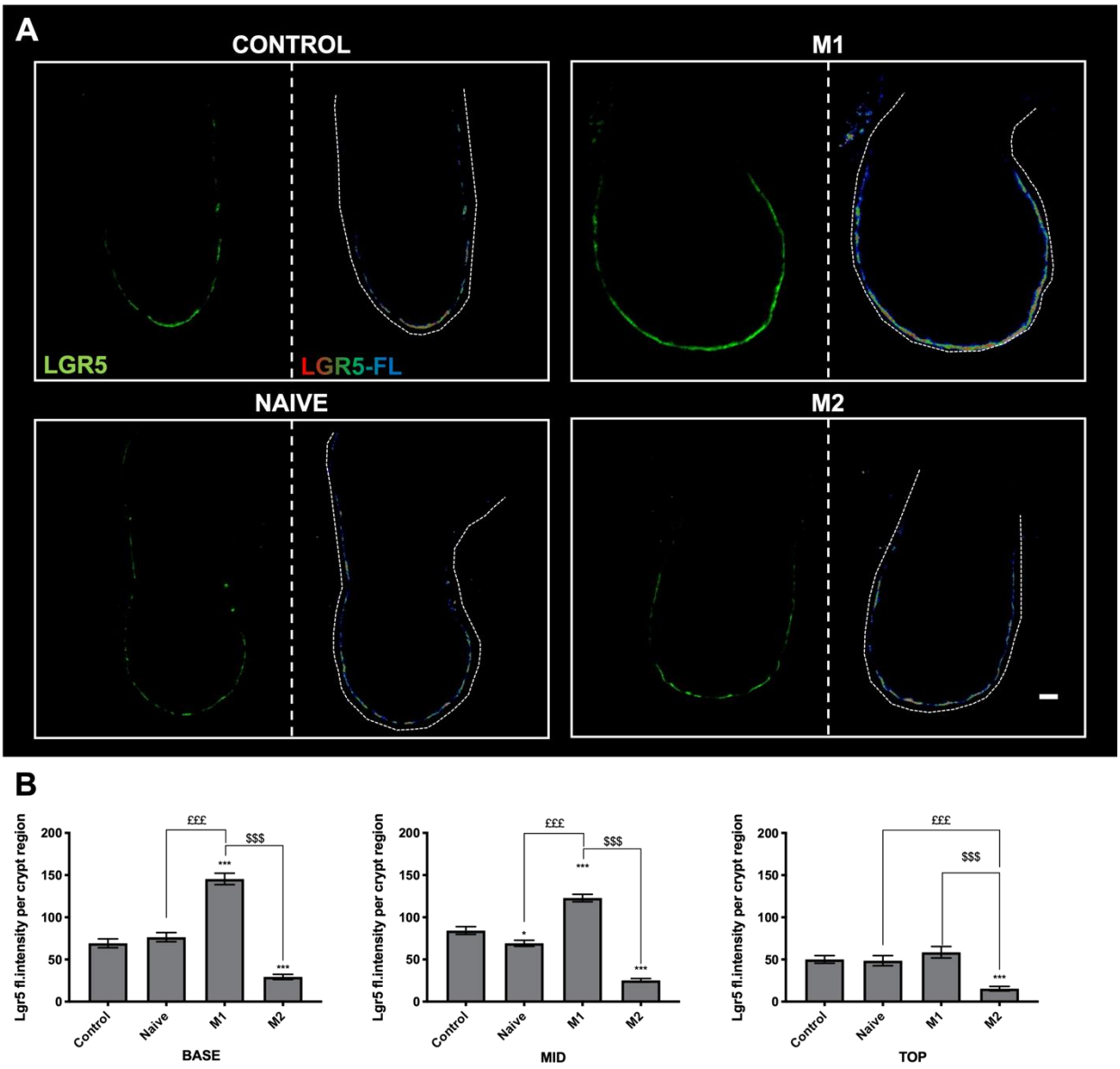

Figure 4.6: M1 but not Naïve or M2 macrophages increase *in vitro* Lgr5 fluorescence intensity in colonic crypts within the co-culture model

A) Representative confocal images showing the fluorescence intensity of Lgr5 (RBG heat map) in each crypt-macrophage subtype co-culture, where blue and red labelling indicate the maximum and minimum fluorescence value expressed, respectively **B)** Histogram showing average fluorescence intensity (arbitrary value) within each crypt region (base, mid, top) *(n=4, N≥36 compared to control *P<0.05, ***P<0.001; $$$ P<0.001 Naïve compared to M1; £££ P<0.001 M2 compared to M1).* Scale bar 20µm.

Epithelial cell type	Marker	Naïve	M1	M2
 Crypt growth	EDU	↑	↑	↑
 Enteroendocrine cell	CRO-A	=	=	=
 Goblet cell	UEA-1	↓	↓	=
 Tuft cell	DCAMKL1	=	↓	=
 stem cell	LGR5	=	↑	=*

Table 6: Diagrammatic summary

Summary table highlighting the differential effects of Naïve, M1 and M2 macrophages on colonic crypt growth and differentiation *in vitro. *(does not refer to Lgr5 fluorescence intensity, which was decreased in crypts cultured with M2 macrophages).*

4.3 Discussion:

In this chapter, we have shown that all macrophage sub-types, non-activated (Naïve), classically activated-M1 or alternatively activated-M2 macrophages-crypt co-cultures were able to induce crypt proliferation in comparison to the control, where proliferation was significantly higher in the M1-crypt co-culture compared to its non-activated and anti-inflammatory counterparts. While Cro-A+ enteroendocrine cell numbers were maintained in crypt when co-cultured with either Naive, M1 or M2 macrophages, UEA-1+ goblet cell numbers were significantly reduced in epithelia co-cultured with either Naive or M1 macrophages but not in M2. While colonic DCAMKL1+ tuft cell numbers were only reduced in crypts cultured with M1 macrophages. Additionally, epithelial Lgr5+ stem cell numbers also remained unchanged in the presence of Naive and M2 macrophages but were significantly higher in M1-crypt co-cultures. This thesis is first to demonstrate that Naive, M1 and M2 macrophages can differentially regulate colonic crypt renewal *in vitro*.

Intestinal macrophages have been implicated in colonic epithelial growth in several *in vivo* mouse models (Saha et al., 2016; Quiros et al., 2017; Sehgal et al., 2018). However, as a myriad of cell types such as fibroblasts, dendritic, T-cells among others are present in the lamina propria *in vivo*, such studies are not able to determine whether the macrophage population and macrophage-derived factors are the causative factor leading to increased crypt growth (Montalban-Arques et al., 2018). Our *in vitro* study is first to demonstrate that all macrophage subtypes despite of their phenotypic differences are able to induce colonic crypt growth via a molecular mechanism yet to be delineated.

In our study, both Naive and M2 macrophages induced comparable levels of crypt proliferation. Although the Naive macrophage population is considered to be a “neutral” and non-polarised macrophages population it could be likely that the presence of colonic crypts induced the education of macrophages to obtain an anti-inflammatory/homeostatic phenotype which according to some *in vivo* studies often resembles the M2 macrophage phenotype (Bain et al., 2014; Hine and Loke., 2019). The environmental cues which could trigger the re-education of Naive macrophages *in vivo* are currently not known and further investigation will be required. In contrast, if Naive macrophages have remained in their non-activated state, it can also be hypothesised that cytokines which have been reportedly unregulated in M2 macrophages such as IL-10, TGF-β and IL-1Rα are not directly influencing

epithelial proliferation and other factors are likely at play instead (Sica and Mantovani., 2012). Other small intestinal studies have suggested that IL-10, which is secreted in large concentrations by M2 but not Naïve or M1 macrophages aids epithelial cell proliferation through CREB signalling and the WISP-1 pathway in injury-induced crypts (Morhardt et al., 2019). Contrarily, this is not the case in our study, as proliferation in crypts cultured with M2 macrophages was comparable the Naive-crypt co-culture condition. However, it should be noted that crypts in Morhardt et al's study were subjected to physical injury, while crypts within our co-culture model remained intact and it may be possible that the IL-10 signalling pathway remains dormant in the steady-state.

In comparison to both Naïve and M2 conditions, M1 macrophages are able to increase epithelial proliferation by a further 30%. Such an increase could potentially be caused by the number of pro-inflammatory cytokines secreted by M1 macrophages such as IL-6, TNF-α, IL-1β and iNOS production (Lopes et al., 2020) . It was previously shown that IL-6 can stimulate epithelial proliferation in injury-induced mice (Kuhn et al., 2014). Furthermore IL-6 stimulation in small intestinal organoids also led to an increase in epithelial proliferation, alluding to the potential role that M1-mediated IL-6 could have in regulating crypt growth (Jeffery et al., 2017). It was also shown that exogenous TNF-α expression can promote intestinal cell proliferation via Wnt and β-catenin signalling (Bradford et al., 2017). A drawback of quantifying epithelial proliferation in this study should also be taken into consideration. Previous studies have established that the rate of turnover of the intestinal epithelium of a mouse lies at around 3-4 days. In this study, the control crypts' rate of cell proliferation average lies at 20% per day, which is lower than the estimated *in vivo* average of 33% per day (Darwich et al., 2014).

Additionally, studies have shown that LPS stimulation within macrophages can lead to the upregulation of NOX-1 which in turn increases the expression of iNOS in macrophages, an archetypical feature of M1 macrophages (Kato et al., 2016; Lui et al., 2020). An *in vivo* study had previously shown that colonic proliferation was reduced in NOX-1 deficient mice treated with DSS by 30% therefore NOX-1 should be considered another downstream target that M1 macrophages could utilise in our model (Coant et al., 2010; Moll et al., 2018).

Prior to the crypt isolation, the *in-situ* crypts were likely in contact with other sub-epithelial cells including residential macrophages. As the crypts were liberated and removed from the

in vivo setting and re-seeded into our 3D co-culture model, it is likely that epithelial turnover is reduced in crypts cultured alone due to the lack of macrophages present in the control group, while the rate of epithelial proliferation of our Naive/M2-crypt co-culture model may match the turnover rate *in vivo*. It should therefore also be considered that the non-activated or anti-inflammatory co-culture may more closely resemble the *in vivo* setting (Kuhn et al., 2014).

Early studies have shown that IL-6 secretion can be stimulated in macrophages following its exposure to LPS. As this thesis utilises the classical activation of macrophages via LPS and IFN-γ, the presumption can be made that the increased proliferation observed may be associated with the pro-inflammatory functions of IL-6 (Mantovani et al., 2004; Manderson et al., 2007). An *in vitro* organoid study has shown that the small intestinal epithelium responds to IL-6 by increasing epithelial proliferation in the steady state of the small intestine (Jeffery et al., 2017) and more relevantly, Kuhn et al. have also demonstrated an increase in epithelial proliferation following acute injury in the colon *in vivo* (Kuhn et al., 2014).

While all macrophage sub-populations were able to induce an increase in colonic crypt proliferation, findings in this chapter show that Naïve, M1 and M2 macrophage also differentially affect the expression of the differentiated cell lineages. Among all macrophage sub-types, a significant reduction in goblet, tuft cells and an increase in stem cell numbers was only observed in crypts from M1-crypt co-cultures. Although further work is required to determine the molecular mechanism which have led to the changes we have observed specifically in this culture model, the factors which could play a potential role in epithelial cell fate regulation have been highlighted below.

Constitutively mucus-producing goblet cells play a vital role in the intestinal homeostasis within the colonic epithelium (Parikh et al., 2019). In our co-culture model, a reduction in goblet cell numbers was displayed in both the Naïve and M1-crypt co-culture. In correlation to this, Sehgal et al's colonic experimental setup in *vivo* demonstrated that goblet cell numbers were also significantly increased in the absence of macrophages following blockade of CSFR1 suggesting that BMD-M1 macrophages may share similar functional properties with residential macrophages (Sehgal et al., 2018). Similarly, to the results of the M1 co-culture, a depletion in goblet cells was also observed in both IBD and ulcerative

colitis, both in which M1 macrophages are constitutively present (Lissner et al., 2015; Gerseman et al., 2009; Strugula et al., 2008). Work from Toth's lab noted that goblet progenitor cells undergo early differentiation and slowly cycle trough the transit-amplifying zone compared to absorptive cells, likely to supply the bottom of the lumen with sufficient mucus, this is also evident in our co-culture, where goblet cells were consistently present within the +4 CBC position (Toth et al., 2017).

Upregulation of NOX-1 in inflammatory macrophages could also play an important role in influencing the secretory goblet cell fate. In a *in vivo* study of the colon, an increase in goblet cells numbers was recorded following the knockout of NOX-1 (Coant et al., 2010). The study demonstrated that NOX-1 can engage the NOTCH1 signalling pathway, subsequently activating downstream stimulation of Hes1 and Hes5 and finally supressing AtOH1 transcription, thereby forcing the cells towards an absorptive cell fate. Consequently, NOTCH1 signalling was downregulated leading to an increased goblet cell expression in NOX-1 KO mice. Whether NOX-1 is involved in causing a reduction in goblet cell numbers will need to be determined in the future. In addition to this, enteroendocrine cells numbers remained unchanged in NOX-1 KO mice, which correlates with our findings (Liu et al., 2020).

As mentioned previously, Th2 response secretion of IL-4 and IL-13 leads to the activation of M2 macrophages which were proven to play a vital role in controlling parasitic invasions (Chen et al., 2012). *In vivo*, Th2-derived IL-13 secretion was also found to induce goblet cell hyperplasia, reportedly aiding to the rapid expulsion of parasitic worms (Gerbe et al., 2016). In contrast, despite the increase in cell proliferation, our findings show that goblet cell numbers were maintained in M2-crypt co-culture conditions compared to M1 and Naive. However, it should be noted that the colonic crypts within our *in vitro* co-culture model were not directly exposed to IL-13, as described in the study above, and it is also a possibility that IL-13 directly stimulates and interacts with the colonic epithelium to induce an increase in goblet cell differentiation.

A signalling pathway which is heavily impaired in IBD is TGF-β signalling, where its suppression contributes to the progression of the disease (Lees et al., 2011). TGF-β signalling is also postulated to play a pivotal role in regulating goblet cell differentiation (Ihara et al., 2016). In a previous study CD11c-*cre* TGFb depleted mice in the colon have shown to cause goblet cell depletion *in vivo*. The study highlighted that TGF-β inhibition

within CD11c+ dendritic cells lead to the upregulation of Jagged1/2, upregulation of Hes1 and consequently a reduction in goblet cells (Ihara et al., 2016). It is currently unknown to which extent CD11c+ macrophages share this phenotype with dendritic cells, however as demonstrated in chapter 3, CD11c was also highly expressed in bone-marrow derived M1 macrophages in our study. In addition, the ablation of TGF-β-RII on CD68+ macrophages led to a reduction in IL-10 production (anti-inflammatory cytokine) and increased susceptibility DSS-induced colitis (Rani et al., 2011). It is therefore likely that the observed goblet cell depletion within our M1-crypt culture condition was caused due to the absence or lack or TGF- β in the co-culture system leading to an upregulation in Notch signalling. In the future, inhibition and blocking experiments of the paracrine mediators mentioned previously could reveal the regulatory role they play within our co-culture model. It should also be noted that colonic crypts in this study were isolated from the mid and distal region, however, goblet cell numbers can differ significantly each colonic region, where goblet cell expression gradually increases from the duodenum to the distal colon (Kim et al., 2010; Karam et al.,1999). To decrease batch to batch variability in our co-culture model, we suggest the isolation of crypts from a single colonic region in future experiments.

In this thesis, tuft cell depletion was observed in M1-crypt culture while expression levels were maintained in Naïve and M2-crypt conditions. Due to its rare occurrence within the intestine, the functions of intestinal tuft cells in colonic crypt homeostasis are not well understood (Gerbe et al., 2011). It has become clear however that DCLK1+ tuft cell fates are differentially regulated in the large and small intestine. *In vivo* ablation of Atoh1 in the colon led to the depletion of DCLKL1+ tuft cells, in contrast Atoh1 deficiency within the small intestine led to tuft cell hyperplasia (Herring et al., 2018). In alignment with the colonic findings, it could therefore be hypothesised that Atoh1 is downregulated in the M1-crypt co-culture, leading to the observed decrease in the DCAMKL1+ tuft cell numbers. Interestingly, ablation of DCAMKL1 in DSS colitis-induced colitis also led to an increase in pro-inflammatory cytokine secretion and inflammation, however the depletion of DCLK1 also resulted in a decrease in Lgr5 mRNA expression (Qu et al., 2014). Whether the tuft cell depletion we have observed in our *in vitro* model is linked to the likely upregulation of M1-derived pro-inflammatory cytokine or is the result of differential cell differentiation will be further investigated in the latter chapters of this study.

Tuft cell's ability to secrete prostaglandin E2 has shown to aid wound repair *in vitro (*Miyoshi et al., 2017*)*. In addition, an *in vivo* colonoid study found that DCLK1+ deficient tuft cells only contribute to epithelial proliferation in the event of chronically induced colitis within the colon (Yi et al., 2018). As our study demonstrated that M1-crypt interactions are leading to an increase in epithelial proliferation, it is likely that tuft cell-mediated prostaglandin secretion does not significantly influence epithelial renewal. However, in an *in vitro* 2D organoid system, PGE_2 supplementation led to the reduction in tuft cell density, suggesting that tuft cells are sensitised to PGE_2 levels (Miyata et al., 2018). It is evident that bone-marrow derived M1 macrophages protein expression of PGE_2 is significantly higher compared to its Naïve and M2 counterpart and COX-2 expression is increased in macrophages in contact with intracellular bacteria in a similar fashion to this studies' M1 macrophage phenotype (Manning et al., 2015). For this reason, the reduction of tuft cells numbers exhibited in our M1 co-culture could be credited to the increasing levels of PGE_2 within the co-culture's microenvironment. The exact mechanism which causes the changes we have observed are currently not known, to further investigate this, future studies should aim to determine the expression of PGE_2 within the co-culture via utilisation of an ELISA kit.

The reduction in tuft cells in the M1 co-culture may also have indirectly reduced goblet cell numbers within the epithelium. Tuft cells secretion of IL-25 *in vivo* plays a vital role in the recruitment of Th2 cells and consequent secretion of IL-4 and IL-13 both of which are required for polarisation of M2 macrophages. An *In vivo* small intestinal study demonstrated that recombinant IL-4 and IL-13 injection led to increased tuft and goblet cell hyperplasia after 5 days, however it was not elucidated whether the changes observed were caused by an increased influx of M2 macrophages (Gerbe et al., 2016; Moltke et al., 2016). Additionally, tuft cells have also been implicated to act as quiescent stem cells within the small intestine, where they can act as a source of Notch for the maintenance of Lgr5+ stem cells following the ablation of Paneth cells; however, to which extent this role is translated across to the colon is not known (Westphalen et al.,2014; Van es et al., 2019).

Altogether the reduction in tuft and goblet cell numbers observed in our M1-crypt co-cultures begs the question as to whether the epithelial cell fate equilibrium has been shifted between the absorptive and secretory cell fate as described.

In this study's co-culture model, enteroendocrine cell (EEC) numbers were not affected by the different macrophage subtypes. Several studies have shown the effects EECs could have on macrophage activity; however, the reciprocal effects have previously not been extensively studied (Miyamoto et al., 2012; Saia et al., 2014; Hogan et al., 2014) Enteroendocrine cells are categorised as secretory cells and Neurogenin 3 has been identified as the critical transcription factors required for the differentiation of enteroendocrine cells. As no changes were detected in our co-culture system it can be assumed that all three macrophage subtypes are unable to influence the EEC differentiation pathway (Jenny et al., 2002).

As colonic renewal has been established to be driven by Lgr5+ stem cells, a particularly compelling finding of this chapter is the significant increase of crypt Lgr5+ stem cells when in culture with M1 macrophages (Barker et al. 2007; Rothenberg 2014). As to why M1 macrophages alone are able to implement such a change within our model is currently not known, however signalling pathways such as Wnt and Notch among others may play a crucial role in engaging intestinal stem cell expansion and is further investigated in **Chapter 6** of this study.

Wnt signalling pathway plays a critical role in the renewal of the epithelium and the maintenance of stem cell activity (Clevers., 2014). Saha et al. have demonstrated that macrophages' extra-vesicular secretion of Wnt is required for epithelial renewal and proliferation Here bone-marrow derived macrophages expressed WNt5a, Wnt6 and Wnt9a (Saha et al., 2016). Where small intestinal crypts can rely on Paneth cells to provide Wnt ligands, specifically, Wnt3a, the exact cause of Wnt signalling in the colon remains an enigma (Sato et al., 2011). The Wnt-signalling paradigm within our co-culture system is further studied in the latter chapters of this thesis.

As mentioned above, M1 macrophage unique pro-inflammatory inventory could prompt a change in epithelial stemness. The inflammatory cytokine TNF-α, is secreted by BMD-M1 macrophages in large quantities (Ying et al., 2013). A recent study has demonstrated that epithelial cells depend on bone-marrow cell derived TNF in mucosal repair following DSS treatment. Interestingly, an increase in Lgr5 mRNA expression was also exhibited in colonoids following treatment with TNF, hinting at the potential role TNF-α may play within our co-culture system (Bradford et al., 2018). Recent work from Koelink et al, has revealed

that anti-TNF therapy utilised to treat patients with Crohn's disease, causes an increase in macrophage derived-IL-10 production which subsequently promotes the differentiation towards an M2 macrophage phenotype, thereby showcasing the potential therapeutic role macrophages play in inflammation resolution (Koelink et al., 2020). It should be noted that although Lgr5 has been established as a robust marker for actively cycling stem cells within the colon, unlike Lgr5+GFP+ mice, the immunofluorescent labelling with an anti-Lgr5 antibody does not allow for lineage tracing and therefore it cannot be established whether the Lgr5+ stem cells identified in our co-culture model are a clonal derivative or arose as a result of de-differentiation (Barker et al., 2007). Furthermore, Cosin-Roger's work has described that M2 macrophages may regulate mucosal repair in colitis-induced mice via a STAT6 dependent pathway, however we did not observe any changes in the expression of Lgr5+ stem cells in our co-culture system where the epithelium largely remained intact (Cosin-Roger et al., 2013). We therefore suggest that the experiments in this chapter are repeated with crypts isolated from DSS-treated mice, so we can further understand whether M1 and M2 macrophages differentially respond to the inflammatory stimuli.

Jeffery et al. have previously shown that the number of Lgr5 positive cells increase following IL-6 treatment *in vivo* and *in vitro*. Interestingly, gene expression of IL-6 is also highly upregulated in classically activated (M1) macrophages but not alternatively activated (M2) macrophages. (Orrecchioni et al., 2019). This also correlates with our current findings of Lgr5 increase in the M1-crypt culture. However, Paneth cells in the small intestine which the IL-6 pathway depends on are not present in the colon and it remains unknown as to how IL-6 signalling may be transmitted to the colonic epithelium (Jeffery et al., 2016). In correlation to the *in vivo* studies mentioned above, Reinecker et al's earlier work has also found that increased levels of lamina propria-derived IL-6 and TNF was present in patients with Crohn's disease (Reinecker et al., 1993). In order to confirm whether macrophage-derived cytokines such as IL-6 and TNF-α are present in our co-culture, the culture medium can be collected and a chemokine/growth factor ELISA can be performed to further understand the differences in cytokine composition in our Naïve, M1 and M2 co-cultures.

In 2020, Meli et al have highlighted that the depletion of YAP, a component of the Hippo signalling pathway, inhibits the activation of macrophages towards an inflammatory phenotype, whereas the overexpression of YAP led to an increase in inflammation (Meli et al., 2020). Similarly, YAP activation was shown to be upregulated in both IBD and following mucosal injury (Tanguchi et al., 2014). A follow up study, further revealed that the polarisation of M2 macrophages was inhibited by YAP, instead enhancing the presence of IL-6 producing M1 macrophages in chronic inflammatory disorders (Tanguchi et al., 2019). Interestingly, the Hippo signalling may also play a regulatory role in the activation of both Wnt and Notch signalling (Zhou et al., 2019). The accumulation of nuclear YAP, which was initiated by the conditional deletion of MST1/2 in intestinal epithelial cells, was shown to upregulate Notch activation (Zhou et al., 2011). It was also demonstrated that the nuclear accumulation of YAP can aid the stabilisation of the β-catenin thereby positively regulating Wnt signalling (Rosenbluh et al., 2012; Heallen et al., 2011). Whether the significant upregulation in colonic crypt proliferation we have observed in M1 macrophages is partly driven by the upregulation in the Hippo signalling pathways as observed in IBD is in in our 3D *in vitro* co-culture model will need to be further investigated in the future.

In an *in vivo* setting, the environmental stimuli often define the macrophage phenotype, as previously described macrophages in the intestinal lamina propria obtain an inflammatory or homeostatic role (Na et al., 2019). Due to the constant presence of stimuli *in vivo* the non-activated/resting 'Naïve' phenotype can only observed in an *in vitro* setting. As it is not known whether the Naïve macrophage were 'conditioned' by nearby colonic crypts to support and regulate colonic crypt renewal within out co-culture model. To do so, future work should aim to investigate whether crypt-derived secretory factors can activate non-stimulated 'Naïve' macrophages.

Another disadvantage of this study was that to visualise and quantify the number of Lgr5+ stem and differentiated cell type, the samples were fixed in PFA and immunofluorescently labelled after 24 hours throughout this study, however this methodology only allows us to study a fixed time-point. With the use of a time-lapse and Lgr5+GFP+ mice co-cultured along with the macrophage subtypes in future experiment we will be able to further understand the epithelium response to macrophage crosstalk.

Conclusion:

This study is the first to demonstrate that pro, anti and non-activated macrophages are able to induce colonic epithelial proliferation *in vitro*. Furthermore, inflammatory macrophages prompt the upregulation of Lgr5+ stem cell expression and a reduction in goblet and tuft cell numbers. The molecular mechanisms behind the differential shift in differentiation remain to be studied however further studies may aid the search for an alternative therapeutic target to regulate said changes and thus control or prevent chronic inflammation within IBD. To refine the search for the influencing factor causing the increase in crypt growth and changes in crypt differentiation, the upcoming chapters strive to investigate whether the changes observed are induced via macrophages' physical contact or secreted factors, while the following chapter will determine whether physical contact between colonic crypts and macrophages exists within our 3D *in vitro* model.

Chapter 5: Spatial Characteristics of Macrophages And Colonic Crypts *In Vitro* Co-culture Model

5.1 Introduction:

The colon is home to the largest macrophage population in the body and its functional role within the lamina propria during the steady state and their presence is only increased during inflammation, while their ablation *in vivo* can exacerbate inflammation in UC and Crohn's disease (Symthies et al., 2005; Rubio et al., 2018).

As previously described in Chapter 3, the intestinal epithelium recruits' monocytes which are then differentiated into tissue-resident macrophages, where the epithelium and the underlying lamina propria utilise chemokine signalling to direct the macrophage localisation towards the crypt perimeter (Kulkarni et al., 2016). The significance of macrophage and crypt interplay has been highlighted in a few studies. For example, early work from Pull et al, noted that DSS-treatment of mice induced an increase in F4/80 positive macrophages which extended processes out towards the pericryptal surface of the colonic epithelium (Pull et al., 2005). Significantly in a homeostatic setting, seminal work from Skoczek et al's have made a number of key findings. Firstly, the luminal stimulation of LPS initiated the recruitment of 7/4+ neutrophils, Ly6C+ monocytes and F4/80+ macrophages, within an explant model, indicating that the epithelium is capable of relaying luminal signals towards underlying immune cells. The Ly6C+ and F4/80+ were then also observed to be directly juxtaposed with LGR5EGFP+ stem cells, while in parallel, LGR5EGFP+ stem cells were shown to extrude cellular processes through the laminin-rich basement membrane to contact nearby immune cells and the cellular protrusions were observed to be in direct contact with F4/80+ macrophages. (Skoczek et al., 2014; Sobolewski and Skoczek, unpublished data).

The macrophage's capacity to form filopodia to apprehend foreign bacteria has been well established over the course of the last 50 years (Horsthemke et al., 2018; Kress et al., 2007). However, with time the multi-functionality of such macrophage filopodia are also being uncovered. Following acute injury, neutrophils are recruited to the site of injury by epithelial-derived CXCL-cytokines (Stillie et al., 2009). Remarkably, to limit an excessive inflammatory response, intestinal macrophages are able to sense microlesions in the epithelium, extend membrane processes towards the site of injury, remove debris and

DAMPs thus dampening the immune response in vivo (Uderhardt et al., 2019). Additionally, work from Resicgno, Chieppa and Niess et al, have demonstrated that CX3CR1+ macrophages, although initially thought to be dendritic cells, were able to form transepithelial dendrites in order to sample luminal antigens and assist in bacterial clearance (Rescigno et al., 2001; Niess et al., 2005; Chieppa et al., 2006).Further evidence of filopodia-mediated macrophage-epithelial crosstalk was reported in zebrafish, where long, thin cellular protrusions named 'airinemes' were found to link epithelial pigment cells directly to macrophages, where the depletion of macrophages coincided with the ablation of airinemes (Eom and Parichy., 2017).

Within an *in vivo* setting, input from other peri-cryptal myofibroblast and mesenchymal cells such as Rspo1-producing trophocytes and BMP ligand-producing telocytes during the steady-state and IBD makes it difficult to determine whether macrophages-derived signals can affect epithelial renewal in an in vivo setting (Lei et al., 2011; McCarthy et al., 2020; Shoshkes-Carmel et al., 2018). For this reason, the use of 3D Matrigel-based organoid cultures has increased exponentially over the last two decades as they allow researchers to gain a better understanding of the physiological functions of each cellular component within the culture model by mimicking the *in vivo* setting as closely as possible (Simian and Bissell., 2016). Although contact between macrophages and the epithelium have been reported in the studies mentioned above, the spatio-temporal characteristics of colonic crypts and the macrophage subsets have not been studied in detail. As work from Chapter 4 has confirmed that Naïve, M1 and M2 macrophage differentially regulate colonic crypts proliferation and differentiation in our 3D co-culture model, in this chapter we aimed to further understand whether the interactions between colonic crypts and Naïve, M1 or M2 macrophage specifically within our 3D Matrigel-based model affect the morphological properties of colonic crypts and the localisation of nearby macrophages. The data in this chapter suggest that the macrophage sub-populations create direct physical contact to the colonic epithelium, adopt a pattern in its localisation and differentially affect crypt architecture *in vitro*.

5.2 Results:

As the presence of CSF-driven macrophage were shown to play a crucial key role in regulating the intestinal stem cell niche *in vivo* (Sehgal et al., 2018), this chapter aims to further study the spatial and temporal characteristics of both macrophages and crypts within the 3D *in vitro* co-culture model. Live-cell imaging and immunofluorescent labelling was used to semi-quantitively characterise macrophage to crypt contact within the co-culture model. Furthermore, the vesicle secretion of the colonic epithelium in the presence of Naïve, M1 and M2 macrophages was also studied.

5.2.1 Colonic crypts cultured with Naïve, M1 and M2 macrophages share similar crypt morphologies *in vitro*

Initially following the culture of crypts with Naïve, M1 and M2 macrophages, its effect on the overall crypt morphology were studied and characterised in **Figure 5.1**, where a variety of crypt morphologies have been identified in the absence of macrophage (Control) and in the presence of Naïve, M1 and M2 macrophages. In **Figure 5.1A,** native crypts in which the width: length ratio lies at approximately 1:3 are shown. Shorter crypts are shown in **Figure 5.1B** and spheroidal crypts are displayed in **Figure 5.1C.** The occurrence of the native, short and spheroidal crypts on Day 1 of culture were analysed in the presence of Naïve, M1 and M2 macrophages over the course of 48 hours are shown in **Figure 5.1D.** The most commonly occurring morphological phenotype observed was the native crypt followed by short crypts, where spheroidal crypt expression was least commonly detected. Native crypts in control remained unchanged on Day 2 compared to Day 1, however a significant decrease in native crypt expression was noted in crypts cultured with Naïve, M1 and M2 macrophages on Day 2 compared to Day 1. The expression of short crypts in control from Day 1 to Day 2 remained unchanged. A significant increase in the expression of short crypt was observed in crypts cultured with either Naïve or M1 macrophages but not in culture with M2 macrophages. The expression of spheroidal crypts remained unchanged both in the absence and presence of Naïve, M1 and M2 macrophages.

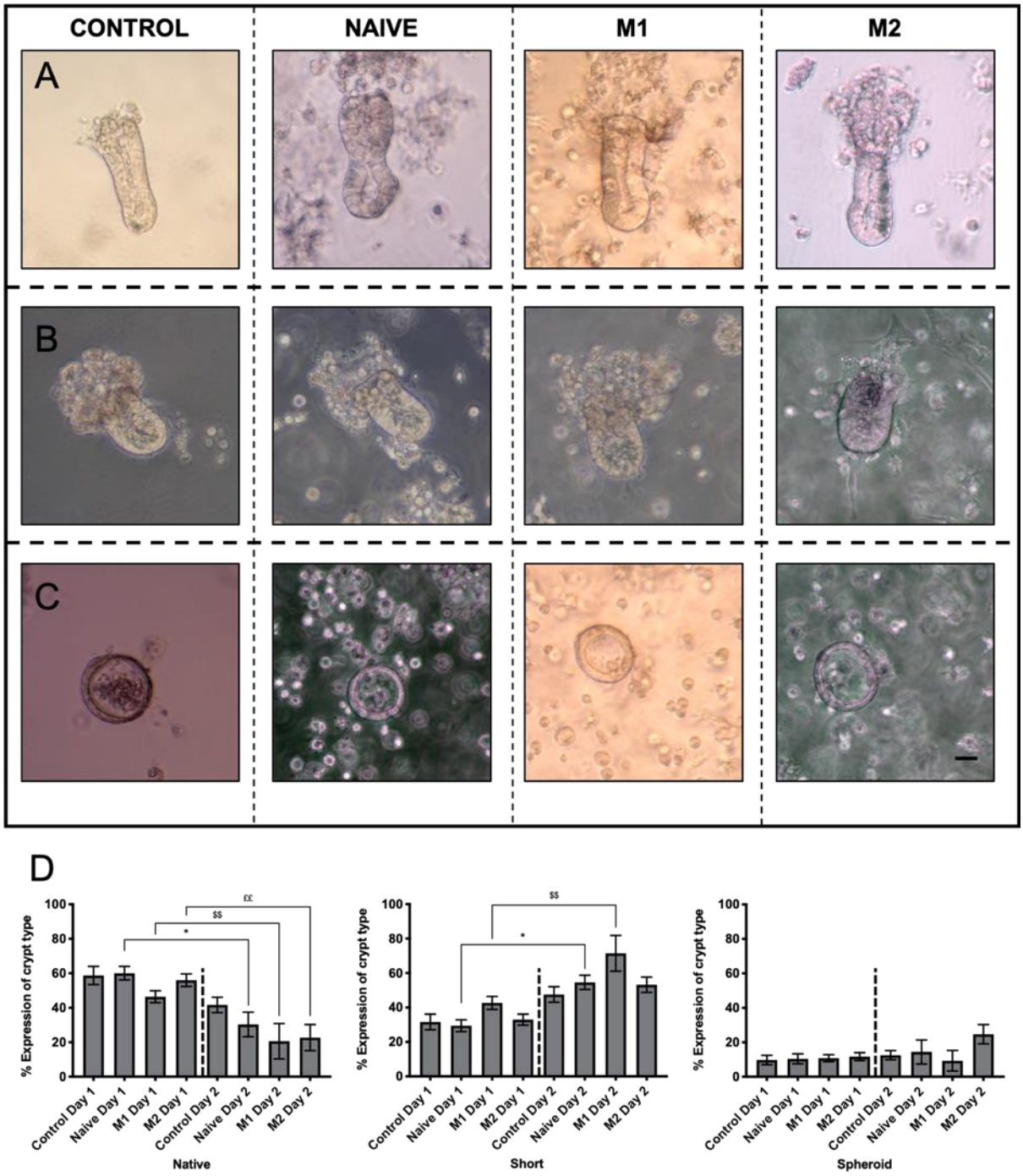

Figure 5.1: Characterisation of colonic crypts morphologies in *in vitro* culture with Naïve, M1 and M2 macrophages

In vitro colonic crypts and co-cultures in 3D Matrigel highlighting varying organoid morphologies. **A)** Native crypt B**)** Shortened crypt C**)** Spheroidal crypt **D)** Histogram showing percentage expression of native, short and spheroid crypts when cultured with Naïve, M1 and M2 macrophages (n=10 N≥68), *P<0.05 Naïve Day 1 compared to Naïve Day 2, $^{\$\$}$P<0.01 M1-Day 1 compared to M1-Day 2, ^{ff}P<0.01 M2-Day 1 compared to M2-Day 2). Scale bar at 25µm.

5.2.2 Crypt length and epithelial area is reduced in culture with M1 macrophages only

To determine whether the culture of Naïve, M1 or M2 macrophages along with colonic crypts has affected the epithelial morphology, the longitudinal crypt length and epithelial area was measured as described in **Section 2.3.7**, where images were captured on Day 1 and Day 2 of co-culture.

In **Figure 5.2A**, representative brightfield images of crypts cultured in the presence of Naïve, M1 and M2 macrophages are shown. The crypt length was analysed in crypts cultured with Naïve, M1 and M2 macrophages following 24 hours (**Figure 5.2Bi**) and 48 hours (**Figure 5.2Bii**) in culture. A significant decrease in crypt length was observed in crypts cultured with M1 macrophages after 24 hours, but not when cultured in the presence of Naïve or M2 macrophages compared to control crypts (**Figure 5.2Bi**). In comparison, no significant changes in crypt length in crypts cultured with Naïve, M1 or M2 macrophages were detected after 48 hours in culture (**Figure 5.2Bii**). Further semi-quantitative analysis of the crypt area also revealed a significant decrease in the average epithelial area of crypts cultured with M1 macrophages compared to control crypts over 24 hours. The epithelial area in crypts cultured with Naïve or M2 macrophages was not affected compared to control crypts. (**Figure 5.2Ci**). The epithelial area in crypts culture in the presence of Naïve, M1 and M2 macrophages did not differ compared to control crypts following 48 hours in culture (**Figure 5.2ii**). In **Figure 5.2D,** the shedding area at the top of the crypt (shedding zone) was measure semi-quantitatively analysed, where similar volume of shedding was found in control crypts compared to crypts cultured with Naïve and M1 macrophages. However, shedding increased significantly in crypts cultured with M2 macrophages compared to control crypts.

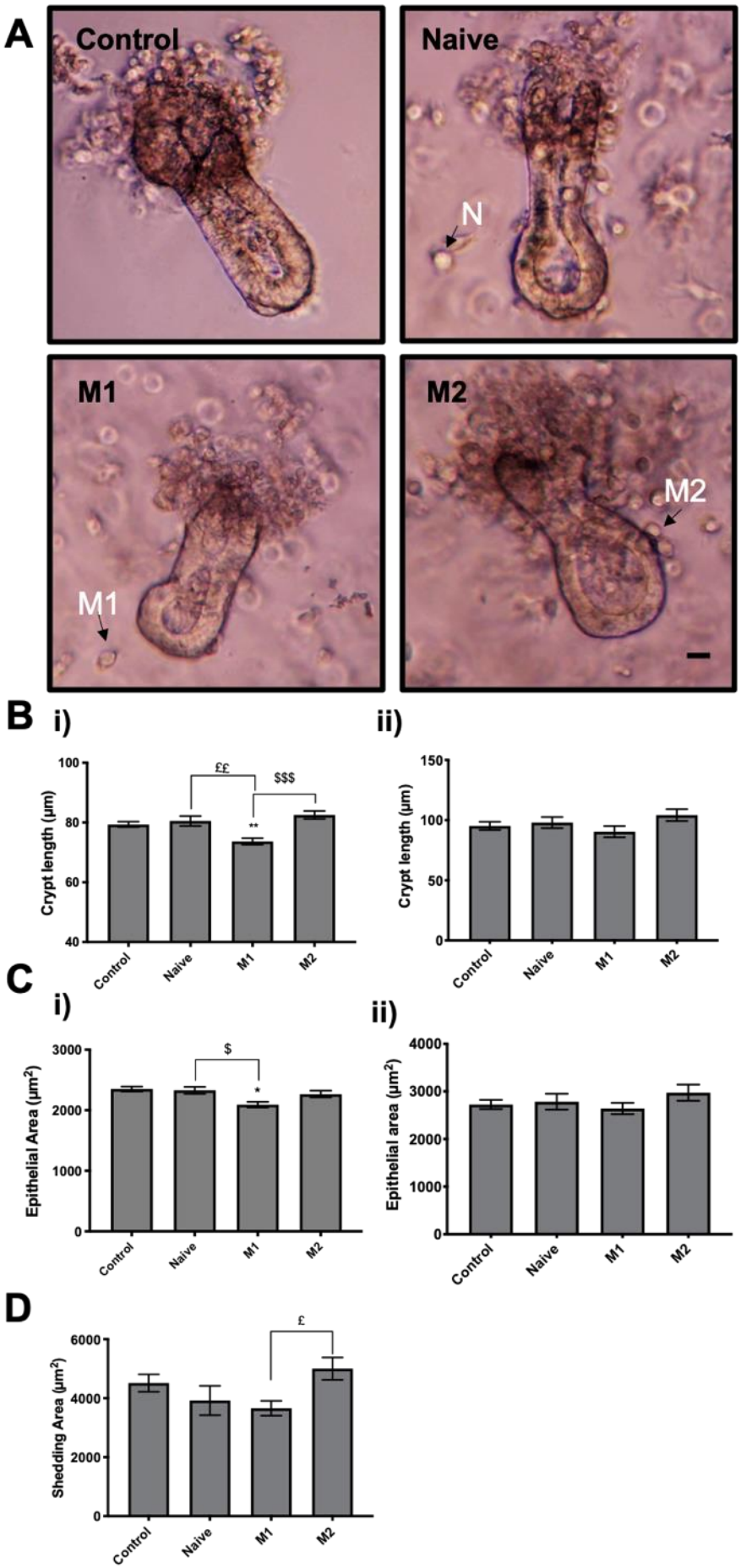
A
Control
Naive
N
M1
M2
M2
M1
B
i)
ii)
Crypt length (µm)
£
$$$
**
Control
Naive
M1
M2
C
i)
ii)
Epithelial Area (µm²)
Epithelial area (µm²)
$
*
D
Shedding Area (µm²)
£

Figure 5.2: Crypt length and epithelial area is reduced *in vitro* when cultured with M1 macrophages only

A) Representative epi-fluorescent images showing crypts in culture with Naïve, M1 or M2 macrophages (arrows). **B)** Histogram showing the average length of crypts in culture with Naïve, M1 or M2 macrophages after 24 hours (n=6, N≥129) **(Bi)** and 48 hours (n=3, N≥29) **(Bii)** (**P<0.01 compared to Control; ^{ff}P<0.01 Naïve compared to M1; ($^{\$\$\$}$P<0.001 M1 compared to M2). **C)** Histogram showing the average epithelial area of crypts cultured alone and with Naïve, M1 or M2 macrophages after 24 hours (n=6, N≥129) (**Ci**) and 48 hours (n=3, N≥29) (**Cii**) (*P<0.05 compared to Control; $^{\$}$P<0.05 Naïve compared to M1). **D)** Histogram showing the average shedding area of crypts cultured alone, with Naïve, M1 or M2 macrophages after 24 hours (n=3, N≥28, $^{£}$P<0.05 M1 compared to M2). Scale bar at 15μm.

Having previously established that native and short crypts are most commonly present within the Naïve, M1 or M2 macrophage-crypt co-culture model, we have further shown that the presence of M1 macrophages induces a significant shortening in colonic crypt length and epithelial when cultured with colonic crypts *in vitro*. Next, we were determined to examine other morphological properties which we have observed within our 3D macrophage-crypt co-culture model, which includes the presence of small vesicles, epithelial processes and "shedding" processes.

5.2.3 Epithelial vesicle expression is reduced in crypts cultured with M1 or M2 macrophages

To understand whether vesicle expression is driven by the presence of macrophages within the *in vitro* co-culture model, brightfield images were captured 3 hours following the co-culture and the presence of epithelial vesicle were analysed in a binarily (as per **Section 2.3.6)**. Representative brightfield images of epithelial vesicles (arrow) in culture with Naïve, M1 or M2 macrophages are shown in **Figure 5.3A**. The average percentage of vesicle expression per crypt in the presence of Naïve, M1 and M2 macrophages are shown in **Figure 5.3B**. Here a decrease was observed in all crypts cultured with Naïve, M1 or M2 macrophages compared to control crypts.

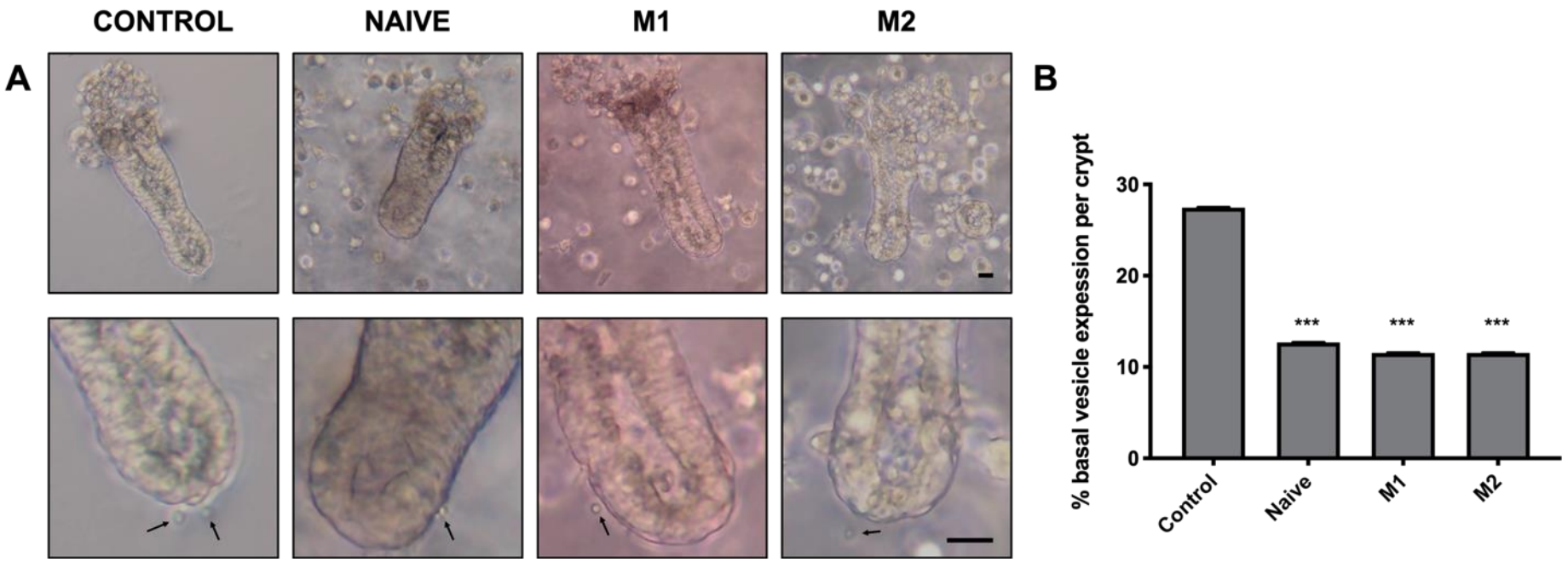

Figure 5.3: Epithelial vesicles expression is reduced in crypt in *in vitro* culture with M1 or M2 macrophages

A) Representative live cell brightfield images showing basal vesicle expression on (arrows) after 3 hours in crypts cultured alone, with Naïve, M1 and M2 macrophages *in vitro*. **B)** Histogram showing the percentage of vesicles per crypt, cultured alone and in the presence of Naïve, M1 or M2 macrophages within each co-culture condition (n=5, N≥51), ***P<0.001 compared to Control. Scale bar at 25µm.

5.2.4 Epithelial processes are present in crypt cultured alone and with Naïve, M1 or M2 macrophages

In our co-culture model, we have noted the presence of epithelial processes protruding from colonic crypts after 1 hours of culture. To understand whether the expression of such epithelial processes is driven by the presence of macrophages within the *in vitro* co-culture model, brightfield-images were captured after 1 hours following the co-culture and the presence of epithelial processes were analysed binarily (as per **Section 2.3.6)**. Representative brightfield images of epithelial vesicles in culture with Naïve, M1 or M2 macrophages are shown in **Figure 5.4A**. The average number of epithelial processes per crypt in the presence of Naïve, M1 and M2 macrophages are shown in **Figure 5.4B** and the average percentage of epithelial processes per crypt in the presence of Naïve, M1 and M2 macrophages are shown in **Figure 5.4C.** Here, a decrease was observed in all crypts cultured with Naïve, M1 or M2 macrophages compared to control crypt.

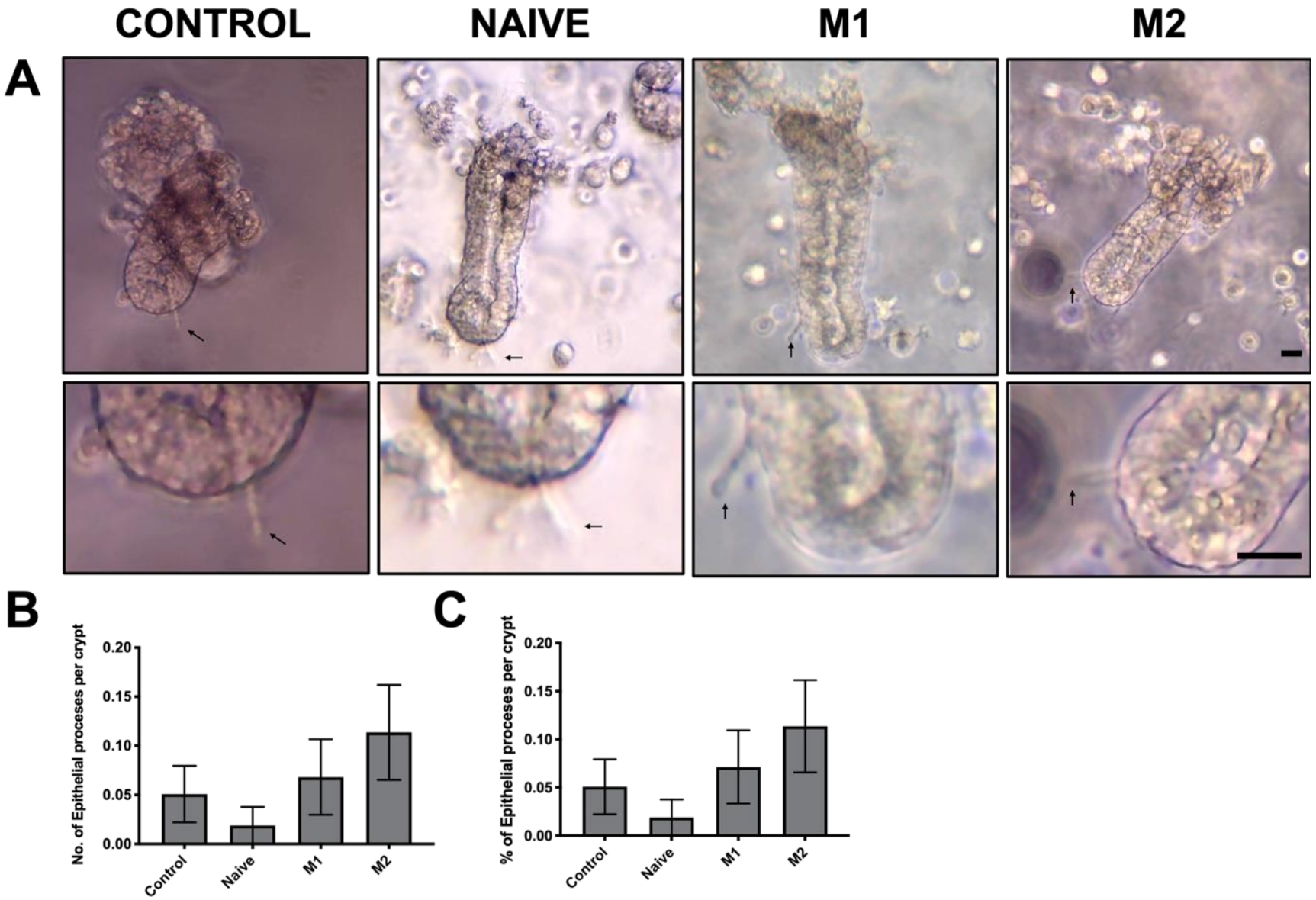
CONTROL
NAIVE
M1
M2
A
B
C
No. of Epithelial proces per crypt
0.20
0.15
0.10
0.05
0.00
Control
Naive
M1
M2
% of Epithelial proces per crypt
0.20
0.15
0.10
0.05
0.00
Control
Naive
M1
M2

Figure 5.4: Epithelial processes are present in *in vitro* crypts cultured alone and with Naïve, M1 or M2 macrophages

A) Examples of live-cell brightfield images showing basal epithelial protrusions (arrows) after 1 hours in crypts cultured alone and with Naïve, M1 or M2 macrophage *in vitro* **B)** Histogram showing the number of epithelial processes present per crypt and **C)** percentage of epithelial protrusions compared to the total number of crypts after 1 hour in crypts cultured alone and with Naïve, M1 or M2 macrophages (n=5, N≥44, non-significant). Scale bar at 25µm.

5.2.5 'Shedding' processes are present in the upper region of crypts cultured alone and with Naïve, M1 or M2 macrophages

In our co-culture model, we have noted the presence of long epithelial processes protruding from the upper region of the colonic crypts. In contrast to other processes previously observed within our 3D Matrigel culture model, rounded cell-like cysts are a hallmark of such 'shedding' processes. To understand whether the expression of such epithelial processes is driven by the presence of macrophages within the *in vitro* co-culture model, brightfield-images were captured after 1 hour following the co-culture and the presence of epithelial processes were analysed binarily (as per **Section 2.3.6)**. Representative brightfield images of such epithelial processes (arrow) in culture with Naïve, M1 or M2 macrophages are shown in **Figure 5.5A**. The average number of processes per crypt in the presence of Naïve, M1 and M2 macrophages are shown in **Figure 5.5B**, whereas **Figure 5.5C** shows the percentage of 'shedding' processes per crypt compared to the total number of crypts analysed. In both, a decrease was observed in all crypts cultured with Naïve, M1 or M2 macrophages compared to control crypts.

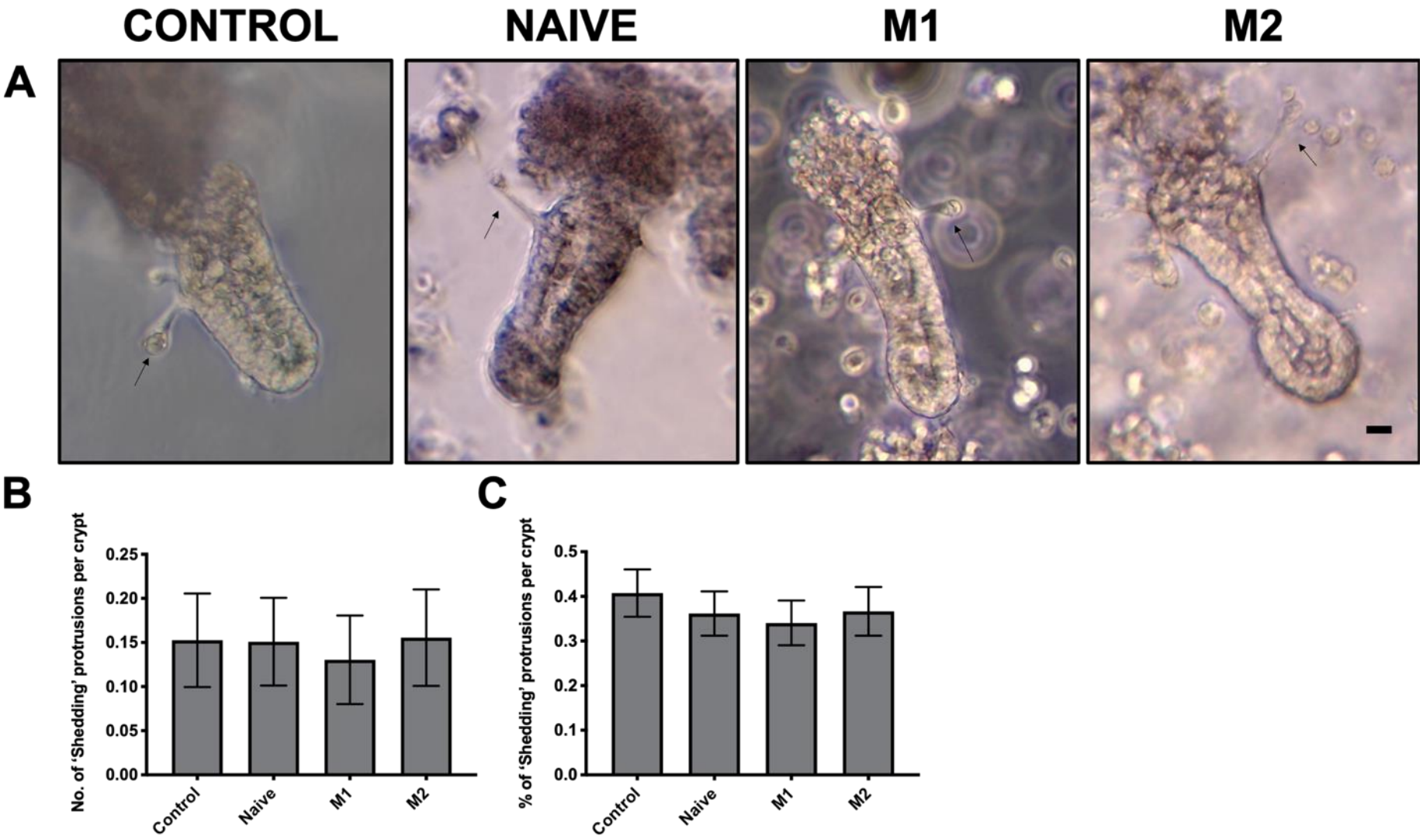
CONTROL
NAIVE
M1
M2
A
B
No. of 'Shedding' protrusions per crypt
0.25
0.20
0.15
0.10
0.05
0.00
Control
Naive
M1
M2
C
% of 'Shedding' protrusions per crypt
0.5
0.4
0.3
0.2
0.1
0.0
Control
Naive
M1
M2

Figure 5.5: 'Shedding' processes are present in the upper region of crypts cultured alone and with Naïve, M1 or M2 macrophages *in vitro*

A) Examples of live-cell brightfield images showing 'shedding' protrusions after 3 hours in crypts cultured alone and with Naïve, M1 or M2 macrophages *in vitro*. Histogram showing **B)** the average number of 'shedding' protrusions present per crypt and **C)** the average percentage of 'shedding' protrusions compared to the total number of crypts in culture after 3 hours cultured alone or with Naïve, M1 or M2 macrophages (n=5, N≥45, non-significant). Scale bar at 15µm.

As the expression of vesicles, epithelial and shedding processes present in colonic crypt cultures and Naïve, M1 or M2 macrophage-crypt co-cultures was determined, we further attempted to determine the frequency, position and classify the method of contact between macrophages and colonic crypts in our 3D macrophage-crypt co-culture model.

5.2.6 M1 and M2 macrophage contact is reduced at the colonic crypt base

To determine the frequency and position of macrophage to crypt contact, the distribution of macrophage contact along the longitudinal crypt-axis was quantified as per **Section 2.3.6.** **Figure 5.6A** shows examples of epithelial-macrophage contact at each crypt region- base (**b**), mid (**m**) and top (**t**) in culture with Naïve, M1 or M2 macrophages. **Figure 5.6B** shows the number of macrophages to crypt contact per crypt region after 24 hours in co-culture whereas only crypts in contact with macrophages and their corresponding positions were analysed in **Figure 5.6C.** Here, Naïve, M1 and M2 macrophages cultured with crypts, commonly located at the base and mid region of the crypt and less at the top. The distribution pattern of M1 macrophages cultured with crypts closely resembled that of crypts cultured in the presence of Naïve macrophages. In contrast, macrophage contact is reduced in crypts when cultured with M2 macrophages, where contact is significantly reduced at the base, mid and top region of the crypt. Here it should also be noted, that the majority of macrophages seeded within our 3D *in vitro* model, were not in contact with the crypts and were in fact some distance apart.

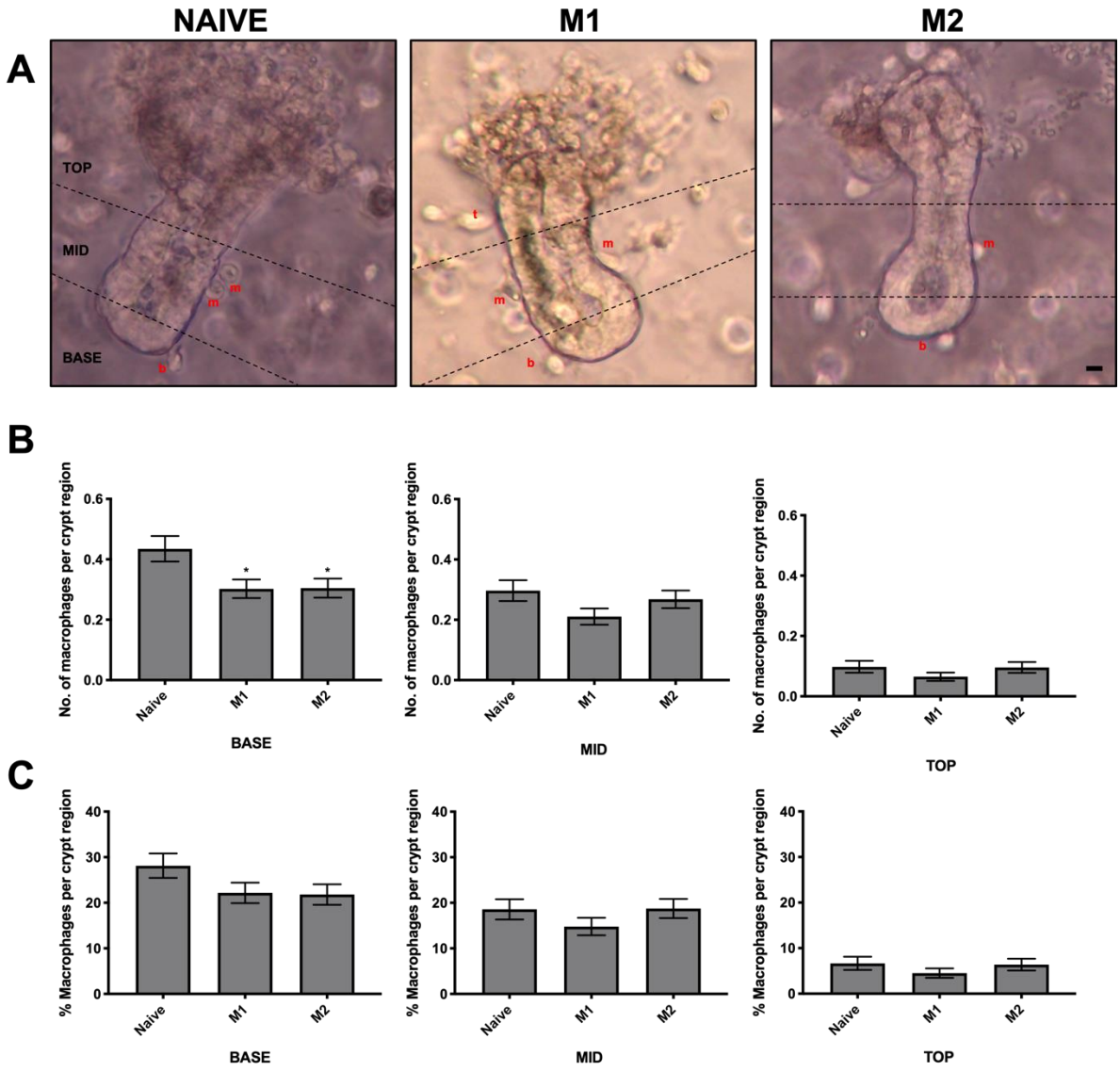

Figure 5.6: Macrophage to crypt contact is reduced in crypts in the presence of M1 and M2 macrophages at the base of the crypt *in vitro*

A) Representative brightfield images showing macrophages at the base (**b**), mid (**m**) and top (**t**) regions of the crypt after 24 hours *in vitro* culture **B)** Histogram showing the average number of macrophages distributed along each crypt region (n=10, N≥ 172) (*P<0.05 compared to Control). **C)** Histogram showing the average percentage of macrophages distributed along each crypt region when in contact with the crypt (n=10, N≥172). Scale bar at 15µm.

5.2.7 Macrophage-body to crypt contact is predominantly observed in co-culture model

As per **Section 2.3.6**, two distinctive macrophage-crypt contact characteristics have been identified in the culture of colonic crypts with Naïve, M1 or M2 macrophages where examples of both the macrophage process (**p**) in contact with the base of the crypt and a macrophage body (**b**) in contact with the base of the crypt are shown in **Figure 5.7A**. The occurrence of both contact phenotypes (**p**) and (**b**) along the longitudinal crypt-axis were analysed semi-quantitatively in **Figure 5.7B,** where all crypts with or without macrophage contact were quantified and **Figure 5.7C**, in which only crypts in contact with macrophages and their corresponding macrophage-crypt contact phenotype was quantified. Here it was shown that macrophage body contact (**b**) was mostly exhibited in Naïve, M1 and M2 macrophages. Significantly less macrophage process contact (**p**) was observed when Naïve, M1 or M2 macrophages were cultured with colonic crypts compared to macrophage body contact (**b**) numbers after 24 hours in co-culture.

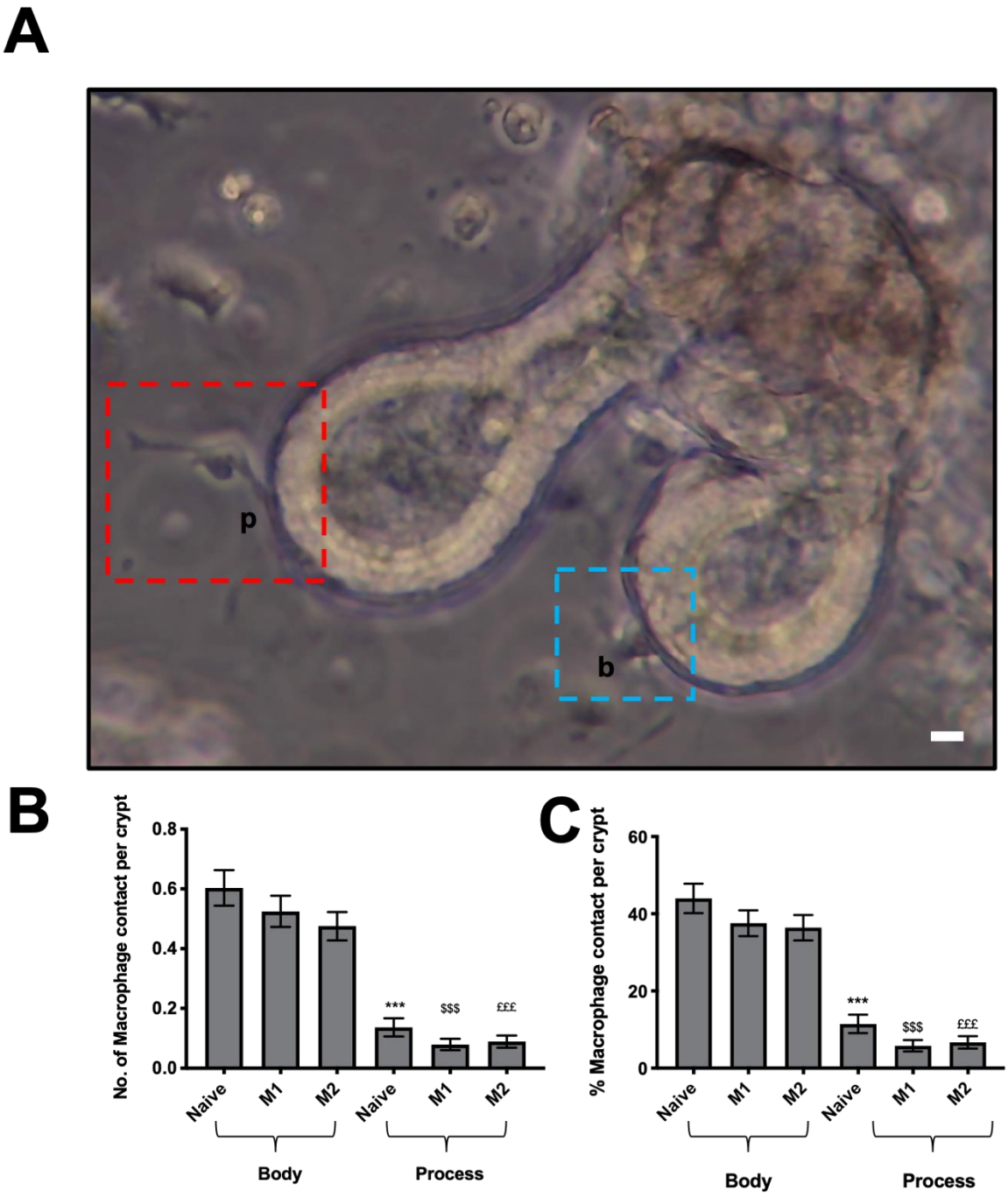

Figure 5.7: **Macrophage-body to crypt contact is predominantly observed in *in vitro* co-culture model**

A) Example of macrophage-process contact (p) and macrophage-body contact (b) shown after 24 hours *in vitro* colonic crypt co-culture **B)** Histogram showing number of macrophage-contact types exhibited in each co-culture condition Scale bar at 10µm (n=10, N≥168 ***P<0.001 Naïve-Body compared to Naïve Process; $$$P<0.001 M1-Body compared to M1-Process; £££P<0.001 M1-Body compared to M1-Process)

C) Histogram showing the percentage of macrophage-contact types per crypt when in contact with the crypt in each co-culture. Scale bar at 10µm (n=10, N≥168 ***P<0.001 Naïve-Body compared to Naïve Process; $$$P<0.001 M1-Body compared to M1-Process; £££P<0.001 M1-Body compared to M1-Process)

Having demonstrated and categorised the preferential mode of contact between macrophages and colonic crypts, we were also determined to show whether the macrophage phenotype was maintained in macrophages which are in contact with the colonic epithelium.

5.2.8 Macrophages maintain phenotypical characteristic when in contact with colonic crypts

To determine whether macrophage in contact with colonic crypts maintain their phenotypic characteristic as previously established in **Chapter 3**, immunofluorescent labelling of macrophage cell surface markers was used to identify bone marrow derived macrophages in contact with colonic crypts *in vitro* following 24 hours in culture. **Figure 5.8Ai)** shows CX3CR1(red) and DAPI (blue) positive Naïve macrophages (white arrows) in contact with a crypt. **Figure 5.8 Aii)** shows F4/80 (red) and DAPI (blue) positive M1 macrophages (white arrows) in contact with colonic crypts labelled with E-cadherin in green. Lastly, **Figure 5.8 Aiii)** shows MHC2 (red), DAPI (blue) positive M1 macrophages (white arrows) in the presence of colonic crypts labelled with E-cadherin (green).

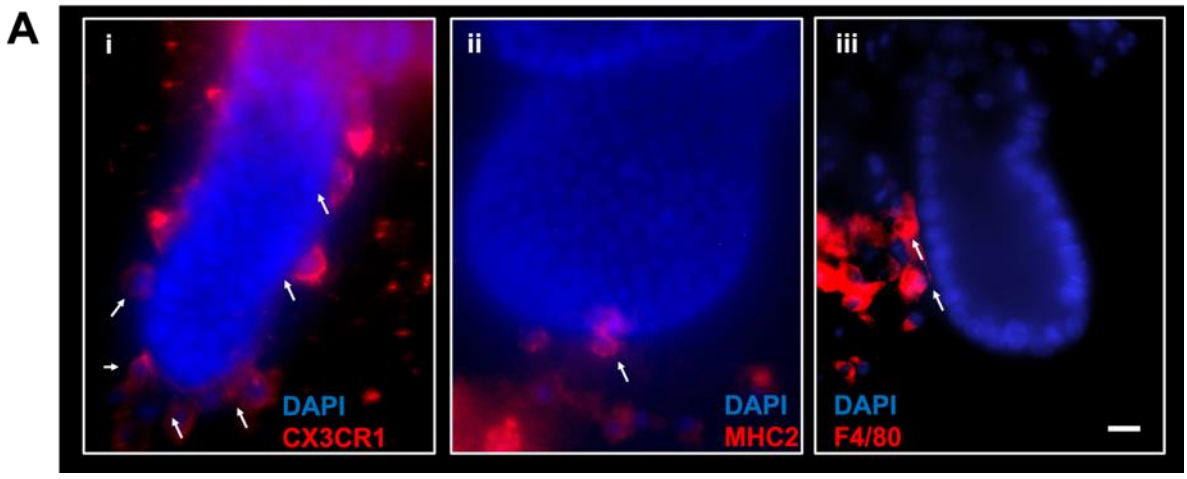

Figure 5.8: Macrophages maintain their macrophage phenotype when in contact with colonic crypts *in vitro*

A) Epi-fluorescent images of crypt-macrophage contact (white arrows) *in vitro* co-cultures showing expression of DAPI (blue) and **Ai)** CX3CR1 (red) positive Naïve macrophages in contact with colonic crypts, **Aii)** MHC-2 (red) positive Naive macrophages in contact colonic crypts and **Aiii)** F4/80 (red) positive M1 macrophages in culture with colonic crypts. Scale bar at 15μm.

As previous results in this chapter have shown that physical contact between macrophages and crypts be made in our *in vitro* macrophage-crypt co-culture model, we then aimed to understand whether the juxtacrine Notch signalling pathway is required to establish cell-cell contact between the macrophages and the colonic epithelium.

5.2.9 M1 macrophage to crypt contact is maintained in the presence of DAPT after 24 hours in co-culture

To understand whether macrophages could maintain cell-cell contact with colonic crypts in the presence of DAPT. Crypts were cultured with M1 macrophages for 24 hours in the presence and absence of DAPT (25μg/ml) and live-cell images were captured under an epi-fluorescent microscope as per **Section 2.3.1. Figure 5.9A** shows representative brightfield images of crypts cultured with M1 macrophages in the presence of DAPT compared to M1 vehicle control (VC). Macrophages (white arrows) are shown as Phagogreen (green) positive. The number of Phagogreen positive cells located along the crypt-axis was analysed in **Figure 5.9B**, in which no significant differences were observed between M1 crypt co-culture treated with DAPT compared to the vehicle control. **Figure 5.10A**, show representative live-cell brightfield images cultured with M1 macrophages in the presence of DAPT compared to M1 vehicle control (VC). The total number of M1 macrophages in contact with colonic crypts were analysed in **Figure 5.10B**, and a non-significant decrease in contact was found in the presence of the γ-secretase inhibitor, DAPT compared to vehicle control (VC). **Figure 5.10C**, the number of M1 macrophages distributed along each crypt region after 1 and 3 hours in co-culture were analysed, where no significance was observed in crypts cultured with M1 (VC) or M1 macrophages in the presence of DAPT. Similarly, in **Figure 5.10D**, where only contact between macrophages were and their position along the crypt-axis was analysed. Here, the percentage of M1 macrophages distributed along each crypt region after 1 and 3 hours in co-culture were analysed, where also no significance was observed in crypts cultured with M1 (VC) or M1 macrophages in the presence of DAPT.

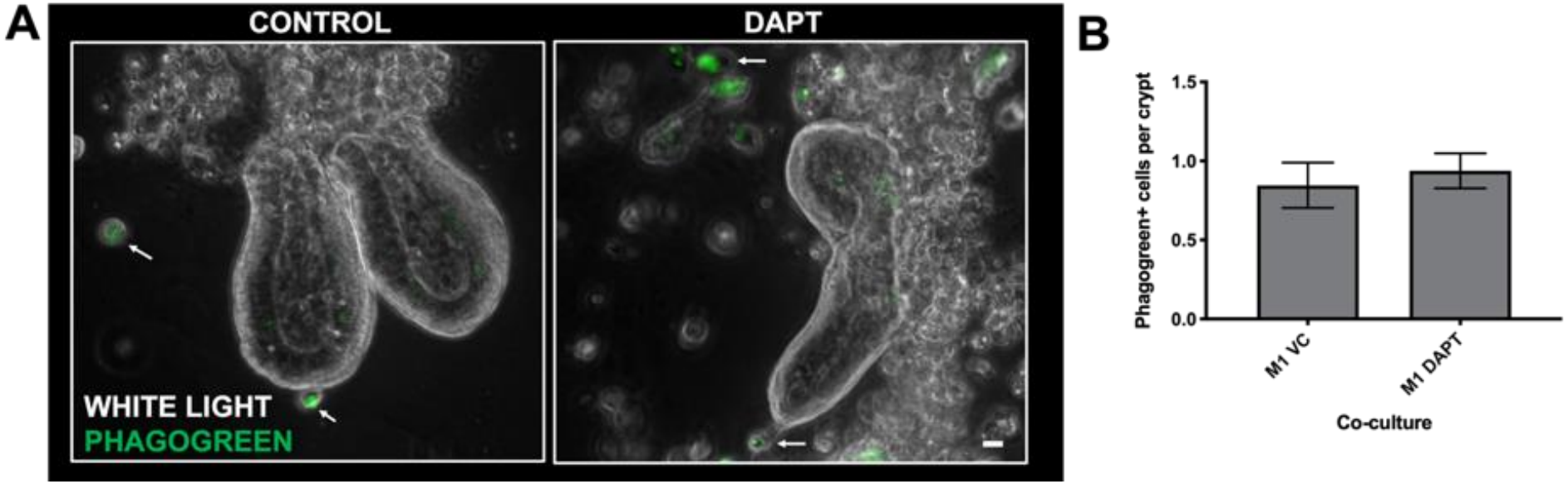

Figure 5.9: Phagogreen+ cells to colonic crypt contact is maintained in M1-crypt co-culture after 24 hours

A) Representative epi-fluorescent brightfield composite image of M1-crypt co-cultures compared to DAPT treated M1-crypt co-culture, showing (green) expression in macrophages (white arrow) Scale bar 10µm (**B)** Histogram showing Phagogreen+ cell expression per crypt in M1 co-culture conditions with VC (Vehicle control) and DAPT (Notch inhibitor). (n=3, N≥16) ns

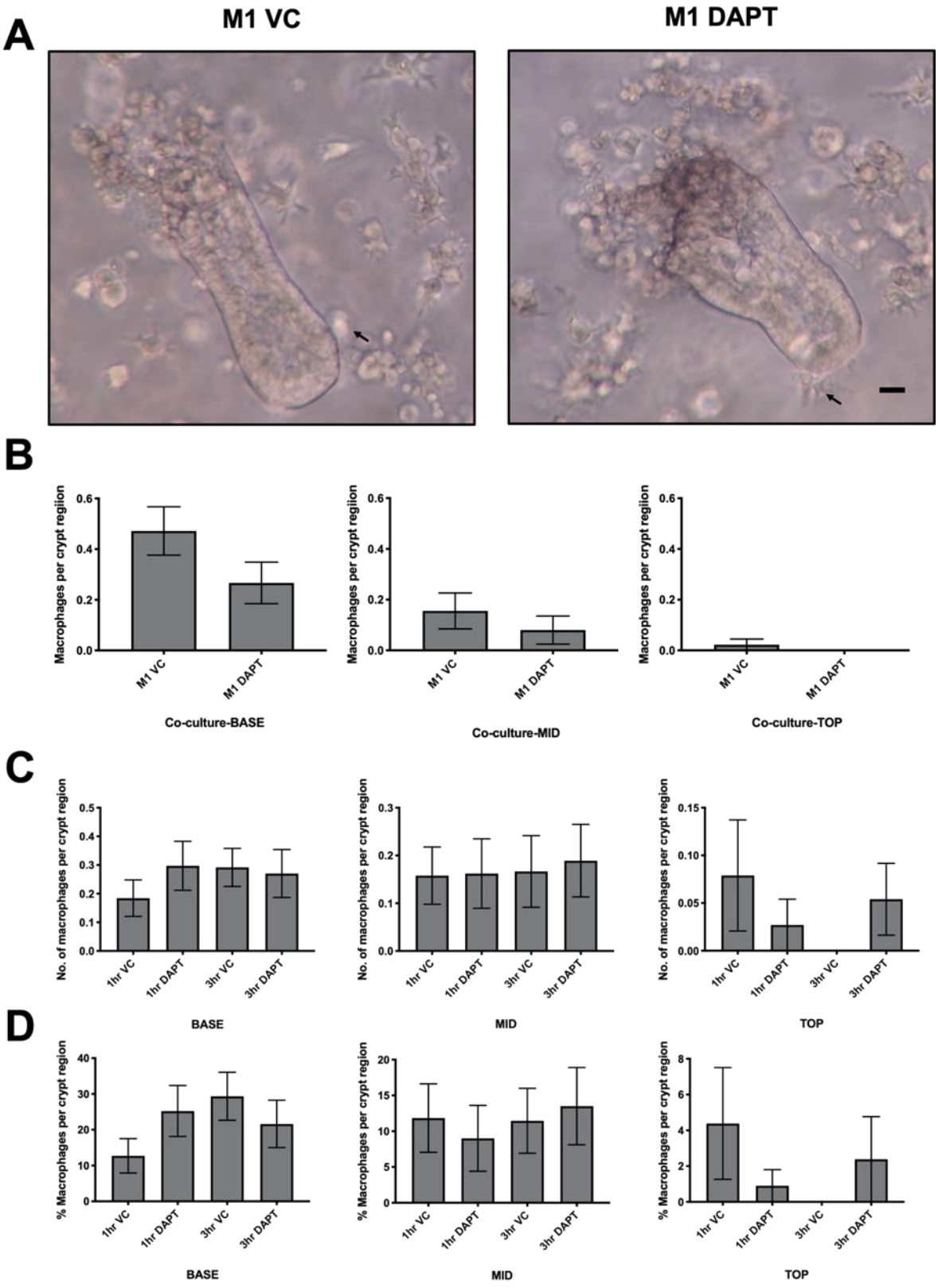
A
M1 VC
M1 DAPT
B
Macrophages per crypt region
M1 VC
M1 DAPT
Co-culture-BASE
Co-culture-MID
Co-culture-TOP
C
No. of macrophages per crypt region
1hr VC
1hr DAPT
3hr VC
3hr DAPT
BASE
MID
TOP
D
% Macrophages per crypt region

Figure 5.10: M1-crypt contact is maintained in the presence of DAPT *in vitro*

A) Representative live-cell brightfield images of colonic crypts cultured with M1 macrophages in the presence of VC (DMSO-vehicle control) or DAPT after 24 hours. **B)** Histogram showing the average number of macrophages per crypt in each culture condition (n=3, N≥37, non-signficant). **C)** Histogram showing the average number of macrophage distributed along each crypt region in each culture condition (n=3, N≥37, non-signficant). **D)** Histogram showing the percentage of macrophages distributed along each crypt region in each culure condition (n=3, N≥37, non-signficant). Scale bar at 15µm.

5.2.10 Appearances of dark, filopodia-like protrusions in colonic crypts cultured alone and in the presence of macrophages

Throughout the culture of colonic crypts alone (**Figure 5.11Ai)** and in the presence of macrophages (**Figure 5.11Aii)**, we have sighted small, dark filopodia-like process protruding from the colonic epithelium. **Figure 5.11A**, show exemplar live-cell brightfield images of the presence of spindle-like shaped filopodia (arrow) with an approximate length of 10-15µm localised near the base of the crypt after 1 hour in culture.

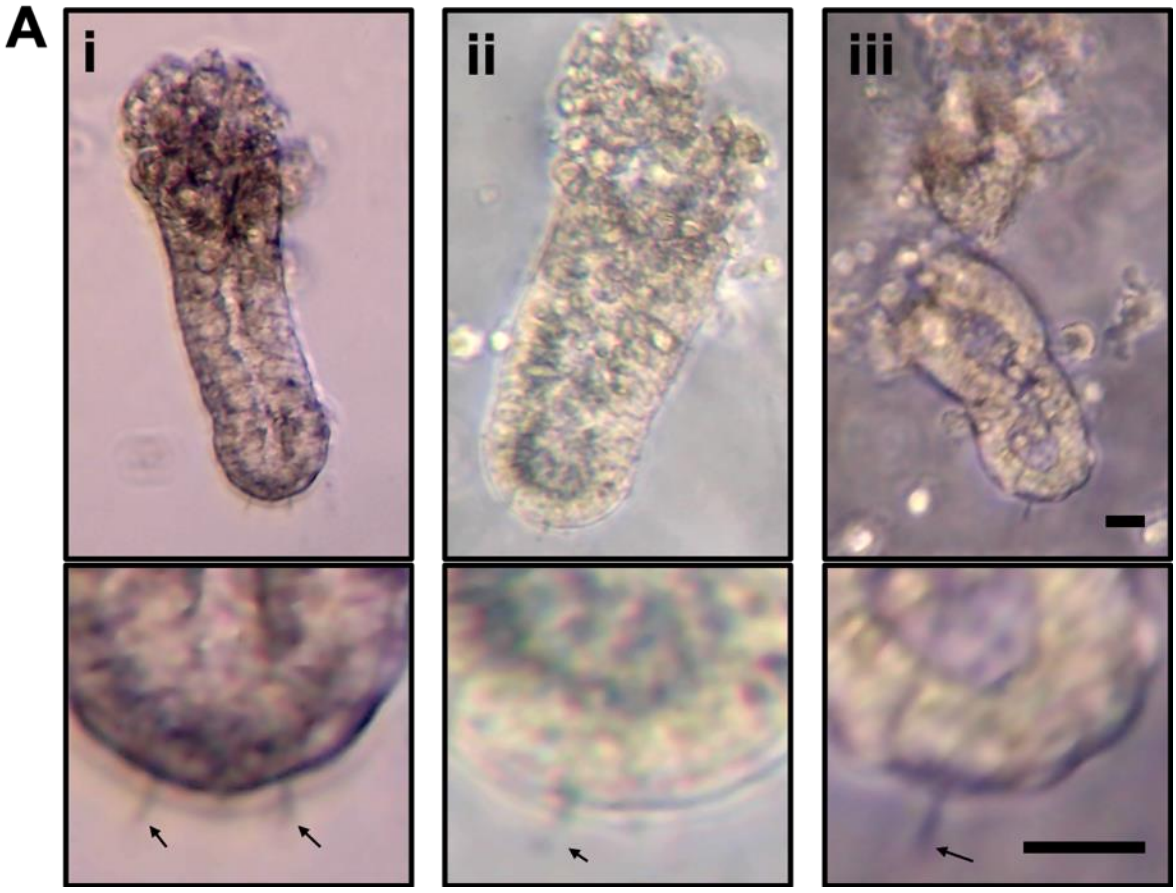

Figure 5.11: Appearances of dark, filopodia-like protrusions in colonic crypts cultured alone and in the presence of macrophages *in vitro*

A) Examples of dark filopodia-like processes protruding from the colonic crypts cultured alone **Ai)** and with M1 **(Aii)** or M2 macrophages **(Aiii)**. Scale bar at 25µm.

5.3 Discussion:

In this chapter of the study, we have cultured colonic crypts along with bone-marrow derived macrophage subtypes (Naïve, M1 and M2) in order to track and characterise the morphological changes both entities undergo over the course of our 3D Matrigel co-culture.

Following the isolation and co-culture of Naïve, M1 or M2 macrophages with colonic crypts, we observed a reduction in the presence of native crypts and an increase in shorter crypts over the course of 48 hours when crypts were cultured with macrophages. As we have shown that all macrophage subtypes are able to substantially upregulate epithelial proliferation on Day 2, it is therefore likely that epithelial turnover has increased in these crypts, thus increasing the rate of shedding. We did not observe any changes in colonic spheroid formation in the presence of either Naïve, M1 or M2 macrophages. This contrasts Ihara's work where, the direct adhesion of CD11c+ dendritic cells induced an increase in spheroid formation (Ihara et al., 2018). To further verify whether macrophages can induce morphological changes in the epithelium, the optical volume of each colonic crypt can be measured by capturing optical confocal slices and summating the epithelial area of each plane using a confocal microscope in future experiments (Sieck et al., 1999).

Interestingly, when colonic crypts were co-cultured with M1 macrophages, the crypt length and epithelial area was significantly reduced compared to crypts cultured alone, with Naïve or M2 macrophages after 24 hours. A detailed morphological study performed by Tan et al, noted that the length of the colonic crypts can differ significantly depending on its position in the colon, where the shortest crypts were found in the proximal colon and longer crypts were present at the distal end (Tan et al., 2013). As crypts used in our co-culture model were isolated from all three sections of the colon and homogenised prior to their co-culture with macrophages in our 3D Matrigel, we can assume that the reduction in crypt length we observed was triggered solely by the presence of M1 macrophage-dependent factor. In contrast to our *in vitro* work in this chapter, a reduction in *in vivo* colonic crypt length was also observed by Skoczek et al following the antibody-blocking of Ly6C+ cells in the mucosa, suggesting that macrophage-predecessors may contribute to crypt atrophy instead. Furthermore, as previously determined in **Chapter 4**, the number of goblet and tuft cells, both derivatives of the secretory cell lineage, were reduced in crypts cultured with M1 macrophages. Whether such as reduction could contribute to the shortening of the crypt is

currently not known and further work is required to determine this. Here a non-toxic nuclear staining dye (NucSpot dye) could be used to track individual cells within the crypts over a period of time.

According to Onfroy-Roy et al, colon deformability can be defined by the intestinal crypts' capacity to elongate or shrink without tearing (Onfroy-Roy et al., 2020). One of the many external factors which must be regulated to maintain colonic crypt survival is the extracellular matrix where, within an *in vivo* setting, colonic crypt morphology is often shaped by the topography of the surrounding extracellular matrix and the rearrangement of ECM composition can play a significant role in the proliferation and differentiation of the epithelium (Basson et al., 1996; Onfroy-Roy et al., 2020). In IBD, the increased influx of neutrophils, T-cells and macrophages often exacerbates ECM degradation via the secretion of various MMPs (matrix metalloprotease) and NEs (neutrophil elastase), naturally leading to a loss in ECM scaffolding, increased epithelial shedding and alterations in cell morphology in vitro. (Groulx et al., 2011). Previous studies have already established that human macrophages are able to remodel and shape the extracellular matrix in order to aid its migration through the interstitial matrix (Bahr et al., 2018). Interestingly, the metal metalloproteinases (MMP), 8,9 and 10 secreted by M1 macrophages are significantly upregulated in the mucosa of IBD patients and colitis-induced mice and often aid the degradation of the extracellular matrix (Pedersen et al., 2009; Sullivan et al., 2014). Furthermore, in early inflammation, M1 macrophages were shown to induce ECM fibrosis and promote the activation of local fibroblasts, whereas M2 macrophages were activated during the latter stages of intestinal scar resolution (Wynn et al., 2010). However, the complete ablation of macrophages also prevents further ECM remodelling required to strengthen epithelial scaffolding and support crypt survival (Valentin et al., 2009).

In vivo, the colonic basement membrane scaffolding components such as laminin (laminin α1 and α2), collagen and elastin provided by mesenchymal cell; localised near the base of the crypt are also essential for the proliferation and differentiation of the stem cell niche (Hughes et al., 2010; Sasaki et al., 2002). However, as our macrophage-crypt co-culture is devoid of other stromal cells, it is likely that M1 macrophages can manipulate colonic crypt deformability by remodelling of the 3D Matrigel's ECM within our co-culture model. Interestingly, recent quasi-3D modelling work in the small intestine, carried out by He et al,

has showcased the importance of extracellular matrix stiffening on epithelial differentiation, where increased stiffening within the culture model, led to an increase in enterocyte and ablation in tuft cell numbers, where Lgr5+ and Ki67+ cells numbers were also found to be reduced at lower stiffnesses (He et al., 2021).

As we were unable to confirm the causative factor which led to the reduction in crypts length within our M1 macrophage-crypt co-culture, to further understand the exact role the macrophage subtypes have on ECM remodelling, we suggest the use of a traction microscopy and displacement fields to identify whether forces/stiffness induced by M1 macrophages and collagen alignment influences crypt size *in vitro*. This will also allow us to understand whether macrophage-mediated changes in ECM stiffness contribute to the changes in epithelial renewal we have observed in the previous chapter (Perez-Gonzalez et al., 2020).

We have also identified and observed a reduction in the presence of extracellular vesicles in the presence of Naïve, M1 and M2 macrophages when compared to crypts cultured alone shortly following their isolation and culture. Although the exact functions of such extracellular vesicles have not been delineated and require further attention, a number of studies have reported similar findings within their culture model. For example, early work from van Niel et al have shown that both human HT29-19A and murine MODE K epithelial cell lines secreted exosome-like vesicles containing HSP-90 (heat shock protein 90), α-enolase, MHC-2, A33 and tubulin from the apical and basal side where its presence was significantly increased following IFN-γ stimulation (Van Niel et al., 2001; Van Niel et al., 2003). In 2010, Barreto et al's work also demonstrated that Caco-2 cells infected with a rotavirus strain, released membrane vesicles slightly larger in size, which just as van Niel's work contained heat-shock proteins and most notably TGF-β, a potent regulator of regulatory T-cell expansion *in vivo* (Barreto et al., 2010; Ihara et al., 2017). Interestingly, advancements in study of intestinal epithelia-derived vesicles were made in 2016, when Jiang et al isolated the TGF-β1, A33+ producing vesicles and transferred them into DSS-induced mice, which significantly reduced IBD severity in mice (Jiang et al., 2016). Similarly, Leoni et al., also identified Annexin A1+ extracellular vesicles which promoted wound repair in DSS-induced mice, where the cleavage of Annexin A1 was dependent on the matrix metalloproteinase MMP9, also commonly expressed by M1 macrophages (Hanania et al.,

2012; Leoni et al., 2015). During inflammation, the expression of chemokines such as IL-8, MCP-1 and MCP-3 among others increases aberrantly, although we have noted that macrophages are pre-dominantly localised around the base and mid-region of the crypt, we are unable to confirm whether epithelial-derived cytokines are involved in the recruitment of Naïve, M1 and M2 macrophages (Wang et al., 2018; Reinecker et al., 1995; Kulkarni et al., 2016). We therefore suggest that chemokine ligand expression in the co-culture media is measured using commercially available ELISA kits.

Additionally, although, work from Oszvald and colleagues has shown that extracellular vesicles within their culture model are able to rescue intestinal stem cell numbers by transporting epidermal growth factors (EGF) following the depletion of exogenous EGF, as the vesicles were derived from fibroblasts rather than the epithelial cells, it is unlikely epithelial-derived vesicles carry a similar function within our 3D co-culture model (Oszvald et al., 2020).

Conventionally, epithelial cells at the base of the crypt can be shed into the apical lumen in order to rid of cells with excessive signalling, in an attempt to reduce tumor formation (Slattum et al., 2009). However, a number of studies have reported a phenomenon in which cells were extruded basally from the intestinal epithelium (Slattum and Rosenblatt, 2014; Rosenblatt et al., 2001; Ohsawa et al., 2018). As mentioned, apoptotic cells are predominantly extruded from the lumen at the top of the crypt, it is likely that 'find-me' and 'eat-me' chemoattractant are being secreted and received by nearby macrophages within the 3D Matrigel co-culture model and we are unable to verify whether such signals play a role in macrophage localisation. To overcome this limitation, we suggest that macrophages are cultured along with an *ex vivo* explant crypt model, within which the epithelial barrier remains intact similarly as to the work performed by Skoczek or Pearce et al (Skoczek et al., 2014; Pearce et al., 2018).

As the colonic crypts are lifted from their *in vivo* environment and transferred *in vitro* Matrigel-based microenvironment it is also likely that the cell polarity and microtubule dynamics within the epithelium have been disturbed following its mechanical dissociation (Muroyama et al., 2018). Here, work from Slattum et al, has confirmed that basal extrusion may occur in an instance in which the microtubules have not been realigned and cause the contraction of neighbouring cells at their apices. It therefore also becomes a possibility the

vesicle-like exosome we have observed basally along the crypt-axis, are apoptotic cells which have been extruded via the mechanisms mentioned above. It should be noted that the size of the extracellular vesicles reported in other intestinal studies were 20-1000nm in size and we lacked the magnification to identify the exosomes of smaller sizes in our study (Bui et al. 2019; Jiang et al., 2016; Niel et al., 2001).We therefore propose the use of transmission electron microscopy (TEM) to quantify the presence of intestinal epithelial derived exosomes, a technique previously utilised in exosome studies of Oszvald and Bui et al. (Oszvald et al., 2019; Bui et al.,2018). Similar to He et al's work, the resolution of TEM imaging could also be utilised to further capture and study the structural properties of filopodial-mediated macrophage-crypt interactions (He et al., 2018). Furthermore, additional work will be required in order to identify the contents of the exosomes which could possibly will give us further insight as to its exact function in the recruitment of macrophages. Although nanoparticle-tracking analysis and exosome-isolation kits and are available and have been utilised previously to profile the proteinic contents of such vesicles, it is challenging to isolate the vesicle we have identified in this manner within our 3D co-culture model, we therefore suggest to immunofluorescently label for apoptotic 'find-me' and 'eat-me' signals as extensively described by Peter's work (Bachurski et al., 2019; Peter et al., 2010; Wong et al., 2016).

We have also identified two archetypical modes of macrophage contact, were the occurrence of macrophage-body to crypt contact occurred more frequently compared to macrophage-filopodia to crypt contact. Recent findings from Chikina et al have demonstrated that macrophages specifically in the distal colon are able to insert ballon-like protrusions (BLP) between epithelial cells (Chikina et al., 2020). Unlike, Rescigno's work in 2001, these BLPS did not reach out to the lumen and were instead positioned between the epithelial cells. Further, phenotyping also revealed that the BLP+ macrophages were $CD11c^{high}$ (Rescigno et al., 2001; Chikina et al., 2020). In crypts cultured with M1 macrophage, which we have previously reported to be CD11c+ in Chapter 3, we did not report an increase in macrophage-body to crypt contact which may have been indicative of BLP formation. We therefore suggest that the capacity of Naïve, M1 and M2 macrophages to form BLPs is investigated further future experiments to understand whether the occurrence of BLPs is linked to the differential changes in epithelial renewal we have

reported in **Chapter 4**. A study from Goodman, has established that the formation of tunnelling nanotubes (TNT) in M1 macrophages was reduced compared to alternatively activated M2 macrophages. Although macrophages in our 3D Matrigel co-culture were shown to express microtubule-like protrusions we did not identify any long and thin TNTs in any of our macrophage subsets. It is likely that the 3D environment in our co-culture, unlike other macrophage-filopodial studies, does not offer sufficient ECM scaffolding support in order to allow the formation of TNTs and a polyacrylamide hydrogel-based co-culture model may need to be developed to further characterise the formation of TNTs and their effect on colonic epithelial renewal (Kress et al., 2007; Goodman et al., 2019). In this chapter, we did not delineate the effect Naïve, M1 or M2 macrophages have on the individual ECM components within Matrigel. Understanding whether macrophage-secreted proteases can affect the ECM scaffolding within our Matrigel-based co-culture model may allow us to link these changes to the findings we have made in the previous chapter. To study this mechanism further we suggest the use of a protein fingerprint assay as previously described by Karsdal et al, in which the accumulation of smaller degraded ECM fragments within the culture media can be characterised via mass spectrometry (Karsdal et al., 2013; Karsdal et al., 2013*). Following the fixation of the crypt-macrophage co-culture with 4% PFA, the Matrigel often disintegrated over the course of the immunohistochemical protocol resulting in the partial loss of both crypts and macrophages. To study the formation of macrophage and epithelial protrusions, we suggest live-imaging of the co-culture with a live-tubulin stain (tubulin tracker) to further characterise the role of microtubules and cellular protrusions play in establishing macrophage-crypt contact.

In macrophage-crypt co-cultures in which Notch signalling was inhibited for 24 hours using a y-secretase inhibitor (DAPT), we noted a decreasing trend in M1 macrophage to crypt contact. This may suggest that Notch signalling needs to be constitutively activated in order for macrophage to remain in contact with colonic crypts, however, to confirm this hypothesis, we will need repeat the experiments and monitor the contact behaviour between the crypts and M1 macrophage over the course of 48 hours.

In this chapter we have also reported the rare sightings of small, dark filopodia protruding from the base of the colonic crypt. In homeostasis, a small population of lymphocytes have reportedly been residing within the epithelial barrier of the small and large intestine, where

its presence decreases, respectively (Hoytema et al., 2017). Research suggests that such intraepithelial lymphocytes (IELs) may play role in maintaining epithelial barrier integrity by encouraging epithelial cells to migrate into the gap created by previously shed cells (Cukrowska et al., 2017; Patterson and Watson., 2017). As we are currently unaware whether the macrophage-IEL crosstalk within our co-culture are able to mediate epithelial renewal via a yet to be identified mechanism, the exact number of IELs within our 3D Matrigel co-culture model must be verified. To do so in the future, we suggest immunofluorescently labelling such cells within our co-culture with the CD8αα and TCRαβ markers which are unique to the IEL population (Ma et al., 2021).

In contrast to findings from Skoczek et al and Pull et al., in which F4/80+ macrophages were recruited towards the crypts base following luminal LPS stimulation, we observed a reduction in M1 and M2 macrophages when cultured with colonic crypts. The reason as to why M1 and M2 macrophage do not contact the crypt's +4 position as frequently as the Naïve macrophage phenotypes remains unclear and must be further investigated. (Skozcek et al., 2014; Pull et al., 2005).

Within this chapter we have also attempted to measure the volume of shed cells extruded into the shedding zone in a semi-quantative manner, in which we measured the shedding zone at the top of crypt. Although we did not find any significant differences in shedding in crypts cultured with macrophages compared to control it should be noted that, we were not able to accurately distinguish apoptotic cells from any macrophages which may have localised within the shedding zone. Furthermore, as crypts are embedded within a three-dimensional space, shedding may occur at different focal planes. For this reason, we suggest immunofluorescently labelling apoptotic cells with a cleaved caspase-3 antibody and capturing live optical slices of the colonic crypt's upper shedding region.

It should also be noted that the majority of macrophages seeded may not have been in direct contact with crypts and it remains unclear whether secretory factors may be secreted. Furthermore, during the co-culture of macrophages and colonic crypts, there is a likelihood of incidentally placing the macrophages near the crypts' basal region, therefore we could not establish whether the macrophages have migrated to its point of interest. To study macrophage migration and localisation towards the epithelium, a chemotactic assay or transwell migratory co-culture assay should be set up in the future allowing us to quantify

the rate of migration and confirm that macrophage have migrated and contact their preferred position of along the crypt axis.

Conclusion:

In this chapter, morphological analysis of colonic crypts and macrophages revealed that, colonic crypts are shortened by the presence of M1 macrophages; M2-crypt contact is reduced compared to Naïve and M1 macrophages and basal extrusion of larger microvesicles is reduced in crypts cultured with M1 and M2 macrophages. Overall, we can confirm physical interactions between Naïve, M1 and M2 macrophages and colonic crypts do occur within our 3D co-culture system and may differentially affect crypt morphology, crypt-vesicle extrusion, and the macrophage localisation along the crypt-axis. Whether macrophages are able to indirectly influence crypt morphology and epithelial renewal through remodelling of the Engelbroth-Holm Swarm-based ECM is yet to be investigated. As we show in this chapter that many macrophages within our 3D *in vitro* model were not in contact with colonic crypts, it is unknown whether nearby macrophages are able to release secretory factors to influence colonic crypt renewal. For this reason, the next chapter will determine whether macrophage- secretory factors or physical contact we have observed can alter colonic crypt renewal.

Chapter 6: Physical Contact and Secretory Factors Differentially Regulate Colonic Crypt Growth and Differentiation *In Vitro*

6.1 Introduction

One of the early hallmarks identified in IBD, was the increased production of monocytes in the bone-marrow which then migrate and differentiate into macrophages. Which are then strategically juxtaposed under the single-cell layer thick epithelium to intercept any foreign invasions. (Meuret et al., 1978; Grimm et al., 1994; Bain et al., 2013). Although the phenotypic characteristics and migratory mechanism of macrophages in IBD versus the steady state have been well defined over the past decade, little is known regarding their reciprocal relationship with the intestinal epithelium (Bain et al., 2013, Orecchioni et al., 2019).

As previously described, work from Skoczek et al, has shown that monocytes are recruited and form contact with Lgr5+GFP+ colonic stem cells following luminal stimulation with LPS and studies from both Niess and Chieppa, were first to show that CX3CR1+ cells are able to form transepithelial dendrites to sample luminal contents, indicating at strong physical contact-depending crosstalk links between macrophages and colonic crypts exists (Skoczek et al., 2014; Niess et al., 2004; Chieppa et al., 2006). Due to the high plasticity and variety of secretory factors intestinal-macrophages are able to synthesise during the steady-state and inflammation, it is difficult to understand whether juxtacrine, paracrine signalling or a combination of both, can affect epithelial renewal in the intestine (Jablonski et al., 2016).

A juxtacrine signalling mechanism most commonly involved in the regulation of epithelial renewal is the Notch pathway. In patients with ulcerative colitis, transcription levels of Notch and Hes1 were significantly elevated (Ghorbaninejad et al., 2019). More recently, work from Kuno et al, have shown that a TNF-α in combination with Notch signalling can upregulate the expression of OLFM4 to promote mucosal regeneration in patients with inflammatory bowel disease (Kuno et al., 2020).

Following the stimulation of from Notch ligands, the NOTCH1 receptor expressing epithelial cells cleave the intracellular NCID, upregulate Hes1 expression which in turn the represses

Atoh1 and consequently the signal-receiving cell does not display any Notch ligand itself (Toth et al., 2016). The balance between the expression of Hath1/Atoh1 and Hes1 in intestinal crypts plays a crucial role in the maintenance of the steady state in the mucosa. An upregulation in Hes1 and suppression of Hath1/Atoh1 was observed in patients with ulcerative colitis which resulted in the depletion of goblet cells (Zheng et al., 2011). Furthermore, the loss of Notch activation, by inhibition of y-secretase, resulted in the exacerbation of inflammation and impaired epithelial repair in colitis-induced mice, highlighting the importance Notch plays in epithelial differentiation. (Okamoto et al., 2008).

Evidence of Notch-mediated crosstalk between macrophages and epithelial cells has been alluded to by several studies. For example, in a co-culture of human macrophages and epithelial cancer cell lines, it was found that M1 but not M2 macrophages showed an increased expression of Notch ligands Jag1 and Dll4 which was dependent on the upregulation of HIF-1, subsequently leading to the increased expression of Hes1 and enterocyte numbers *in vitro* (Ortiz-Masia et al., 2016). In other studies, monocytes expressing Dll4 were recruited and interacted with hepatic epithelial cells following the complete depletion of Kupfer cells *in vitro* (Bonnardel et al., 2019). Aziz et al, have also identified that an increase in Jagged1 and Notch1 in colitis-induced mice was linked with the proportional activation of flagellin-induced toll-like receptor 5 (TLR5) expression in the colon. Interestingly, CD11c+ cells in the lamina propria and alveolar macrophages were also demonstrated to express TLR5, thus it should be questioned whether the upregulation in Notch/juxtacrine signalling observed by Aziz's work is linked to the previously reported surge of macrophages present in IBD (Aziz et al., 2013; Uematsu et al, 2006; Lei et al, 2021).

In contrast to the juxtacrine Notch signalling pathway, Wnt signalling largely operates in a paracrine and autocrine manner (Koch et al., 2017). Understanding of the role of Wnt signalling in inflammatory diseases is limited, however the aberrant activation of Wnt components in cases of chronic IBD and colitis-induced mouse/rat models has become apparent. Dysregulated Wnt signalling was frequently observed in the colon, where in 2018, Swafford et al have demonstrated that the genetic deletion of LRP5/6 in CD11c+ antigen-presenting cells led to a notable increase in disease-severity in colitis-induce mice (Clevers., 2006; Swafford et al., 2018).Genetic mutations of the APC gene in canonical Wnt signalling causing the dysregulated stabilisation of β-catenin, were observed in more than 80% of all

colorectal cancer patients and in patients with Crohn's disease, the expression of the Wnt-downstream transcription factors TCF-1, TCF-4 and LRP6 was significantly reduced likely contributing impaired barrier function (Miyoshi et al., 1992; Beisner et al., 2013; Koslowski et al., 2012). Interestingly, Wnt target transcription factor, TCF-4 and LEF1 expression were considered positive prognostic factors contributing to longer overall survival rates in patients with colorectal cancer by Kriegl and colleagues, once again showcasing the effect Wnt signalling plays in the regulation of epithelial homeostasis (Kriegl et al., 2010).

In colitis-induced models, the expression of Wnt3a and β-catenin were upregulated and a 10-fold increase in CyclinD1 expression was noted in rat models (Xing et al., 2015; Serafino et al., 2014). Curiously, macrophages have also retained the ability to secrete a number of Wnt ligands including Wnt3a, however a definitive link between macrophage mediated Wnt secretion and intestinal inflammation is yet to be made (Malsin et al., 2019).

As we have observed a significant increase in Lgr5+ stem cell expression in colonic crypts cultured with M1 macrophages in the previous chapter. We next aimed to determine whether this phenomenon was reliant on secretory factors or physical contact between the M1 macrophages and the epithelium in the first instance as this work can indicate whether Notch or secreted factor dependent signalling pathway such as Wnt, Hippo etc could have implications for the mechanisms by which potential changes in differentiation and growth can occur. With increasing interest in utilising macrophages as a therapeutic target against intestinal inflammation, we hope to further shed some light on the preferred mechanism of macrophage-crypt crosstalk in this chapter (Na et al., 2019).

In the steady state of the colon, changes in external stimuli can prompt changes within the stem cell nice. As crypt progenitors are able to produce more than 300 crypt cells per day, balanced renewal is key in organoid growth, as aberrant or insufficient proliferation can lead to impaired barrier function and promote inflammation (Marshman et al., 2002). Therefore, we also aimed to determine whether prolonged culture of crypts with M1 macrophages encourages or impairs colonoid formation in our 3D *in vitro* co-culture model. The findings in this chapter suggest that M1 macrophages can utilise a physical contact mechanism to regulate colonic crypt renewal.

6.2 Results

In this chapter a novel *in vitro* 'conditioned media (CM)' co-culture model was utilised as described in **Section 2.2.10,** allowing the comparison of the effects of macrophage to crypt contact and co-culture derived-secretory factors on epithelial crypt growth and differentiation via the incorporation of EdU and immunofluorescent labelling of epithelial tuft, enteroendocrine, goblet and stem cells.

As a result of previous findings in **Chapter 4**, this chapter aimed to determine whether colonic crypt proliferation is dependent on direct contact between Naïve, M1 and M2 macrophage and colonic crypts. Furthermore, as we observed an increase in Lgr5+ stem cells and reduction in UEA-1+ goblet cell numbers in colonic crypts cultured with M1 macrophages in the previous chapter, we next studied whether the alterations in epithelial differentiation is dependent on physical contact between the 'inflammatory' M1 macrophages and colonic crypts. Therefore, goblet (UEA-1+), tuft (DCAMKL1) and stem cell (Lgr5) expression in crypts were measured when cultured with M1 macrophages (M1 co-culture), without direct contact to M1 macrophages but placed in vicinity of a M1-crypt co-culture (M1 cond.media) and cultured in vicinity to M1 macrophages seeded alone (M1-only) . Additionally, Wnt target gene expression of LEF1 and CyclinD1 in crypts within the M1 co-culture, M1 cond. media and M1-only culture models were semi-quantitatively analysed using immunofluorescently labelling.

6.2.1 Secreted factors from M1-crypt co-cultures, but not M1-crypt physical contact is required for M1-induced increase in EdU incorporation.

As EdU incorporation was shown to significantly increase in crypts cultured with Naïve, M1 and M2 macrophages in **Chapter 4.2.1**, this chapter aims to determine whether physical cell-cell contact between macrophages and colonic crypt cells or secretory products derived from crypts cultured with macrophages is the causative factor for the observed increase.

Figure 6.1A show representative images of EdU (green) incorporation in crypts-(cells in red) cultured in the presence of Naïve, M1 or M2 macrophages (co-culture) and crypts cultured without direct contact to Naïve, M1 or M2 macrophages (conditioned media-CM) but placed in vicinity to a co-culture. Semi-quantitative analysis of the percentage of EdU+ positive cells compared to the total number of DAPI positive cells are shown in **Figure 6.1B**. In crypts directly cultured with Naïve, M1 and M2 macrophages a significant increase in the percentage of EdU incorporation was observed compared to control crypts.

Colonic crypts cultured without direct contact between naïve macrophages but placed in vicinity of a Naïve-crypt co-culture (Naïve CM), the percentage of EdU incorporation remained unchanged compared to control crypts. When crypts were cultured without direct contact with M1 macrophages (M1-CM) but placed in vicinity to an M1-crypt co-culture, the percentage of EdU incorporation was significantly increased compared to control crypts. No significant changes in the percentage of EdU incorporation were found in crypts cultured without direct contact with M2 macrophages (M2-CM) but placed in vicinity to the M2-crypt co-culture compared to control crypts. Additionally, it should also be noted that the percentage of EdU incorporation was also significantly higher in M1-CM in comparison to Naïve-CM or M2-CM.

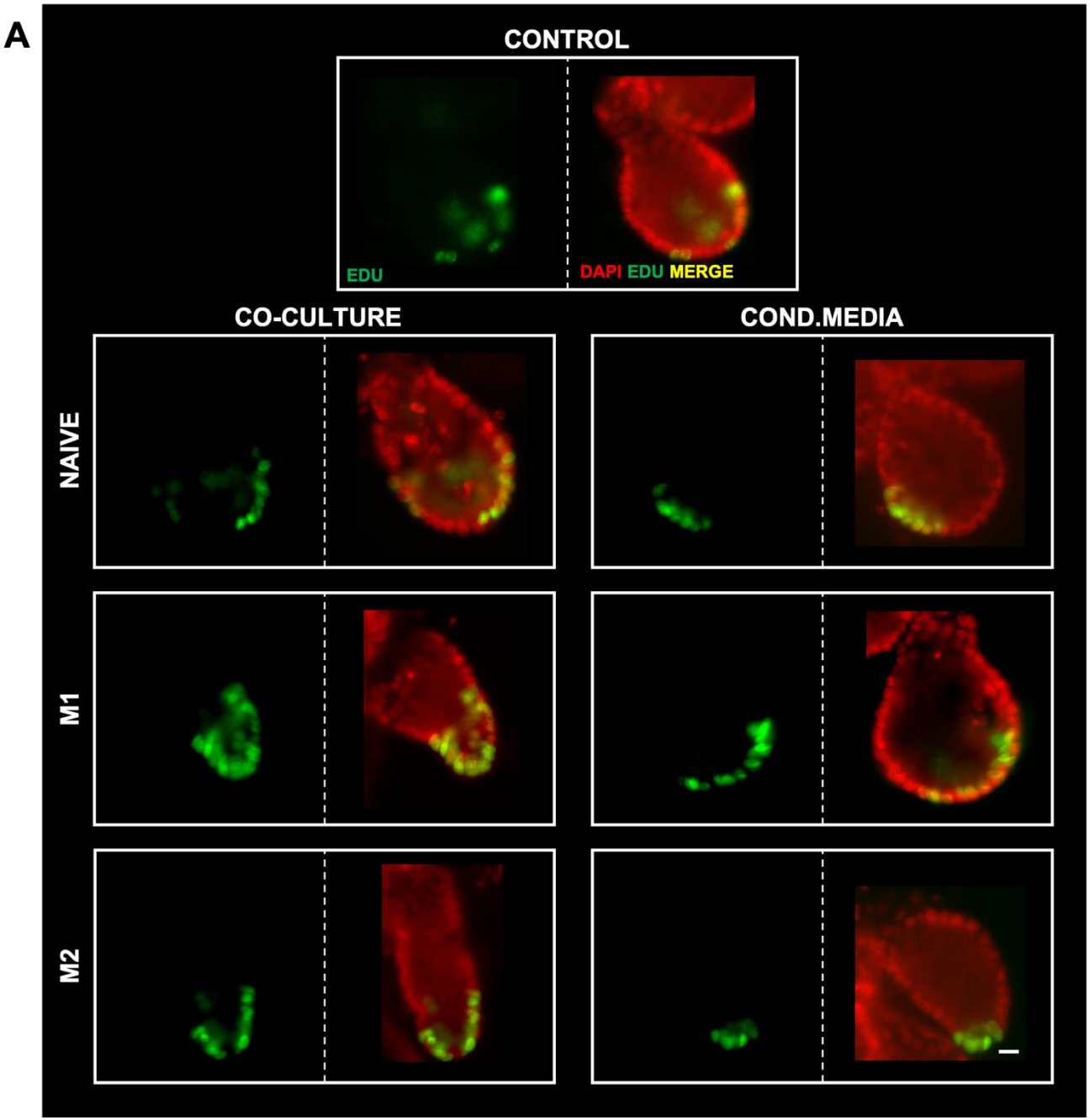
A
CONTROL
EDU
DAPI EDU MERGE
CO-CULTURE
COND.MEDIA
NAIVE
M1
M2

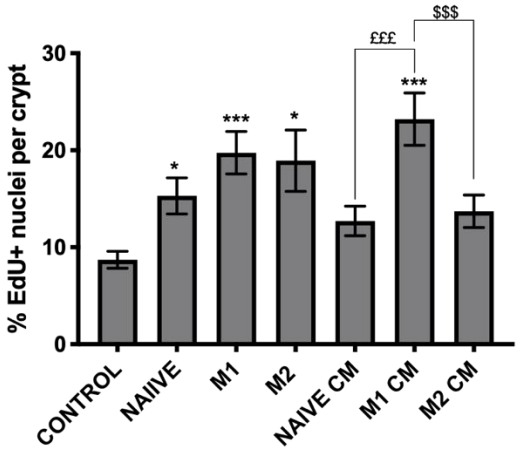
B
% EdU+ nuclei per crypt
30
20
10
0
*
***
*
£££
***
$$$
CONTROL
NAIVE
M1
M2
NAIVE CM
M1 CM
M2 CM

Figure 6.1: Secreted factors from M1-crypt co-cultures, but not M1-crypt physical contact, is required for M1-induced increase in EdU incorporation *in vitro*

A) Representative epi-fluorescent images showing EdU incorporation (green) in the nuclei (red) within colonic crypt-macrophage co-culture and conditioned media. **B)** Histogram showing the percentage of EdU positive nuclei per crypt within each co-culture and secreted factor (CM) condition. (n=4, N ≥35, compared to Control *P<0.05, **P<0.01, ***P<0.001; Naïve compared to M1 £P<0.05; M1 compared to M2 $$P<0.01) Scale bar at 15µm.

Here we have established that Naïve and M2 macrophages are only capable of inducing colonic crypt proliferation through physical contact in our 3D *in vitro* co-culture model, while M1 macrophages were able to induce crypt cell proliferation via physical contact and in a secretory manner. As we have previously shown in **Chapter 4** that UEA-1+ goblet cell and DCAMKL1+ tuft cells were significantly reduced in crypts cultured with M1 macrophages and Lgr5+ stem cell numbers increased,next, we were determined to investigate whether the changes we have observed were dependent on M1 macrophages physical contact or secretory factors in our 3D macrophage-crypt co-culture model.

6.2.2 Physical contact between M1 macrophages and colonic crypts but not secretory factors decrease UEA-1+ cell expression

To determine whether the reduction in UEA-1 positive cell expression in crypts cultured with M1 macrophages were induced by physical macrophage to crypt contact or via co-culture derived secretory factors is revealed in **Figure 6.2. Figure 6.2A** show, representative confocal images of crypts cultured alone, cultured along with M1 macrophages (M1 co-culture), crypts cultured without direct contact to a M1-crypt co-culture (M1 cond.media) and crypts cultured alone but placed in vicinity to M1 macrophages (M1-only). UEA-1 staining is shown in green throughout the crypt lumen, with E-cadherin (cell-cell adhesion molecule) shown in red and DAPI positive cells shown in blue. In UEA-1 positive cells (white arrows), UEA-1 labelling is extended from the crypt lumen into the cell's vacuole. In **Figure 6.2B** the expression of the number of UEA-1 positive cells per crypt was analysed, where numbers in crypts of M1 cond. media and M1-only culture models were maintained. However, a significant decrease in the number of UEA-1 positive cell expression was observed in crypts cultured in the presence of M1 macrophages compared to control crypts. In **Figure 6.2C**, the percentage of DAPI positive cells that are UEA-1 positive per crypt were measured, where the expression was maintained in all three, M1 co-culture, M1 cond. media and M1-only culture models. Although non-significant it should be noted that UEA-1 expression was reduced in crypts cultured in the presence of M1 macrophage.

In **Figure 6.2D**, the distribution of UEA-1 positive cells in each region along the crypt-axis was quantified. In control, UEA-1 positive cells were mostly located at the base and mid region of the crypt with lower expression found at the top of the crypt region. UEA-1 positive cell numbers at the base of crypt in the M1 co-culture, M1 cond. media and M1-only culture model remained unchanged. The number of UEA-1 positive cells expressed in the mid region was also maintained in crypts in the M1 cond. media and M1-only culture model, however a significant decrease in UEA-1 positive cell numbers was observed in crypts cultured along with M1 macrophages compared to both control crypts and the M1 cond.media model. UEA-1 positive cell expression at the top of the crypt-axis was maintained throughout crypts in M1 cond. media, M1-only culture models and crypts cultured in the presence of M1 macrophages (M1 co-culture).

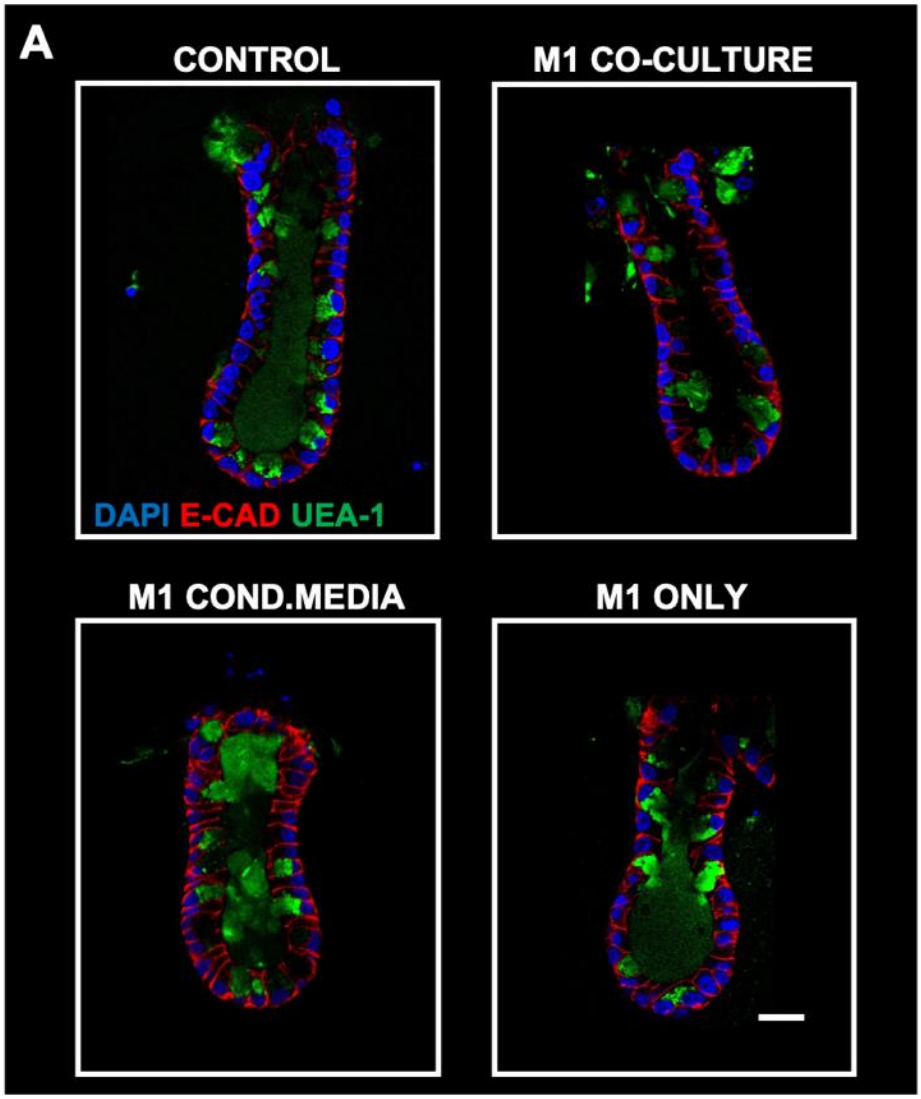
A
CONTROL
M1 CO-CULTURE
DAPI E-CAD UEA-1
M1 COND.MEDIA
M1 ONLY

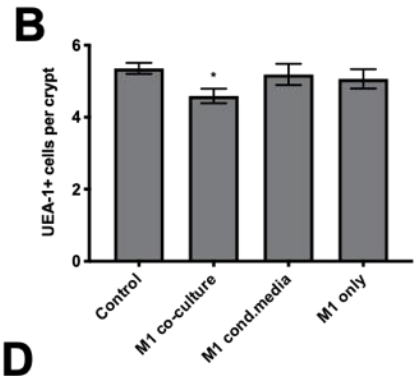
B
UEA-1+ cells per crypt
0
2
4
6
*
Control
M1 co-culture
M1 cond.media
M1 only

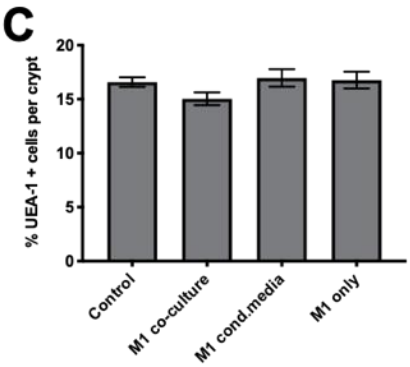
C
% UEA-1 + cells per crypt
0
5
10
15
20
Control
M1 co-culture
M1 cond.media
M1 only

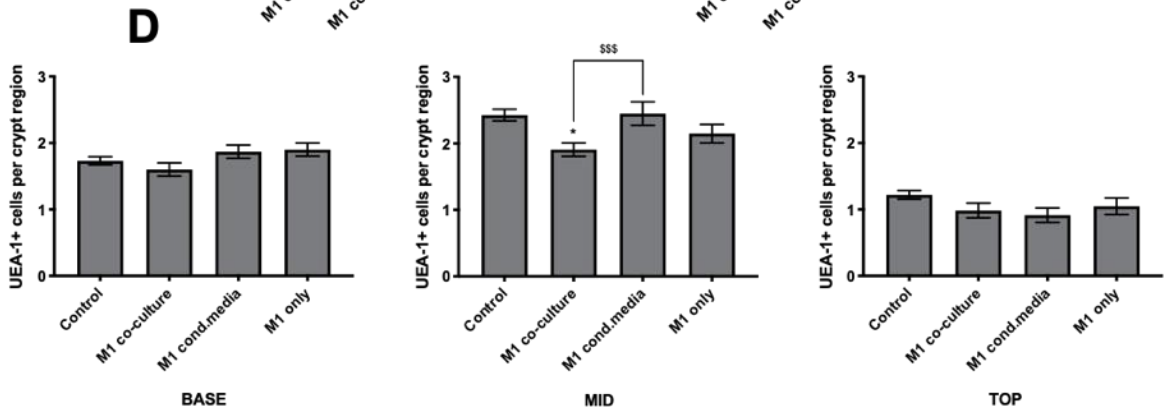
D
UEA-1+ cells per crypt region
0
1
2
3
Control
M1 co-culture
M1 cond.media
M1 only
BASE
$$$
*
MID
TOP

Figure 6.2: **Physical contact between M1 macrophages and colonic crypts but not secretory factors decrease UEA-1+ cell expression in crypts *in vitro***

A) Representative confocal images showing UEA-1 expression (green), nuclei (blue) and E-cadherin (red) in crypts cultured in the M1 co-culture, M1 cond. media and M1-only culture models. **B)** Histogram showing the average number of UEA-1 positive cells per crypt cultured in the M1 co-culture, M1 cond. media and M1-only culture models. **C)** Histogram showing the percentage of UEA-1 positive cells per crypt cultured in the M1 co-culture, M1 cond. media and M1-only culture models **D)** Histogram showing the average number of UEA-1 positive cells per crypt region when cultured in the M1 co-culture, M1 cond. media and M1 only culture models. (n=6, N≥*76, *P<0.05 compared to Control;* $^{\$\$\$}$*P<0.001 compared to M1 co-culture)* Scale bar 20μm.

6.2.3 Physical contact between M1 macrophages and colonic crypts but not secretory factors decrease DCAMKL1+ cell expression

To determine whether the decrease of DCAMKL1 positive cells in crypts cultured with M1 macrophages observed previously in **Chapter 4**, was induced by cell-cell contact between M1 macrophages and colonic crypts or by co-culture derived secretory factors, the 'conditioned media' co-culture model was utilised and DCAMKL1 positive cell expression analysed. In **Figure 6.3A**, representative confocal images of crypts from the M1 co-culture, M1 cond. media and M1-only model are shown, where DCAMKL1 positive cells are visualised by green intracellular labelling enveloping DAPI (blue) positive cells within the confines of the E-cadherin (cell-cell adhesion molecules) borders. The number of DCAMKL1 positive cells per crypt are shown in **Figure 6.3B**. Although statistically non-significant, a reduction of DCAMKL1 positive cells was observed in crypts cultured with M1 macrophages compared to control crypts. In comparison, the number of DCAMKL1 positive cells in crypts of the M1 cond. media and M1-only culture model were maintained compared to control crypts. In **Figure 6.3C**, the percentage of DCAMKL1 positive cells was compared to the total number of DAPI positive cells per crypt, though non-significant the culture of M1 macrophages with colonic crypts resulted in a reduction in the percentage of DCAMKL1 positive cell expression compared to control crypts. In M1 cond. media and M1-only culture models, DCAMKL1 expression in crypts was maintained compared to control crypts.

The distribution of DCAMKL1 positive cells in each region along the longitudinal crypt-axis was analysed in **Figure 6.3D**. In control crypts, the majority of DCAMKL1 positive cells were located at the base of the crypt, with fewer distributed across the mid and top region of the crypt; this pattern was also observed in crypts from M1 cond. media and M1-only culture models. In contrast, the expression of DCAMKL1 positive cells detected at the base of crypts cultured in the presence of M1 macrophages was significantly reduced compared to control crypts. The number of DCAMKL1 positive cells located at the mid and top region of crypts in culture with M1 macrophages was also similar to crypts in control.

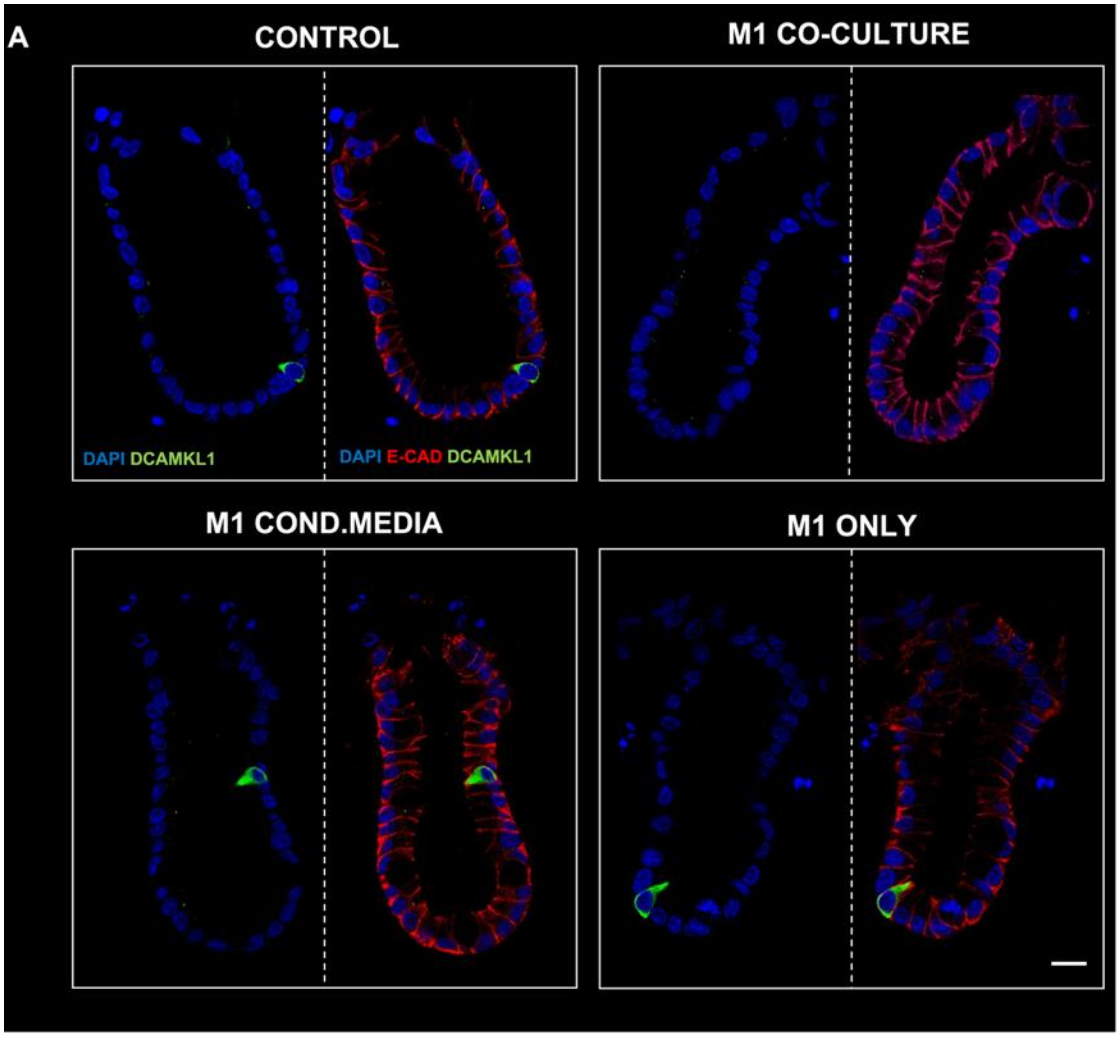
A
CONTROL
M1 CO-CULTURE
M1 COND.MEDIA
M1 ONLY
DAPI DCAMKL1
DAPI E-CAD DCAMKL1

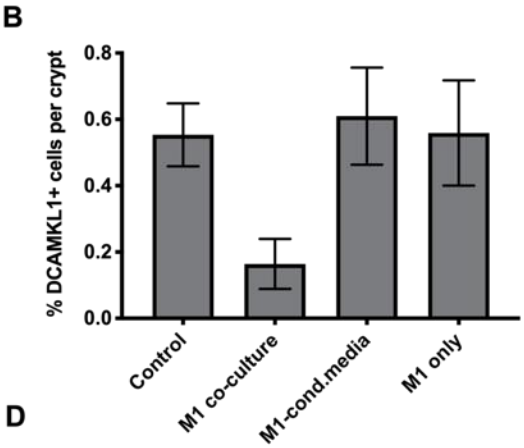
B
% DCAMKL1+ cells per crypt
0.0
0.2
0.4
0.6
0.8
Control
M1 co-culture
M1-cond.media
M1 only

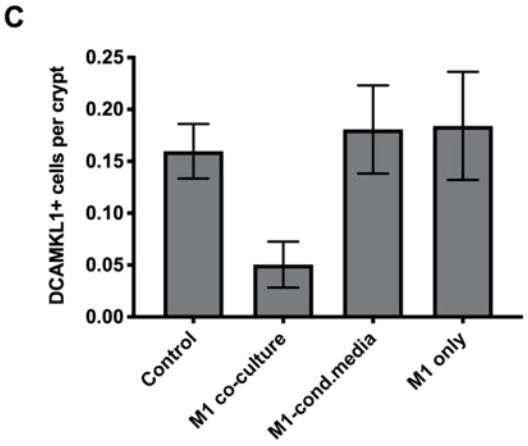
C
DCAMKL1+ cells per crypt
0.00
0.05
0.10
0.15
0.20
0.25
Control
M1 co-culture
M1-cond.media
M1 only

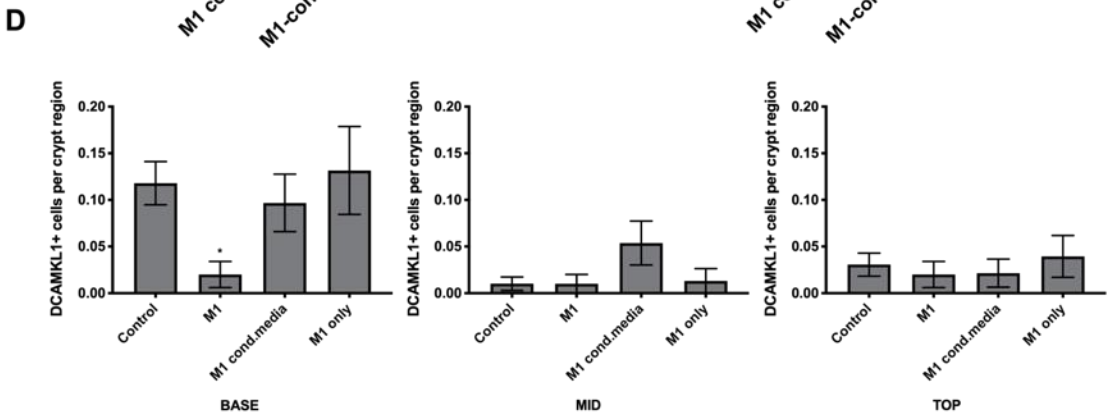
D
DCAMKL1+ cells per crypt region
0.00
0.05
0.10
0.15
0.20
Control
M1
M1 cond.media
M1 only
BASE
MID
TOP

Figure 6.3: Physical contact between M1 macrophages and colonic crypts but not secretory factors decrease DCAMKL1+ cell expression in crypts *in vitro*

A) Representative confocal images showing DCAMKL1 expression (green), nuclei (blue) in crypts cultured in the M1 co-culture, M1 cond. media and M1-only culture models**. B)** Histogram showing the average number of DCAMKL1 positive cells per crypt cultured in the M1 co-culture, M1 cond.media and M1-only culture models **C)** Histogram showing the percentage of DCAMKL1 positive cells per crypt cultured in the M1 co-culture, M1 cond.media and M1-only culture models **D)** Histogram showing the position of DCAMKL1+ cells per crypt region in M1 co-culture, M1 cond.media and M1-only culture models. (n=6, N≥*76, *P<0.05 compared to Control)* Scale bar 20µm.

As the results above confirm that M1 macrophage are only capable of reducing colonic crypt UEA-1+ goblet cells and DCAMKL1+ tuft cell numbers through physical macrophage-crypt contact in our 3D *in vitro* co-culture model. As results from **Chapter 4** suggested that M1 macrophages can increase Lgr5+ crypt stem cell numbers in our 3D *in vitro* macrophage-crypt co-culture, we therefore aimed to further investigate whether physical contact or secretory factors are required to induce such changes.

6.2.4 Physical contact in M1-crypt co-cultures but not secretory factors from M1-crypt culture induce an increase in Lgr5+ cell expression.

As a significant increase in Lgr5 expression was detected in crypts co-cultured with M1 macrophages, it was determined, whether cell-cell contact between M1 macrophages and crypts or crypt-macrophage co-culture-derived secretory factors induce such changes in **Figure 6.4.** Representative confocal images showing basal Lgr5 expression (green) along the crypt axis, in control crypts, crypts in the presence of M1 macrophages (M1 co-culture), crypts cultured alone but placed in vicinity to M1-crypt co-culture (M1 cond.media) and crypts cultured alone but placed in vicinity to M1 macrophages alone (M1-only) are shown in **Figure 6.4A.** A Lgr5 gradient, originating from the base of the crypt and gradually weakening towards the upper region is visualised in green and Lgr5 positive cells were identified with the aid of E-cadherin (red) and DAPI (blue) as per **Section 2.3.3.** The number of Lgr5 positive cells per crypt was significantly increased in crypts cultured in the presence of M1 macrophages compared to control crypts. However, in crypts of M1 cond. media and M1-only culture models, Lgr5 positive cell numbers were maintained compared to control. Furthermore, crypts cultured along with M1 macrophages also expressed significantly more Lgr5 positive cells in comparison to crypts within the M1 cond. media and M1-only culture models.

In **Figure 6.4B**, the percentage of Lgr5 positive cells per crypt are compared to the total number of DAPI positive cells per crypt, where a significant increase was detected in crypts cultured with M1 macrophages compared to control crypts, however in crypts cultured under the M1 cond.media and M1-only culture model, the percentage of Lgr5 expression was maintained compared to control crypts. The distribution of Lgr5 positive cells along the longitudinal crypt-axis was analysed in **Figure 6.4D**. In control crypts, the majority of Lgr5 positive cells were located at the base of the crypts with fewer located at the mid region and the lowest numbers found at the top. Significantly more Lgr5 positive cells were expressed at the base of the crypt cultured with M1 macrophages, where numbers in the mid and top region were similar compared to control crypts. The number of Lgr5 positive cells expressed at the base, mid and top region of crypts in the M1 cond. media and M1-only model were also similar to control crypts.

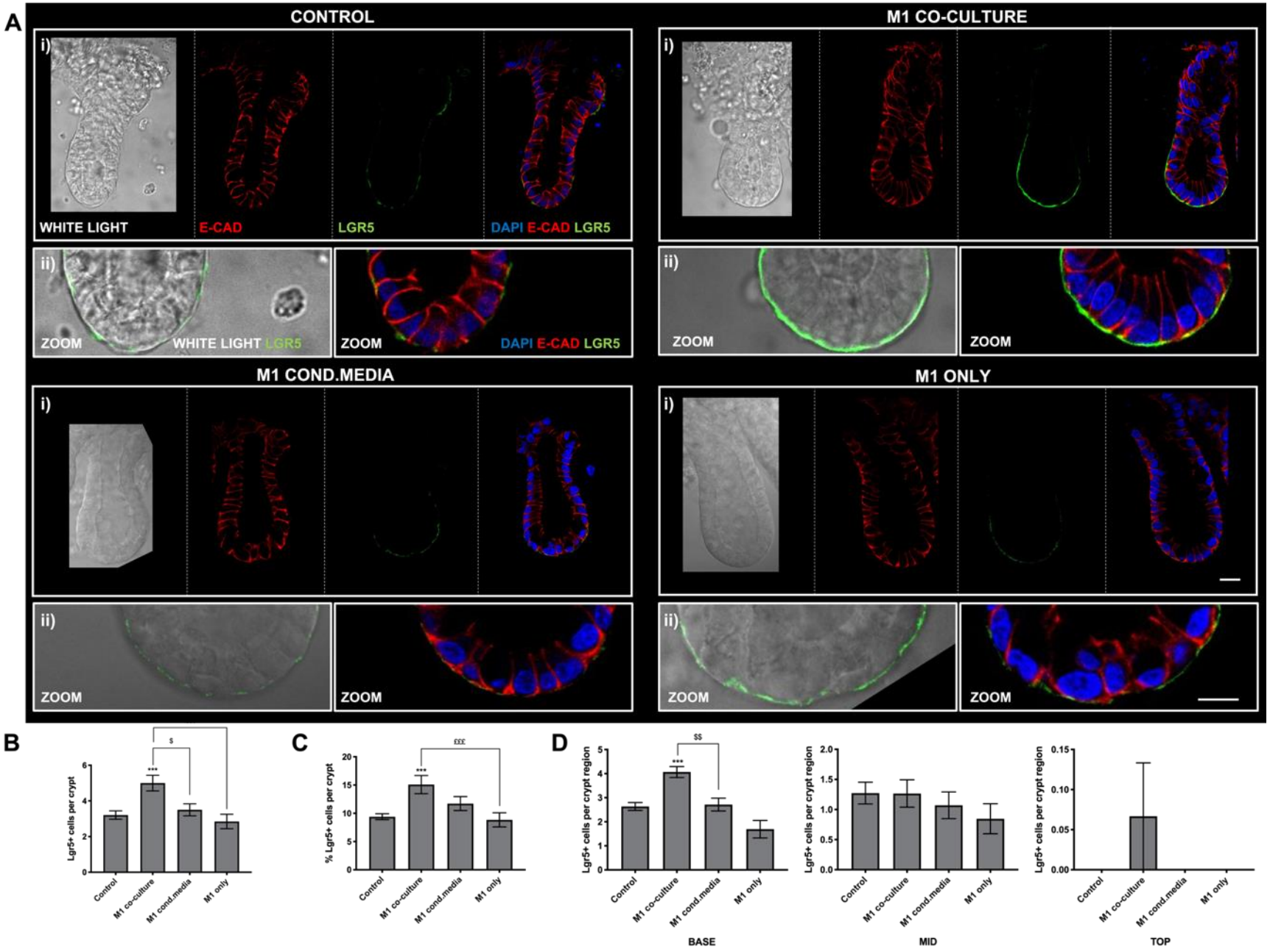
A
CONTROL
M1 CO-CULTURE
M1 COND.MEDIA
M1 ONLY
i)
ii)
WHITE LIGHT
E-CAD
LGR5
DAPI E-CAD LGR5
ZOOM
WHITE LIGHT LGR5
B
Lgr5+ cells per crypt
C
% Lgr5+ cells per crypt
D
Lgr5+ cells per crypt region
BASE
MID
TOP
Control
M1 co-culture
M1 cond.media
M1 only

Figure 6.4: M1 macrophages induce an increase in Lgr5+ cell expression via physical contact; not secretory factors in colonic crypts *in vitro*

Ai) Representative confocal images showing basal Lgr5 expression (green), nuclei (blue) and E-cadherin (red) in crypts from M1 co-cultures, M1 cond. media and M1-only culture models. **Aii)** Enlarged confocal images showing expression of Lgr5 (green) along the base of the crypt alongside white light or DAPI (blue), E-cadherin (red) when cultured in M1 co-culture, M1 cond. media or M1-only models. **B)** Histogram showing the average number of Lgr5 positive cells per crypt cultured in M1 co-culture, M1 cond. media and M1 only culture models. **C)** Histogram showing the percentage of DCAMKL1 positive cells per crypt cultured in M1 co-culture, M1 cond. media and M1-only models. **D)** Histogram showing the position of DCAMKL1+ cells per crypt region when cultured in M1 co-culture, M1 cond. media and M1-only models. (n=3, N≥*20, ***P<0.001 compared to Control; $P<0.05, $$P<0.01 M1 co-culture compared to M1 cond. media; £££P<0.001 M1 co-culture compared to M1-only)*. Scale bar at 20µm.

6.2.5 Physical and secreted factors increase Lgr5 fluorescence intensity in colonic crypts cultured with M1 macrophages

To semi-quantitively determine whether Lgr5 protein expression was affected by physical contact between crypts and M1 macrophages or co-culture-derived secretory factors, the crypt's Lgr5 fluorescence intensity was measured and experiments were setup as per **Section 2.3.3.**

In **Figure 6.5A** crypts, cultured with M1 macrophages (M1 co-culture), cultured alone and placed in vicinity to a M1-crypt co-culture (M1 cond. media) and crypts cultured alone and placed in vicinity to M1 macrophages alone (M1-only). Here Lgr5 fluorescence labelling is basally expressed in RGB colours along the crypt-axis. **Figure 6.5B**, shows the average Lgr5 fluorescence intensity along the base, mid and top region of the crypt. In control crypts, Lgr5 fluorescence intensity was observed to be highest at the base and mid region with lowest values recorded at the top region. Lgr5 fluorescence intensity in crypts cultured in the presence of M1 macrophages (M1 co-culture) was shown to be significantly higher at the base, mid and top region compared to control crypts. Crypts cultured without direct contact to M1 macrophages but placed in vicinity to M1-crypt co-culture (M1 cond. media) was also shown to be significantly higher at the base, mid and top crypt region compared to control crypts. Crypts alone cultured without direct contact to M1 macrophages (M1-only), Lgr5 fluorescence intensity remained unchanged at the base and top of the crypt, however a significant decrease was noted at the mid crypt region compared to control crypts. Furthermore, Lgr5 fluorescence intensity in crypts cultured along with M1 macrophages (M1 co-culture) were also significantly higher compared to crypt in M1 cond. media and M1-only culture model.

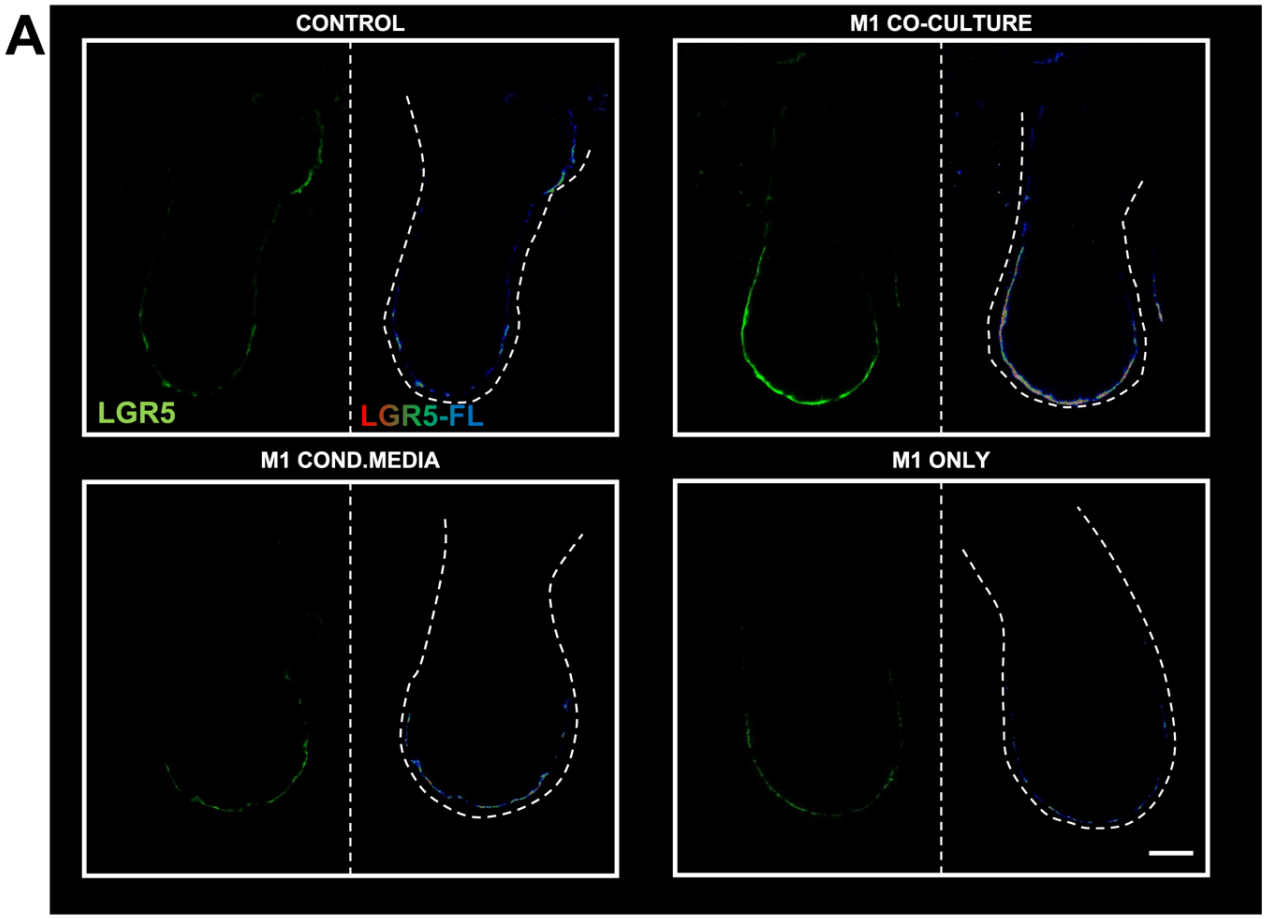
A
CONTROL
M1 CO-CULTURE
LGR5
LGR5-FL
M1 COND.MEDIA
M1 ONLY

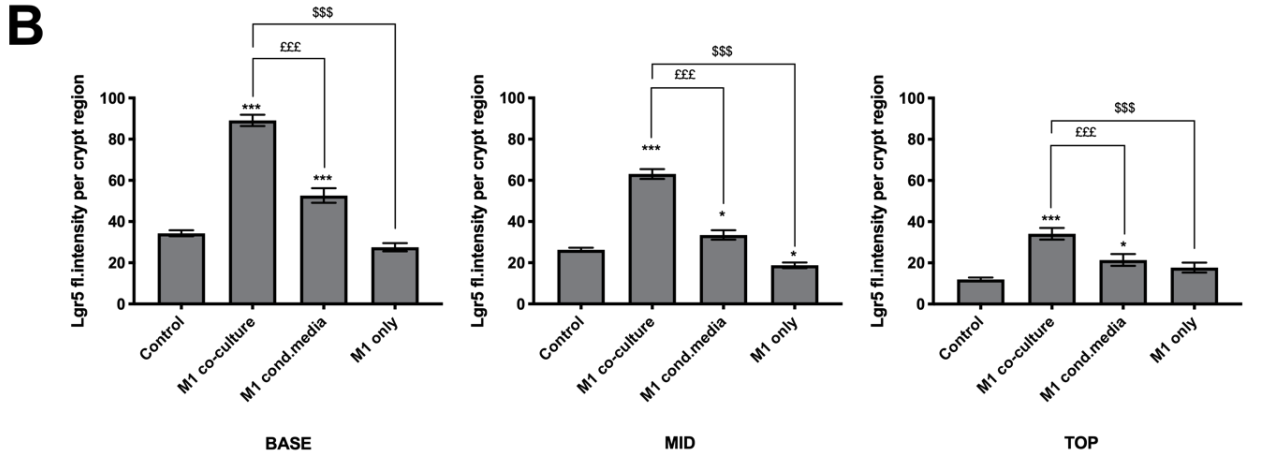
B
Lgr5 fl.intensity per crypt region
Control
M1 co-culture
M1 cond.media
M1 only
BASE
MID
TOP
$$$
£££
***
*

Figure 6.5: Physical contact between M1 macrophages and colonic crypts and co-culture derived secretory factors cause an increase in LGR5 fluorescence intensity *in vitro*

A) Representative confocal images showing the fluorescence intensity of Lgr5 (RBG heat map) in each crypt-M1macrophage co-culture and 'conditioned media' co-culture model, where blue and red labelling indicate the maximum and minimum fluorescence value expressed, respectively. **B)** Histogram showing average fluorescence intensity (arbitrary value) within each crypt region (base, mid, top) (n=4, N≥20 *P<0.05, ***P<0.001 *compared to Control*; $^{£££}$P<0.001 *M1 co-culture compared to M1 cond.media;* $^{\$\$\$}$ P<0.001; *M2 co-culture compared to M1-only*.) Scale bar at 20µm

Having demonstrated that physical contact between M1 macrophages and colonic crypts is required to increase Lgr5+ crypt stem cell expression and reduce UEA-1+ goblet cell and DCAMKL1+ tuft cell numbers *in vitro,* we were next determined to investigate whether these changes are dependent on the Wnt signalling and quantified the expression of the Wnt target genes, CyclinD1 and LEF1 in our M1 macrophage-crypt co-culture model.

6.2.6 M1 macrophages increase CyclinD1 expression in co-culture with crypts

To determine whether physical cell-cell contact between macrophages and colonic crypts, or co-culture derived secretory factors differentially affect CyclinD1 expression was further studied in **Figure 6.6. Figure 6A** show representative confocal images where CyclinD1 expression (red) is expressed within DAPI (blue) positive cells in colonic epithelial cells in control crypts, crypts cultured in the presence of M1 macrophages (M1 co-culture), crypts cultured without direct contact to M1 macrophages but placed in vicinity to a M1-crypt co-culture (M1 cond.media) and crypts cultured without direct contact to M1 macrophages but placed in vicinity of M1 macrophages alone (M1-only).

Figure 6.6B shows the mean fluorescence intensity of CyclinD1 expression in crypt regions of all culture models as described above. In control crypts, similar expression of CyclinD1 was found at the base, mid and top of the crypt. In crypts cultured in the presence of M1 macrophages (M1 co-culture) a significant increase in CyclinD1 expression was noted at the base of the crypt compared to control crypts, however CyclinD1 expression was maintained at the mid and top region of crypts. In crypts cultured without direct contact to M1 macrophages but placed in vicinity of a M1-crypt co-culture (M1 cond. media), the mean fluorescence intensity of CyclinD1 expression remained unchanged at the base, mid and top region of the crypt compared to control crypts. In crypts cultured without direct contact to M1 macrophages but placed in vicinity of M1 macrophages alone (M1-only), the mean fluorescence intensity of CyclinD1 expression also remained unchanged compared to control crypts. Notably, the mean CyclinD1 fluorescence intensity in crypts cultured in the presence of macrophages (M1 co-culture) were significantly higher compared to crypts from the M1-only culture model.

Figure 6.6D show the total mean fluorescence intensity of CyclinD1 per crypt, where a significant increase in crypts cultured with M1 macrophages was detected compared to control crypts. In contrast, the total mean fluorescence intensity of CyclinD1 expression in crypts cultured in M1 cond. media and M1 only culture models were maintained compared to control crypts. In **Figure 6.6E**, CyclinD1 positive cells were identified as per **Section 2.3.4** and the percentage of CyclinD1 positive cells was compared to the total number of DAPI positive cells per crypt. Here, significantly more CyclinD1 positive cells were identified in

crypts cultured in the presence of M1 macrophages (M1 co-culture) compared to control crypts. No significant changes in the number of CyclinD1 positive cells in crypts cultured in M1 cond. media and M1-only culture model were shown when compared to control crypts. Notably, the number of CyclinD1 positive cells was also significantly higher in crypts cultured along with M1 macrophages (M1 co-culture) when compared to crypts from the M1 cond.media and M1 only culture model.

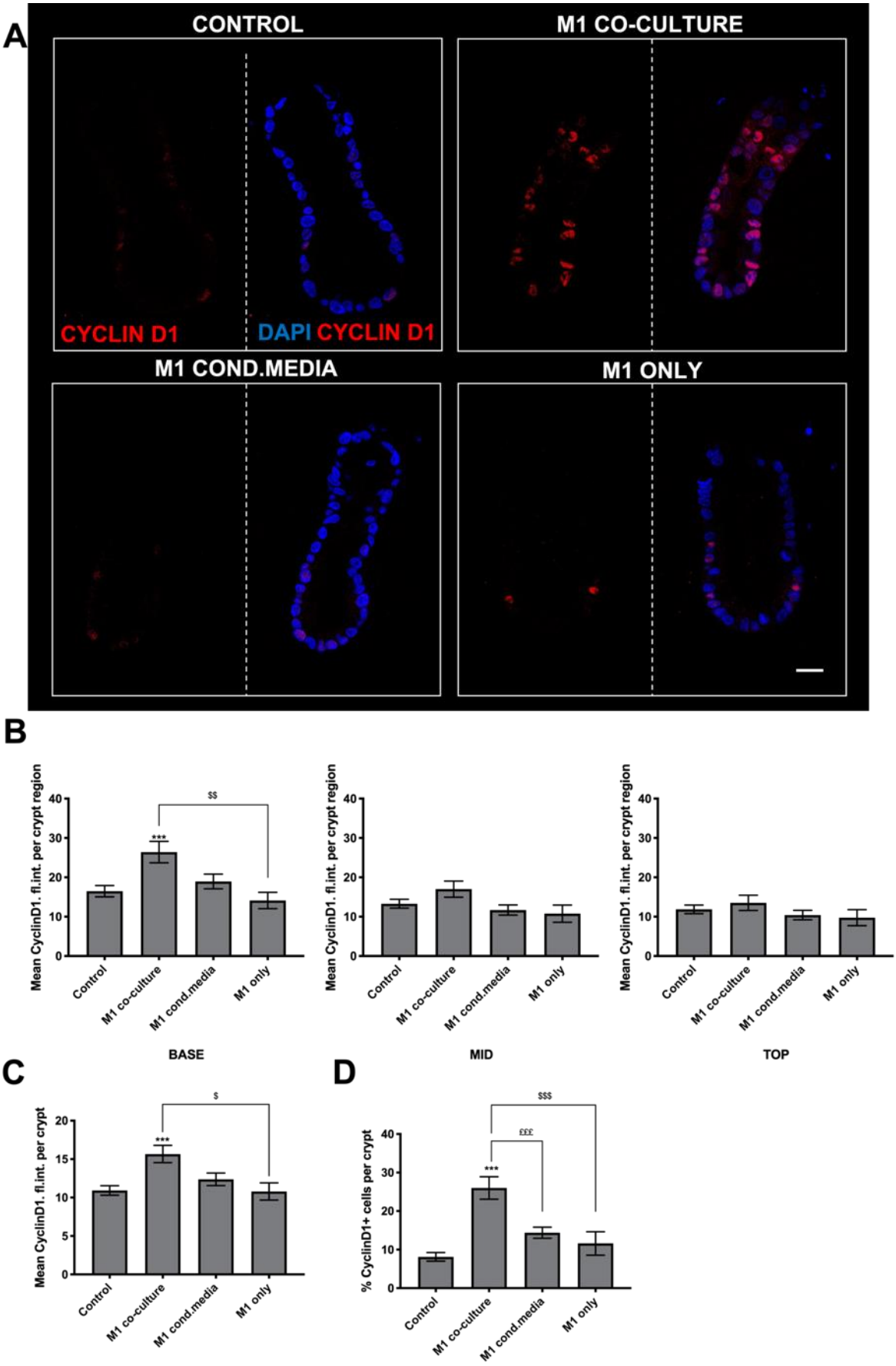
A
CONTROL
M1 CO-CULTURE
CYCLIN D1
DAPI CYCLIN D1
M1 COND.MEDIA
M1 ONLY
B
Mean CyclinD1. fl.int. per crypt region
Control
M1 co-culture
M1 cond.media
M1 only
BASE
MID
TOP
C
Mean CyclinD1. fl.int. per crypt
D
% CyclinD1+ cells per crypt

Figure 6.6: M1 macrophages induce an increase in CyclinD1+ cell expression via physical contact; not secretory factors in colonic crypts *in vitro*

A) Representative confocal images showing nuclear LEF1 expression (red), nuclei (blue) in each crypt-M1 co-culture and 'conditioned media' co-culture experiment. **B)** Histogram showing the average fluorescence intensity of CyclinD1 within each crypt co-culture/conditioned media experiment per crypt region. **C)** Histogram showing the average fluorescence intensity of CyclinD1 per crypt **D)** Histogram showing the percentage of DAPI labelled nuclei that are CyclinD1+ cells per crypt (n=3, N≥*10,* ***P<0.001 *compared to Control;* £££P<0.001 *M1 co-cultured compared to M1 cond.media;* $P<0.05,$$*P<0.01,*$$$*P<0.001 M1 co-culture compared to M1 only.* Scale bar at 20 µm.

6.2.7 M1 macrophages increase LEF1 expression in co-culture and conditioned media models but not within the M1 only model

To determine whether LEF1 expression is affected by physical contact between M1 macrophages and crypts or via crypt-M1 macrophage co-culture-derived secretory factors or M1 secreted factors alone, the culture model was utilised. Representative confocal images of LEF1 expression (red) localised within DAPI positive cells (blue) in all culture models described above are shown in **Figure 6.7A**. Semi-quantitative analysis of the mean fluorescence intensity of LEF1 expression per crypt region is shown in **Figure 6.7B**, where the mean fluorescence intensity of LEF1 expression in control crypts is shown to be evenly distributed along the longitudinal crypt-axis, in comparison, LEF1 expression in crypts cultured in the presence of M1 macrophages was significantly higher at the base, mid and top region of the crypts compared to control, M1 cond.media and M1-only crypts. A significant increase in mean fluorescence intensity of LEF1 was also observed at the base, mid and top region of crypts cultured without direct contact to M1 macrophages but placed in vicinity of M1-crypt co-culture (M1 cond. media) compared to control and M1-only crypts. A significant decrease in the mean fluorescence intensity of LEF1 expression was also found in crypts cultured alone but placed in vicinity to M1 macrophage (M1-only) compared to control, M1 co-culture and M1 cond.media crypts. **Figure 6.7C**, shows the total mean fluorescence intensity of LEF1 expression along the entire longitudinal crypt-axis, where a significant increase in crypts cultured along with M1 macrophages (M1 co-culture) was found compared to control, M1 cond.media and M1-only crypts. Crypts cultured without

direct contact to M1 macrophages but placed in vicinity of M1-crypt co-cultures (M1-cond media) remained unchanged compared to control crypts. A significant reduction in the mean fluorescence intensity of LEF1 was noted in crypts cultured alone but placed in vicinity to M1 macrophages (M1-only) compared to control and M1 co-culture crypts. It should be noted that crypts in the M1 co-culture model also expressed significantly higher LEF1 fluorescence intensity when compared to crypts from M1 cond. media and M1 only culture models.

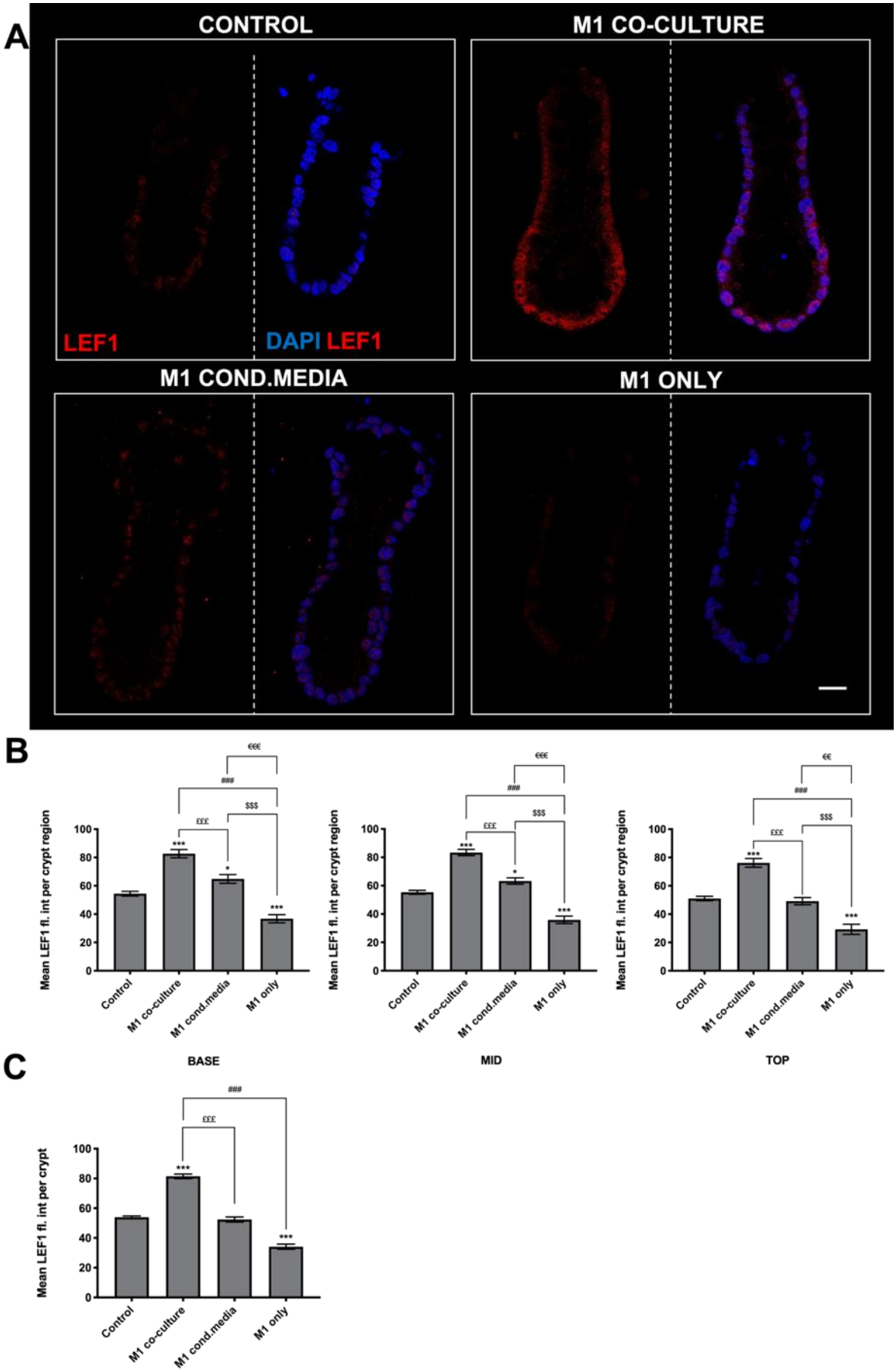
A
CONTROL
M1 CO-CULTURE
LEF1
DAPI LEF1
M1 COND.MEDIA
M1 ONLY
B
Mean LEF1 fl. int per crypt region
Control
M1 co-culture
M1 cond.media
M1 only
BASE
MID
TOP
C
Mean LEF1 fl. int per crypt

Figure 6.7: M1 macrophages increase LEF1 expression through physical contact and secretory factors in crypts *in vitro*, but not within the M1-only culture model

A) Representative confocal images showing nuclear LEF1 expression (red), nuclei (blue) in each crypt-M1 co-culture and 'conditioned media' co-culture experiment. **B)** Histogram showing the average fluorescence intensity of CyclinD1 within each crypt region **C)** Histogram showing the average fluorescence intensity of LEF1 per crypt (n=3, N≥*14 compared to Control* *$P<0.05$,***$P<0.001$;$^{£££}P<0.01$ *M1 co-culture compared to M1 cond.media ;* $^{###}P<0.0$ *M1 co-culture compared to M1-only;* $^{€€}P<0.01$,$^{€€€}P<0.001$ *M1 cond.media compared to M1 only)* Scale bar at 20 µm.

As we have confirmed in this chapter that M1 macrophage-crypt contact increases Lgr5+ stem cell expansion, we finally sought to investigate the effects of these findings in prolonged M1 macrophage-crypt co-culture, in which colonic crypt budding was determined.

6.2.8 M1 macrophages stimulate an increase in colonic crypt budding

In **Figure 8,** the organoid budding capacity of crypts cultured with M1 macrophages compared to control crypts was assessed. Representative brightfield images of colonic crypt budding (white arrows) in control and M1 macrophage-crypt co-culture on Day 0 and Day 6 are shown in **Figure 6.8A**. The number of buds per crypt within control crypts and crypts cultured with M1 macrophages are shown in **Figure 6.8B**, where a significant increase in crypt budding was observed on Day 6 and 7 compared to control crypts. The percentage of organoid survival in control crypts and crypts cultured along with M1 macrophages are shown in **Figure 6.8C.** A steady decrease in organoid survival was noted in both control crypts and crypts cultured with M1 macrophages, however no significant changes in the percentage of organoid survival was found when compared to each day between crypts cultured along with M1 macrophages and control crypts.

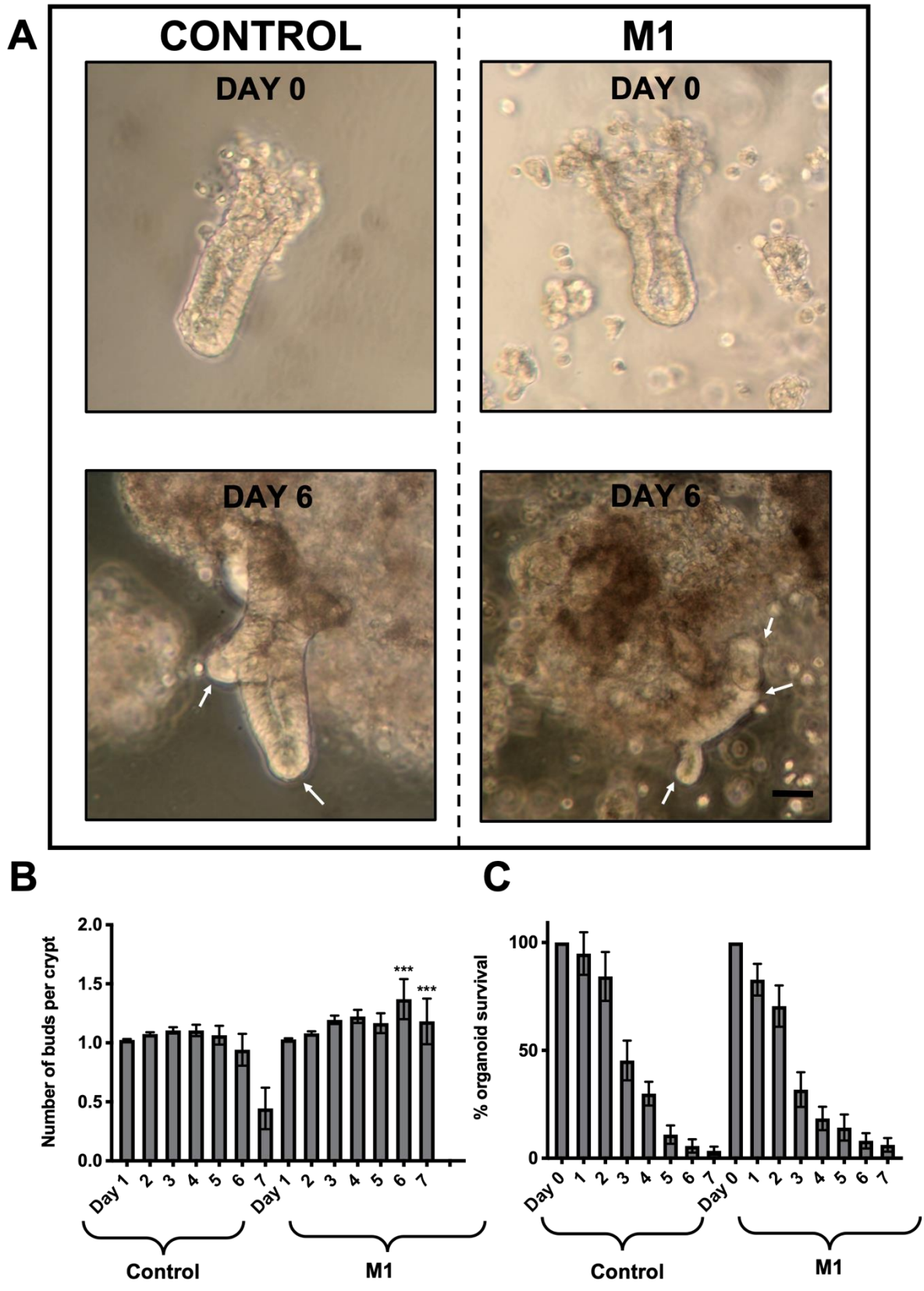
A
CONTROL
M1
DAY 0
DAY 0
DAY 6
DAY 6
B
Number of buds per crypt
2.0
1.5
1.0
0.5
0.0
***
***
Day 1 2 3 4 5 6 7
Day 1 2 3 4 5 6 7
Control
M1
C
% organoid survival
100
50
0
Day 0 1 2 3 4 5 6 7
Day 0 1 2 3 4 5 6 7
Control
M1

Figure 6.8: M1 macrophages stimulate an increase in colonic crypt budding *in vitro*

A) Representative white light images (x10) of colonic crypts on Day 0 and Day 6 of (co)-culture. **B)** Histogram showing the number of buds per crypt expressed over the course of 7 days in Control compared to M1-crypt co-culture (n=3; N>9 Control vs M1 ***P<0.0001). **C)** Histogram showing the percentage organoid survival per coverslip in Control compared to M1-crypt co-culture (n=3; N>16) Scale bar at 25µm.

In this chapter, the results reveal that secretory factors derived from crypts cultured only with M1 macrophages but not Naive or M2 macrophages increase colonic crypt growth; M1 macrophage to crypt contact is essential for inducing differential changes in Lgr5 and UEA-1 crypt cell as well as LEF1 and CyclinD1 expression in colonic crypts and lastly, long-term *In vitro* culture of crypts with M1 macrophages drives organoid crypt budding *in vitro*.

6.3 Discussion

This chapter demonstrated that Naïve and M2 macrophages induce colonic epithelial proliferation only via physical contact in contrast to M1 macrophages which induce crypt proliferation via both physical contact and secretory factors. Similarly, direct contact between crypts and M1 macrophages but not secretory factors resulted in an increase in Lgr5+ stem cell, LEF1 and CyclinD1 expression as well as a reduction in UEA-1+ goblet cell numbers. Furthermore, prolonged co-culture of M1 macrophages with colonic crypts resulted in an increase in crypt budding in our 3D *in vitro* co-culture model. Proliferation experiments in this chapter, demonstrated that direct contact between Naïve, M1 and M2 macrophages to crypts can induce an increase in colonic proliferation, however only M1 macrophages could induce a proliferative response without direct immune-crypt contact.

The findings in this chapter suggest that M1-crypt contact derived secretory factors may diffuse across the media to induce colonic crypt cell proliferation in crypt cultured alone. As this phenomenon was exclusively observed within the M1 macrophage population, we assume that M1 macrophage-derived secretory factors which are yet to be identified are the causative factor.

Over the last decade, the pro-inflammatory cytokines generated by classically activated M1 macrophages have been well documented, where an increased production of IL-6, TNFα, HIF1α and iNOS have predominantly been associated with the M1 macrophage phenotype and were not found to be generated by the M2 macrophage population (Shapouri-Moghaddam et al., 2018). In 2014, Kuhn et al, have demonstrated that IL-6 is critically required to aid epithelial proliferation early on following colitis induced injury in the colon *in vivo*, where M1 macrophage presence is also often highest during the early acute inflammatory stages of injury (Kuhn et al., 2014; Krzyszczyk et al., 2018). However, inhibition of IL-6 in the latter stages of colitis where M2 macrophages are predominantly present, did not impair epithelial proliferation. These findings could suggest that M1-derived secretion of IL-6 triggers intestinal proliferation during colitis (Kuhn et al., 2014).

As mentioned briefly in **Chapter 4**, iNOS mediated production of nitric oxide by M1 macrophages could also induce epithelial proliferation (Rath et al., 2014). A study from

2013 has shown the production of reactive oxygen species such as NO can initiate an increase in epithelial proliferation when exposed to commensal bacteria in mice *in vivo* (Jones et al., 2013). One of the major regulators of ROS production in the colon is the NADPH oxidase subunit, NoxO1 which was shown to play a critical role in wound repair of DSS-induced injury in mice, where knockout of NoxO1 caused an increase in epithelial proliferation (Moll et al., 2018). Interestingly, NoxO1 expression was also reduced in M1 macrophage *in vitro*, possible causing the increase in epithelial proliferation we observed without direct M1 to crypt contact (Wang et al., 2020).

Other studies have also found an upregulated mRNA expression of the hypoxia induced factor 1α (HIF1α) in M1 macrophages (Ortiz-Masia et al., 2016; Nakayama et al., 2013). Hypoxia in the intestinal tissue can be caused by epithelial injury and breach of the barrier function, HIF1 stabilisation then allows for the transcription of genes promoting wound repair following injury (Goggins et al., 2013). Most recently it was found that stabilising HIF1α in TNBS induced mice led to an increase in epithelial proliferation in *in vitro* (Goggins et al., 2021). During inflammatory bowel disease, where hypoxia levels within the tissue are high, HIF1α cannot be hydroxylated and is instead stabilised and highly expressed in the cells due to the presence of pro-inflammatory cytokines such as TNF-α, a known secretory product of M1 macrophages. To understand whether HIF-1α is upregulated in our macrophage-crypt co-culture model, its presence within the co-culture model can be detected via the use of commercially available HIF-1α ELISA kits, where its presence within cell lysates is measured (Lee and Simon, 2015).

Whereas the previously described studies have reported an increase in intestinal proliferation only in injury-induced colitis models to our understanding we are the first to confirm that inflammatory M1 macrophages derived-secretory factors can trigger epithelial proliferation in colonic crypts in their steady state (Kaunitz and Akiba., 2019).

Following the epithelial proliferation experiments we have carried out during this chapter, it was clear that we were unable determine whether Naïve, M1 and M2 macrophages are able to utilise secretory factors independently of macrophage-crypt crosstalk. Future experiments should include an experimental condition in which Naïve, M1 and M2 macrophages are separated and cultured separately from the crypts to understand whether macrophages are prompted to secrete cytokines and chemokines and affect epithelial

proliferation without the requirement for direct contact between the macrophages and colonic crypts. This experimental condition was utilised henceforth and described as the "M1-only" condition in further experiments in this chapter.

Furthermore, as we are currently unsure as to which exact M1-secretory factors are causing an increase in epithelial proliferation and the conditioned media should be tested for pro-inflammatory cytokine levels via the aid of ELISA kits in the future.

As we aimed to understand the epithelial renewal and have successfully identified a few distinct epithelial cell lineages such as the Lgr5+ stem cells, UEA-1+ goblet cells and DCAMKL1+ tuft cells, it remains unknown which effect M1 macrophages have on the transit-amplifying cell lineage within the colonic epithelium. As such cells are unlikely to express the markers previously mentioned, we suggest the use of CD24, Bmi1 and/or HopX to label for progenitor cells and self-renewing stem cells located in the +4 position (Furstenberg et al., 2011; Barker et al., 2012). Furthermore, identification of the ckit+ deep secretory goblet cell progenitors as performed by Rothenberg et al would also widen our understanding of the effect M1 macrophages have on the process of epithelial proliferation and differentiation in the colon (Rothenberg et al., 2012).

While colonic crypt proliferation experiments from this chapter suggest that M1 macrophages can increase crypt cell proliferation via secretory mechanism and findings in **Chapter 4** suggested that the colonic epithelium's differentiated cell lineages and Lgr5+ stem cell numbers can only be influenced by the presence of M1 macrophages, we directed our focus towards understanding whether physical contact or secretory factors are required to regulate colonic crypt renewal in the latter part of this chapter.

Since we have reported that crypts cultured with direct contact to M1 macrophages were shown to increase Lgr5+ stem cell numbers (**Chapter 4)**, it begs the question as to whether this mechanism is dependent on juxtacrine signalling or short-range paracrine signalling. Over time it was recognised that Notch signalling is a potent regulator of the intestinal stem cell niche both in the small and large intestine, where it maintains the stem cell pool via the 'lateral inhibition' and negative regulation of Notch (Sancho et al., 2015). Thus, by altering Notch signalling within the intestinal epithelium it is entirely possible to affect the epithelium's balance of self-renewal (Stamataki et al., 2011).

Treatment of the small intestine with DBZ (a y-secretase Notch inhibitor) led to an 84% reduction in Lgr5EFGP+ stem cell numbers within the epithelium and subsequently, intestinal differentiation was also perturbed (Van Dussen et al., 2012). Lgr5+ stem cells themselves are highly expressive of both the Notch receptor, NOTCH1 and NOTCH2, where the double deletion of such receptors leads to the complete loss of stem cells within the intestine. Although, single deletion of the Notch ligand Dll-1 and Dll-4 did not affect Lgr5+ stem cell numbers, double mutant mice showed a reduction in the stem cell pool, furthermore individual loss of NOTCH1 or Dll-1 also led to an increase in goblet cell numbers, while ISC number were maintained (Pellegrinet et al., 2011). In the small intestine, the Lgr5+ stem cell niche is maintained by the constitutive stimulation of the stem cell's NOTCH 1 and 2 receptor by neighbouring Paneth cells which express Dll-1 and Dll-4, however, to date it is not fully understood how Lgr5+ stem cells in the colon maintain their stem cell pool in the absence of Paneth cells (Sato et al., 2011).

Shimizu et al's colonic experiments show that Dll-1+ cells commonly reside at the bottom of the crypt, whereas Dll-4+ cells reside in the upper part of the colonic crypt. Additionally, both Dll1 and Dll-4+ epithelial cells were shown to be Atoh1+ (expressed in cells of the secretory lineage) but Hes-1 negative (an inhibitor of Atoh1+ allowing for lateral inhibition and negative regulation) (Shimizu et al., 2014). Li et al's, recent mRNA quantification of Notch ligands Jag1,2 and Dll-1,4 in BMDM derived M1 and M2 macrophages has shown that both Jag1 (2-fold increase) and Dll-1 (12-fold increase) are highly expressed in M1 macrophages in comparison to M0 (Naïve) (Li et al., 2018).Interestingly, a study from Ito et al in 2011, demonstrated that exposure of bone-marrow derived dendritic cells to LPS did not increase Dll-1 ligand expression however in stark contrast, LPS exposure to bone-marrow derived macrophages did lead to a significant increase in Dll-1 expression thereby alluding to the observed increase in Lgr5 expression observed in our 3D M1-crypt co-culture model, in which M1 macrophages were also differentiated via its exposure to LPS (and IFN-γ). (Ito et al., 2011). Whether Jag1 or Dll-1 in M1 macrophage affect the notch-responsive intestinal stem cell niche via this juxtacrine mechanism within our 3D co-culture model is yet to be determined.

Over the past decade, a number of studies have also revealed that Notch signalling can play a crucial role in mediating intestinal crypt differentiation (Spit et al., 2018). Notch inhibitory

studies have reported goblet cell hyperplasia, increased Paneth, enteroendocrine and tuft cell marker expression (Van Dussen et al., 2012; Van Es et al., 2005). In addition, Atoh1/Math1 was identified as a crucial regulator of the secretory cell lineage, where the depletion of Atoh1 can results in the ablation of goblet cells within the intestinal epithelium (Shroyer et al., 2007). In 2016, Ihara et al, have previously demonstrated an increased expression of both Jag1 and Jag2 in CD11c+ dendritic cells which was also associated with the depletion of goblet cells in colitis induced mice. This study also reflects the findings of this chapter where we also found a reduction in UEA-1+ goblet cell numbers in crypts in direct contact with M1 macrophages (Ihara et al., 2016). Ihara further suggested that the increase in Notch ligands could activate Notch signalling in the colon further leading to the inhibition of goblet cell differentiation. Similar findings were reported by Pope et al, where the abnormal activation of Notch coincided with reduced mucus production and a reduction in goblet cell number *in vivo* (Pope et al., 2014). In a subsequent study in 2018, Ihara et al., confirmed the reduction in of both the goblet cell marker Muc2 and upregulation of Hes1 (absorptive lineage marker) but most notably did not find a significant difference in mRNA expression of Lgr5 (Ihara et al., 2018). Another *in vitro* study indicated that the increased presence of HIF-1α is required to induce the increased expression of Notch ligands Jag1 and Dll-4 in M1 macrophages, consequently the upregulation resulted in the increased expression in Hes1 and increased enterocyte presence in Caco-2 and HT29 epithelial cell lines (Ortiz-Masia et al., 2016).

It has been well established that Notch-high cells can give rise to enterocytes on the other hand Delta-like ligand-high expressing cells differentiate into secretory cells. The colonic crypts follow a stochastic differentiation pattern subsequently leading to a enterocyte: goblet cell ratio of 3:1 in vivo (Collier et al., 1996; Zecchini et al., 2005). Crucially, Toth et al has shown that the ratio is initiated in the commitment zone located two rows above the +4 stem cell zone and relies on the lateral inhibition of Delta-Notch ligands (Toth et al., 2017). It is therefore likely that the hyper-stimulation of Notch receptors by M1 macrophages resulted in impaired differentiation of secretory goblet cells and is highlighted in our direct M1-crypt co-culture by the reduction of goblet cells in the crypt's mid region, although this will have to verified in future studies.

Although the findings in this chapter indicate that M1 macrophage-crypt contact is required to affect epithelial differentiation, we were unable to identify which juxtacrine or short-range signal is required to bring about the changes we have observed, and we were unable to prove whether Notch or other juxtacrine signalling pathways such as Eph-Ephrin were the causative factors leading to the observed increase in Lgr5+ stem cells. In order to understand the role Notch signalling plays in more detail, the next step is to identify the signal receiving/sending ligands and receptors within this co-culture model by immunofluorescently labelling for Jag1/2, Dll-1/4 ligands and Notch1/2 receptors. Additionally, labelling the intestinal epithelial cells with the transcription factors Atoh1 and Hes1 as performed by previous studies will allow us to analyse the shift in balance between the secretory and absorptive cell lineage in the presence of M1 macrophages (Ishibashi et al., 2018; Gracz et al., 2018; Zheng et al., 2011).

Interestingly, in our M1-crypt co-culture, the increase in Lgr5+ also coincides with the depletion of UEA-1+ goblet cells. In the small intestine, a number of secretory progenitors were shown to de-differentiate in order to replenish the intestinal stem cell pool following tissue damage (Buczacki et al., 2013). Furthermore, colonic work from Rothenberg et al, has previously identified a subset of goblet cells, which express c-kit+, Dll1, Dll4 and EGF the expression of which was increased in when crypts were treated with the Notch inhibitor DAPT (y-secretase inhibitor) and the formation of organoids was promoted. Vice versa, the depletion of c-kit+ cells via toxin-conjugated antibodies led to a decrease in organoid formation, highlighting their importance in maintaining stemness (Rothenberg et al., 2012). More recently, Murata et al's work has found that, following the ablation of Lgr5, the replenishment of the stem cell niche is highly dependent on the transcription factor Ascl2 in both the colon and small intestine and can be expressed by secretory and absorptive progenitors located in the transit-amplifying zone. Following injury, these cells are recruited towards the base of the crypt where they eventually express Lgr5 (Murata et al., 2020). Furthermore, early work from Barker et al also identified the presence of LGR5+GFP- cells along with LGR5+GFP+ in the colon but not in the small intestine, indicating that all not all colonic stem cells are clonally derived, thus progenitor de-differentiation may be more prevalent in the colon compared to the small intestine (Barker et al., 2007). In 2016, Sasaki et al's novel work also identified the presence of Reg4+ and c-kit+ deep secretory cells in the

colon, which when ablated led to a loss of stem cells and reduced colonoid growth. (Sasaki et al., 2016). This was followed by further findings in which it was confirmed that Atoh1, the Notch transcription factor predominantly expressed in the secretory cell lineage, are able to replace Lgr5+ cells following epithelial injury (Castillo-Azofeifa et al., 2019). Although injury was not induced in our co-culture experiments, the presence of M1 macrophages may mimic inflammation and trigger the mechanism of de-differentiation within the epithelium causing the increase in Lgr5. Furthermore, the loss of secretory progenitors may also explain the decreased presence of UEA-1+ goblet cells and tuft cells in our co-culture model, as stem cell de-differentiation may be preferred.

Similarly, to goblet cells, tuft cells also rely on the expression of Hath1/Atoh1 for its differentiation, however they also require the expression Pou2f3 (Pou domain, class 2 transcription factor 3) (Gerbe et al., 2012). Unlike goblet cells, the functions of tuft cells have not been delineated although some research has shown they may play a role in promoting epithelial repair following DSS and radiation injury (May et al., 2014). Additionally, it was also found that the deletion of DCAMKL1 in the small intestine resulted in the enhanced expression of Notch1, a receptor also commonly expressed on Lgr5+ stem cells (Mourao et al., 2019). Whereas we recorded a significant decrease in tuft cell numbers in crypts when cultured with M1 macrophages in **Chapter 4** and a decreasing trend in tuft cell presence, the findings in the current chapter were not statistically significant. As only 0.4% of the epithelial population consists of tuft cells *in vivo*, a large sample size is required in order to identify any changes (McKinley et al., 2017). In this study, a 10µm Z-stack (optical slice) was used to identify any DCAMKl1+ tuft cells within the region, however as the average crypt width lies at around 40µm the likelihood that the tuft cell within the crypt was not recognised is high, henceforth we suggest that the entirety of the crypt is imaged in future experiments (Tan et al., 2013).

In this chapter we have also demonstrated that direct contact between M1 macrophages and colonic crypt results in the overall upregulation of the downstream Wnt transcription factor LEF1. A number of Wnt ligands have been recognised to stimulate the intestinal epithelium including Wnt3a, Wnt5a, Wnt6 and Wnt9b, however as LEF1 can only be activated via the β-catenin dependent canonical Wnt pathway it can be inferred that the non-canonical Wnt ligands Wnt5a and Wnt6 did not initiate the increase in LEF1 localisation

in our co-culture model (Komiya and Habas., 2008; Flanagan et al., 2018; Niehrs et al., 2012). In the small intestine, niche factors such as Wnt3a and R-spondin are provided to Lgr5+ stem cells by neighbouring Paneth cells, in contrast, the colonic epithelium must rely on external cells such as mesenchymal cells, myofibroblasts and macrophages to provide such factors. Specifically, macrophages recruited following injury in colitis-induced mice are able to secrete Wnt3a to support epithelial restitution (Saha et al., 2016; Aoki et al., 2016; Valenta et al., 2016).

In the intestinal epithelium, a gradual Wnt gradient can often be observed with high expression of Wnt localised at the base of the crypt and the least located at the top of the crypt, however a number of studies have established that Wnt signalling occurs over a short-range. In 2016, novel work from Farin et al, has demonstrated that Wnt3a secreted from Paneth cells is directly transferred to Lgr5+ stem cells bound to the Fzd receptor, which then diluted the ligands along the crypt-axis via cell division rather than cellular division, thus proving that Paneth cell derived Wnt3a does not freely diffuse. Promisingly, work from Skoczek et al, has shown that 'inflammatory' monocytes were recruited directly towards Lgr5+GFP+ stem cells in the colonic epithelium *ex vivo*, however as the phenomenon of short-range signalling has not been widely studied, it will need to be determined whether Wnt3a producing macrophage utilise this mechanism in the future (Farin et al., 2016; Skoczek et al., 2014).

During tissue damage, neutrophils often arrive at the site of inflammation via transepithelial migration which requires the expression of ICAM-1. Here ICAM-1 was shown to engage the AKT which in turn drives β-catenin and subsequently epithelial repair is promoted (Luissant et al., 2016; Miyoshi et al., 2017). Interestingly, ICAM-1 is also upregulated in M1 macrophages via a NF-κb dependent pathway, and especially high expression of ICAM-1 was also noted in the colon of colitis-induced mice (Wiesolek et al., 2020; Orrechioni et al., 2019; Yang et al., 2015). Whether the upregulation of ICAM-1 contributed to the observed increase in LEF1 expression in our co-culture model will need to be further explored in future experiment.

Interestingly, in 2018, it was reported that signalling filopodia, known as cytonemes were able to transport Wnt8a, a β-catenin target ligand at the tip of the cytoneme to neighbouring cells, where they were bound to Fzd/Lrp6 to activate β-catenin in zebrafish

and gastric cancer cells (Mattes et al., 2018). Furthermore, in response to intestinal inflammation among other Wnt ligands, Wnt8a expression is especially high in colonic macrophages (Swafford et al., 2018). As both our study in **Chapter 5** and Skoczek's work in 2014 have reported the occasional presence of cellular processes within the respective colonic co-culture models and the increase in epithelial LEF1 expression in this chapter is M1 macrophage contact dependent, this emerging mechanism may play a role in regulating Wnt signalling and epithelial renewal and its involvement will need to be studied further in the future (Skoczek et al., 2014).

Along with LEF1, the expression of the Wnt target gene Cyclin D1 was also highly upregulated following epithelial contact with M1 macrophages. Cyclin D1 is the most abundant cyclin and is commonly expressed throughout the large intestine. Cyclin D1 and has long been established to be a key regulator required for the transition of cells from the G1 to S phase in the cell cycle, where elevated levels of cyclin D1 are often found at the M and G2 phase (Yang et al., 2006; Shtutman et al., 1999; Stacey D.W., 2003). Furthermore, an overexpression of CyclinD1 has frequently been noted in patients with colorectal cancer, where akin to our M1-crypt co-culture model, epithelial proliferation is upregulated when compared to the healthy mucosa (Shakoori et al., 2005; Maeda et al., 1998). In the embryonic pancreatic epithelium, it was shown that M2 macrophages were able to regulate the epithelial progenitor cell's exit from the cell cycle and differentiation towards the islet cell lineages, however to our knowledge it is now understood whether intestinal macrophage can control the intestinal cell cycle *in vivo* or *in vitro* (Mussar et al., 2014). To understand whether M1 macrophages differentially regulate the cell cycle in colonic crypts compared to control crypts, we suggest immunofluorescently co-labelling for CyclinD1, CyclinE2 and Cyclin A, potentially giving us further insight into each cell's current cell cycle progression.

An interesting study from 2020 has observed that the deletion of the extracellular signalling kinase 1 and 2 (ERK1/2) from intestinal epithelial cells during postnatal development led to a significant increase epithelial proliferation and activation of Wnt-target gene Cyclin D1. Furthermore, real-time PCR analysis revealed a dramatic increase in the expression of the Notch ligands Dll-1/4, Jag1/2 and Notch receptors Notch1 as well as increase in the transcription factor Hes1, where similar to our study, these results were accompanied by a

reduction in goblet cell numbers, which could later only be recovered via the inhibition of Notch1 *in vivo* (Wei et al., 2020). Whether M1 macrophages are able to inhibit ERK1/2 in order to activate the Ras/Akt/mTOR and upregulate Wnt signalling is currently not known and will need to be investigated further in the future.

Unlike, Notch signalling, the Wnt pathway does not require cell-cell contact to transduce its signal, this begs the question as to why we have observed an increase in Wnt signalling following direct contact with M1 macrophages. Previous studies have shown that both Wnt and Notch can be regulated by each other to some extent (Collu et al., 2014). Here Foltz et al, demonstrated that GSK3β is able to stabilise the NICD1 domain thereby positively regulating Notch signalling (Foltz et al., 2002). Where one study has shown that Notch1 can tether itself to non-phosphorylated β-catenin thereby dampening its effect on downstream Wnt target genes, another study found that another study found that the interaction between Notch1/NICD and β-catenin, reduces the ubiquitination and subsequently enhances Hes1 expression *in vivo* (Jin et al., 2009). In addition to expressing Notch ligands, early research has that the exposure of macrophage to LPS and IFN-γ also leads to the increased protein levels of the signal receiving Notch1 receptor in RAW 264.6 macrophages (Monsalve et al., 2006). Notably, the mammary gland stem cells in mice, also rely on macrophage's-derived Wnt ligands to maintain its stem cell niche, where its secretion was dependent on the expression of mammary stem cell-mediated Dll-1 signalling (Chakrabarti et al., 2018). It could therefore also be a likely possibility that this mechanism is mimicked our M1-crypt co-culture model. The crosstalk between Wnt and Notch will need to be studied further to understand whether such a correlation is existent within our M1-crypt co-culture model.

Following our previous findings in which we have shown that Lgr5+ stem cells and newly proliferated cell numbers were increased we then further investigated whether these factors can affect the prolonged culture of colonoids within our M1-crypt co-culture model. Indeed, the continuous culture of colonic crypts and M1 macrophages led to increased presence of organoid budding after six days within the 3D *in vitro* co-culture model, suggesting that the inflammatory M1 macrophages may contribute to the long-term survival of colonic organoids.

We also noted a decline in colonoid numbers in both crypts cultured alone and in the presence with M1 macrophages over the course of seven days. As mentioned previously, the colonic epithelium relies on external stimuli to provide the growth factors required for survival, however such factors can be quickly diminished within an Matrigel-based organoid model (Meran et al., 2017). One of the major stem cell niche's supporting factors are the ECM components such as laminin, collagen IV and entactin which when degraded forces the Matrigel to lose its structural rigidity and is unable to maintain the 3D scaffold, thus no longer supporting organoid formation (Aisenbrey and Murphy., 2020). As organoid survival remained consistent in both culture conditions, it can also be assumed that the M1 macrophages did not differentially degrade the extracellular matrix components. A recent study has previously described that M2 macrophages but not M1 macrophages are able to influence the remodelling of the ECM by aiding matrix alignment *in vitro*, whether M1-driven ECM remodelling occurred within our co-culture model cannot be confirmed and is yet to be determined (Witherel et al., 2020). Although the 3D *in vitro* growth factor-reduced Matrigel has been utilised throughout this study, it has been identified as a product with high batch-to-batch variability, where varying protein contents may have an unidentified effect on the macrophages and the colonic epithelium. (Aisenbrey and Murphy., 2020). As a resolution, Sachs et al have suggested the use of synthetic collagen gels in order to grow small intestinal organoids thus reducing batch-to-batch variability. Interestingly, small intestinal organoids within a collagen-gel model were self-organized into a continuous tube-like structure, which could also potentially allow us to study and compare epithelial renewal between neighbouring crypt domains in the future (Sachs et al., 2017). A study from 2018 also found that when M1 macrophages were cultured in Matrigel-containing laminin, an increase in arginase-1 producing M2-like macrophages was found and that ECM1 (extracellular matrix protein 1) expressed in tissue-infiltrated 'inflammatory' macrophages are also aberrantly upregulated in IBD, where the knockout of ECM1 resulted in the impaired polarisation of M1 macrophages and increased production of arginase-1, commonly secreted by M2 macrophages (Luu and Liu., 2018; Zhang et al., 2020). For these reasons it cannot be confirmed whether M1 macrophages have maintained their phenotype and function throughout the course of the organoid culture experiment as M1 macrophages can potentially re-differentiate into a M2 macrophage phenotype as previously described by Orrechioni's work (Orrechioni et al., 2018).

A recent study into the culture conditions for the growth of colonoids has revealed that recombinant Wnt3a does not support the long-term survival of human and mouse colonoids, secretory Wnt3a derived from L-Wnt3a was suggested to be more suitable to the maintenance of the stem cell niche. Furthermore, the study revealed that the absence of Wnt3a, Noggin and R-spondin leads to increased colonoid differentiation and a reduction in Lgr5+ stem cells (Wilson et al., 2021). Although we also relied on the use of recombinant Wnt3a as many other organoid studies have utilised in the past, with the replenishment of growth-factor containing culture media every two days of culture we were unable maintain intact colonoids for a longer time period, whether the use of L-Wnt3a cells derived Wnt3a as suggested by Wilson et al would prolong their colonoid survival will have to be determined in future experiments. (Fair et al., 2018; Clevers, 2016).

Lastly, a myriad of inhibitory drugs are available to be used in the future to delineate the individual pathways macrophages utilise to communicate with epithelial cells. To determine whether M1-derived stimulation via the expression of delta-like ligand or jagged, we suggest that M1 macrophages are pre-incubated in the inhibitor drug prior to the co-culture, allowing us to determine the ligands required for M1 to crypt cell signalling. The use of 5-ASA (aminosalicylates) for alleviating chronic inflammation has long been recognised as a well-known inhibitor of the Wnt/β-catenin pathway, where β-catenin and cyclinD1 were significantly downregulated in colon cancer cell lines (Bos et al., 2006; Munding et al., 2012). Similarly, anti-TNF-α therapy also downregulated β-catenin to challenge inflammation in IBD (Li et al., 2011; Bradford et al., 2017). In future experiments, we would like to understand the effects 5-ASA and anti-TNFα have on macrophage-crypt crosstalk and will allow us to evaluate whether the inhibition of Wnt signalling is sufficient to inhibit stem cell expansion within our M1-crypt co-culture model or a non-canonical Wnt pathway is utilised instead.

Conclusion:

Under *in vivo* conditions, the presence of M1 macrophages in the lamina propria usually represents one of many inflammatory factors which the colonic epithelium can be exposed to (Rees et al., 2020). Due to the unique experimental setup, by minimising the environmental factors the colonic crypts are subjected to, we were able to confirm that, the unique M1 macrophage phenotype can increase colonic proliferation in a paracrine manner, and juxtacrine signalling mediated crosstalk between 'inflammatory' M1 macrophages and colonic crypts regulates stem cell expansion, the differentiation of tuft and goblet cells as well as promote organoid budding in prolonged co-culture with colonic crypts *in vitro*.

Chapter 7: General Discussion and Future Outlook

In this study, our key findings demonstrate that macrophage subtypes differentially regulate colonic crypt proliferation and differentiation in **Chapter 4**, characterised the spatio-temporal interactions between macrophages and colonic crypts in our 3D Matrigel-based co-culture (**Chapter 5**) and further demonstrated the capacity of M1 macrophages to promote colonic Lgr5+ stem cell expansion in a juxtacrine-signal dependent manner in **Chapter 6**. Overall, our findings showcase the influence non-activated, pro-inflammatory, and anti-inflammatory macrophages have on colonic crypt renewal. In this chapter we will discuss the potential implications of our findings on future research and offer an outlook into novel experimental models which may be utilised to further our understanding of macrophage-epithelial crosstalk in the future.

As the colon houses the largest microbiome population in the body, continual insults to the epithelial barrier function must be maintained to remain in homoeostasis. The ever-present macrophages in the underlying lamina propria partially modulate barrier integrity by resolving pathogen-driven inflammation via its highly conserved role as a phagocyte. Over the last two decades however, its malleable nature has allowed it to take on further functions and were shown to play a crucial role in the maintenance of the intestinal steady state. In this study, our key findings demonstrate that macrophage, depending on its metabolic state (Naive, M1 or M2), engage with the colonic epithelium and subsequently increase epithelial proliferation and alter epithelial differentiation, as summarised in **Figure 7.1**. More prominently, **Figure 7.2**, summarises our work from **Chapter 6**, in which we identified that M1 macrophages are able regulate epithelial renewal in a contact-dependent manner.

Conventionally, a breach in the epithelial barrier triggers the recruitment of Th1 or Th2 immune cells towards the site of inflammation, where in turn either pro-inflammatory IFN-γ or anti-inflammatory IL-13 and IL-4 cytokines are secreted, respectively (Kayama and Takeda., 2012). Residential macrophages and inflammatory macrophages are then educated to obtain a 'inflammatory' M1 macrophage phenotype. However, within an in vivo setting, it is unlikely that steady-state colonic crypts will encounter M1 macrophages, and it thereby becomes difficult to study the 'inflammatory' M1 macrophages effect on the epithelial

signalling. Unlike other *in vivo* studies, the use of our 3D macrophage-crypt co-culture allows us to further study the effect individual macrophages states (Naïve, M1 and M2) on epithelial renewal without disturbing crypt homeostasis.

Based on our findings in this study, future work should endeavour to identify the signalling pathways which prompted the changes in epithelial renewal within our co-culture model (**Figure 7.3**). In the intestinal epithelium, colonic proliferation and differentiation is closely regulated by the activation and inhibition of various signalling pathways, including Wnt, Notch, Hedgehog, BMP and Eph-Ephrin signalling, where disruption to one of the aforementioned pathways could potentially cause a rippling effect leading to the dysregulation in epithelial renewal. In **Chapter 6,** we have alluded to the potential knock-on effect contact-dependent signalling may have on Wnt target genes. Although the role of individual signalling pathways within the intestine have been well defined, little research has characterised the reciprocal relationship between the signalling pathways in either health or disease. To utilise macrophages as a therapeutic target, the signalling pathways which are either up or down regulated in the absence and presence of macrophages must therefore be profiled in detail. As a next step we therefore suggest the use of proteomic profiling and immunofluorescently co-labelling of key Notch, Wnt,BMP and Hedgehog target genes to further understand the signalling triggers required to result in the changes we have observed in **Chapter 4** and **6**.

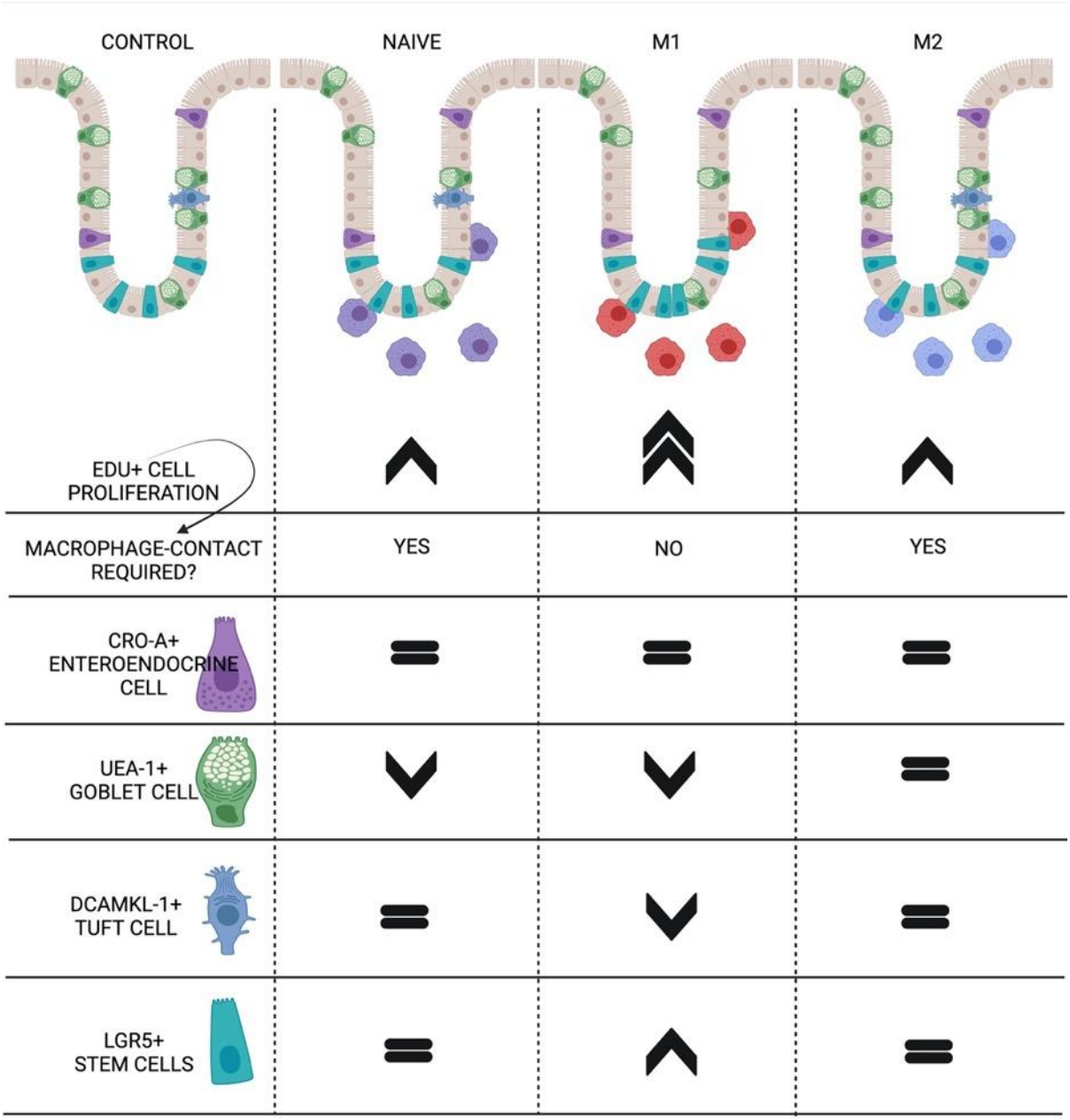

Figure 7.1: Summary of key findings in the co-culture of Naïve, M1 and M2 macrophages with colonic crypts

Schematic table summarising the effect of Naïve, M1 and M2 macrophages on epithelial proliferation, enteroendocrine, goblet cells, tuft cell and stem cell numbers within the 3D co-culture model. Created on Biorender (2021).

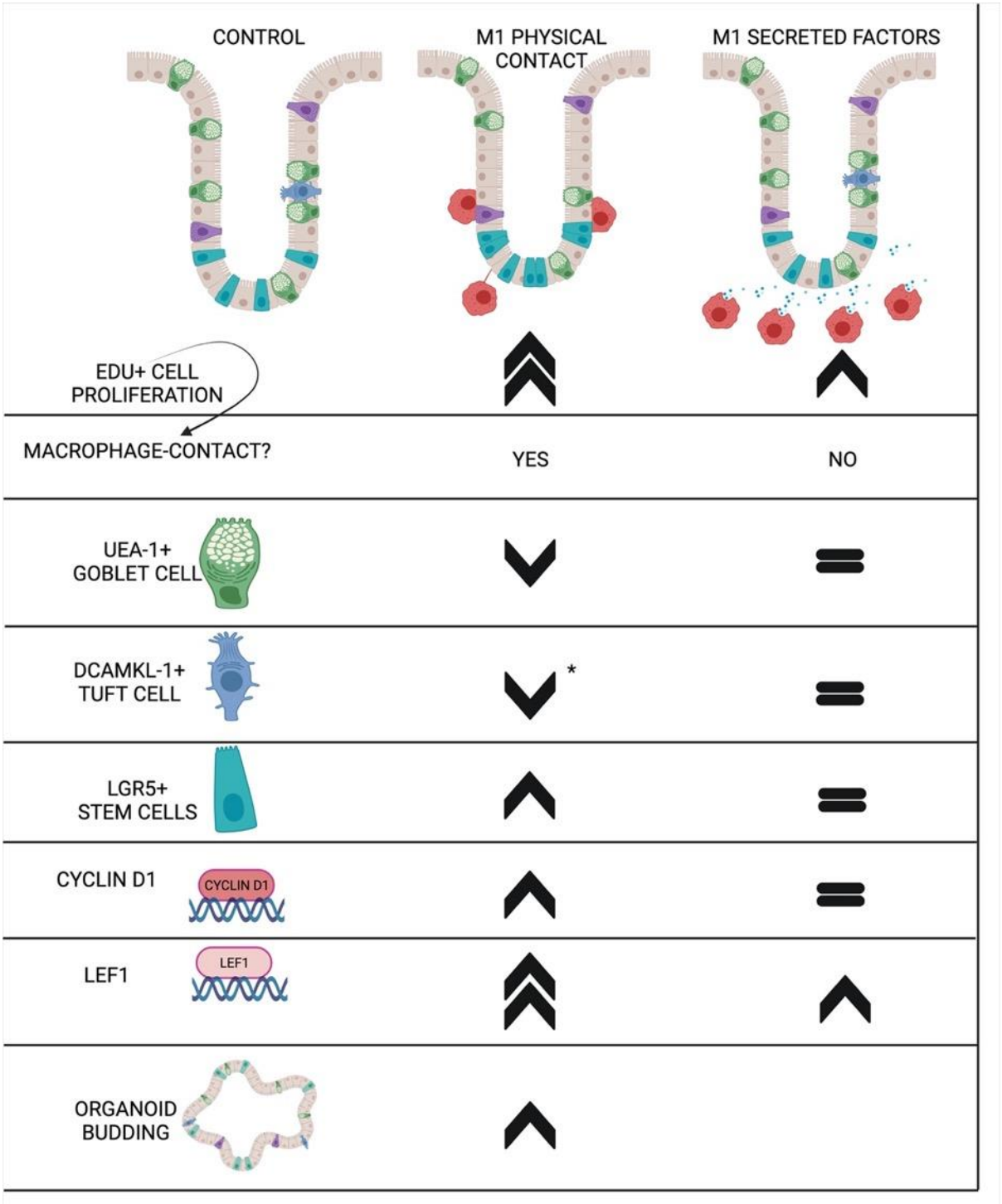

Figure 7.2: Summary of key findings of the M1-crypt conditioned media experiments

Schematic table summarising the effects of M1-crypt contact and M1-secretory factors on colonic proliferation, epithelial differentiated cells, Wnt targets genes (CyclinD1 and LEF1) and organoid budding efficiency within our 3D co-culture model. Created on Biorender (2021)

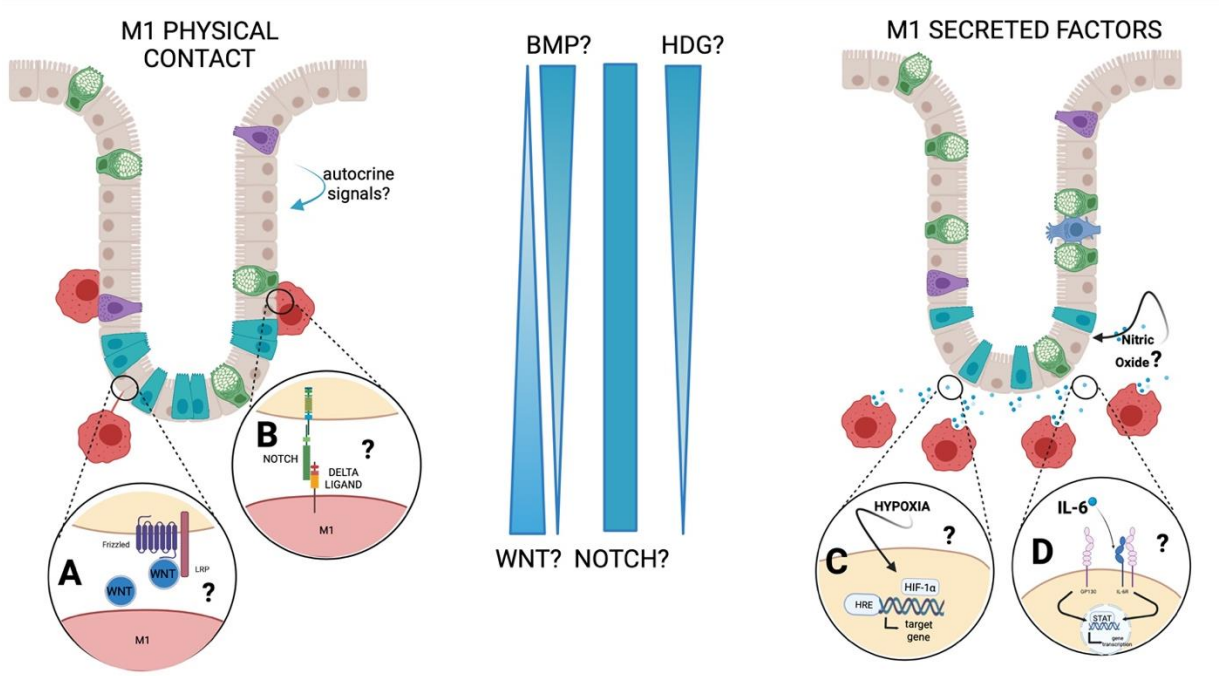

Figure 7.3: Potential signalling pathways requiring further investigation

Diagram outlining the potential signalling mechanisms involved in M1-driven epithelial renewal and the role of **A)** Wnt signalling pathway and Notch signalling **B)** in M1 contact dependent epithelial renewal. **C)** The role of M1-induced hypoxia and **D)** M1-derived IL-6 secretion on epithelial proliferation. Created on Biorender (2021).

7.1 Non-epithelial influences on macrophage phenotype and intestinal epithelial renewal

In this study, specifically **in Chapter 4** and **6**, we have demonstrated that the presence of Naïve, M1 and M2 macrophages can differentially influence epithelial renewal *in vitro*. Whether macrophages can regulate epithelial cell proliferation and differentiation with the same potency *in vivo* is currently unknown. By excluding, other external lamina propria cells from our 3D co-culture model, we have precluded macrophages from interacting with other variables, and regulating the intestinal epithelium in an indirect paracrine manner within our co-culture model.

One of the cell types residing in the lamina propria are FoxP3+ cells, known to suppress the immune response and promote oral tolerance within the lamina propria as a preventative measure to reduce inflammation-driven damage (Cosovanu and Neumann., 2020). In the dynamic *in vivo* microenvironment, constitutive secretion of IL-10 by tissue-resident M2-like macrophages leads to the maintenance of FoxP3+ T regulatory cells (Hadis et al., 2011). T-reg derived secretion of IL-10 was later found to support epithelial Lgr5+ stem cell renewal, while the depletion of Treg cells *in vivo* of the small intestine led to an increase in epithelial differentiation (Biton et al., 2018). Although currently, there is no evidence to suggest that the depletion of macrophages, could affect the capacity of T regulatory cells to maintain the stem cell niche, the possibility exists for residential macrophages to regulate the stem cell niche in conjunction with FoxP3+ regulatory T cells.

The underlying stromal cells, such a fibroblasts, myofibroblasts and mesenchymal stem cells and lamina propria-resident T-cells are all able to regulate the activation of macrophages *in vivo* (Yip et al., 2021). For example, mesenchymal stem cells were shown to direct macrophages towards a M2 macrophage phenotype in a tumor microenvironment, leading to decreased production of iNOS and other pro-inflammatory cytokines (Mantovani et al., 2012). Furthermore, when mesenchymal stem cells were introduced to DSS-colitis induced mice, an increase in IL-10 and a reduction of iNOS was reported, possibly suggesting that the inflammatory macrophage phenotype has been de-polarised towards an anti-inflammatory M2-like phenotype (Mao et al.,2017).

In the intestine, the stem cell niche is also in close contact with α-SMA+ myofibroblasts, which were demonstrated to provide the niche with R-spondin, hepatocyte-growth factor (HGF) and PGE2 (Sigal et al., 2017; Pastula and Macrinkiewicz., 2019). Karpus et al, was also able to identify CD90+ fibroblasts exclusively localised near the colonic stem cell niche, which induced stem cell proliferation via the secretion of semaphorin-3 in a NRP2-dependent manner (Karpus et al., 2019) During inflammation, activated fibroblasts were also shown to polarise macrophages towards the M1 phenotype, thus indicating that macrophages are also able to respond to fibroblast-derived secretory factors (Onfroy-Roy et al., 2021). **Figure 7.4** highlights the potential stromal-macrophage interactions which may contribute to intestinal epithelial renewal and their synergistic effects on colonic proliferation and differentiation should also be studied further in the future.

Although this reductionist *in vitro* co-culture model was not intended to include other endogenous stromal cells, we were unable to determine whether other lymphocytic cells are present within our co-culture model. As previously mentioned in **Chapter 5** of this study, we have reported sightings of small dark filopodial processes which we were unable to identify further, as these processes were also visible in crypts cultured alone, it is entirely possible that a fraction of lamina-propria resident cells have been isolated and seeded during the colonic crypt isolation. Here, unpublished work from the Sobolewski lab have shown that CD103+ intraepithelial lymphocytes were present in crypts cultured *in vitro* 3D Matrigel were present, which resembled dark filopodial like processes as we have previously described in **Chapter 5**. Interestingly, transfer of such CD103+, α4β7+ γδ- T lymphocytes into the intestinal tissue resulted in an increase in Th1/Th17 accumulation likely exacerbating disease progression (Jeong-su Do et al., 2017). Whether such intraepithelial lymphocytes are present and could interact with the macrophage's subtypes present within our co-culture model is yet to be determined and requires further work to understand their potential effects on epithelial renewal. Other sub-epithelial resident cells such as pericytes and neural cells, also play a crucial role in supporting the epithelial homeostasis of the intestinal crypt and were shown to affect intestinal stem cells division and differentiation (Powell et al., 2011). Interestingly, here enteric glial cells were shown to inhibit intestinal proliferation via the secretion of TGF-β1, while contractile pericytes interlaced in the basement membrane *in vivo* are commonly involved in the angiogenesis and

revascularization (Neunlist et al., 2007; Mifflin et al., 2011). . As we have not confirmed the absence or presence of either cell types within our co-culture model, we are unsure whether pericytes or glial-macrophage crosstalk as described by Grubisic and colleagues could affect macrophage function and therefore cause the differential regulation in epithelial renewal (Grubisic et al., 2020). Previously, little was known regarding the presence of the above mentioned stromal and mesenchymal cells following a colonic crypt isolation, however recent work from Bruegger and colleagues have shown following the isolation of crypts and cell sorting that almost 95% of all cells were of epithelial origin, less than 4% of lymphocytic cells and 1% of mesenchymal cells lineage (Bruegger et al., 2020).

As crosstalk between stromal cells, mesenchymal cells and macrophages is evidently crucial to intestinal homeostasis, we therefore also suggest that future work should attempt to determine whether lamina propria-resident cells mentioned above including Fox-P3+ T-cells, CD90+ myofibroblasts, CD103+intraepithelial lymphocytes and Connexin-43+ glial cells are present within our crypt-macrophage co-culture model and to further help us understand whether crosstalk between other lamina propria-resident tissue cells and macrophages can contribute to the differential changes in epithelial renewal as we have previously reported in **Chapter 4** and **6** (Stevens et al., 2020).

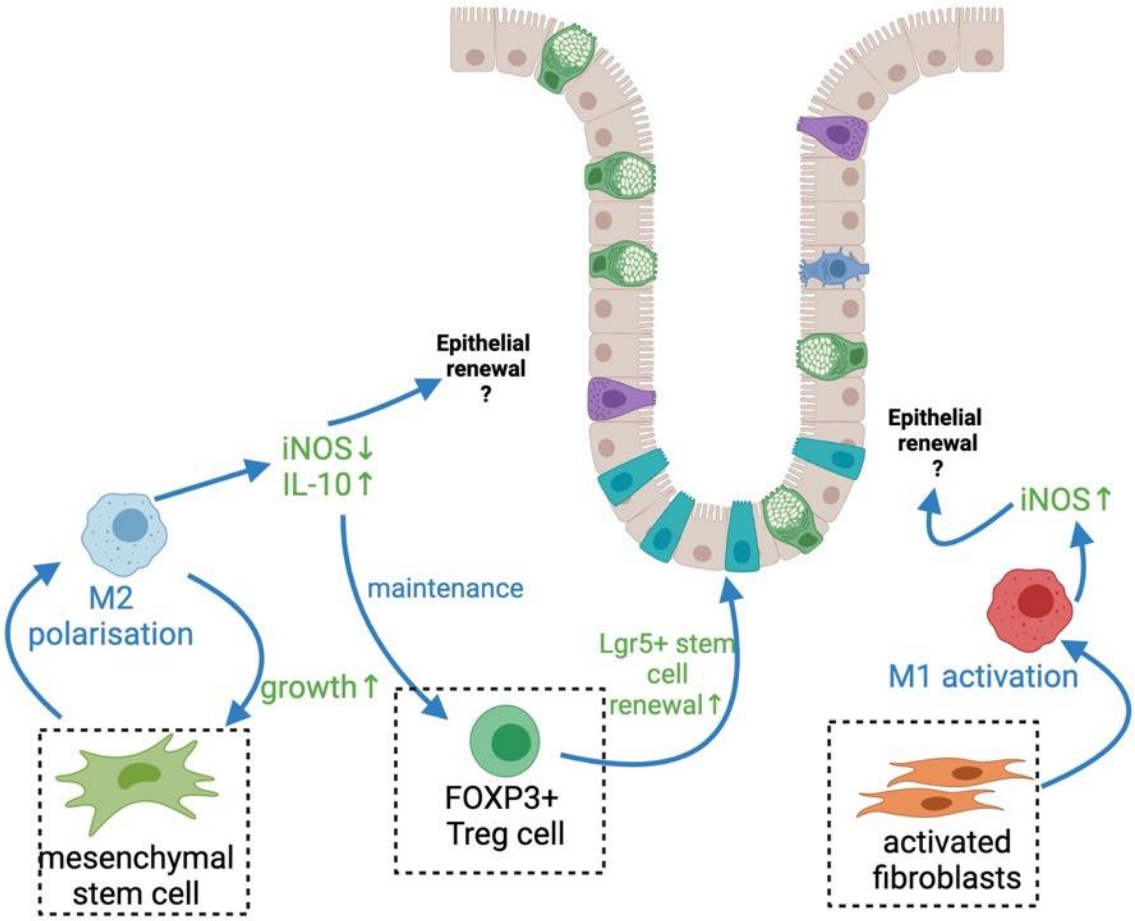

Figure 7.4: Intestinal stromal cell-macrophage crosstalk

Diagram highlighting the potential stromal-macrophage crosstalk links and their potential effect on epithelial renewal to be investigated in the future. Created on BioRender (2021).

7.2 Emerging organoid culture and IBD models

In the last decade several epithelial- non-parenchymal co-culture models have been developed to study the mechanism of inter-epithelial crosstalk. Over time, several culture models have been developed and refined to more closely mimic certain aspects of intestinal in vivo microenvironment while also giving researcher more control over the variable factors in culture. While 2D co-culture models as setup by Kaempfer et al, where Caco-2 epithelial cells were co-cultured with THP-1 monocytes allow us to gain a better fundamental understanding the reciprocal effects on cytokine secretion and epithelial integrity in a bid to closely mimic the physiological conditions of intestinal homeostasis and inflammation, increasingly complex culture model have been developed (Kaempfer et al., 2017).

A novel culture technique which is increasingly gaining traction is the use of the organ-on a chip model (Low et al., 2020). In this miniature microfluidic culture model, a well-defined microenvironment can be created with the use of photolithography where patterns and scaffoldings are etched onto the base of the chip and later coated with ECM components such as collagen and laminin, allowing the culture of epithelial cells. This method allows the user to predetermine the organoid's shape and size thus yielding more predictable data. Although previously, Caco-2 epithelial cell lines were cultured onto the microchips, advanced work from Verhulsel et al., has demonstrated that the culture of small intestinal epithelial monolayers derived from mouse-organoids is feasible. Furthermore, the presence of stromal cells can also be incorporated within the dynamic chip model (Verhulsel et al., 2020). An additional advantage of culturing intestinal epithelial cells in within a microfluidic chip chamber, is that the fluid flow can mimic the peristaltic flow within an in vivo environment. Not only can this influence the physiological characteristics of the epithelium, it can also regulate the chemical gradient of growth factors within the chamber (**Figure 7.5A)** (Lentle and Janssen., 2008: McCarthy et al., 2020*).

Similarly, microfluidic models have also been utilised to create co-culture 'droplets', which can produce intestinal spheroids (Collins et al., 2015). In 2016, Dura et al have also utilised a microfluidic model to study individual cell-cell interactions between NK cells and leukemia cell lines order to observe single-cell interactions (Dura et al., 2016).

ECM are commonly derived from animal sources, scaffolding support within this study, is provided by the Engelbroth-Holm Swarm mouse tumor, mainly consisting of laminin (60%), collagen type IV (30%) and entactin (8%), which can promote the formation of colonic organoids in an in vitro setting (Corning Matrigel datasheet., accessed 2021). However, as Hughes et al has noted, along with the ECM components, varying concentrations of intracellular proteins were also present within the Matrigel and is therefore unlikely to gain FDA approval for future therapeutic use (Hughes et al., 2010). To overcome this limitations, crosslinked polyethylene glycol (PEG) hydrogels are also utilised to embed tissue onto, providing more control over the matrix stiffness. However, the growth of organoids on such a platform remains problematic and requires further optimisation as described in detail by Magno and colleagues (Wen et al., 2014; Magno et al., 2020).

The intestinal basement membrane which offers structural support to the overlaying epithelium is largely composed of laminin and collage type IV, the production of which is mediated by epithelial and stromal cells (Roulis and Flavell., 2016). Although it is unknown whether endogenous stromal cells are present in our co-culture model and whether such cells could potentially be regulated by differential macrophage subtypes to cooperatively regulate colonic epithelial renewal *in vitro,* analysis of previous colonic crypt isolations performed by Bruegger et al have shown that less than 1% of all cells where of mesenchymal origin (Bruegger et al., 2020). As the intestinal extracellular matrix is a highly complex in nature and consists of several hundreds of molecules which are involved in the maintenance of tissue architecture, barrier function and migration, it is likely that both the colonic epithelium and macrophages utilise this network to its advantage *in vivo* (Pompili et al., 2021). Supporting this, work from Luu and colleagues have suggested that differing ECM proteins can indeed regulate both macrophage morphology and function. Here the adhesion of macrophages to either laminin, Matrigel or vitronectin resulted in an enhanced M2-like phenotype expression compared to their adhesion to collagen, fibronectin, or fibrinogen (Luu et al., 2018). Furthermore, *in vivo* work from Skoczek et al have noted that Lgr5-GFP+ stem cell processes from colonic crypts were shown protruding through the laminin-rich basement membrane to contact monocytes in the lamina propria (Skoczek et al., 2014). As laminin is the major component of the Matrigel used within our co-culture model, it begs the question as to whether this phenomenon prevails within our *in vitro*

model. For the reasons stated above, we therefore suggest that future work should endeavour to determine, whether the ECM components specifically present within our co-culture model are able to regulate or interact with differential macrophages subtypes and subsequently affect colonic crypt renewal. Specifically, the role of the ECM1 gene, previously discussed in **Chapter 6**, should be further studied as it's upregulation in M1 macrophages evidently plays a major role in IBD's pathogenesis (Zhang et al., 2020).

As we have established in **Chapter 3**, the intestinal epithelium in our 3D culture model remained intact and therefore resembled crypt in the *in vivo* steady state. To understand whether the role and effect macrophages have on epithelial renewal differs in damage-induced crypts several colitis-models can be utilised in the future. For example, Liso et al., have utilised *Winnie* mice, in which a mutation in the *Muc2* gene altered mucus production thus causing colonic inflammation in mice (**Figure 7.5B)**. Furthermore, their work reported an increase in MHC2+ immune cell recruitment and an alteration in the commensal microbiome in *Winnie* mice compared to control (Liso et al., 2019).

As M1 and M2 macrophage activation depends on the secretory response of Th1 and Th2 cells, respectively (Mills et al., 2001). Spontaneous inflammation is triggered in SAMP1/yit mice, in which a Th1-cell response is triggered and thus likely activates macrophages towards the M1 phenotype. This would allow us to potentially study M1 macrophage-crypt contact further within in an *in vivo* setting rather than *in vitro* as performed in Chapter 5. Additionally, following the isolation and co-culture of SAMP1/yit mice we could further investigate whether Naïve, M1 or M2 macrophages are able to normalise epithelial renewal *in vitro* (Pizarro et al., 2011). A similar inflammatory response can also be triggered in mice in which IL-10 was targeted for deletion (**Figure 7.5C)** (Roers et al., 2004). Whether the organoid co-culture of *Winnie* with either Naïve, M1 or M2 macrophages can alleviate or further exacerbate epithelial renewal could widen our understanding of the differential capacities the macrophage activation states (Naïve, M1 or M2) have on wound repair and renewal.

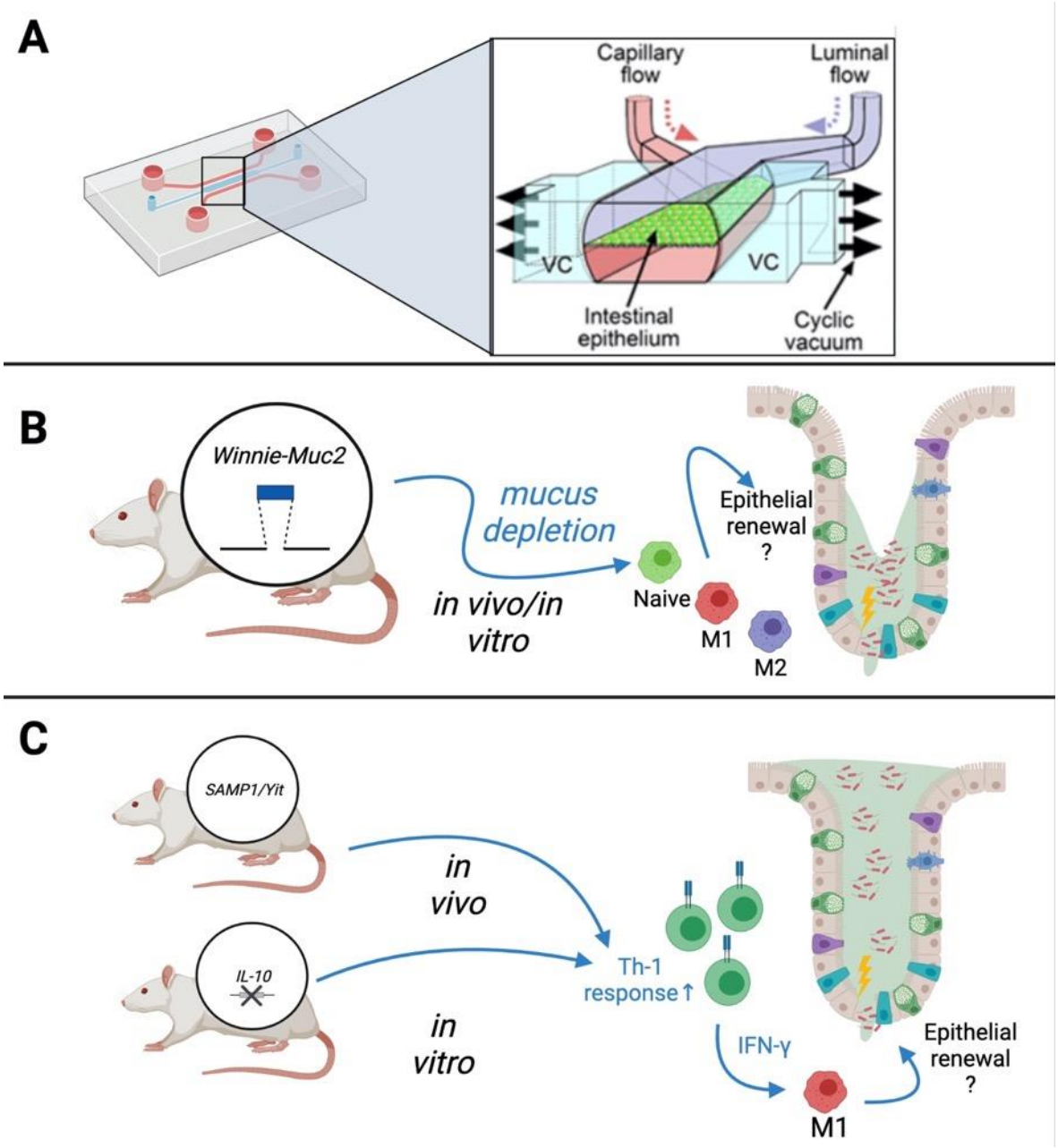

Figure 7. 5: Emerging organoid culture and IBD models

Diagram showing **A)** the experimental setup of an organ-on-chip model, where intestinal epithelial cells are cultured on a photolithography-sculpted scaffold and laminal flow is created to mimic peristalsis. (schematic adapted from Bein et al., 2018). **B)** The potential use of *Winnie* mice to either study the M1's macrophages restitutional abilities *in vivo* or the effect of Naïve, M1 and M2 macrophages in a *Winnie* crypt-macrophage co-culture model. **C)** the potential study of *in vivo* M1 macrophages and their role in wound repair and epithelial renewal *in vivo/in vitro.* Created on Biorender (2021).

7.3 Therapeutic targets against IBD and the role of macrophages

During inflammatory bowel disease, the aberrant production of cytokines produced by multiple source such as macrophage, dendritic and T-cells, are directly linked with the deterioration of the intestinal tissue observed in UC and CD. For this reason, studies in the last two decades have focused their attention to specifically targeting immune cells with varying degrees of success.

Along with the increase in inflammatory monocytes and macrophages, another hallmark of inflammatory bowel disease is the increased presence of Th-17 helper cells. Pro-inflammatory macrophages are able to secrete Th-17 cell-recruiting cytokines such as IL-12 and IL-23 which then exacerbate tissue damage. Initial clinical trials have attempted to aid intestinal resolution by introducing anti-inflammatory cytokines such as IL-10 and IL-11, while also inhibiting IL-12 and Il-23, however the direct induction of anti-inflammatory cytokines displayed low efficacy in IBD patients (Rang Na et al., 2018; Ogino et al., 2013).

In recent years, the use anti-TNF treatment has prominently featured as a preferred treatment method in IBD patients with chronic inflammation and heavily relies on the inhibition of inflammatory macrophages, subsequently preventing the recruitment of T-cell and reducing pathogenesis in IBD patients. Here TNF-receptor targeting drugs such as infliximab and azathioprine, promote the maintenance of 'regulatory' M2-like macrophages in IBD patients, while inhibiting the activation of inflammatory signalling pathways in macrophages (**Figure 7.6A**) (Vos et al., 2013). However due to varying efficacies in patients and the occurrence of severe side-effects, alternative therapies are still being pursued (Shivaji et al., 2019).

A promising new therapeutic drug named Alequel, which aims to increase the oral tolerance in IBD patients and was recently proven to alleviate inflammation in CD patients, where initial clinical trials were shown to reduce IFN-γ and increase in IL-10 and IL-4 levels, thereby likely promoting the polarisation of anti-inflammatory M2 macrophage rather than M1 macrophage phenotype. The oral administration of AlequelTM is currently in phase 2 of the clinical trials (**Figure 7.6B**) (Israeli and Ilan., 2010; National Library of Medicine, NCT02185183, accessed 2021). Similarly, the PDE4 (phosophodisesterase-4) inhibitor, Apremiliast, is also showing promising results in the alleviation of inflammation in UC patients and is currently in phase 2 of the clinical trial study. Here, Apremilast suppressed

the inflammatory response in macrophages following stimulation with LPS in a PKA-CREB pathway-dependent manner while also inhibiting proliferation and cytokine production in Caco-2 cells *in vitro (***Figure 7.6C**) (Li et al., 2018; National Library of Medicine, NCT02289417, accessed 2021).

The risk of developing intestinal cancer in patients with inflammatory bowel disease increases depending on the extend of the colonic disease and the disease duration (Greuter et al., 2020). Macrophages are also being increasingly utilised as an alternative approach to tackling and inhibiting intestinal tumour metastasis and growth. For example, Zanganeh et al, exposure of macrophages to an iron-oxide containing nanoparticle, induced a Th-1 type response and an increase in M1 macrophages while also significantly inhibited the growth of adenocarcinoma *in vitro* (Zanganeh et al., 2016). In colorectal tumours, tumour associated macrophages (TAMs), largely share a similar phenotype to M2 macrophages and are commonly present within the tumour environment in which they are known to promote tumour cell proliferation (Lin et al, 2019). Promising work from Song et al., reported that manganese dioxide nanoparticles are able to trigger the re-education of such TAMs towards the M1-like phenotypes, which reduced the expression VEGF and HIF-1α within tumours *in vivo* (Song et al., 2016). Although the use of macrophages to treat tumour formation are increasing, little to no studies have investigated whether macrophages can be manipulated in order to prevent the exacerbation of inflammatory bowel disease and requires more attention (Sun et al., 2021). As persistently increasing cellular proliferation is often observed in patients with colitis/IBD and colorectal cancers, in which the constitutive secretion of pro-inflammatory cytokines maintains chronic inflammation *in vivo* (Lyons et al., 2018). We have also reported that inflammatory macrophages significantly upregulate crypt proliferation in **Chapter 4** and is therefore important to understand and identify a therapeutic approach to reverse excessive proliferation and reduce the risk of tumour formation.

In comparison to the previously mentioned drugs, the favonol, quercetin which is found in a number of fruits and vegetables, was also demonstrated to alleviate colitis and increase microbiota diversity in mice (Lin et al., 2019). Interestingly, exposing colonic organoid to LPS while treating them with quercetin, led to a significant suppression of inflammation *in vitro*. Specifically, the mRNA expression of *TNF-α*, *Slpi* (serine protease inhibitor) and *LCN-2* was reduced in the presence of quercetin (DiCarclo et al., 2019). As other studies have shown

that the knockout of *Slpi* in M1 and M2 macrophages can lead to an increase in iNOS and arginase activity, respectively, while increased *LCN-2* expression was considered a M1-polarisation factor, it should be questioned whether quercetin can directly influence the metabolic state of macrophages in homeostasis and inflammation in order to reverse the effects in epithelial renewal we have reported in **Chapter 4 (Figure 7.6D**) (McCartney-Francis et al., 2014; Cheng et al., 2015). The previously mentioned therapeutic drugs which may rely on the activation of M1 or M2 macrophages for epithelial wound repair are summarised in **Figure 7.6**.

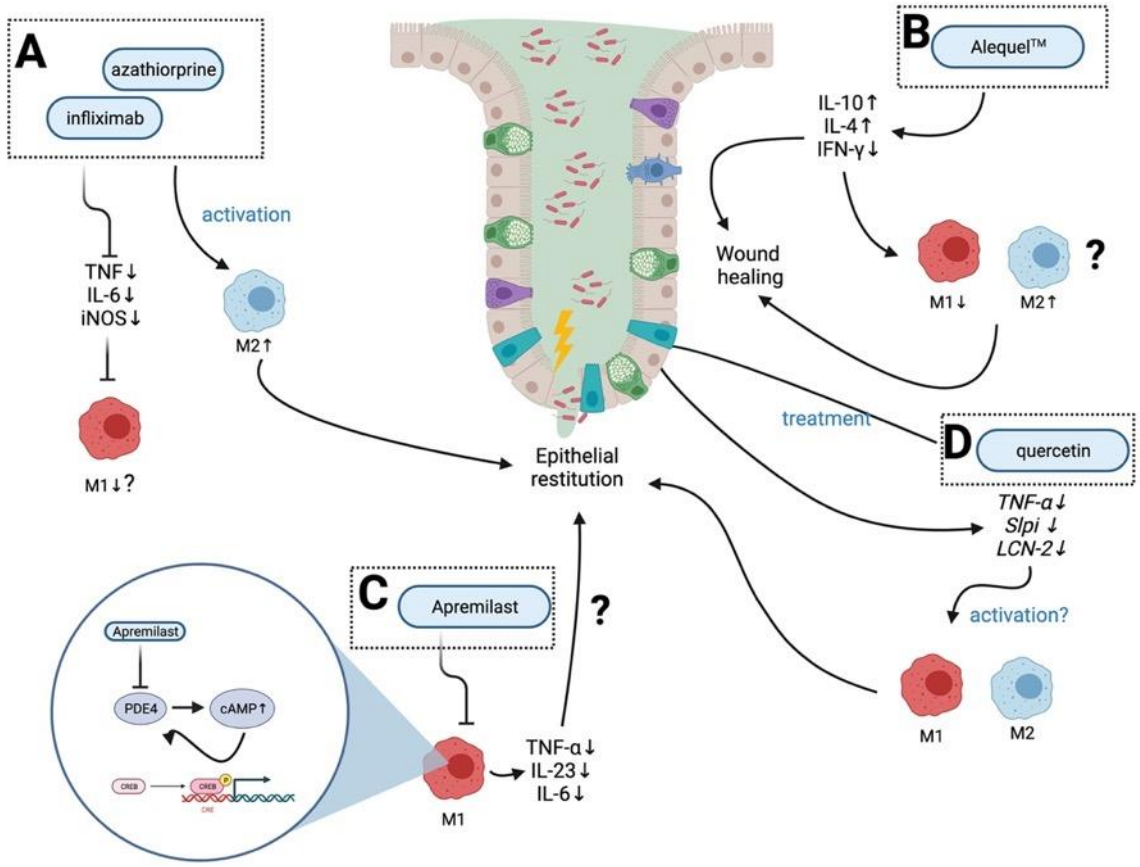

Figure 7.6: Therapeutic targets against IBD and the role of macrophages

Diagram highlighting current drugs and their utilisation of macrophages as a therapeutic target **A)** The effect of anti-TNF therapy on the polarisation of M1 and M2 macrophages **B)** The potential downstream effects of Alequel on M1 and M2 macrophage activation **C)** The effect of Apremilast on M1 macrophages to downregulate inflammation *in vivo* ***D)*** The effect of quercetin and the potential downstream effects on M1 and M2 macrophage activation. Created on Biorender (2021).

7.4 Concluding remarks

In conclusion, we have utilised a unique 3D macrophage-crypt co-culture model in order to demonstrate the differential effects of non-activated (Naïve), inflammatory (M1) and anti-inflammatory (M2) macrophages have on epithelial proliferation and differentiation, importantly, this study describes the phenomenon in which inflammatory (M1) macrophage unlike its anti-inflammatory (M2) or non-activated (Naïve) counterpart are able to promote Lgr5+ stem cell expansion in a contact-dependent manner *in vitro*. Further work should be directed to determining the causative signalling mechanism which have prompted the macrophage-driven changes we have observed in the colonic epithelium. We anticipate that the findings in this study will contribute to our understanding of the dynamic relationship between macrophages and colonic crypts in homeostasis and aid the development of preventative strategies and new therapeutic targets against IBD.

Bibliography:

Andrä, I., Ulrich, H., Dürr, S., Soll, D., Henkel, L., Angerpointner, C., Ritter, J., Przibilla, S., Stadler, H., Effenberger, M., Busch, D. H. and Schiemann, M. (2020) 'An Evaluation of T-Cell Functionality After Flow Cytometry Sorting Revealed p38 MAPK Activation', Cytometry Part A, 97(2), pp. 171–183. doi: 10.1002/cyto.a.23964.

Ahlman, H. and Nilsson, O. (2001) 'The gut as the largest endocrine organ in the body', *Annals of Oncology*, 12(SUPPLE. 2), pp. S63–S68. doi: 10.1093/annonc/12.suppl_2.s63.

Aisenbrey, E. A. and Murphy, W. L. (2020) *Synthetic alternatives to Matrigel*, *Nature Reviews Materials*. doi: 10.1038/s41578-020-0199-8.

Allaire, J. M., Crowley, S. M., Law, H. T., Chang, S. Y., Ko, H. J. and Vallance, B. A. (2018) 'The Intestinal Epithelium: Central Coordinator of Mucosal Immunity', *Trends in Immunology*, 39(9), pp. 677–696. doi: 10.1016/j.it.2018.04.002.

Amici, S. A., Young, N. A., Narvaez-Miranda, J., Jablonski, K. A., Arcos, J., Rosas, L., Papenfuss, T. L., Torrelles, J. B., Jarjour, W. N. and Guerau-de-Arellano, M. (2018) 'CD38 is robustly induced in human macrophages and monocytes in inflammatory conditions', *Frontiers in Immunology,* 9(JUL), pp. 1–13. doi: 10.3389/fimmu.2018.01593.

Andrianifahanana, M., Moniaux, N. and Batra, S. K. (2006) 'Regulation of mucin expression: Mechanistic aspects and implications for cancer and inflammatory diseases', *Biochimica et Biophysica Acta - Reviews on Cancer*, 1765(2), pp. 189–222. doi: 10.1016/j.bbcan.2006.01.002.

Antonios, J. K., Yao, Z., Li, C., Rao, A. J. and Goodman, S. B. (2013) 'Macrophage polarization in response to wear particles in vitro', *Cellular and Molecular Immunology*, 10(6), pp. 471–482. doi: 10.1038/cmi.2013.39.

Arrieta, M. C., Madsen, K., Doyle, J. and Meddings, J. (2009) 'Reducing small intestinal permeability attenuates colitis in the IL10 gene-deficient mouse', *Gut*, 58(1), pp. 41–48. doi: 10.1136/gut.2008.150888.

Aziz, M., Ishihara, S., Ansary, M. U., Sonoyama, H., Tada, Y., Oka, A., Kusunoki, R., Tamagawa, Y., Fukuba, N., Mishima, Y., Mishiro, T., Oshima, N., Moriyama, I., Ishimura, N., Sato, S., Yuki, T., Kawashima, K. and Kinoshita, Y. (2013) 'Crosstalk between TLR5 and

Notch1 signalling in epithelial cells during intestinal inflammation', *International Journal of Molecular Medicine*, 32(5), pp. 1051–1062. doi: 10.3892/ijmm.2013.1501.

Bachurski, D., Schuldner, M., Nguyen, P. H., Malz, A., Reiners, K. S., Grenzi, P. C., Babatz, F., Schauss, A. C., Hansen, H. P., Hallek, M. and Pogge von Strandmann, E. (2019) 'Extracellular vesicle measurements with nanoparticle tracking analysis–An accuracy and repeatability comparison between NanoSight NS300 and ZetaView', *Journal of Extracellular Vesicles*, 8(1). doi: 10.1080/20013078.2019.1596016.

Bahr, J. and Weiss, S. (2018) 'Macrophage-Dependent Trafficking and Remodeling of the Basement Membrane-Interstitial Matrix Interface', *bioRxiv*, p. 364422. doi: 10.1101/364422.

Bain, C. C., Oliphant, C. J., Thomson, C. A., Kullberg, M. C. and Mowat, A. M. (2018) 'Proinflammatory role of monocyte-derived CX3CR1int macrophages in Helicobacter hepaticus-induced colitis', *Infection and Immunity*, 86(2). doi: 10.1128/IAI.00579-17.

Barker, N., Van Es, J. H., Kuipers, J., Kujala, P., Van Den Born, M., Cozijnsen, M., Haegebarth, A., Korving, J., Begthel, H., Peters, P. J. and Clevers, H. (2007) 'Identification of stem cells in small intestine and colon by marker gene Lgr5', *Nature*, 449(7165), pp. 1003–1007. doi: 10.1038/nature06196.

Barker, N., Van Oudenaarden, A. and Clevers, H. (2012) 'Identifying the stem cell of the intestinal crypt: Strategies and pitfalls', *Cell Stem Cell*, 11(4), pp. 452–460. doi: 10.1016/j.stem.2012.09.009.

Barreto, A., Rodríguez, L. S., Rojas, O. L., Wolf, M., Greenberg, H. B., Franco, M. A. and Angel, J. (2010) 'Membrane vesicles released by intestinal epithelial cells infected with rotavirus inhibit T-cell function', *Viral Immunology*, 23(6), pp. 595–608. doi: 10.1089/vim.2009.0113.

Barros, M. H. M., Hauck, F., Dreyer, J. H., Kempkes, B. and Niedobitek, G. (2013) 'Macrophage polarisation: An immunohistochemical approach for identifying M1 and M2 macrophages', *PLoS ONE*, 8(11), pp. 1–11. doi: 10.1371/journal.pone.0080908.

Basson, M. D., Turowski, G. and Emenaker, N. J. (1996) 'Regulation of human (Caco-2) intestinal epithelial cell differentiation by extracellular matrix proteins', *Experimental Cell Research*, 225(2), pp. 301–305. doi: 10.1006/excr.1996.0180.

Beisner, J., Teltschik, Z., Ostaff, M. J., Tiemessen, M. M., Staal, F. J. T., Wang, G., Gersemann, M., Perminow, G., Vatn, M. H., Schwab, M., Stange, E. F. and Wehkamp, J. (2014) 'TCF-1-mediated Wnt signaling regulates Paneth cell innate immune defense effectors HD-5 and -6: Implications for Crohn's disease', *American Journal of Physiology - Gastrointestinal and Liver Physiology*, 307(5), pp. 487–498. doi: 10.1152/ajpgi.00347.2013.

Berger, A. (2000) 'Science commentary: Th1 and Th2 responses: What are they?', *British Medical Journal*, 321(7258), p. 424. doi: 10.1136/bmj.321.7258.424.

Berghe, T. Vanden, Linkermann, A., Jouan-Lanhouet, S., Walczak, H. and Vandenabeele, P. (2014) 'Regulated necrosis: The expanding network of non-apoptotic cell death pathways', *Nature Reviews Molecular Cell Biology*, 15(2), pp. 135–147. doi: 10.1038/nrm3737.

Bersudsky, M., Luski, L., Fishman, D., White, R. M., Ziv-Sokolovskaya, N., Dotan, S., Rider, P., Kaplanov, I., Aychek, T., Dinarello, C. A., Apte, R. N. and Voronov, E. (2014) 'Non-redundant properties of IL-1α and IL-1β during acute colon inflammation in mice', *Gut*, 63(4), pp. 598–609. doi: 10.1136/gutjnl-2012-303329.

Berwick, D. C. and Harvey, K. (2013) 'LRRK2: An éminence grise of Wnt-mediated neurogenesis?', *Frontiers in Cellular Neuroscience*, 7(MAY), pp. 1–13. doi: 10.3389/fncel.2013.00082.

Bhasin, J. M., Chakrabarti, E., Peng, D. Q., Kulkami, A., Chen, X. and Smith, J. D. (2008) 'Sex specific gene regulation and expression QTLs in mouse macrophages from a strain intercross', *PLoS ONE*, 3(1). doi: 10.1371/journal.pone.0001435.

Bhattacharjee, J., Das, B., Mishra, A., Sahay, P. and Upadhyay, P. (2017) 'Monocytes isolated by positive and negative magnetic sorting techniques show different molecular characteristics and immunophenotypic behaviour', F1000Research, 6(0), p. 2045. doi: 10.12688/f1000research.12802.1.

Birchenough, G. M. H., Johansson, M. E. V., Gustafsson, J. K., Bergström, J. H. and Hansson, G. C. (2015) 'New developments in goblet cell mucus secretion and function', *Mucosal Immunology*, 8(4), pp. 712–719. doi: 10.1038/mi.2015.32.

Bissonnette, E. Y., Lauzon-Joset, J. F., Debley, J. S. and Ziegler, S. F. (2020) 'Cross-Talk Between Alveolar Macrophages and Lung Epithelial Cells is Essential to Maintain Lung

Homeostasis', *Frontiers in Immunology*, 11(October), pp. 1–12. doi: 10.3389/fimmu.2020.583042.

Biton, M. *et al.* (2019) 'HHS Public Access', 175(5), pp. 1307–1320. doi: 10.1016/j.cell.2018.10.008.T.Bjerknes, M., Cheng, H. and Toronto, U. O. (2002) 'Multipotential stem cells in adult mouse gastric epithelium', *American Journal of Physiology - Gastrointestinal and Liver Physiology*, 283(3 46-3). doi: 10.1152/ajpgi.00415.2001.

Blander, J. M. (2018) 'On cell death in the intestinal epithelium and its impact on gut homeostasis', *Current Opinion in Gastroenterology*, 34(6), pp. 413–419. doi: 10.1097/MOG.0000000000000481.

Bogunovic, D., O'Neill, D. W., Belitskaya-Levy, I., Vacic, V., Yu, Y. Lo, Adams, S., Darvishian, F., Berman, R., Shapiro, R., Pavlick, A. C., Lonardi, S., Zavadil, J., Osman, I. and Bhardwaj, N. (2009) 'Immune profile and mitotic index of metastatic melanoma lesions enhance clinical staging in predicting patient survival', *Proceedings of the National Academy of Sciences of the United States of America*, 106(48), pp. 20429–20434. doi: 10.1073/pnas.0905139106.

Bonecchi, R., Bianchi, G., Bordignon, P. P., D'Ambrosio, D., Lang, R., Borsatti, A., Sozzani, S., Allavena, P., Gray, P. A., Mantovani, A. and Sinigaglia, F. (1998) 'Differential expression of chemokine receptors and chemotactic responsiveness of type 1 T helper cells (Th1s) and Th2s', *Journal of Experimental Medicine*, 187(1), pp. 129–134. doi: 10.1084/jem.187.1.129.

Bonnardel, J. *et al.* (2019) 'Stellate Cells, Hepatocytes, and Endothelial Cells Imprint the Kupffer Cell Identity on Monocytes Colonizing the Liver Macrophage Niche', *Immunity*, 51(4), pp. 638-654.e9. doi: 10.1016/j.immuni.2019.08.017.

Boocock, C. A., Jones, G. E., Stanley, E. R. and Pollard, J. W. (1989) 'Colony-stimulating factor-1 induces rapid behavioural responses in the mouse macrophage cell line, BAC1.2F5', *Journal of Cell Science*, 93(3), pp. 447–456.

Boom, W., Liano, D. and Abbas, A. K. (1988) 'Heterogeneity of helper/inducer T lymphocytes: II. Effects of interleukin 4- and interleukin 2-producing T cell clones on resting B lymphocytes', *Journal of Experimental Medicine*, 167(4), pp. 1350–1363. doi: 10.1084/jem.167.4.1350.

Bos, C. L., Diks, S. H., Hardwick, J. C. H., Walburg, K. V., Peppelenbosch, M. P. and Richel, D. J. (2006) 'Protein phosphatase 2A is required for mesalazine-dependent inhibition of Wnt/β-catenin pathway activity', *Carcinogenesis*, 27(12), pp. 2371–2382. doi: 10.1093/carcin/bgl071.

Bradford, E. M., Ryu, S. H., Singh, A. P., Lee, G., Goretsky, T., Sinh, P., Williams, D. B., Cloud, A. L., Gounaris, E., Patel, V., Lamping, O. F., Lynch, E. B., Moyer, M. P., De Plaen, I. G., Shealy, D. J., Yang, G.-Y. and Barrett, T. A. (2017) 'Epithelial TNF Receptor Signaling Promotes Mucosal Repair in Inflammatory Bowel Disease', *The Journal of Immunology*, 199(5), pp. 1886–1897. doi: 10.4049/jimmunol.1601066.

Bruegger David., Tomas Valenta., Fazilaty, H., Hausmann, G. and Basler, K. (2020) 'Distinct populations of crypt-associated fibroblasts act as signaling hubs to control colon homeostasis', *PLoS Biology,* 18(12), pp. 1–20. doi: 10.1371/journal.pbio.3001032.

Buczacki, S. J. A., Zecchini, H. I., Nicholson, A. M., Russell, R., Vermeulen, L., Kemp, R. and Winton, D. J. (2013) 'Intestinal label-retaining cells are secretory precursors expressing lgr5', *Nature*, 495(7439), pp. 65–69. doi: 10.1038/nature11965.

Bui, T. M., Mascarenhas, L. A. and Sumagin, R. (2018) 'Extracellular vesicles regulate immune responses and cellular function in intestinal inflammation and repair', *Tissue Barriers*, 6(2), pp. 1–14. doi: 10.1080/21688370.2018.1431038.

Bullen, T. F., Forrest, S., Campbell, F., Dodson, A. R., Hershman, M. J., Pritchard, D. M., Turner, J. R., Montrose, M. H. and Watson, A. J. M. (2006) 'Characterization of epithelial cell shedding from human small intestine', *Laboratory Investigation*, 86(10), pp. 1052–1063. doi: 10.1038/labinvest.3700464.

Burgess, M., Wicks, K., Gardasevic, M. and Mace, K. A. (2019) 'Cx3CR1 Expression Identifies Distinct Macrophage Populations That Contribute Differentially to Inflammation and Repair', *ImmunoHorizons*, 3(7), pp. 262–273. doi: 10.4049/immunohorizons.1900038.

Burgueño, J. F. and Abreu, M. T. (2020) 'Epithelial Toll-like receptors and their role in gut homeostasis and disease', *Nature Reviews Gastroenterology and Hepatology*, 17(5), pp. 263–278. doi: 10.1038/s41575-019-0261-4.

Butcher, S. K., O'Carroll, C. E., Wells, C. A. and Carmody, R. J. (2018) 'Toll-like receptors drive specific patterns of tolerance and training on restimulation of macrophages', *Frontiers in Immunoloy*, 9(MAY). doi: 10.3389/fimmu.2018.00933.

Camargo, F. D., Gokhale, S., Johnnidis, J. B., Fu, D., Bell, G. W., Jaenisch, R. and Brummelkamp, T. R. (2007) 'YAP1 Increases Organ Size and Expands Undifferentiated Progenitor Cells', *Current Biology*, 17(23), pp. 2054–2060. doi: 10.1016/j.cub.2007.10.039.

Castillo-Azofeifa, D., Fazio, E. N., Nattiv, R., Good, H. J., Wald, T., Pest, M. A., Sauvage, F. J., Klein, O. D. and Asfaha, S. (2019) ' Atoh1 + secretory progenitors possess renewal capacity independent of Lgr5 + cells during colonic regeneration ', *The EMBO Journal*, 38(4), pp. 1–16. doi: 10.15252/embj.201899984.

Cerovic, V., Bain, C. C., Mowat, A. M. and Milling, S. W. F. (2014) 'Intestinal macrophages and dendritic cells: What's the difference?', *Trends in Immunology*, 35(6), pp. 270–277. doi: 10.1016/j.it.2014.04.003.

Cerutti, A. (2008) 'The regulation of IgA class switching', *Nature Reviews Immunology*, 8(6), pp. 421–434. doi: 10.1038/nri2322.Chakrabarti, R., Celià-terrassa, T., Kumar, S., Hang, X., Wei, Y., Gao, J., Es, J. Van, Li, M. O., Aifantis, I. and Clevers, H. (2021) 'Dll1-mediated macrophageal niche for mammary gland stem cells', 360(6396). doi: 10.1126/science.aan4153.Dll1-mediated.

Chang, P. V., Hao, L., Offermanns, S. and Medzhitov, R. (2014) 'The microbial metabolite butyrate regulates intestinal macrophage function via histone deacetylase inhibition', *Proceedings of the National Academy of Sciences of the United States of America*, 111(6), pp. 2247–2252. doi: 10.1073/pnas.1322269111.

Chen, F., Liu, Z., Wu, W., Rozo, C., Bowdridge, S., Rooijen, N. Van, Jr, J. F. U., Wynn, T. A. and William, C. (2012) 'Damage During Helminth Infection', 18(2), pp. 260–266. doi: 10.1038/nm.2628.An.

Chen, X., Song, C.-H., Feng, B.-S., Li, T.-L., Li, P., Zheng, P.-Y., Chen, X.-M., Xing, Z. and Yang, P.-C. (2011) 'Intestinal epithelial cell-derived integrin αβ6 plays an important role in the

induction of regulatory T cells and inhibits an antigen-specific Th2 response', *Journal of Leukocyte Biology*, 90(4), pp. 751–759. doi: 10.1189/jlb.1210696.

Cheng, H. and Leblond, C. P. (1974) 'Origin, differentiation and renewal of the four main epithelial cell types in the mouse small intestine I. Columnar cell', *American Journal of Anatomy*, 141(4), pp. 461–479. doi: 10.1002/aja.1001410403.

Cheng, L., Xing, H., Mao, X., Li, L., Li, X. and Li, Q. (2015) 'Lipocalin-2 promotes M1 macrophages polarization in a mouse cardiac ischaemia-reperfusion injury model', *Scandinavian Journal of Immunology*, 81(1), pp. 31–38. doi: 10.1111/sji.12245.

Chieppa, M., Rescigno, M., Huang, A. Y. C. and Germain, R. N. (2006) 'Dynamic imaging of dendritic cell extension into the small bowel lumen in response to epithelial cell TLR engagement', *Journal of Experimental Medicine*, 203(13), pp. 2841–2852. doi: 10.1084/jem.20061884.

Chikina, A. S., Nadalin, F., Maurin, M., San-Roman, M., Thomas-Bonafos, T., Li, X. V., Lameiras, S., Baulande, S., Henri, S., Malissen, B., Lacerda Mariano, L., Barbazan, J., Blander, J. M., Iliev, I. D., Matic Vignjevic, D. and Lennon-Duménil, A. M. (2020) 'Macrophages Maintain Epithelium Integrity by Limiting Fungal Product Absorption', *Cell*, 183(2), pp. 411-428.e16. doi: 10.1016/j.cell.2020.08.048.

Choi, K. M., Kashyap, P. C., Dutta, N., Stoltz, G. J., Ordog, T., Shea Donohue, T., Bauer, A. J., Linden, D. R., Szurszewski, J. H., Gibbons, S. J. and Farrugia, G. (2010) 'CD206-Positive M2 Macrophages That Express Heme Oxygenase-1 Protect Against Diabetic Gastroparesis in Mice', *Gastroenterology*, 138(7), pp. 2399-2409.e1. doi: 10.1053/j.gastro.2010.02.014.

Choy, M. C., Visvanathan, K. and De Cruz, P. (2017) 'An overview of the innate and adaptive immune system in inflammatory bowel disease', *Inflammatory Bowel Diseases*, 23(1), pp. 2–13. doi: 10.1097/MIB.0000000000000955.

Clevers, H. (2013) 'XThe intestinal crypt, a prototype stem cell compartment', *Cell*, 154(2), p. 274. doi: 10.1016/j.cell.2013.07.004.Clevers, H., Loh, K. M. and Nusse, R. (2014) 'An integral program for tissue renewal and regeneration: Wnt signaling and stem cell control', *Science*, 346(6205). doi: 10.1126/science.1248012.Coant, N. *et al.* (2010) 'NADPH Oxidase 1

Modulates WNT and NOTCH1 Signaling To Control the Fate of Proliferative Progenitor Cells in the Colon', *Molecular and Cellular Biology*, 30(11), pp. 2636–2650. doi: 10.1128/mcb.01194-09.

Collier, J. R., Monk, N. A. M., Maini, P. K. and Lewis, J. H. (1996) 'Pattern formation by lateral inhibition with feedback: A mathematical model of delta-notch intercellular signalling', *Journal of Theoretical Biology*, 183(4), pp. 429–446. doi: 10.1006/jtbi.1996.0233.

Collins, D. J., Neild, A., deMello, A., Liu, A. Q. and Ai, Y. (2015) 'The Poisson distribution and beyond: Methods for microfluidic droplet production and single cell encapsulation', *Lab on a Chip*, 15(17), pp. 3439–3459. doi: 10.1039/c5lc00614g.

Collu, G. M., Hidalgo-Sastre, A. and Brennan, K. (2014) 'Wnt-Notch signalling crosstalk in development and disease', *Cellular and Molecular Life Sciences*, 71(18), pp. 3553–3567. doi: 10.1007/s00018-014-1644-x.

Cong, F., Schweizer, L. and Varmus, H. (2004) 'Wnt signals across the plasma membrane to activate the β-catenin pathway by forming oligomers containing its receptors, Frizzled and LRP', *Development*, 131(20), pp. 5103–5115. doi: 10.1242/dev.01318.

Cosín-Roger, J., Ortiz-Masiá, D., Calatayud, S., Hernández, C., Esplugues, J. V. and Barrachina, M. D. (2016) 'The activation of Wnt signaling by a STAT6-dependent macrophage phenotype promotes mucosal repair in murine IBD', *Mucosal Immunology*, 9(4), pp. 986–998. doi: 10.1038/mi.2015.123.

Cosovanu, C. and Neumann, C. (2020) 'The Many Functions of Foxp3+ Regulatory T Cells in the Intestine', *Frontiers in Immunology*, 11(October), pp. 1–9. doi: 10.3389/fimmu.2020.600973.

Cristina, M. L., Lehy, T., Zeitoun, P. and Dufougeray, F. (1978) 'Fine Structural Classification and Comparative Distribution of Endocrine Cells in Normal Human Large Intestine', *Gastroenterology*, 75(1), pp. 20–28. doi: 10.1016/0016-5085(78)93758-7.

Dagenais, M., Douglas, T. and Saleh, M. (2014) 'Role of programmed necrosis and cell death in intestinal inflammation', *Current Opinion in Gastroenterology*, 30(6), pp. 568–575. doi: 10.1097/MOG.0000000000000117.

Dai, X. M., Ryan, G. R., Hapel, A. J., Dominguez, M. G., Russell, R. G., Kapp, S., Sylvestre, V. and Stanley, E. R. (2002) 'Targeted disruption of the mouse colony-stimulating factor 1 receptor gene results in osteopetrosis, mononuclear phagocyte deficiency, increased primitive progenitor cell frequencies, and reproductive defects', *Blood*, 99(1), pp. 111–120. doi: 10.1182/blood.V99.1.111.

Dai, X. M., Zong, X. H., Sylvestre, V. and Stanley, E. R. (2004) 'Incomplete restoration of colony-stimulating factor 1 (CSF-1) function in CSF-1-deficient Csf1op/Csf1op mice by transgenic expression of cell surface CSF-1', *Blood*, 103(3), pp. 1114–1123. doi: 10.1182/blood-2003-08-2739.

Daley, J. M., Brancato, S. K., Thomay, A. A., Reichner, J. S. and Albina, J. E. (2010) 'The phenotype of murine wound macrophages', *Journal of Leukocyte Biology*, 87(1), pp. 59–67. doi: 10.1189/jlb.0409236.

Damiano, S., Morano, A., Ucci, V., Accetta, R., Mondola, P., Paternò, R., Avvedimento, V. E. and Santillo, M. (2015) 'Dual oxidase 2 generated reactive oxygen species selectively mediate the induction of mucins by epidermal growth factor in enterocytes', *International Journal of Biochemistry and Cell Biology*, 60, pp. 889–893. doi: 10.1016/j.biocel.2014.12.014.

Darwich, A. S., Aslam, U., Ashcroft, D. M. and Rostami-Hodjegan, A. (2014) 'Meta-analysis of the turnover of intestinal epithelia in preclinical animal species and humans', *Drug Metabolism and Disposition*, 42(12), pp. 2016–2022. doi: 10.1124/dmd.114.058404.

de Lau, W., Peng, W. C., Gros, P. and Clevers, H. (2014) 'The R-spondin/Lgr5/Rnf43 module: Regulator of Wnt signal strength', *Genes and Development*, 28(4), pp. 305–316. doi: 10.1101/gad.235473.113.

De Schepper, S. *et al.* (2018) 'Self-Maintaining Gut Macrophages Are Essential for Intestinal Homeostasis', *Cell*, 175(2), pp. 400-415.e13. doi: 10.1016/j.cell.2018.07.048.Delgado, M. E., Grabinger, T. and Brunner, T. (2016) 'Cell death at the intestinal epithelial front line', *FEBS Journal*, pp. 2701–2719. doi: 10.1111/febs.13575.

Demitrack, E. S. and Samuelson, L. C. (2016) 'Notch regulation of gastrointestinal stem cells', *Journal of Physiology*, 594(17), pp. 4791–4803. doi: 10.1113/JP271667.

Denning, T. L., Norris, B. A., Medina-Contreras, O., Manicassamy, S., Geem, D., Madan, R., Karp, C. L. and Pulendran, B. (2011) 'Functional Specializations of Intestinal Dendritic Cell and Macrophage Subsets That Control Th17 and Regulatory T Cell Responses Are Dependent on the T Cell/APC Ratio, Source of Mouse Strain, and Regional Localization', *The Journal of Immunology*, 187(2), pp. 733–747. doi: 10.4049/jimmunol.1002701.

Denning, T. L., Wang, Y. C., Patel, S. R., Williams, I. R. and Pulendran, B. (2007) 'Lamina propria macrophages and dendritic cells differentially induce regulatory and interleukin 17-producing T cell responses', *Nature Immunology*, 8(10), pp. 1086–1094. doi: 10.1038/ni1511.

Doyle, C. M., Vine, E. E., Bertram, K. M., Baharlou, H., Rhodes, J. W., Dervish, S., Gosselink, M. P., Di Re, A., Collins, G. P., Reza, F., Toh, J. W. T., Pathma-Nathan, N., Ahlenstiel, G., Ctercteko, G., Cunningham, A. L., Harman, A. N. and Byrne, S. N. (2021) 'Optimal Isolation Protocols for Examining and Interrogating Mononuclear Phagocytes From Human Intestinal Tissue', *Frontiers in Immunology, 12*(9), pp. 1–14. doi: 10.3389/fimmu.2021.727952.

Desalegn, G. and Pabst, O. (2019) 'Inflammation triggers immediate rather than progressive changes in monocyte differentiation in the small intestine', *Nature Communications*, 10(1), pp. 1–14. doi: 10.1038/s41467-019-11148-2.

Dicarlo, M., Teti, G., Verna, G., Liso, M., Cavalcanti, E., Sila, A., Raveenthiraraj, S., Mastronardi, M., Santino, A., Serino, G., Lippolis, A., Sobolewski, A., Falconi, M. and Chieppa, M. (2019) 'Quercetin exposure suppresses the inflammatory pathway in intestinal organoids from winnie mice', *International Journal of Molecular Sciences*, 20(22), pp. 1–15. doi: 10.3390/ijms20225771.

Dunay, I. R., DaMatta, R. A., Fux, B., Presti, R., Greco, S., Colonna, M. and Sibley, L. D. (2008) 'Gr1+ Inflammatory Monocytes Are Required for Mucosal Resistance to the Pathogen Toxoplasma gondii', *Immunity*, 29(2), pp. 306–317. doi: 10.1016/j.immuni.2008.05.019.

Duque, G. A. and Descoteaux, A. (2014) 'Macrophage cytokines: Involvement in immunity and infectious diseases', *Frontiers in Immunology*, 5(OCT), pp. 1–12. doi: 10.3389/fimmu.2014.00491.Duque, G. A. and Descoteaux, A. (2014) 'Macrophage cytokines: Involvement in immunity and infectious diseases', *Frontiers in Immunology*, 5(OCT), pp. 1–12. doi: 10.3389/fimmu.2014.00491.

Dura, B., Servo, M. M., Barry, R. M., Ploeghf, H. L., Dougand, S. K. and Voldman, J. (2016) 'Longitudinal multiparameter assay of lymphocyte interactions from onset by microfluidic cell pairing and culture', *Proceedings of the National Academy of Sciences of the United States of America*, 113(26), pp. E3599–E3608. doi: 10.1073/pnas.1515364113.

Egberts, H. J., Koninkx, J. F., van Dijk, J. E. and Mouwen, J. M. (1984) 'Biological and pathobiological aspects of the glycocalyx of the small intestinal epithelium. A review.', *The Veterinary quarterly*, 6(4), pp. 186–199. doi: 10.1080/01652176.1984.9693936.

Egerod, K. L., Engelstoft, M. S., Grunddal, K. V., Nøhr, M. K., Secher, A., Sakata, I., Pedersen, J., Windeløv, J. A., Füchtbauer, E. M., Olsen, Jørgen, Sundler, F., Christensen, J. P., Wierup, N., Olsen, Jesper V., Holst, J. J., Zigman, J. M., Poulsen, S. S. and Schwartz, T. W. (2012) 'A major lineage of enteroendocrine cells coexpress CCK, secretin, GIP, GLP-1, PYY, and neurotensin but not somatostatin', *Endocrinology*, 153(12), pp. 5782–5795. doi: 10.1210/en.2012-1595.

Eom, D. S. (2020) 'Airinemes: Thin cellular protrusions mediate long-distance signalling guided by macrophages', *Open Biology*. doi: 10.1098/rsob.200039.

Fair, K. L., Colquhoun, J. and Hannan, N. R. F. (2018) 'Intestinal organoids for modelling intestinal development and disease', *Philosophical Transactions of the Royal Society B: Biological Sciences*, 373(1750). doi: 10.1098/rstb.2017.0217.

Farin, H. F., Jordens, I., Mosa, M. H., Basak, O., Korving, J., Tauriello, D. V. F., De Punder, K., Angers, S., Peters, P. J., Maurice, M. M. and Clevers, H. (2016) 'Visualization of a short-range Wnt gradient in the intestinal stem-cell niche', *Nature*, 530(7590), pp. 340–343. doi: 10.1038/nature16937.

Fevr, T., Robine, S., Louvard, D. and Huelsken, J. (2007) 'Wnt/β-Catenin Is Essential for Intestinal Homeostasis and Maintenance of Intestinal Stem Cells', *Molecular and Cellular Biology*, 27(21), pp. 7551–7559. doi: 10.1128/mcb.01034-07.

Finkelman, F. D., Shea-Donohue, T., Morris, S. C., Gildea, L., Strait, R., Madden, K. B., Schopf, L. and Urban, J. F. (2004) 'Interleukin-4- and interleukin-13-mediated host protection against

intestinal nematode parasites', *Immunological Reviews*, 201(1), pp. 139–155. doi: 10.1111/j.0105-2896.2004.00192.x.

Flanagan, D. J., Austin, C. R., Vincan, E. and Phesse, T. J. (2018) 'Wnt signalling in gastrointestinal epithelial stem cells', *Genes*, 9(4). doi: 10.3390/genes9040178.Fouquet, S., Lugo-Martínez, V. H., Faussat, A. M., Renaud, F., Cardot, P., Chambaz, J., Pinçon-Raymond, M. and Thenet, S. (2004) 'Early loss of E-cadherin from cell-cell contacts is involved in the onset of anoikis in enterocytes', *Journal of Biological Chemistry*, 279(41), pp. 43061–43069. doi: 10.1074/jbc.M405095200.

Fre, S., Huyghe, M., Mourikis, P., Robine, S., Louvard, D. and Artavanis-Tsakonas, S. (2005) 'Notch signals control the fate of immature progenitor cells in the intestine', *Nature*, 435(7044), pp. 964–968. doi: 10.1038/nature03589.

Geissmann, F., Jung, S. and Littman, D. R. (2003) 'Blood monocytes consist of two principal subsets with distinct migratory properties', *Immunity*, 19(1), pp. 71–82. doi: 10.1016/S1074-7613(03)00174-2.

Gerbe, F., Brulin, B., Makrini, L., Legraverend, C. and Jay, P. (2009) 'DCAMKL-1 Expression Identifies Tuft Cells Rather Than Stem Cells in the Adult Mouse Intestinal Epithelium', *Gastroenterology*, 137(6), pp. 2179–2180. doi: 10.1053/j.gastro.2009.06.072.

Gerbe, F., Legraverend, C. and Jay, P. (2012) 'The intestinal epithelium tuft cells: Specification and function', *Cellular and Molecular Life Sciences*, 69(17), pp. 2907–2917. doi: 10.1007/s00018-012-0984-7.

Gerbe, F., Van Es, J. H., Makrini, L., Brulin, B., Mellitzer, G., Robine, S., Romagnolo, B., Shroyer, N. F., Bourgaux, J. F., Pignodel, C., Clevers, H. and Jay, P. (2011) 'Distinct ATOH1 and Neurog3 requirements define tuft cells as a new secretory cell type in the intestinal epithelium', *Journal of Cell Biology*, 192(5), pp. 767–780. doi: 10.1083/jcb.201010127.

Gersemann, M., Becker, S., Kübler, I., Koslowski, M., Wang, G., Herrlinger, K. R., Griger, J., Fritz, P., Fellermann, K., Schwab, M., Wehkamp, J. and Stange, E. F. (2009) 'Differences in goblet cell differentiation between Crohn's disease and ulcerative colitis', *Differentiation*, 77(1), pp. 84–94. doi: 10.1016/j.diff.2008.09.008.

Ghahremani Piraghaj, M., Soudi, S., Ghanbarian, H., Bolandi, Z., Namaki, S. and Hashemi, S. M. (2018) 'Effect of efferocytosis of apoptotic mesenchymal stem cells (MSCs) on C57BL/6 peritoneal macrophages function', *Life Sciences*, 212, pp. 203–212. doi: 10.1016/j.lfs.2018.09.052.

Ghorbaninejad, M., Heydari, R., Mohammadi, P., Shahrokh, S., Haghazali, M., Khanabadi, B. and Meyfour, A. (2019) 'Contribution of NOTCH signaling pathway along with TNF-α in the intestinal inflammation of ulcerative colitis', *Gastroenterology and Hepatology from Bed to Bench*, 12, pp. S80–S86. doi: 10.22037/ghfbb.v12i0.1821.

Ginhoux, F. and Jung, S. (2014) 'Monocytes and macrophages: Developmental pathways and tissue homeostasis', *Nature Reviews Immunology*, 14(6), pp. 392–404. doi: 10.1038/nri3671.

Girard-Madoux, M. J. H., Ober-Blöbaum, J. L., Costes, L. M. M., Kel, J. M., Lindenbergh-Kortleve, D. J., Brouwers-Haspels, I., Heikema, A. P., Samsom, J. N. and Clausen, B. E. (2016) 'IL-10 control of CD11c+ myeloid cells is essential to maintain immune homeostasis in the small and large intestine', *Oncotarget*, 7(22), pp. 32015–32030. doi: 10.18632/oncotarget.8337.

Goggins, B. J., Minahan, K., Sherwin, S., Soh, W. S., Pryor, J., Bruce, J., Liu, G., Mathe, A., Knight, D. A., Horvat, J. C., Walker, M. and Keely, S. (2021) 'Pharmacological HIF-1 stabilization promotes intestinal epithelial healing through regulation of α-integrin expression and function', *American Journal of Physiology-Gastrointestinal and Liver Physiology*, (December 2020). doi: 10.1152/ajpgi.00192.2020.

Goodman, S., Naphade, S., Khan, M., Sharma, J. and Cherqui, S. (2019) 'Macrophage polarization impacts tunneling nanotube formation and intercellular organelle trafficking', *Scientific Reports*, 9(1), pp. 1–15. doi: 10.1038/s41598-019-50971-x.

Gosse, S. G., Bourgin, C., Liu, W. Q., Garbay, C. and Mouchiroud, G. (2005) 'M-CSF stimulated differentiation requires persistent MEK activity and MAPK phosphorylation independent of Grb2-Sos association and phosphatidylinositol 3-kinase activity', *Cellular Signalling*, 17(11), pp. 1352–1362. doi: 10.1016/j.cellsig.2005.02.002.

Gracz, A. D., Samsa, L. A., Fordham, M. J., Trotier, D. C., Zwarycz, B., Lo, Y. H., Bao, K., Starmer, J., Raab, J. R., Shroyer, N. F., Reinhardt, R. L. and Magness, S. T. (2018) 'Sox4 Promotes Atoh1-Independent Intestinal Secretory Differentiation Toward Tuft and

Enteroendocrine Fates', *Gastroenterology*, 155(5), pp. 1508-1523.e10. doi: 10.1053/j.gastro.2018.07.023.

Gregorieff, A. and Clevers, H. (2005) 'Wnt signaling in the intestinal epithelium: From endoderm to cancer', *Genes and Development*, 19(8), pp. 877–890. doi: 10.1101/gad.1295405.

Gregorieff, A., Liu, Y., Inanlou, M. R., Khomchuk, Y. and Wrana, J. L. (2015) 'Yap-dependent reprogramming of Lgr5+ stem cells drives intestinal regeneration and cancer', *Nature*, 526(7575), pp. 715–718. doi: 10.1038/nature15382.

Greuter, T., Vavricka, S., König, A. O., Beaugerie, L. and Scharl, M. (2020) 'Malignancies in Inflammatory Bowel Disease', *Digestion*, 101(Suppl1), pp. 136–145. doi: 10.1159/000509544.

Gribble, F. M. and Reimann, F. (2016) 'Enteroendocrine Cells: Chemosensors in the Intestinal Epithelium', *Annual Review of Physiology*, 78, pp. 277–299. doi: 10.1146/annurev-physiol-021115-105439.

Grimm, M., Pullmann, W., Bennet, G., Sullivan, P., Pavli, P. and Doe, W. (1995) 'Direct evidence of monocyte recruitment to inflammatory bowel disease mucosa', *Journal of Gastroenterology and Hepatology*, 10(4), pp. 387–395. doi: 10.1111/j.1440-1746.1995.tb01589.x.

Groschwitz, K. R. and Hogan, S. P. (2009) 'Intestinal barrier function: Molecular regulation and disease pathogenesis', *Journal of Allergy and Clinical Immunology*, 124(1), pp. 3–20. doi: 10.1016/j.jaci.2009.05.038.

Groulx, J. F., Gagné, D., Benoit, Y. D., Martel, D., Basora, N. and Beaulieu, J. F. (2011) 'Collagen VI is a basement membrane component that regulates epithelial cell-fibronectin interactions', *Matrix Biology*, 30(3), pp. 195–206. doi: 10.1016/j.matbio.2011.03.002.

Guarner, F. and Malagelada, J.-R. (2003) 'Gut flora in health and disease', *The Lancet*, 361(9356), pp. 512–519. doi: 10.1016/S0140-6736(03)12489-0.

Grubišić, V., McClain, J. L., Fried, D. E., Grants, I., Rajasekhar, P., Csizmadia, E., Ajijola, O. A., Watson, R. E., Poole, D. P., Robson, S. C., Christofi, F. L. and Gulbransen, B. D. (2020) 'Enteric

Glia Modulate Macrophage Phenotype and Visceral Sensitivity following Inflammation', *Cell Reports,* 32(10). doi: 10.1016/j.celrep.2020.108100.

Guilbert, L. J. and Stanley, E. R. (1980) 'Specific interaction of murine colony-stimulating factor with mononuclear phagocytic cells', *Journal of Cell Biology*, 85(1), pp. 153–159. doi: 10.1083/jcb.85.1.153.

Gutzeit, C., Magri, G. and Cerutti, A. (2014) 'Intestinal IgA production and its role in host-microbe interaction', *Immunological Reviews*, 260(1), pp. 76–85. doi: 10.1111/imr.12189.

Hadis, U., Wahl, B., Schulz, O., Hardtke-Wolenski, M., Schippers, A., Wagner, N., Müller, W., Sparwasser, T., Förster, R. and Pabst, O. (2011) 'Intestinal Tolerance Requires Gut Homing and Expansion of FoxP3+ Regulatory T Cells in the Lamina Propria', *Immunity*, 34(2), pp. 237–246. doi: 10.1016/j.immuni.2011.01.016.

Hagbom, M., Istrate, C., Engblom, D., Karlsson, T., Rodriguez-Diaz, J., Buesa, J., Taylor, J. A., Loitto, V. M., Magnusson, K. E., Ahlman, H., Lundgren, O. and Svensson, L. (2011) 'Rotavirus stimulates release of serotonin (5-HT) from human enterochromaffin cells and activates brain structures involved in nausea and vomiting', *PLoS Pathogens*, 7(7), pp. 1–10. doi: 10.1371/journal.ppat.1002115.

Hanania, R., Sun, H. S., Xu, K., Pustylnik, S., Jeganathan, S. and Harrison, R. E. (2012) 'Classically activated macrophages use stable microtubules for matrix metalloproteinase-9 (MMP-9) secretion', *Journal of Biological Chemistry*, 287(11), pp. 8468–8483. doi: 10.1074/jbc.M111.290676.

Hansson, G. C. and Johansson, M. E. V. (2010) 'The inner of the two Muc2 mucin-dependent mucus layers in colon is devoid of bacteria', *Gut Microbes*, 1(1), pp. 51–54. doi: 10.4161/gmic.1.1.10470.

He, S., Lei, P., Kang, W., Cheung, P., Xu, T., Mana, M. and Park, C. Y. (2021) 'Stiffness Regulates Intestinal Stem Cell Fate Does fibrotic gut stiffening caused by inflammatory bowel diseases (IBD) direct the fate of intestinal', *BioRxiv* pp. 1–56. Doi:https: 10.1101/2021.03.15.435410.

Heallen, T., Zhang, M., Wang, J., Bonilla-Claudio, M., Klysik, E., Johnson, R. L. and Martin, J. F. (2011) 'Hippo pathway inhibits wnt signaling to restrain cardiomyocyte proliferation and heart size', *Science*, 332(6028), pp. 458–461. doi: 10.1126/science.1199010.

Henson, P. M. and Hume, D. A. (2006) 'Apoptotic cell removal in development and tissue homeostasis', *Trends in Immunology*, 27(5), pp. 244–250. doi: 10.1016/j.it.2006.03.005.

Hesketh, M., Sahin, K. B., West, Z. E. and Murray, R. Z. (2017) 'Macrophage phenotypes regulate scar formation and chronic wound healing', *International Journal of Molecular Sciences*, 18(7), pp. 1–10. doi: 10.3390/ijms18071545.

Hine, A. M. and Loke, P. (2019) 'Intestinal Macrophages in Resolving Inflammation', *The Journal of Immunology*, 203(3), pp. 593–599. doi: 10.4049/jimmunol.1900345.

Hirsch, S., Austyn, J. M. and Gordon, S. (1981) 'Expression of the macrophage-specific antigen F4/80 during differentiation of mouse bone marrow cells in culture.', *Journal of Experimental Medicine*, 154(3), pp. 713–725. doi: 10.1084/jem.154.3.713.

Hooper, L. V. (2015) *Epithelial Cell Contributions to Intestinal Immunity*. 1st edn, *Advances in Immunology*. 1st edn. Elsevier Inc. doi: 10.1016/bs.ai.2014.11.003.

Horsthemke, M., Wilden, J., Bachg, A. C. and Hanley, P. J. (2018) 'Time-lapse 3D imaging of phagocytosis by mouse macrophages', *Journal of Visualized Experiments*, 2018(140), pp. 1–9. doi: 10.3791/57566.

Howitt, M. R., Lavoie, S., Michaud, M., Blum, A. M., Tran, S. V, Weinstock, J. V., Gallini, C. A., Redding, K., Margolskee, R. F., Osborne, L. C., Artis, D. and Garrett, W. S. (2016) 'Tuft cells, taste-chemosensory cells, orchestrate parasite type 2 immunity in the gut', *Science*, 351(6279), pp. 1329–1333. doi: 10.1126/science.aaf1648.

Hsu, D., Fukata, M., Hernandez, Y. G., Sotolongo, J. P., Goo, T., Maki, J., Hayes, L. A., Ungaro, R. C., Chen, A., Breglio, K. J., Xu, R. and Abreu, M. T. (2010) 'Toll-like receptor 4 differentially regulates epidermal growth factor-related growth factors in response to intestinal mucosal injury', *Laboratory Investigation*, 90(9), pp. 1295–1305. doi: 10.1038/labinvest.2010.100.

Hsu, K. W., Hsieh, R. H., Huang, K. H., Li, A. F. Y., Chi, C. W., Wang, T. Y., Tseng, M. J., Wu, K. J. and Yeh, T. S. (2012) 'Activation of the Notch1/STAT3/Twist signaling axis promotes gastric cancer progression', *Carcinogenesis*, 33(8), pp. 1459–1467. doi: 10.1093/carcin/bgs165.

Hughes, C. S., Postovit, L. M. and Lajoie, G. A. (2010) 'Matrigel: a complex protein mixture required for optimal growth of cell culture.', *Proteomics*, 10(9), pp. 1886–1890. doi: 10.1002/pmic.200900758.

Ivanov, I. I., Frutos, R. de L., Manel, N., Yoshinaga, K., Rifkin, D. B., Sartor, R. B., Finlay, B. B. and Littman, D. R. (2008) 'Specific Microbiota Direct the Differentiation of IL-17-Producing T-Helper Cells in the Mucosa of the Small Intestine', *Cell Host & Microbe*, 4(4), pp. 337–349. doi: 10.1016/j.chom.2008.09.009.

Ihara, S., Hirata, Y., Hikiba, Y., Yamashita, A., Tsuboi, M., Hata, M., Konishi, M., Suzuki, N., Sakitani, K., Kinoshita, H., Hayakawa, Y., Nakagawa, H., Ijichi, H., Tateishi, K. and Koike, K. (2018) 'Adhesive Interactions between Mononuclear Phagocytes and Intestinal Epithelium Perturb Normal Epithelial Differentiation and Serve as a Therapeutic Target in Inflammatory Bowel Disease', *Journal of Crohn's & colitis*, 12(10), pp. 1219–1231. doi: 10.1093/ecco-jcc/jjy088.

Ihara, S., Hirata, Y. and Koike, K. (2017) 'TGF-β in inflammatory bowel disease: a key regulator of immune cells, epithelium, and the intestinal microbiota', *Journal of Gastroenterology*, 52(7), pp. 777–787. doi: 10.1007/s00535-017-1350-1.

Ihara, S., Hirata, Y., Serizawa, T., Suzuki, N., Sakitani, K., Kinoshita, H., Hayakawa, Y., Nakagawa, H., Ijichi, H., Tateishi, K. and Koike, K. (2016) 'TGF-β Signaling in Dendritic Cells Governs Colonic Homeostasis by Controlling Epithelial Differentiation and the Luminal Microbiota', *The Journal of Immunology*, 196(11), pp. 4603–4613. doi: 10.4049/jimmunol.1502548.

Ip, W. K. E., Hoshi, N., Shouval, D. S., Snapper, S. and Medzhitov, R. (2017) 'Anti-inflammatory effect of IL-10 mediated by metabolic reprogramming of macrophages', *Science*, 356(6337), pp. 513–519. doi: 10.1126/science.aal3535.

Ishibashi, F., Shimizu, H., Nakata, T., Fujii, S., Suzuki, K., Kawamoto, A., Anzai, S., Kuno, R., Nagata, S., Ito, G., Murano, T., Mizutani, T., Oshima, S., Tsuchiya, K., Nakamura, T., Watanabe, M. and Okamoto, R. (2018) 'Contribution of ATOH1+ Cells to the Homeostasis, Repair, and Tumorigenesis of the Colonic Epithelium', *Stem Cell Reports*, 10(1), pp. 27–42. doi: 10.1016/j.stemcr.2017.11.006.

Ishida, Y., Gao, J.-L. and Murphy, P. M. (2008) 'Chemokine Receptor CX3CR1 Mediates Skin Wound Healing by Promoting Macrophage and Fibroblast Accumulation and Function', *The Journal of Immunology*, 180(1), pp. 569–579. doi: 10.4049/jimmunol.180.1.569.

Israeli, E. and Ilan, Y. (2010) 'Oral administration of Alequel, a mixture of autologous colon-extracted proteins for the treatment of Crohn's disease', *Therapeutic Advances in Gastroenterology*, 3(1), pp. 23–30. doi: 10.1177/1756283X09351733.

Ito, T., Allen, R. M., Carson IV, W. F., Schaller, M., Cavassani, K. A., Hogaboam, C. M., Lukacs, N. W., Matsukawa, A. and Kunkel, S. L. (2011) 'The critical role of Notch ligand delta-like 1 in the pathogenesis of influenza a virus (H1N1) infection', *PLoS Pathogens*, 7(11). doi: 10.1371/journal.ppat.1002341.

Jablonski, K. A., Amici, S. A., Webb, L. M., Ruiz-Rosado, J. D. D., Popovich, P. G., Partida-Sanchez, S. and Guerau-De-arellano, M. (2015) 'Novel markers to delineate murine M1 and M2 macrophages', *PLoS ONE*, 10(12), pp. 5–11. doi: 10.1371/journal.pone.0145342.

Jaensson, E., Uronen-Hansson, H., Pabst, O., Eksteen, B., Tian, J., Coombes, J. L., Berg, P. L., Davidsson, T., Powrie, F., Johansson-Lindbom, B. and Agace, W. W. (2008) 'Small intestinal CD103+ dendritic cells display unique functional properties that are conserved between mice and humans', *Journal of Experimental Medicine*, 205(9), pp. 2139–2149. doi: 10.1084/jem.20080414.

Jan, R. and Chaudhry, G.-S. (2019) 'Understanding Apoptosis and Apoptotic Pathways Targeted Cancer Therapeutics', *Advanced Pharmaceutical Bulletin*, 9(2), pp. 205–218. doi: 10.15171/apb.2019.024.Janeway, C. A. (2001) 'How the immune system protects the host from infection', *Microbes and Infection*, 3(13), pp. 1167–1171. doi: 10.1016/S1286-4579(01)01477-0.

Jeffery, V., Goldson, A. J., Dainty, J. R., Chieppa, M. and Sobolewski, A. (2017) 'IL-6 Signaling Regulates Small Intestinal Crypt Homeostasis', *The Journal of Immunology*, 199(1), pp. 304–311. doi: 10.4049/jimmunol.1600960.

Jenny, M., Uhl, C., Roche, C., Duluc, I., Guillermin, V., Guillemot, F., Jensen, J., Kedinger, M. and Gradwohl, G. (2002) 'Neurogenin3 is differentially required for endocrine cell fate specification in the intestinal and gastric epithelium', *EMBO Journal*, 21(23), pp. 6338–6347. doi: 10.1093/emboj/cdf649.

Jensen, J., Pedersen, E. E., Galante, P., Hald, J., Heller, R. S., Ishibashi, M., Kageyama, R., Guillemot, F., Serup, P. and Madsen, O. D. (2000) 'Control of endodermal endocrine development by Hes-1', *Nature Genetics*, 24(1), pp. 36–44. doi: 10.1038/71657.

Do, J., Kim, S., Keslar, K., Jang, E., Huang, E., Fairchild, R. L., Pizarro, T. T. and Min, B. (2017) 'γδ T Cells Coexpressing Gut Homing α4β7 and αE Integrins Define a Novel Subset Promoting Intestinal Inflammation', *The Journal of Immunology,* 198(2), pp. 908–915. doi: 10.4049/jimmunol.1601060.

Jiang, L., Shen, Y., Guo, D., Yang, D., Liu, J., Fei, X., Yang, Y., Zhang, B., Lin, Z., Yang, F., Wang, X., Wang, K., Wang, J. and Cai, Z. (2016) 'EpCAM-dependent extracellular vesicles from intestinal epithelial cells maintain intestinal tract immune balance', *Nature Communications*, 7, pp. 1–15. doi: 10.1038/ncomms13045.

Jin, Y. H., Kim, H., Ki, H., Yang, I., Yang, N., Lee, K. Y., Kim, N., Park, H.-S. and Kim, K. (2009) 'B-catenin modulates the level and transcriptional activity of Notch1/NICD through its direct interaction', *Biochimica et Biophysica Acta (BBA) - Molecular Cell Research*, 1793(2), pp. 290–299. doi: 10.1016/j.bbamcr.2008.10.002.

Johansson, M. E. V., Gustafsson, J. K., Holmen-Larsson, J., Jabbar, K. S., Xia, L., Xu, H., Ghishan, F. K., Carvalho, F. A., Gewirtz, A. T., Sjovall, H. and Hansson, G. C. (2014) 'Bacteria penetrate the normally impenetrable inner colon mucus layer in both murine colitis models and patients with ulcerative colitis', *Gut*, 63(2), pp. 281–291. doi: 10.1136/gutjnl-2012-303207.

Jones, G. R., Bain, C. C., Fenton, T. M., Kelly, A., Brown, S. L., Ivens, A. C., Travis, M. A., Cook, P. C. and MacDonald, A. S. (2018) 'Dynamics of colon monocyte and macrophage activation during colitis', *Frontiers in Immunology*, 9(NOV). doi: 10.3389/fimmu.2018.02764.

Josefowicz, S. Z., Lu, L. F. and Rudensky, A. Y. (2012) 'Regulatory T cells: Mechanisms of differentiation and function', *Annual Review of Immunology*, 30, pp. 531–564. doi: 10.1146/annurev.immunol.25.022106.141623.

Kämpfer, A. A. M., Urbán, P., Gioria, S., Kanase, N., Stone, V. and Kinsner-Ovaskainen, A. (2017) 'Development of an in vitro co-culture model to mimic the human intestine in healthy and diseased state', *Toxicology in Vitro*, 45(August), pp. 31–43. doi: 10.1016/j.tiv.2017.08.011.

Karam, S. M. (1999) 'Lineage commitment and maturation of epithelial cells in the gut.', *Frontiers in bioscience : a journal and virtual library*, 4(1), pp. 286–298. doi: 10.2741/a426.

Karpus, O. N., Westendorp, B. F., Vermeulen, J. L. M., Meisner, S., Koster, J., Muncan, V., Wildenberg, M. E. and van den Brink, G. R. (2019) 'Colonic CD90+ Crypt Fibroblasts Secrete Semaphorins to Support Epithelial Growth', *Cell Reports*, 26(13), pp. 3698-3708.e5. doi: 10.1016/j.celrep.2019.02.101.

Karsdal, M. A., Bay-Jensen, A. C., Leeming, D. J., Henriksen, K. and Christiansen, C. (2013) 'Quantification of "end products" of tissue destruction in inflammation may reflect convergence of cytokine and signaling pathways-implications for modern clinical chemistry', *Biomarkers*, 18(5), pp. 375–378. doi: 10.3109/1354750X.2013.789084.

Karsdal, M. A., Nielsen, M. J., Sand, J. M., Henriksen, K., Genovese, F., Bay-Jensen, A. C., Smith, V., Adamkewicz, J. I., Christiansen, C. and Leeming, D. J. (2013) 'Extracellular matrix remodeling: The common denominator in connective tissue diseases possibilities for evaluation and current understanding of the matrix as more than a passive architecture, but a key player in tissue failure', *Assay and Drug Development Technologies*, 11(2), pp. 70–92. doi: 10.1089/adt.2012.474.

Kato, M., Marumo, M., Nakayama, J., Matsumoto, M., Yabe-Nishimura, C. and Kamata, T. (2016) 'The ROS-generating oxidase Nox1 is required for epithelial restitution following colitis', *Experimental Animals*, 65(3), pp. 197–205. doi: 10.1538/expanim.15-0127.

Kaunitz, J. D. and Akiba, Y. (2019) 'Control of Intestinal Epithelial Proliferation and Differentiation: The Microbiome, Enteroendocrine L Cells, Telocytes, Enteric Nerves, and GLP, Too', *Digestive Diseases and Sciences*, 64(10), pp. 2709–2716. doi: 10.1007/s10620-019-05778-1.

Kayama, H. and Takeda, K. (2012) 'Regulation of intestinal homeostasis by innate and adaptive immunity', *International Immunology*, 24(11), pp. 673–680. doi: 10.1093/intimm/dxs094.

Kelm, M. (1999) 'Nitric oxide metabolism and breakdown', *Biochimica et Biophysica Acta - Bioenergetics*, 1411(2–3), pp. 273–289. doi: 10.1016/S0005-2728(99)00020-1.Kiesslich, R., Duckworth, C. A., Moussata, D., Gloeckner, A., Lim, L. G., Goetz, M., Pritchard, D. M., Galle, P. R., Neurath, M. F. and Watson, A. J. M. (2012) 'Local barrier dysfunction identified by confocal laser endomicroscopy predicts relapse in inflammatory bowel disease', *Gut*, 61(8), pp. 1146–1153. doi: 10.1136/gutjnl-2011-300695.

Kiesslich, R., Duckworth, C. A., Moussata, D., Gloeckner, A., Lim, L. G., Goetz, M., Pritchard, D. M., Galle, P. R., Neurath, M. F. and Watson, A. J. M. (2012) 'Local barrier dysfunction identified by confocal laser endomicroscopy predicts relapse in inflammatory bowel disease', *Gut*, 61(8), pp. 1146–1153. doi: 10.1136/gutjnl-2011-300695.

Kiesslich, R., Goetz, M., Lammersdorf, K., Schneider, C., Burg, J., Stolte, M., Vieth, M., Nafe, B., Galle, P. R. and Neurath, M. F. (2007) 'Chromoscopy-Guided Endomicroscopy Increases the Diagnostic Yield of Intraepithelial Neoplasia in Ulcerative Colitis', pp. 874–882. doi: 10.1053/j.gastro.2007.01.048.

Kim, C. K., Yang, V. W. and Bialkowska, A. B. (2017) 'The Role of Intestinal Stem Cells in Epithelial Regeneration Following Radiation-Induced Gut Injury', *Current Stem Cell Reports*, 3(4), pp. 320–332. doi: 10.1007/s40778-017-0103-7.

Kim, K. A., Kakitani, M., Zhao, J., Oshima, T., Tang, T., Binnerts, M., Liu, Y., Boyle, B., Park, E., Emtage, P., Funk, W. D. and Tomizuka, K. (2005) 'Medicine: Mitogenic influence of human R-spondin1 on the intestinal epithelium', *Science*, 309(5738), pp. 1256–1259. doi: 10.1126/science.1112521.

Knoop, K. A., McDonald, K. G., McCrate, S., McDole, J. R. and Newberry, R. D. (2015) 'Microbial sensing by goblet cells controls immune surveillance of luminal antigens in the colo', *Mucosal Immunology*, 8(1), pp. 198–210. doi: 10.1038/mi.2014.58.

Koch, S. (2017) 'Extrinsic control of Wnt signaling in the intestine', *Differentiation*, 97(June), pp. 1–8. doi: 10.1016/j.diff.2017.08.003.

Koelink, P. J., Bloemendaal, F. M., Li, B., Westera, L., Vogels, E. W. M., Van Roest, M., Gloudemans, A. K., Van 'T Wout, A. B., Korf, H., Vermeire, S., Te Velde, A. A., Ponsioen, C. Y., D'Haens, G. R. A. M., Verbeek, J. S., Geiger, T. L., Wildenberg, M. E. and Van Den Brink, G. R. (2020) 'Anti-TNF therapy in IBD exerts its therapeutic effect through macrophage IL-10 signalling', *Gut*, 69(6), pp. 1053–1063. doi: 10.1136/gutjnl-2019-318264.

Komiya, Y. and Habas, R. (2008) 'Wnt Secretion and Extra-Cellular Regulators', 4(2), pp. 68–75. Available at: www.landesbioscience.com.Konsavage, W. M. and Yochum, G. S. (2012) 'Intersection of Hippo / YAP and Wnt / b-catenin signaling pathways Hippo / YAP Signaling Pathway', *Acta Biochimica et Biophysica Sinica Advance Access*, (September 2012), pp. 1–9. doi: 10.1093/abbs/gms084.Advance.

Korinek, V., Barker, N., Moerer, P., Van Donselaar, E., Huls, G., Peters, P. J. and Clevers, H. (1998) 'Depletion of epithelial stem-cell compartments in the small intestine of mice lacking Tcf-4', *Nature Genetics*, 19(4), pp. 379–383. doi: 10.1038/1270.

Kosinski, C., Li, V. S. W., Chan, A. S. Y., Zhang, J., Ho, C., Wai, Y. T., Tsun, L. C., Mifflin, R. C., Powell, D. W., Siu, T. Y., Suet, Y. L. and Chen, X. (2007) 'Gene expression patterns of human colon tops and basal crypts and BMP antagonists as intestinal stem cell niche factors', *Proceedings of the National Academy of Sciences of the United States of America*, 104(39), pp. 15418–15423. doi: 10.1073/pnas.0707210104.

Koslowski, M. J., Teltschik, Z., Beisner, J., Schaeffeler, E., Wang, G., Kübler, I., Gersemann, M., Cooney, R., Jewell, D., Reinisch, W., Vermeire, S., Rutgeerts, P., Schwab, M., Stange, E. F. and Wehkamp, J. (2012) 'Association of a functional variant in the wnt co-receptor LRP6

with early onset ileal Crohn's Disease', *PLoS Genetics*, 8(2). doi: 10.1371/journal.pgen.1002523.

Kress, H., Stelzer, E. H. K., Holzer, D., Buss, F., Griffiths, G. and Rohrbach, A. (2007) 'Filopodia act as phagocytic tentacles and pull with discrete steps and a load-dependent velocity', *Proceedings of the National Academy of Sciences of the United States of America*, 104(28), pp. 11633–11638. doi: 10.1073/pnas.0702449104.

Kriz, V. and Korinek, V. (2018) 'WNT, RSPO and hippo signalling in the intestine and intestinal stem cells', *Genes*, 9(1), pp. 1–18. doi: 10.3390/genes9010020.

Krzyszczyk, P., Schloss, R., Palmer, A. and Berthiaume, F. (2018) 'The role of macrophages in acute and chronic wound healing and interventions to promote pro-wound healing phenotypes', *Frontiers in Physiology*, 9(MAY), pp. 1–22. doi: 10.3389/fphys.2018.00419.

Kuhn, K. A., Manieri, N. A., Liu, T. C. and Stappenbeck, T. S. (2014) 'IL-6 stimulates intestinal epithelial proliferation and repair after injury', *PLoS ONE*, 9(12), pp. 1–18. doi: 10.1371/journal.pone.0114195.

Kuhnert, F., Davis, C. R., Wang, H. T., Chu, P., Lee, M., Yuan, J., Nusse, R. and Kuo, C. J. (2004) 'Essential requirement for Wnt signaling in proliferation of adult small intestine and colon revealed by adenoviral expression of Dickkopf-1', *Proceedings of the National Academy of Sciences of the United States of America*, 101(1), pp. 266–271. doi: 10.1073/pnas.2536800100.

Kulkarni, N., Pathak, M. and Lal, G. (2017) 'Role of chemokine receptors and intestinal epithelial cells in the mucosal inflammation and tolerance', *Journal of Leukocyte Biology*, 101(2), pp. 377–394. doi: 10.1189/jlb.1ru0716-327r.

Kuno, R., Ito, G., Kawamoto, A., Hiraguri, Y., Sugihara, H. Y., Takeoka, S., Nagata, S., Takahashi, J., Tsuchiya, M., Anzai, S., Mizutani, T., Shimizu, H., Yui, S., Oshima, S., Tsuchiya, K., Watanabe, M. and Okamoto, R. (2021) 'Notch and TNF-α signaling promote cytoplasmic accumulation of OLFM4 in intestinal epithelium cells and exhibit a cell protective role in the inflamed mucosa of IBD patients', *Biochemistry and Biophysics Reports*, 25(December 2020), p. 100906. doi: 10.1016/j.bbrep.2020.100906.

Lau, E., Marques, C., Pestana, D., Santoalha, M., Carvalho, D., Freitas, P. and Calhau, C. (2016) 'The role of I-FABP as a biomarker of intestinal barrier dysfunction driven by gut microbiota changes in obesity', *Nutrition and Metabolism*, 13(1), pp. 1–7. doi: 10.1186/s12986-016-0089-7.

Lecarpentier, Y., Schussler, O., Hébert, J. L. and Vallée, A. (2019) 'Multiple Targets of the Canonical WNT/β-Catenin Signaling in Cancers', *Frontiers in Oncology*, 9(November), pp. 1–17. doi: 10.3389/fonc.2019.01248.

Lee, B., Moon, K. M. and Kim, C. Y. (2018) 'Tight junction in the intestinal epithelium: Its association with diseases and regulation by phytochemicals', *Journal of Immunology Research*, 2018(Figure 2). doi: 10.1155/2018/2645465.

Lee, K. E. and Simon, M. C. (2015) 'SnapShot: Hypoxia-Inducible Factors', *Cell*, 163(5), pp. 1288.e1-1288.e1. doi: 10.1016/j.cell.2015.11.011.

Leggett, R., Thomas, P., Marín, M. J., Gavrilovic, J. and Russell, D. A. (2017) 'Imaging of compartmentalised intracellular nitric oxide, induced during bacterial phagocytosis, using a metalloprotein-gold nanoparticle conjugate', *Analyst*, 142(21), pp. 4099–4105. doi: 10.1039/c7an00898h.

Lentle, R. G. and Janssen, P. W. M. (2008) 'Physical characteristics of digesta and their influence on flow and mixing in the mammalian intestine: A review', *Journal of Comparative Physiology B: Biochemical, Systemic, and Environmental Physiology*, 178(6), pp. 673–690. doi: 10.1007/s00360-008-0264-x.

Leoni, G., Neumann, P. A., Sumagin, R., Denning, T. L. and Nusrat, A. (2015) 'Wound repair: Role of immune-epithelial interactions', *Mucosal Immunology*, 8(5), pp. 959–968. doi: 10.1038/mi.2015.63.Li, H., Fan, C., Feng, C., Wu, Y., Lu, H., He, P., Yang, X., Zhu, F., Qi, Q., Gao, Y., Zuo, J. and Tang, W. (2019) 'Inhibition of phosphodiesterase-4 attenuates murine ulcerative colitis through interference with mucosal immunity', *British Journal of Pharmacology*, 176(13), pp. 2209–2226. doi: 10.1111/bph.14667.

Li, N., Lu, N. and Xie, C. (2019) 'The Hippo and Wnt signalling pathways: crosstalk during neoplastic progression in gastrointestinal tissue', *FEBS Journal*, 286(19), pp. 3745–3756. doi: 10.1111/febs.15017.

Liao, D. H., Zhao, J. B. and Gregersen, H. (2009) 'Gastrointestinal tract modelling in health and disease', *World Journal of Gastroenterology*, 15(2), pp. 169–176. doi: 10.3748/wjg.15.169.

Lin, R., Piao, M. and Song, Y. (2019) 'Dietary Quercetin Increases Colonic Microbial Diversity and Attenuates Colitis Severity in Citrobacter rodentium-Infected Mice', *Frontiers in Microbiology*, 10(MAY), pp. 1–8. doi: 10.3389/fmicb.2019.01092.

Liso, M., De Santis, S., Verna, G., Dicarlo, M., Calasso, M., Santino, A., Gigante, I., Eri, R., Raveenthiraraj, S., Sobolewski, A., Palmitessa, V., Lippolis, A., Mastronardi, M., Armentano, R., Serino, G., De Angelis, M. and Chieppa, M. (2020) 'A Specific Mutation in Muc2 Determines Early Dysbiosis in Colitis-Prone Winnie Mice', *Inflammatory Bowel Diseases*, 26(4), pp. 546–556. doi: 10.1093/ibd/izz279.Lissner, D., Schumann, M., Batra, A., Kredel, L. I., Kühl, A. A., Erben, U., May, C., Schulzke, J. D. and Siegmund, B. (2015) 'Monocyte and M1 macrophage-induced barrier defect contributes to chronic intestinal inflammation in IBD', *Inflammatory Bowel Diseases*, 21(6), pp. 1297–1305. doi: 10.1097/MIB.0000000000000384.

Litvak, Y., Byndloss, M. X. and Bäumler, A. J. (2018) 'Colonocyte metabolism shapes the gut microbiota', *Science*, 362(6418), pp. 1–15. doi: 10.1126/science.aat9076.

Liu-Chittenden, Y., Huang, B., Shim, J. S., Chen, Q., Lee, S. J., Anders, R. A., Liu, J. O. and Pan, D. (2012) 'Genetic and pharmacological disruption of the TEAD-YAP complex suppresses the oncogenic activity of YAP', *Genes and Development*, 26(12), pp. 1300–1305. doi: 10.1101/gad.192856.112.

Liu, J., Iwata, K., Zhu, K., Matsumoto, M., Matsumoto, K., Asaoka, N., Zhang, X., Ibi, M., Katsuyama, M., Tsutsui, M., Kato, S. and Yabe-Nishimura, C. (2020) 'NOX1/NADPH oxidase in bone marrow-derived cells modulates intestinal barrier function', *Free Radical Biology and Medicine*, 147, pp. 90–101. doi: 10.1016/j.freeradbiomed.2019.12.009.

Liu, Y. H., Ding, Y., Gao, C. C., Li, L. S., Wang, Y. X. and Xu, J. D. (2018) 'Functional macrophages and gastrointestinal disorders', *World Journal of Gastroenterology*, 24(11), pp. 1181–1195. doi: 10.3748/wjg.v24.i11.1181.

Lloberas, J., Valverde-Estrella, L., Tur, J., Vico, T. and Celada, A. (2016) 'Mitogen-activated protein kinases and mitogen kinase phosphatase 1: A critical interplay in macrophage biology', *Frontiers in Molecular Biosciences*, 3(JUN), pp. 1–8. doi: 10.3389/fmolb.2016.00028.

Low, L. A., Mummery, C., Berridge, B. R., Austin, C. P. and Tagle, D. A. (2020) 'Organs-on-chips: into the next decade', *Nature Reviews Drug Discovery*. doi: 10.1038/s41573-020-0079-3.

Lumeng, C. N., Delproposto, J. B., Westcott, D. J. and Saltiel, A. R. (2008) 'Phenotypic switching of adipose tissue macrophages with obesity is generated by spatiotemporal differences in macrophage subtypes', *Diabetes*, 57(12), pp. 3239–3246. doi: 10.2337/db08-0872.

Luu, T. U. and Liu, W. F. (2018) 'Regulation of Macrophages by Extracellular Matrix Composition and Adhesion Geometry', *Regenerative Engineering and Translational Medicine*, 4(4), pp. 238–246. doi: 10.1007/s40883-018-0065-z.

Lyons, J., Ghazi, P. C., Starchenko, A., Tovaglieri, A., Baldwin, K. R., Poulin, E. J., Gierut, J. J., Genetti, C., Yajnik, V., Breault, D. T., Lauffenburger, D. A. and Haigis, K. M. (2018) 'The colonic epithelium plays an active role in promoting colitis by shaping the tissue cytokine profile', *PLoS Biology*, 16(3), pp. 1–24. doi: 10.1371/journal.pbio.2002417.

Ma, H., Qiu, Y. and Yang, H. (2021) 'Intestinal intraepithelial lymphocytes: Maintainers of intestinal immune tolerance and regulators of intestinal immunity', *Journal of Leukocyte Biology*, 109(2), pp. 339–347. doi: 10.1002/JLB.3RU0220-111.

Ma, X. and Shah, Y. M. (2018) *The Role of Hippo Signaling in Intestinal Homeostasis*. Sixth Edit, *Physiology of the Gastrointestinal Tract: Sixth Edition*. Sixth Edit. Elsevier Inc. doi: 10.1016/B978-0-12-809954-4.00005-0.

Maeda, K., Chung, Y. S., Kang, S. M., Ogawa, M., Onoda, N., Nishiguch, Y., Ikehara, T., Nakata, B., Okuno, M. and Sowa, M. (1998) 'Cyclin D1 overexpression and prognosis in colorectal adenocarcinoma', *Oncology*, 55(2), pp. 145–151. doi: 10.1159/000011849.

Magno, V., Meinhardt, A. and Werner, C. (2020) 'Polymer Hydrogels to Guide Organotypic and Organoid Cultures', *Advanced Functional Materials*, 30(48). doi: 10.1002/adfm.202000097.Magrone, T. and Jirillo, E. (2013) 'The interaction between gut microbiota and age-related changes in immune function and inflammation', *Immunity and Ageing*, 10(1), p. 1. doi: 10.1186/1742-4933-10-31.

Mah, A. T., Yan, K. S. and Kuo, C. J. (2016) 'Wnt pathway regulation of intestinal stem cells', *Journal of Physiology*, 594(17), pp. 4837–4847. doi: 10.1113/JP271754.Malsin, E. S., Kim, S., Lam, A. P. and Gottardi, C. J. (2019) 'Macrophages as a Source and Recipient of Wnt Signals', *Frontiers in immunology*, 10(July), p. 1813. doi: 10.3389/fimmu.2019.01813.

Malsin, E. S., Kim, S., Lam, A. P. and Gottardi, C. J. (2019) 'Macrophages as a Source and Recipient of Wnt Signals', *Frontiers in immunology,* 10(July), p. 1813. doi: 10.3389/fimmu.2019.01813.

Man, A. L., Gicheva, N., Regoli, M., Rowley, G., De Cunto, G., Wellner, N., Bassity, E., Gulisano, M., Bertelli, E. and Nicoletti, C. (2017) 'CX 3 CR1 + Cell–Mediated Salmonella Exclusion Protects the Intestinal Mucosa during the Initial Stage of Infection', *The Journal of Immunology*, 198(1), pp. 335–343. doi: 10.4049/jimmunol.1502559.

Manderson, A. P., Kay, J. G., Hammond, L. A., Brown, D. L. and Stow, J. L. (2007) 'Subcompartments of the macrophage recycling endosome direct the differential secretion of IL-6 and TNFα', *Journal of Cell Biology*, 178(1), pp. 57–69. doi: 10.1083/jcb.200612131.

Manning, C. N., Martel, C., Sakiyama-Elbert, S. E., Silva, M. J., Shah, S., Gelberman, R. H. and Thomopoulos, S. (2015) 'Adipose-derived mesenchymal stromal cells modulate tendon fibroblast responses to macrophage-induced inflammation in vitro', *Stem Cell Research and Therapy*, 6(1), pp. 1–14. doi: 10.1186/s13287-015-0059-4.

Mantovani, A., Biswas, S. K., Galdiero, M. R., Sica, A. and Locati, M. (2013) 'Macrophage plasticity and polarization in tissue repair and remodelling', *Journal of Pathology*, 229(2), pp. 176–185. doi: 10.1002/path.4133.

Mao, F., Wu, Y., Tang, X., Kang, J., Zhang, B., Yan, Y., Qian, H., Zhang, X. and Xu, W. (2017) 'Exosomes Derived from Human Umbilical Cord Mesenchymal Stem Cells Relieve

Inflammatory Bowel Disease in Mice', *BioMed Research International*, 2017. doi: 10.1155/2017/5356760.

Marchiando, A. M., Shen, L., Graham, W. V., Edelblum, K. L., Duckworth, C. A., Guan, Y., Montrose, M. H., Turner, J. R. and Watson, A. J. M. (2011) 'The epithelial barrier is maintained by in vivo tight junction expansion during pathologic intestinal epithelial shedding', *Gastroenterology*, 140(4), pp. 1208-1218.e2. doi: 10.1053/j.gastro.2011.01.004.

Marshman, E., Booth, C. and Potten, C. S. (2002) 'The intestinal epithelial stem cell', *BioEssays*, 24(1), pp. 91–98. doi: 10.1002/bies.10028.Martinez, F. O. and Gordon, S. (2014) 'The M1 and M2 paradigm of macrophage activation: Time for reassessment', *F1000Prime Reports*, 6(March), pp. 1–13. doi: 10.12703/P6-13.

Martinez, F. O., Gordon, S., Locati, M. and Mantovani, A. (2006) 'Transcriptional Profiling of the Human Monocyte-to-Macrophage Differentiation and Polarization: New Molecules and Patterns of Gene Expression', *The Journal of Immunology*, 177(10), pp. 7303–7311. doi: 10.4049/jimmunol.177.10.7303.

Matsuo, K., Ota, H., Akamatsu, T., Sugiyama, A. and Katsuyama, T. (1997) 'Histochemistry of the surface mucous gel layer of the human colon', *Gut*, 40(6), pp. 782–789. doi: 10.1136/gut.40.6.782.

Mattes, B. and Scholpp, S. (2018) 'Emerging role of contact-mediated cell communication in tissue development and diseases', *Histochemistry and Cell Biology*, 150(5), pp. 431–442. doi: 10.1007/s00418-018-1732-3.

May, R., Qu, D., Weygant, N., Chandrakesan, P., Ali, N., Lightfoot, S. A., Li, L., Sureban, S. M. and Houchen, C. W. (2014) 'Brief Report: Dclk1 Deletion in Tuft Cells Results in Impaired Epithelial Repair After Radiation Injury', *Stem Cells* 32(3), pp. 822–827. doi: 10.1002/stem.1566.

Mazzini, E., Massimiliano, L., Penna, G. and Rescigno, M. (2014) 'Oral Tolerance Can Be Established via Gap Junction Transfer of Fed Antigens from CX3CR1+ Macrophages to CD103+ Dendritic Cells', *Immunity*, 40(2), pp. 248–261. doi: 10.1016/j.immuni.2013.12.012.

McCarthy, N., Kraiczy, J. and Shivdasani, R. A. (2020) 'Cellular and molecular architecture of the intestinal stem cell niche', *Nature Cell Biology*, 22(9), pp. 1033–1041. doi: 10.1038/s41556-020-0567-z.

McCarthy, N., Manieri, E., Storm, E. E., Saadatpour, A., Luoma, A. M., Kapoor, V. N., Madha, S., Gaynor, L. T., Cox, C., Keerthivasan, S., Wucherpfennig, K., Yuan, G. C., de Sauvage, F. J., Turley, S. J. and Shivdasani, R. A. (2020) 'Distinct Mesenchymal Cell Populations Generate the Essential Intestinal BMP Signaling Gradient', *Cell Stem Cell*, 26(3), pp. 391-402.e5. doi: 10.1016/j.stem.2020.01.008.

McCartney-Francis, N., Jin, W., Belkaid, Y., McGrady, G. and Wahl, S. M. (2014) ' Aberrant host defense against Leishmania major in the absence of SLPI ', *Journal of Leukocyte Biology*, 96(5), pp. 917–929. doi: 10.1189/jlb.4a0612-295rr.

McEntee, C. P., Finlay, C. M. and Lavelle, E. C. (2019) 'Divergent roles for the IL-1 family in gastrointestinal homeostasis and inflammation', *Frontiers in Immunology*, 10(JUN), pp. 1–23. doi: 10.3389/fimmu.2019.01266.

McGuckin, M. A. and Hasnain, S. Z. (2017) 'Goblet cells as mucosal sentinels for immunity', *Mucosal Immunology*, 10(5), pp. 1118–1121. doi: 10.1038/mi.2016.132.McKenzie, G. J., Bancroft, A., Grencis, R. K. and McKenzie, A. N. J. (1998) 'A distinct role for interleukin-13 in Th2-cell-mediated immune responses', *Current Biology*, 8(6), pp. 339–342. doi: 10.1016/S0960-9822(98)70134-4.

McKinley, E. T., Sui, Y., Al-Kofahi, Y., Millis, B. A., Tyska, M. J., Roland, J. T., Santamaria-Pang, A., Ohland, C. L., Jobin, C., Franklin, J. L., Lau, K. S., Gerdes, M. J. and Coffey, R. J. (2017) 'Optimized multiplex immunofluorescence single-cell analysis reveals tuft cell heterogeneity', *JCI insight*, 2(11). doi: 10.1172/jci.insight.93487.

Medina-Contreras, O., Geem, D., Laur, O., Williams, I. R., Lira, S. A., Nusrat, A., Parkos, C. A. and Denning, T. L. (2011) 'CX3CR1 regulates intestinal macrophage homeostasis, bacterial translocation, and colitogenic Th17 responses in mice', *Journal of Clinical Investigation*, 121(12), pp. 4787–4795. doi: 10.1172/JCI59150.

Meli, V. S., Atcha, H., Veerasubramanian, P. K., Nagalla, R. R., Luu, T. U., Chen, E. Y., Guerrero-Juarez, C. F., Yamaga, K., Pandori, W., Hsieh, J. Y., Downing, T. L., Fruman, D. A., Lodoen, M. B., Plikus, M. V., Wang, W. and Liu, W. F. (2020) 'YAP-mediated mechanotransduction tunes the macrophage inflammatory response', *Science Advances*, 6(49), pp. 1–14. doi: 10.1126/sciadv.abb8471.

Meran, L., Baulies, A. and Li, V. S. W. (2017) 'Intestinal Stem Cell Niche: The Extracellular Matrix and Cellular Components', *Stem Cells International*, 2017. doi: 10.1155/2017/7970385.

Merritt, A. J., Potten, C. S., Watson, A. J. M., Loh, D. Y., Nakayama -i., K., Nakayama, K. and Hickman, J. A. (1995) 'Differential expression of bcl-2 in intestinal epithelia. Correlation with attenuation of apoptosis in colonic crypts and the incidence of colonic neoplasia', *Journal of Cell Science*, 108(6), pp. 2261–2271.

Meuret, G., Bitzi, A. and Hammer, B. (1978) 'Macrophage turnover in Crohn's disease and ulcerative colitis', *Gastroenterology*, 74(3), pp. 501–503. doi: 10.1016/0016-5085(78)90285-8.

Rothenberg,, Ysbrand Nusse, Tomer Kalisky, John J. Lee,‖, Piero Dalerba, Ferenc Scheeren, Neethan Lobo, Subhash Kulkarni, Sopheak Sim, Dalong Qian, Philip A. Beachy, Pankaj J. Pasricha, Stephen R. Quake, and M. F. C. (2014) 'Identification of a cKit+ Colonic Crypt Base Secretory Cell That Supports Lgr5+ Stem Cells in Mice Michael', 142(5), pp. 1195–1205. doi: 10.1053/j.gastro.2012.02.006.

R. C. Mifflin, I. V. Pinchuk, J. I. Saada, and D. W. Powell, "Intestinal myofibroblasts: targets for stem cell therapy," *American Journal of Physiology Gastrointestinal and Liver Physiology,* vol. 300, pp. G684–G696, 2011.

Mills, C. D. (1991) 'Molecular basis of "suppressor" macrophages. Arginine metabolism via the nitric oxide synthetase pathway.', *Journal of immunology (Baltimore, Md. : 1950)*, 146(8), pp. 2719–23. Available at: http://www.ncbi.nlm.nih.gov/pubmed/1707918.

Mills, C. D., Kincaid, K., Alt, J. M., Heilman, M. J. and Hill, A. M. (2000) 'M-1/M-2 Macrophages and the Th1/Th2 Paradigm', *The Journal of Immunology*, 164(12), pp. 6166–6173. doi: 10.4049/jimmunol.164.12.6166.

Miron, N. and Cristea, V. (2012) 'Enterocytes: Active cells in tolerance to food and microbial antigens in the gut', *Clinical and Experimental Immunology*, 167(3), pp. 405–412. doi: 10.1111/j.1365-2249.2011.04523.x.

Miyata, N. *et al.* (2018) 'Microbial Sensing by Intestinal Myeloid Cells Controls Carcinogenesis and Epithelial Differentiation', *Cell Reports*, 24(9), pp. 2342–2355. doi: 10.1016/j.celrep.2018.07.066.

Miyoshi, H., VanDussen, K. L., Malvin, N. P., Ryu, S. H., Wang, Y., Sonnek, N. M., Lai, C. and Stappenbeck, T. S. (2017) 'Prostaglandin E2 promotes intestinal repair through an adaptive cellular response of the epithelium', *The EMBO Journal*, 36(1), pp. 5–24. doi: 10.15252/embj.201694660.

Miyoshi, H., VanDussen, K. L., Malvin, N. P., Ryu, S. H., Wang, Y., Sonnek, N. M., Lai, C. and Stappenbeck, T. S. (2017) 'Prostaglandin E2 promotes intestinal repair through an adaptive cellular response of the epithelium', *The EMBO Journal*, 36(1), pp. 5–24. doi: 10.15252/embj.201694660.

Miyoshi, Y., Ando, H., Nagase, H., Nishisho, I., Horii, A., Miki, Y., Mori, T., Utsunomiya, J., Baba, S. and Petersen, G. (1992) 'Germ-line mutations of the APC gene in 53 familial adenomatous polyposis patients.', *Proceedings of the National Academy of Sciences*, 89(10), pp. 4452–4456. doi: 10.1073/pnas.89.10.4452.

Moll, F., Walter, M., Rezende, F., Helfinger, V., Vasconez, E., De Oliveira, T., Greten, F. R., Olesch, C., Weigert, A., Radeke, H. H. and Schröder, K. (2018) 'NoxO1 controls proliferation of colon epithelial cells', *Frontiers in Immunology*, 9(MAY), pp. 1–11. doi: 10.3389/fimmu.2018.00973.

Moorefield, E. C., Blue, R. E., Quinney, N. L., Gentzsch, M. and Ding, S. (2018) 'Generation of renewable mouse intestinal epithelial cell monolayers and organoids for functional analyses', *BMC Cell Biology*, 19(1), pp. 1–11. doi: 10.1186/s12860-018-0165-0.

Morhardt, T. L., Hayashi, A., Kao, J. Y. and Kamada, N. (2018) 'Regional Control of Regulatory Immune Cells in the Intestine', *Current Pathobiology Reports*, 6(1), pp. 29–34. doi: 10.1007/s40139-018-0156-z.

Morhardt, T. L., Hayashi, A., Ochi, T., Quirós, M., Kitamoto, S., Nagao-Kitamoto, H., Kuffa, P., Atarashi, K., Honda, K., Kao, J. Y., Nusrat, A. and Kamada, N. (2019) 'IL-10 produced by macrophages regulates epithelial integrity in the small intestine', *Scientific Reports*, 9(1), pp. 1–10. doi: 10.1038/s41598-018-38125-x.

Moroishi, T., Park, H. W., Qin, B., Chen, Q., Meng, Z., Plouffe, S. W., Taniguchi, K., Yu, F. X., Karin, M., Pan, D. and Guan, K. L. (2015) 'A YAP/TAZ-induced feedback mechanism regulates Hippo pathway homeostasis', *Genes and Development*, 29(12), pp. 1271–1284. doi: 10.1101/gad.262816.115.

Mossadegh-Keller, N., Sarrazin, S., Kandalla, P. K., Espinosa, L., Richard Stanley, E., Nutt, S. L., Moore, J. and Sieweke, M. H. (2013) 'M-CSF instructs myeloid lineage fate in single haematopoietic stem cells', *Nature*, 497(7448), pp. 239–243. doi: 10.1038/nature12026.

Mosser, D. M. and Edwards, J. P. (2008) 'Exploring the full spectrum of macrophage activation', *Nature Reviews Immunology*, 8(12), pp. 958–969. doi: 10.1038/nri2448.

Mourao, L., Jacquemin, G., Huyghe, M., Nawrocki, W. J., Menssouri, N., Servant, N. and Fre, S. (2019) 'Lineage tracing of Notch1-expressing cells in intestinal tumours reveals a distinct population of cancer stem cells', *Scientific Reports*, 9(1), pp. 1–14. doi: 10.1038/s41598-018-37301-3.

Mowat, A. M. and Agace, W. W. (2014) 'Regional specialization within the intestinal immune system', *Nature Reviews Immunology*, 14(10), pp. 667–685. doi: 10.1038/nri3738.

Mowat, A. M. I. and Bain, C. C. (2011) 'Mucosal macrophages in intestinal homeostasis and inflammation', *Journal of Innate Immunity*, 3(6), pp. 550–564. doi: 10.1159/000329099.

Mowat, A. M. I., Scott, C. L. and Bain, C. C. (2017) 'Barrier-tissue macrophages: Functional adaptation to environmental challenges', *Nature Medicine*, 23(11), pp. 1258–1270. doi: 10.1038/nm.4430.

Munding, J., Ziebarth, W., Pox, C. P., Ladigan, S., Reiser, M., Hüppe, D., Brand, L., Schmiegel, W., Tannapfel, A. and Reinacher-Schick, A. C. (2012) 'The influence of 5-aminosalicylic acid on the progression of colorectal adenomas via the ß-catenin signaling pathway', *Carcinogenesis*, 33(3), pp. 637–643. doi: 10.1093/carcin/bgr306.

Murai, M., Turovskaya, O., Kim, G., Madan, R., Karp, C. L., Cheroutre, H. and Kronenberg, M. (2009) 'Interleukin 10 acts on regulatory T cells to maintain expression of the transcription factor Foxp3 and suppressive function in mice with colitis', *Nature Immunology*, 10(11), pp. 1178–1184. doi: 10.1038/ni.1791.

Murata, K., Jadhav, U., Madha, S., van Es, J., Dean, J., Cavazza, A., Wucherpfennig, K., Michor, F., Clevers, H. and Shivdasani, R. A. (2020) 'Ascl2-Dependent Cell Dedifferentiation Drives Regeneration of Ablated Intestinal Stem Cells', *Cell Stem Cell*, 26(3), pp. 377-390.e6. doi: 10.1016/j.stem.2019.12.011.

Muroyama, A., Terwilliger, M., Dong, B., Suh, H. and Lechler, T. (2018) 'Genetically induced microtubule disruption in the mouse intestine impairs intracellular organization and transport', *Molecular Biology of the Cell*, 29(13), pp. 1533–1541. doi: 10.1091/mbc.E18-01-0057.

Murray, P. J. *et al.* (2014) 'Macrophage Activation and Polarization: Nomenclature and Experimental Guidelines', *Immunity*, 41(1), pp. 14–20. doi: 10.1016/j.immuni.2014.06.008.

Mussar, K., Tucker, A., McLennan, L., Gearhart, A., Jimenez-Caliani, A. J., Cirulli, V. and Crisa, L. (2014) 'Macrophage/epithelium cross-talk regulates cell cycle progression and migration in pancreatic progenitors', *PLoS ONE*, 9(2). doi: 10.1371/journal.pone.0089492.

Mutoh, H., Sakamoto, H., Hayakawa, H., Arao, Y., Satoh, K., Nokubi, M. and Sugano, K. (2006) 'The intestine-specific homeobox gene Cdx2 induces expression of the basic helix-loop-helix transcription factor Math1', *Differentiation*, 74(6), pp. 313–321. doi: 10.1111/j.1432-0436.2006.00074.x.

Na, Y. R., Stakenborg, M., Seok, S. H. and Matteoli, G. (2019) 'Macrophages in intestinal inflammation and resolution: a potential therapeutic target in IBD', *Nature Reviews Gastroenterology and Hepatology*, 16(9), pp. 531–543. doi: 10.1038/s41575-019-0172-4.

Negroni, A., Cucchiara, S. and Stronati, L. (2015) 'Apoptosis, necrosis, and necroptosis in the gut and intestinal homeostasis', *Mediators of Inflammation*, 2015. doi: 10.1155/2015/250762.

Neunlist, M., Aubert, P., Bonnaud, S., Van Landeghem, L., Coron, E., Wedel, T., Naveilhan, P., Ruhl, A., Lardeux, B., Savidge, T., Paris, F. and Galmiche, J. P. (2007) 'Enteric glia inhibit

intestinal epithelial cell proliferation partly through a TGF-β1-dependent pathway', *American Journal of Physiology - Gastrointestinal and Liver Physiology*, 292(1), pp. 231–241. doi: 10.1152/ajpgi.00276.2005.

Neurath, M. F. (2014) 'Cytokines in inflammatory bowel disease', Nature Reviews Immunology, 14(5), pp. 329–342. doi: 10.1038/nri3661.

Neurath, M. F., Finotto, S. and Glimcher, L. H. (2002) 'The role of TH1/TH2 polarization in mucosal immunity', *Nature Medicine*, 8(6), pp. 567–573. doi: 10.1038/nm0602-567.

Niehrs, C. (2012) 'The complex world of WNT receptor signalling', *Nature Reviews Molecular Cell Biology*, 13(12), pp. 767–779. doi: 10.1038/nrm3470.

Nibali, L., Henderson, B., Sadiq, S. T. and Donos, N. (2014) 'Genetic dysbiosis: The role of microbial insults in chronic inflammatory diseases', Journal of Oral Microbiology, 6(1). doi: 10.3402/jom.v6.22962.

Niess, J. H., Brand, S., Gu, X., Landsman, L., Jung, S., McCormick, B. A., Vyas, J. M., Boes, M., Ploegh, H. L., Fox, J. G., Littman, D. R. and Reinecker, H. C. (2005) 'CX3CR1-mediated dendritic cell access to the intestinal lumen and bacterial clearance', *Science*, 307(5707), pp. 254–258. doi: 10.1126/science.1102901.

Norlén, P., Curry, W. J., Björkqvist, M., Maule, A., Cunningham, R. T., Hogg, R. B., Harriott, P., Johnston, C. F., Hutton, J. C. and Håkanson, R. (2001) 'Cell-specific processing of chromogranin A in endocrine cells of the rat stomach', *Journal of Histochemistry and Cytochemistry*, 49(1), pp. 9–18. doi: 10.1177/002215540104900102.

O'Rourke, S. A., Dunne, A. and Monaghan, M. G. (2019) 'The Role of Macrophages in the Infarcted Myocardium: Orchestrators of ECM Remodeling', *Frontiers in Cardiovascular Medicine*, 6(July), pp. 1–12. doi: 10.3389/fcvm.2019.00101.

O'Sullivan, S., Gilmer, J. F. and Medina, C. (2014) 'Matrix metalloproteinases in inflammatory bowel disease: An update', *Mediators of Inflammation*, 2015. doi: 10.1155/2015/964131.

Ogino, T., Nishimura, J., Barman, S., Kayama, H., Uematsu, S., Okuzaki, D., Osawa, H., Haraguchi, N., Uemura, M., Hata, T., Takemasa, I., Mizushima, T., Yamamoto, H., Takeda, K., Doki, Y. and Mori, M. (2013) 'Increased Th17-inducing activity of CD14+ CD163low myeloid

cells in intestinal lamina propria of patients with Crohn's disease', *Gastroenterology*, 145(6), pp. 1380-1391.e1. doi: 10.1053/j.gastro.2013.08.049.

Ohsawa, S., Vaughen, J. and Igaki, T. (2018) 'Cell Extrusion: A Stress-Responsive Force for Good or Evil in Epithelial Homeostasis', *Developmental Cell*, 44(3), pp. 284–296. doi: 10.1016/j.devcel.2018.01.009.

Okeke, E. B. and Uzonna, J. E. (2019) 'The pivotal role of regulatory T cells in the regulation of innate immune cells', *Frontiers in Immunology*, 10(APR), pp. 1–12. doi: 10.3389/fimmu.2019.00680.

Onfroy-Roy, L., Hamel, D., Foncy, J., Malaquin, L. and Ferrand, A. (2020) 'Extracellular Matrix Mechanical Properties and Regulation of the Intestinal Stem Cells: When Mechanics Control Fate', *Cells*, 9(12), pp. 1–23. doi: 10.3390/cells9122629.

Orecchioni, M., Ghosheh, Y., Pramod, A. B. and Ley, K. (2019) 'Macrophage polarization: Different gene signatures in M1(Lps+) vs. Classically and M2(LPS-) vs. Alternatively activated macrophages', *Frontiers in Immunology*, 10(MAY), pp. 1–14. doi: 10.3389/fimmu.2019.01084.

Ortiz-Masiá, D., Cosín-Roger, J., Calatayud, S., Hernández, C., Alós, R., Hinojosa, J., Esplugues, J. V. and Barrachina, M. D. (2016) 'M1 macrophages activate notch signalling in epithelial cells: Relevance in Crohn's disease', *Journal of Crohn's and Colitis*, 10(5), pp. 582–592. doi: 10.1093/ecco-jcc/jjw009.

Parikh, K. *et al.* (2019) 'Colonic epithelial cell diversity in health and inflammatory bowel disease', *Nature*, 567(7746), pp. 49–55. doi: 10.1038/s41586-019-0992-y.

Park, J., Lim, D. H., Lim, H. J., Kwon, T., Choi, J. S., Jeong, S., Choi, I. H. and Cheon, J. (2011) 'Size dependent macrophage responses and toxicological effects of Ag nanoparticles', *Chemical Communications*, 47(15), pp. 4382–4384. doi: 10.1039/c1cc10357a.

Pastuła, A. and Marcinkiewicz, J. (2019) 'Cellular Interactions in the Intestinal Stem Cell Niche', *Archivum Immunologiae et Therapiae Experimentalis*, 67(1), pp. 19–26. doi: 10.1007/s00005-018-0524-8.

Patterson, A. M. and Watson, A. J. M. (2017) 'Deciphering the complex signaling systems that regulate intestinal epithelial cell death processes and shedding', *Frontiers in Immunology*, 8(JUL), pp. 1–7. doi: 10.3389/fimmu.2017.00841.

Pearce, S. C., Coia, H. G., Karl, J. P., Pantoja-Feliciano, I. G., Zachos, N. C. and Racicot, K. (2018) 'Intestinal in vitro and ex vivo Models to Study Host-Microbiome Interactions and Acute Stressors', *Frontiers in Physiology*, 9(NOV). doi: 10.3389/fphys.2018.01584.

Pedersen, G., Saermark, T., Kirkegaard, T. and Brynskov, J. (2009) 'Spontaneous and cytokine induced expression and activity of matrix metalloproteinases in human colonic epithelium', *Clinical and Experimental Immunology*, 155(2), pp. 257–265. doi: 10.1111/j.1365-2249.2008.03836.x.

Pellegrinet, L., Rodilla, V., Liu, Z., Chen, S., Koch, U., Espinosa, L., Kaestner, K. H., Kopan, R., Lewis, J. and Radtke, F. (2011) 'Dll1- and Dll4-Mediated Notch Signaling Are Required for Homeostasis of Intestinal Stem Cells', *Gastroenterology*, 140(4), pp. 1230-1240.e7. doi: 10.1053/j.gastro.2011.01.005.

Pérez-González, C., Ceada, G., Greco, F., Matejcic, M., Gómez-González, M., Castro, N., Kale, S., Álvarez-Varela, A., Roca-Cusachs, P., Batlle, E., Matic Vignjevic, D., Arroyo, M., Trepat, X. and Matic Vignjevic, D. (2020) 'Mechanical compartmentalization of the intestinal organoid enables crypt folding and collective cell migration', *bioRxiv*, pp. 1–26. Available at: https://doi.org/10.1101/2020.09.20.299552.

Peter, C., Wesselborg, S., Herrmann, M. and Lauber, K. (2010) 'Dangerous attraction: Phagocyte recruitment and danger signals of apoptotic and necrotic cells', *Apoptosis*, 15(9), pp. 1007–1028. doi: 10.1007/s10495-010-0472-1.

Petrey, A. C. and De La Motte, C. A. (2017) 'The extracellular matrix in IBD: A dynamic mediator of inflammation', *Current Opinion in Gastroenterology*, 33(4), pp. 234–238. doi: 10.1097/MOG.0000000000000368.

Piazzi, G., Fini, L., Selgrad, M., Garcia, M., Daoud, Y., Wex, T., Malfertheiner, P., Gasbarrini, A., Romano, M., Meyer, R. L., Genta, R. M., Fox, J. G., Boland, C. R., Bazzoli, F. and Ricciardiello, L. (2011) 'Epigenetic regulation of Delta-Like1 controls Notch1 activation in gastric cancer', *Oncotarget*, 2(12), pp. 1291–1301. doi: 10.18632/oncotarget.414.

Pixley, F. J. (2012) 'Macrophage migration and its regulation by CSF-1', *International Journal of Cell Biology*, 2012. doi: 10.1155/2012/501962.

Pizarro, T. T., Pastorelli, L., Bamias, G., Garg, R. R., Reuter, B. K., Mercado, J. R., Chieppa, M., Arseneau, K. O., Ley, K. and Cominelli, F. (2011) 'SAMP1/YitFc mouse strain: A spontaneous model of Crohn's disease-like ileitis', *Inflammatory Bowel Diseases*, 17(12), pp. 2566–2584. doi: 10.1002/ibd.21638.

Platt, A. M., Bain, C. C., Bordon, Y., Sester, D. P. and Mowat, A. M. (2010) 'An Independent Subset of TLR Expressing CCR2-Dependent Macrophages Promotes Colonic Inflammation', *The Journal of Immunology*, 184(12), pp. 6843–6854. doi: 10.4049/jimmunol.0903987.

Pompili, S., Latella, G., Gaudio, E., Sferra, R. and Vetuschi, A. (2021) 'The Charming World of the Extracellular Matrix: A Dynamic and Protective Network of the Intestinal Wall', Frontiers in Medicine, 8(April), pp. 1–19. doi: 10.3389/fmed.2021.610189.

Powell, I. V. Pinchuk, J. I. Saada, X. Chen, and R. C. Mifflin, "Mesenchymal cells of the intestinal lamina propria," Annual Review of Physiology, vol. 73, pp. 213– 237, 2011.

Proto, J. D., Doran, A. C., Gusarova, G., Yurdagul, A., Sozen, E., Subramanian, M., Islam, M. N., Rymond, C. C., Du, J., Hook, J., Kuriakose, G., Bhattacharya, J. and Tabas, I. (2018) 'Regulatory T Cells Promote Macrophage Efferocytosis during Inflammation Resolution', *Immunity*, 49(4), pp. 666-677.e6. doi: 10.1016/j.immuni.2018.07.015.

Pull, S. L., Doherty, J. M., Mills, J. C., Gordon, J. I. and Stappenbeck, T. S. (2005) 'Activated macrophages are an adaptive element of the colonic epithelial progenitor niche necessary for regenerative responses to injury', *Proceedings of the National Academy of Sciences of the United States of America*, 102(1), pp. 99–104. doi: 10.1073/pnas.0405979102.

Qi, Z., Li, Y., Zhao, B., Xu, C., Liu, Y., Li, H., Zhang, B., Wang, X., Yang, X., Xie, W., Li, B., Han, J. D. J. and Chen, Y. G. (2017) 'BMP restricts stemness of intestinal Lgr5 + stem cells by directly suppressing their signature genes', *Nature Communications*, 8. doi: 10.1038/ncomms13824.

Qin, S., Zheng, J. hong, Xia, Z. huan, Qian, J., Deng, C. liang and Yang, S. lin (2019) 'CTHRC1 promotes wound repair by increasing M2 macrophages via regulating the TGF-β and notch pathways', *Biomedicine and Pharmacotherapy*, 113(November 2018), p. 108594. doi: 10.1016/j.biopha.2019.01.055.

Qu, D., May, R., Sureban, S. M., Weygant, N., Chandrakesan, P., Ali, N., Li, L., Barrett, T. and Houchen, C. W. (2014) 'Inhibition of Notch signaling reduces the number of surviving Dclk1+ reserve crypt epithelial stem cells following radiation injury', *American Journal of Physiology - Gastrointestinal and Liver Physiology*, 306(5), pp. 404–411. doi: 10.1152/ajpgi.00088.2013.

Qualls, J. E., Kaplan, A. M., Van Rooijen, N. and Cohen, D. A. (2006) 'Suppression of experimental colitis by intestinal mononuclear phagocytes', *Journal of Leukocyte Biology*, 80(4), pp. 802–815. doi: 10.1189/jlb.1205734.

Quiros, M. *et al.* (2017) 'Macrophage-derived IL-10 mediates mucosal repair by epithelial WISP-1 signaling', *Journal of Clinical Investigation*, 127(9), pp. 3510–3520. doi: 10.1172/JCI90229.

Rabbi, M. F., Eissa, N., Munyaka, P. M., Laëtitia Kermarrec, Elgazzar, O., Khafipour, E., Bernstein, C. N. and Ghia, J. E. (2017) 'Reactivation of intestinal inflammation is suppressed by catestatin in a murine model of colitis via M1 macrophages and not the gut microbiota', *Frontiers in Immunology*, 8(AUG), pp. 1–17. doi: 10.3389/fimmu.2017.00985.

Rakoff-Nahoum, S., Paglino, J., Eslami-Varzaneh, F., Edberg, S. and Medzhitov, R. (2004) 'Recognition of commensal microflora by toll-like receptors is required for intestinal homeostasis', *Cell*, 118(2), pp. 229–241. doi: 10.1016/j.cell.2004.07.002.

Rani, R., Smulian, A. G., Greaves, D. R., Hogan, S. P. and Herbert, D. R. (2011) 'TGF-β limits IL-33 production and promotes the resolution of colitis through regulation of macrophage function', *European Journal of Immunology*, 41(7), pp. 2000–2009. doi: 10.1002/eji.201041135.

Rath, M., Müller, I., Kropf, P., Closs, E. I. and Munder, M. (2014) 'Metabolism via arginase or nitric oxide synthase: Two competing arginine pathways in macrophages', *Frontiers in Immunology*, 5(OCT), pp. 1–10. doi: 10.3389/fimmu.2014.00532.

Reed, K. K. and Wickham, R. (2009) 'Review of the Gastrointestinal Tract: From Macro to Micro', *Seminars in Oncology Nursing*, 25(1), pp. 3–14. doi: 10.1016/j.soncn.2008.10.002.

Rees, W. D., Sly, L. M. and Steiner, T. S. (2020) 'How do immune and mesenchymal cells influence the intestinal epithelial cell compartment in inflammatory bowel disease? Let's

crosstalk about it!', *Journal of Leukocyte Biology*, 108(1), pp. 309–321. doi: 10.1002/JLB.3MIR0120-567R.

Regoli, M., Bertelli, E., Gulisano, M. and Nicoletti, C. (2017) 'The Multifaceted Personality of Intestinal CX3CR1+ Macrophages', *Trends in Immunology*, 38(12), pp. 879–887. doi: 10.1016/j.it.2017.07.009.

Reinecker, H., Steffen, M., Witthoeft, T., Pflueger, I. and Schreiber, S. (1993) '<Reinecker-1993-Enhanced secretion o.pdf>', pp. 174–181.

Rescigno, M., Urbano, M., Valzasina, B., Francolini, M., Rotta, G., Bonasio, R., Granucci, F., Kraehenbuhl, J. P. and Ricciardi-Castagnoli, P. (2001) 'Dendritic cells express tight junction proteins and penetrate gut epithelial monolayers to sample bacteria', *Nature Immunology*, 2(4), pp. 361–367. doi: 10.1038/86373.

Rindi, G., Leiter, A. B., Kopin, A. S., Bordi, C. and Solcia, E. (2004) 'The "normal" endocrine cell of the gut: Changing concepts and new evidences', *Annals of the New York Academy of Sciences*, 1014, pp. 1–12. doi: 10.1196/annals.1294.001.

Ritsma, L., Ellenbroek, S. I. J., Zomer, A., Snippert, H. J., De Sauvage, F. J., Simons, B. D., Clevers, H. and Van Rheenen, J. (2014) 'Intestinal crypt homeostasis revealed at single-stem-cell level by in vivo live imaging', *Nature*, 507(7492), pp. 362–365. doi: 10.1038/nature12972.

Rivollier, A., He, J., Kole, A., Valatas, V. and Kelsall, B. L. (2012) 'Inflammation switches the differentiation program of Ly6chi monocytes from antiinflammatory macrophages to inflammatory dendritic cells in the colon', *Journal of Experimental Medicine*, 209(1), pp. 139–155. doi: 10.1084/jem.20101387.

Roers, A., Siewe, L., Strittmatter, E., Deckert, M., Schlüter, D., Stenzel, W., Gruber, A. D., Krieg, T., Rajewsky, K. and Müller, W. (2004) 'T cell-specific inactivation of the interleukin 10 gene in mice results in enhanced T cell responses but normal innate responses to lipopolysaccharide or skin irritation', *Journal of Experimental Medicine*, 200(10), pp. 1289–1297. doi: 10.1084/jem.20041789.

Role, P. and Cxcr, M. (2018) 'crossm Macrophages in Helicobacter hepaticus -Induced Colitis'.Ronald, P. C. and Beutler, B. (2010) 'Plant and animal sensors of conserved microbial signatures', *Science*, 330(6007), pp. 1061–1064. doi: 10.1126/science.1189468.

Rosenbluh, J. *et al.* (2012) 'β-Catenin-driven cancers require a YAP1 transcriptional complex for survival and tumorigenesis', *Cell*, 151(7), pp. 1457–1473. doi: 10.1016/j.cell.2012.11.026.

Rothenberg, M. E., Nusse, Y., Kalisky, T., Lee, J. J., Dalerba, P., Scheeren, F., Lobo, N., Kulkarni, S., Sim, S., Qian, D., Beachy, P. A., Pasricha, P. J., Quake, S. R. and Clarke, M. F. (2012) 'Identification of a cKit+ Colonic Crypt Base Secretory Cell That Supports Lgr5+ Stem Cells in Mice', *Gastroenterology*, 142(5), pp. 1195-1205.e6. doi: 10.1053/j.gastro.2012.02.006.

Roulis, M. and Flavell, R. A. (2016) 'Fibroblasts and myofibroblasts of the intestinal lamina propria in physiology and disease', *Differentiation*, 92(3), pp. 116–131. doi: 10.1016/j.diff.2016.05.002.

Rubio, C. A. and Schmidt, P. T. (2018) 'Morphological classification of corrupted colonic crypts in ulcerative colitis', *Anticancer Research*, 38(4), pp. 2253–2259. doi: 10.21873/anticanres.12469.

Rugtveit, J., Nilsen, E. M., Bakka, A., Carlsen, H., Brandtzaeg, P. and Scott, H. (1997) 'Cytokine profiles differ in newly recruited and resident subsets of mucosal macrophages from inflammatory bowel disease', *Gastroenterology*, 112(5), pp. 1493–1505. doi: 10.1016/S0016-5085(97)70030-1.

Ryan, G. R., Dai, X. M., Dominguez, M. G., Tong, W., Chuan, F., Chisholm, O., Russell, R. G., Pollard, J. W. and Richard Stanley, E. (2001) 'Rescue of the colony-stimulating factor 1 (CSF-1)-nullizygous mouse (Csf1op/Csf1op) phenotype with a CSF-1 transgene and identification of sites of local CSF-1 synthesis', *Blood*, 98(1), pp. 74–84. doi: 10.1182/blood.V98.1.74.

Sachs, N., Tsukamoto, Y., Kujala, P., Peters, P. J. and Clevers, H. (2017) 'Intestinal epithelial organoids fuse to form self-organizing tubes in floating collagen gels', *Development (Cambridge)*, 144(6), pp. 1107–1112. doi: 10.1242/dev.143933.

Saha, S., Aranda, E., Hayakawa, Y., Bhanja, P., Atay, S., Brodin, N. P., Li, J., Asfaha, S., Liu, L., Tailor, Y., Zhang, J., Godwin, A. K., Tome, W. A., Wang, T. C., Guha, C. and Pollard, J. W. (2016) 'Macrophage-derived extracellular vesicle-packaged WNTs rescue intestinal stem cells and enhance survival after radiation injury', *Nature Communications*, 7, pp. 1–16. doi: 10.1038/ncomms13096.

Saia, R. S., Mestriner, F. L., Bertozi, G., Cunha, F. Q. and Cárnio, E. C. (2014) 'Cholecystokinin Inhibits Inducible Nitric Oxide Synthase Expression by Lipopolysaccharide-Stimulated Peritoneal Macrophages', *Mediators of Inflammation*, 2014. doi: 10.1155/2014/896029.

Sailaja, B. S., He, X. C. and Li, L. (2016) 'The regulatory niche of intestinal stem cells', *Journal of Physiology*, 594(17), pp. 4827–4836. doi: 10.1113/JP271931.

Sancho, R., Cremona, C. A. and Behrens, A. (2015) 'Stem cell and progenitor fate in the mammalian intestine: Notch and lateral inhibition in homeostasis and disease', *EMBO reports*, 16(5), pp. 571–581. doi: 10.15252/embr.201540188.

Santos, A. J. M., Lo, Y. H., Mah, A. T. and Kuo, C. J. (2018) 'The Intestinal Stem Cell Niche: Homeostasis and Adaptations', *Trends in Cell Biology*, 28(12), pp. 1062–1078. doi: 10.1016/j.tcb.2018.08.001.

Sasaki, N., Sachs, N., Wiebrands, K., Ellenbroek, S. I. J., Fumagalli, A., Lyubimova, A., Begthel, H., Van Born, M. Den, Van Es, J. H., Karthaus, W. R., Li, V. S. W., López-Iglesias, C., Peters, P. J., Van Rheenen, J., Van Oudenaarden, A. and Clevers, H. (2016) 'Reg4+ deep crypt secretory cells function as epithelial niche for Lgr5+ stem cells in colon', *Proceedings of the National Academy of Sciences of the United States of America*, 113(37), pp. E5399–E5407. doi: 10.1073/pnas.1607327113.

Sasaki, S., Yoneyama, H., Suzuki, K., Suriki, H., Aiba, T., Watanabe, S., Kawauchi, Y., Kawachi, H., Shimizu, F., Matsushima, K., Asakura, H. and Narumi, S. (2002) 'Blockade of CXCL 10 protects mice from acute colitis and enhances crypt cell survival', *European Journal of Immunology*, 32(11), pp. 3197–3205. doi: 10.1002/1521-4141(200211)

Sato, A. (2007) 'Tuft cells', *Anatomical Science International*, 82(4), pp. 187–199. doi: 10.1111/j.1447-073X.2007.00188.x.

Sato, T., van Es, J. H., Snippert, H. J., Stange, D. E., Vries, R. G., van den Born, M., Barker, N., Shroyer, N. F., van de Wetering, M. and Clevers, H. (2011) 'Paneth cells constitute the niche for Lgr5 stem cells in intestinal crypts', *Nature*, 469(7330), pp. 415–418. doi: 10.1038/nature09637.

Schmitz, H., Fromm, M., Bentzel, C. J., Scholz, P., Detjen, K., Mankertz, J., Bode, H., Epple, H. J., Riecken, E. O. and Schulzke, J. D. (1999) 'Tumor necrosis factor-α (TNFα) regulates the epithelial barrier in the human intestinal cell line HT-29/B6.', *Journal of cell science*, 112 (Pt 1(1), pp. 137–46. Available at: http://www.ncbi.nlm.nih.gov/pubmed/9841910.

Schridde, A., Bain, C. C., Mayer, J. U., Montgomery, J., Pollet, E., Denecke, B., Milling, S. W. F., Jenkins, S. J., Dalod, M., Henri, S., Malissen, B., Pabst, O. and McL Mowat, A. (2017) 'Tissue-specific differentiation of colonic macrophages requires TGFβ receptor-mediated signaling', *Mucosal Immunology*, 10(6), pp. 1387–1399. doi: 10.1038/mi.2016.142.

Scoville, D. H., Sato, T., He, X. C. and Li, L. (2008) 'Current View: Intestinal Stem Cells and Signaling', *Gastroenterology*, 134(3), pp. 849–864. doi: 10.1053/j.gastro.2008.01.079.

Sehgal, A., Donaldson, D. S., Pridans, C., Sauter, K. A., Hume, D. A. and Mabbott, N. A. (2018) 'The role of CSF1R-dependent macrophages in control of the intestinal stem-cell niche', *Nature Communications*, 9(1), pp. 1–17. doi: 10.1038/s41467-018-03638-6.

Seo, Y., Park, S. Y., Kim, H. S. and Nam, J. S. (2020) 'The hippo–yap signaling as guardian in the pool of intestinal stem cells', *Biomedicines*, 8(12), pp. 1–20. doi: 10.3390/biomedicines8120560.

Serafino, A., Moroni, N., Zonfrillo, M., Andreola, F., Mercuri, L., Nicotera, G., Nunziata, J., Ricci, R., Antinori, A., Rasi, G. and Pierimarchi, P. (2014) 'WNT-pathway components as predictive markers useful for diagnosis, prevention and therapy in inflammatory bowel disease and sporadic colorectal cancer', *Oncotarget*, 5(4), pp. 978–992. doi: 10.18632/oncotarget.1571.

Shakoori, A., Ougolkov, A., Zhi, W. Y., Zhang, B., Modarressi, M. H., Billadeau, D. D., Mai, M., Takahashi, Y. and Minamoto, T. (2005) 'Deregulated GSK3β activity in colorectal cancer: Its association with tumor cell survival and proliferation', *Biochemical and Biophysical Research Communications*, 334(4), pp. 1365–1373. doi: 10.1016/j.bbrc.2005.07.041.

Shapouri-Moghaddam, A., Mohammadian, S., Vazini, H., Taghadosi, M., Esmaeili, S. A., Mardani, F., Seifi, B., Mohammadi, A., Afshari, J. T. and Sahebkar, A. (2018) 'Macrophage plasticity, polarization, and function in health and disease', *Journal of Cellular Physiology*, 233(9), pp. 6425–6440. doi: 10.1002/jcp.26429.

Shaw, T. N., Houston, S. A., Wemyss, K., Bridgeman, H. M., Barbera, T. A., Zangerle-Murray, T., Strangward, P., Ridley, A. J. L., Wang, P., Tamoutounour, S., Allen, J. E., Konkel, J. E. and Grainger, J. R. (2018) 'Tissue-resident macrophages in the intestine are long lived and defined by Tim-4 and CD4 expression', *Journal of Experimental Medicine*, 215(6), pp. 1507–1518. doi: 10.1084/jem.20180019.

Shimizu, H., Okamoto, R., Ito, G., Fujii, S., Nakata, T., Suzuki, K., Murano, T., Mizutani, T., Tsuchiya, K., Nakamura, T., Hozumi, K. and Watanabe, M. (2014) 'Distinct expression patterns of Notch ligands, Dll1 and Dll4, in normal and inflamed mice intestine', *PeerJ*, 2014(1), pp. 1–18. doi: 10.7717/peerj.370.

Shivaji, U. N., Sharratt, C. L., Thomas, T., Smith, S. C. L., Iacucci, M., Moran, G. W., Ghosh, S. and Bhala, N. (2019) 'Review article: managing the adverse events caused by anti-TNF therapy in inflammatory bowel disease', Alimentary Pharmacology and Therapeutics, 49(6), pp. 664–680. doi: 10.1111/apt.15097.

Shoshkes-Carmel, M., Wang, Y. J., Wangensteen, K. J., Tóth, B., Kondo, A., Massassa, E. E., Itzkovitz, S. and Kaestner, K. H. (2018) 'Subepithelial telocytes are an important source of Wnts that supports intestinal crypts', *Nature*, 557(7704), pp. 242–246. doi: 10.1038/s41586-018-0084-4.

Shroyer, N. F., Helmrath, M. A., Wang, V. Y. C., Antalffy, B., Henning, S. J. and Zoghbi, H. Y. (2007) 'Intestine-Specific Ablation of Mouse atonal homolog 1 (Math1) Reveals a Role in Cellular Homeostasis', *Gastroenterology*, 132(7), pp. 2478–2488. doi: 10.1053/j.gastro.2007.03.047.

Shtutman, M., Zhurinsky, J., Simcha, I., Albanese, C., D'Amico, M., Pestell, R. and Ben-Ze'ev, A. (1999) 'The cyclin D1 gene is a target of the β-catenin/LEF-1 pathway', *Proceedings of the National Academy of Sciences of the United States of America*, 96(10), pp. 5522–5527. doi: 10.1073/pnas.96.10.5522.

Shull, M. M., Ormsby, I., Kier, A. B., Pawlowski, S., Diebold, R. J., Yin, M., Allen, R., Sidman, C., Proetzel, G., Calvin, D., Annunziata, N. and Doetschman, T. (1992) 'Targeted disruption of the mouse transforming growth factor-β1 gene results in multifocal inflammatory disease [14]', *Nature*, 359(6397), pp. 693–699. doi: 10.1038/359693a0.

Sica, A. and Mantovani, A. (2012) 'Macrophage plasticity and polarization: In vivo veritas', *Journal of Clinical Investigation*, 122(3), pp. 787–795. doi: 10.1172/JCI59643.

Sica, A. and Mantovani, A. (2012) 'Macrophage plasticity and polarization: in vivo veritas', *Journal of Clinical Investigation*, 122(3), pp. 787–795. doi: 10.1172/JCI59643.

Sieck, G. C., Mantilla, C. B. and Prakash, Y. S. (1999) 'Volume measurements in confocal microscopy', *Methods in Enzymology*, 307(1993), pp. 296–315. doi: 10.1016/S0076-6879(99)07019-6.

Sigal, M., Logan, C. Y., Kapalczynska, M., Mollenkopf, H. J., Berger, H., Wiedenmann, B., Nusse, R., Amieva, M. R. and Meyer, T. F. (2017) 'Stromal R-spondin orchestrates gastric epithelial stem cells and gland homeostasis', *Nature*, 548(7668), pp. 451–455. doi: 10.1038/nature23642.

Skoczek, D. A., Walczysko, P., Horn, N., Parris, A., Clare, S., Williams, M. R. and Sobolewski, A. (2014) 'Luminal Microbes Promote Monocyte–Stem Cell Interactions Across a Healthy Colonic Epithelium', *The Journal of Immunology*, 193(1), pp. 439–451. doi: 10.4049/jimmunol.1301497.

Slattum, G. M. and Rosenblatt, J. (2014) 'Tumour cell invasion: an emerging role for basal epithelial cell extrusion', *Nature Reviews Cancer*, 14(7), pp. 495–501. doi: 10.1038/nrc3767.

Slattum, G., McGee, K. M. and Rosenblatt, J. (2009) 'P115 RhoGEF and microtubules decide the direction apoptotic cells extrude from an epithelium', *Journal of Cell Biology*, 186(5), pp. 693–702. doi: 10.1083/jcb.200903079.

Smythies, L. E., Sellers, M., Clements, R. H., Mosteller-Barnum, M., Meng, G., Benjamin, W. H., Orenstein, J. M. and Smith, P. D. (2005) 'Human intestinal macrophages display profound inflammatory anergy despite avid phagocytic and bacteriocidal activity', *Journal of Clinical Investigation*, 115(1), pp. 66–75. doi: 10.1172/JCI200519229.

Spalinger, M. R., Sayoc-Becerra, A., Santos, A. N., Shawki, A., Canale, V., Krishnan, M., Niechcial, A., Obialo, N., Scharl, M., Li, J., Nair, M. G. and McCole, D. F. (2020) 'PTPN2 Regulates Interactions Between Macrophages and Intestinal Epithelial Cells to Promote Intestinal Barrier Function', *Gastroenterology*, 159(5), pp. 1763-1777.e14. doi: 10.1053/j.gastro.2020.07.004.

Spit, M., Koo, B. K. and Maurice, M. M. (2018) 'Tales from the crypt: Intestinal niche signals in tissue renewal, plasticity and cancer', *Open Biology*, 8(9). doi: 10.1098/rsob.180120.

Stacey, D. W. (2003) 'Cyclin D1 serves as a cell cycle regulatory switch in actively proliferating cells', *Current Opinion in Cell Biology*, 15(2), pp. 158–163. doi: 10.1016/S0955-0674(03)00008-5.

Stamataki, D., Holder, M., Hodgetts, C., Jeffery, R., Nye, E., Spencer-Dene, B., Winton, D. J. and Lewis, J. (2011) 'Delta1 expression, cell cycle exit, and commitment to a specific secretory fate coincide within a few hours in the mouse intestinal stem cell system', *PLoS ONE*, 6(9). doi: 10.1371/journal.pone.0024484.

Stanley, E. R., Chen, D. M. and Lin, H. S. (1978) 'Induction of macrophage production and proliferation by a purified colony stimulating factor [22]', *Nature*, 274(5667), pp. 168–170. doi: 10.1038/274168a0.

Stevens, H. Y., Bowles, A. C., Yeago, C. and Roy, K. (2020) 'Molecular Crosstalk Between Macrophages and Mesenchymal Stromal Cells', *Frontiers in Cell and Developmental Biology*, 8(12), pp. 1–18. doi: 10.3389/fcell.2020.600160.

Stillie, R., Farooq, S. M., Gordon, J. R. and Stadnyk, A. W. (2009) 'The functional significance behind expressing two IL-8 receptor types on PMN', *Journal of Leukocyte Biology*, 86(3), pp. 529–543. doi: 10.1189/jlb.0208125.

Strugala, V., Dettmar, P. W. and Pearson, J. P. (2008) 'Thickness and continuity of the adherent colonic mucus barrier in active and quiescent ulcerative colitis and Crohn's disease', *International Journal of Clinical Practice*, 62(5), pp. 762–769. doi: 10.1111/j.1742-1241.2007.01665.x.

Sun, Q., Arif, M., Chi, Z., Li, G. and Liu, C. G. (2021) 'Macrophages-targeting mannosylated nanoparticles based on inulin for the treatment of inflammatory bowel disease (IBD)',

International Journal of Biological Macromolecules, 169, pp. 206–215. doi: 10.1016/j.ijbiomac.2020.12.094.

Suzuki, A., Sekiya, S., Gunshima, E., Fujii, S. and Taniguchi, H. (2010) 'EGF signaling activates proliferation and blocks apoptosis of mouse and human intestinal stem/progenitor cells in long-term monolayer cell culture', *Laboratory Investigation*, 90(10), pp. 1425–1436. doi: 10.1038/labinvest.2010.150.

Swafford, D., Shanmugam, A., Ranganathan, P., Hussein, M. S., Koni, P. A., Prasad, P. D., Thangaraju, M. and Manicassamy, S. (2018) ' Canonical Wnt Signaling in CD11c + APCs Regulates Microbiota-Induced Inflammation and Immune Cell Homeostasis in the Colon ', *The Journal of Immunology*, 200(9), pp. 3259–3268. doi: 10.4049/jimmunol.1701086.

Szabo, S. J., Kim, S. T., Costa, G. L., Zhang, X., Fathman, C. G. and Glimcher, L. H. (2000) 'A novel transcription factor, T-bet, directs Th1 lineage commitment', *Cell*, 100(6), pp. 655–669. doi: 10.1016/S0092-8674(00)80702-3.

Takeda, K. and Akira, S. (2005) 'Toll-like receptors in innate immunity', *International Immunology*, 17(1), pp. 1–14. doi: 10.1093/intimm/dxh186.

Tamoutounour, S., Henri, S., Lelouard, H., de Bovis, B., de Haar, C., van der Woude, C. J., Woltman, A. M., Reyal, Y., Bonnet, D., Sichien, D., Bain, C. C., Mowat, A. M., Reis e Sousa, C., Poulin, L. F., Malissen, B. and Guilliams, M. (2012) 'CD64 distinguishes macrophages from dendritic cells in the gut and reveals the Th1-inducing role of mesenteric lymph node macrophages during colitis', *European Journal of Immunology*, 42(12), pp. 3150–3166. doi: 10.1002/eji.201242847.

Tan, C. W., Hirokawa, Y., Gardiner, B. S., Smith, D. W. and Burgess, A. W. (2013) 'Colon Cryptogenesis: Asymmetric Budding', *PLoS ONE*, 8(10), pp. 1–18. doi: 10.1371/journal.pone.0078519.

Tang, X., Liu, H., Yang, S., Li, Z., Zhong, J. and Fang, R. (2016) 'Epidermal Growth Factor and Intestinal Barrier Function', *Mediators of Inflammation*, 2016, pp. 27–30. doi: 10.1155/2016/1927348.

Taniguchi, K. *et al.* (2017) 'YAP-IL-6ST autoregulatory loop activated on APC loss controls colonic tumorigenesis', *Proceedings of the National Academy of Sciences of the United States of America*, 114(7), pp. 1643–1648. doi: 10.1073/pnas.1620290114.

Taniguchi, K., Wu, L., Grivennikov, S. I., de Jong, P. R., Lian, I., Yu, F., Wang, K., Ho, S. B., Boland, B. S., Chang, J. T., Sandborn, W. J., Hardiman, G., Raz, E., Maehara, Y., Yoshimura, A., Zucman-Rossi, J., Guan, K. and Karin, M. (2015) 'A gp130–Src–YAP module links inflammation to epithelial regeneration', *Nature*, 519(7541), pp. 57–62. doi: 10.1038/nature14228.

Tetteh, P. W., Basak, O., Farin, H. F., Wiebrands, K., Kretzschmar, K., Begthel, H., Van Den Born, M., Korving, J., De Sauvage, F., Van Es, J. H., Van Oudenaarden, A. and Clevers, H. (2016) 'Replacement of Lost Lgr5-Positive Stem Cells through Plasticity of Their Enterocyte-Lineage Daughters', *Cell Stem Cell*, 18(2), pp. 203–213. doi: 10.1016/j.stem.2016.01.001.

Tiemessen, M. M., Jagger, A. L., Evans, H. G., Van Herwijnen, M. J. C., John, S. and Taams, L. S. (2007) 'CD4+CD25+Foxp3+ regulatory T cells induce alternative activation of human monocytes/macrophages', *Proceedings of the National Academy of Sciences of the United States of America*, 104(49), pp. 19446–19451. doi: 10.1073/pnas.0706832104.

Tóth, B., Ben-Moshe, S., Gavish, A., Barkai, N. and Itzkovitz, S. (2017) 'Early commitment and robust differentiation in colonic crypts', *Molecular Systems Biology*, 13(1), p. 902. doi: 10.15252/msb.20167283.

Tsou, C. L., Peters, W., Si, Y., Slaymaker, S., Aslanian, A. M., Weisberg, S. P., Mack, M. and Charo, I. F. (2007) 'Critical roles for CCR2 and MCP-3 in monocyte mobilization from bone marrow and recruitment to inflammatory sites', *Journal of Clinical Investigation*, 117(4), pp. 902–909. doi: 10.1172/JCI29919.

Tsujimoto, Y. (1998) 'Role of Bcl-2 family proteins in apoptosis: Apoptosomes or mitochondria?', *Genes to Cells*, 3(11), pp. 697–707. doi: 10.1046/j.1365-2443.1998.00223.x.

Tushinski, R. J., Oliver, I. T., Guilbert, L. J., Tynan, P. W., Warner, J. R. and Stanley, E. R. (1982) 'Survival of mononuclear phagocytes depends on a lineage-specific growth factor that the differentiated cells selectively destroy', *Cell*, 28(1), pp. 71–81. doi: 10.1016/0092-8674(82)90376-2.

Uderhardt, S., Martins, A. J., Tsang, J. S., Lämmermann, T. and Germain, R. N. (2019) 'Resident Macrophages Cloak Tissue Microlesions to Prevent Neutrophil-Driven Inflammatory Damage', *Cell*, 177(3), pp. 541-555.e17. doi: 10.1016/j.cell.2019.02.028.

Uematsu, S., Jang, M. H., Chevrier, N., Guo, Z., Kumagai, Y., Yamamoto, M., Kato, H., Sougawa, N., Matsui, H., Kuwata, H., Hemmi, H., Coban, C., Kawai, T., Ishii, K. J., Takeuchi, O., Miyasaka, M., Takeda, K. and Akira, S. (2006) 'Detection of pathogenic intestinal bacteria by Toll-like receptor 5 on intestinal CD11c+ lamina propria cells', *Nature Immunology*, 7(8), pp. 868–874. doi: 10.1038/ni1362.

Valenta, T., Degirmenci, B., Moor, A. E., Herr, P., Zimmerli, D., Moor, M. B., Hausmann, G., Cantù, C., Aguet, M. and Basler, K. (2016) 'Wnt Ligands Secreted by Subepithelial Mesenchymal Cells Are Essential for the Survival of Intestinal Stem Cells and Gut Homeostasis'*, Cell Reports*, 15(5), pp. 911–918. doi: 10.1016/j.celrep.2016.03.088.

Valentin, J. E., Stewart-Akers, A. M., Gilbert, T. W. and Badylak, S. F. (2009) 'Macrophage participation in the degradation and remodeling of extracellular matrix scaffolds', *Tissue Engineering - Part A*, 15(7), pp. 1687–1694. doi: 10.1089/ten.tea.2008.0419.

Van Dyken, S. J. and Locksley, R. M. (2013) 'Interleukin-4- and Interleukin-13-Mediated Alternatively Activated Macrophages: Roles in Homeostasis and Disease', *Annual Review of Immunology*, 31(1), pp. 317–343. doi: 10.1146/annurev-immunol-032712-095906.

Van Dussen, K. L., Carulli, A. J., Keeley, T. M., Patel, S. R., Puthoff, B. J., Magness, S. T., Tran, I. T., Maillard, I., Siebel, C., Kolterud, Å., Grosse, A. S., Gumucio, D. L., Ernst, S. A., Tsai, Y. H., Dempsey, P. J. and Samuelson, L. C. (2012) 'Notch signaling modulates proliferation and differentiation of intestinal crypt base columnar stem cells', *Development*, 139(3), pp. 488–497. doi: 10.1242/dev.070763.

Van Es, J. H., Sato, T., Van De Wetering, M., Lyubimova, A., Yee Nee, A. N., Gregorieff, A., Sasaki, N., Zeinstra, L., Van Den Born, M., Korving, J., Martens, A. C. M., Barker, N., Van Oudenaarden, A. and Clevers, H. (2012) 'Dll1 + secretory progenitor cells revert to stem cells upon crypt damage', *Nature Cell Biology*, 14(10), pp. 1099–1104. doi: 10.1038/ncb2581.

Van Niel, G., Mallegol, J., Bevilacqua, C., Candalh, C., Brugière, S., Tomaskovic-Crook, E., Heath, J. K., Cerf-Bensussan, N. and Heyman, M. (2003) 'Intestinal epithelial exosomes carry

MHC class II/peptides able to inform the immune system in mice', *Gut*, 52(12), pp. 1690–1697. doi: 10.1136/gut.52.12.1690.

Van Niel, G., Raposo, G., Candalh, C., Boussac, M., Hershberg, R., Cerf-Bensussan, N. and Heyman, M. (2001) 'Intestinal epithelial cells secrete exosome-like vesicles', *Gastroenterology*, 121(2), pp. 337–349. doi: 10.1053/gast.2001.26263.

Van Konijnenburg, D. P. and Mucida, D. (2017) 'Intraepithelial lymphocytes', *Current Biology*, 27(15), pp. R737–R739. doi: 10.1016/j.cub.2017.05.073.

Varelas, X., Samavarchi-Tehrani, P., Narimatsu, M., Weiss, A., Cockburn, K., Larsen, B. G., Rossant, J. and Wrana, J. L. (2010) 'The Crumbs Complex Couples Cell Density Sensing to Hippo-Dependent Control of the TGF-β-SMAD Pathway', *Developmental Cell*, 19(6), pp. 831–844. doi: 10.1016/j.devcel.2010.11.012.

Varol, C., Vallon-Eberhard, A., Elinav, E., Aychek, T., Shapira, Y., Luche, H., Fehling, H. J., Hardt, W. D., Shakhar, G. and Jung, S. (2009) 'Intestinal Lamina Propria Dendritic Cell Subsets Have Different Origin and Functions', *Immunity*, 31(3), pp. 502–512. doi: 10.1016/j.immuni.2009.06.025.

Verhulsel, M., Simon, A., Bernheim-Dennery, M., Gannavarapu, V. R., Gérémie, L., Ferraro, D., Krndija, D., Talini, L., Viovy, J. L., Vignjevic, D. M. and Descroix, S. (2021) 'Developing an advanced gut on chip model enabling the study of epithelial cell/fibroblast interactions', *Lab on a Chip*, 21(2), pp. 365–377. doi: 10.1039/d0lc00672f.

Veremeyko, T., Yung, A. W. Y., Anthony, D. C., Strekalova, T. and Ponomarev, E. D. (2018) 'Early growth response gene-2 is essential for M1 and M2 macrophage activation and plasticity by modulation of the transcription factor CEBPβ', *Frontiers in Immunology*, 9(NOV), pp. 1–23. doi: 10.3389/fimmu.2018.02515.

Viola, M. F. and Boeckxstaens, G. (2020) 'Intestinal resident macrophages: Multitaskers of the gut', *Neurogastroenterology and Motility*, 32(8), pp. 1–12. doi: 10.1111/nmo.13843.

Von Furstenberg, R. J., Gulati, A. S., Baxi, A., Doherty, J. M., Stappenbeck, T. S., Gracz, A. D., Magness, S. T. and Henning, S. J. (2011) 'Sorting mouse jejunal epithelial cells with CD24 yields a population with characteristics of intestinal stem cells', *American Journal of*

Physiology - Gastrointestinal and Liver Physiology, 300(3), pp. 409–417. doi: 10.1152/ajpgi.00453.2010.

Von Moltke, J., Ji, M., Liang, H. E. and Locksley, R. M. (2016) 'Tuft-cell-derived IL-25 regulates an intestinal ILC2-epithelial response circuit', *Nature*, 529(7585), pp. 221–225. doi: 10.1038/nature16161.

Vos, A. C. W., Wildenberg, M. E., Arijs, I., Duijvestein, M., Verhaar, A. P., De Hertogh, G., Vermeire, S., Rutgeerts, P., Van Den Brink, G. R. and Hommes, D. W. (2012) 'Regulatory macrophages induced by infliximab are involved in healing in vivo and in vitro', *Inflammatory Bowel Diseases*, 18(3), pp. 401–408. doi: 10.1002/ibd.21818.

Wang, L., Zhu, L. and Qin, S. (2019) 'Gut Microbiota Modulation on Intestinal Mucosal Adaptive Immunity', Journal of Immunology Research, 2019. doi: 10.1155/2019/4735040.

Wang, R. N. *et al.* (2014) 'Bone Morphogenetic Protein (BMP) signaling in development and human diseases', *Genes and Diseases*, 1(1), pp. 87–105. doi: 10.1016/j.gendis.2014.07.005.

Wang, S. and Chen, Y. G. (2018) 'BMP signaling in homeostasis, transformation and inflammatory response of intestinal epithelium', Science China Life Sciences, 61(7), pp. 800–807. doi: 10.1007/s11427-018-9310-7.

Wang, Y., Giel-Moloney, M., Rindi, G. and Leiter, A. B. (2007) 'Enteroendocrine precursors differentiate independently of Wnt and form serotonin expressing adenomas in response to active β-catenin', *Proceedings of the National Academy of Sciences of the United States of America*, 104(27), pp. 11328–11333. doi: 10.1073/pnas.0702665104.

Wang, Y., Kim, R., Hwang, S. H. J., Dutton, J., Sims, C. E. and Allbritton, N. L. (2018) 'Analysis of Interleukin 8 Secretion by a Stem-Cell-Derived Human-Intestinal-Epithelial-Monolayer Platform', *Analytical Chemistry*, 90(19), pp. 11523–11530. doi: 10.1021/acs.analchem.8b02835.

Wei, G., Gao, N., Chen, J., Fan, L., Zeng, Z., Gao, G., Li, L., Fang, G., Hu, K., Pang, X., Fan, H. Y., Clevers, H., Liu, M., Zhang, X. and Li, D. (2020) 'Erk and MAPK signaling is essential for intestinal development through Wnt pathway modulation', *Development (Cambridge, England)*, 147(17). doi: 10.1242/dev.185678.

Wen, J. H., Vincent, L. G., Fuhrmann, A., Choi, Y. S., Hribar, K. C., Taylor-Weiner, H., Chen, S. and Engler, A. J. (2014) 'Interplay of matrix stiffness and protein tethering in stem cell differentiation', *Nature Materials*, 13(10), pp. 979–987. doi: 10.1038/nmat4051.

West, N. J., Courtney, E. D. J., Poullis, A. P. and Leicester, R. J. (2009) 'Apoptosis in the colonic crypt, colorectal adenomata, and manipulation by chemoprevention', *Cancer Epidemiology Biomarkers and Prevention*, 18(6), pp. 1680–1687. doi: 10.1158/1055-9965.EPI-09-0006.

Westphalen, C. B., Asfaha, S., Hayakawa, Y., Takemoto, Y., Lukin, D., Nuber, A., Brandtner, A., Setlik, W., Remotti, H., Muley, A., Chen, X., May, R., Houchen, C., Fox, J., Gershon, M., Quante, M. and Wang, T. (2014) 'Long-lived intestinal tuft cells serve as colon cancer–initiating cells', *Journal of Clinical Investigation*, 124(3), pp. 1283–1295. doi: 10.1172/JCI73434DS1.

Wick, G., Backovic, A., Rabensteiner, E., Plank, N., Schwentner, C. and Sgonc, R. (2010) 'The immunology of fibrosis: innate and adaptive responses', *Trends in Immunology*, 31(3), pp. 110–119. doi: 10.1016/j.it.2009.12.001.

Wiesolek, H. L., Bui, T. M., Lee, J. J., Dalal, P., Finkielsztein, A., Batra, A., Thorp, E. B. and Sumagin, R. (2020) 'Intercellular Adhesion Molecule 1 Functions as an Efferocytosis Receptor in Inflammatory Macrophages', *American Journal of Patholog*y, 190(4), pp. 874–885. doi: 10.1016/j.ajpath.2019.12.006.

Wilkinson, H. N., Upson, S. E., Banyard, K. L., Knight, R., Mace, K. A. and Hardman, M. J. (2019) 'Reduced Iron in Diabetic Wounds: An Oxidative Stress-Dependent Role for STEAP3 in Extracellular Matrix Deposition and Remodeling', *Journal of Investigative Dermatology*, 139(11), pp. 2368-2377.e7. doi: 10.1016/j.jid.2019.05.014.

Williams, J. M., Duckworth, C. A., Burkitt, M. D., Watson, A. J. M., Campbell, B. J. and Pritchard, D. M. (2015) 'Epithelial Cell Shedding and Barrier Function: A Matter of Life and Death at the Small Intestinal Villus Tip', *Veterinary Pathology*, 52(3), pp. 445–455. doi: 10.1177/0300985814559404.

Witherel, C. E., Sao, K., Brisson, B. K., Han, B., Volk, S. W., Petrie, R. J., Han, L. and Spiller, K. L. (2021) 'Regulation of extracellular matrix assembly and structure by hybrid M1/M2

macrophages', Biomaterials, 269(August 2020), p. 120667. doi: 10.1016/j.biomaterials.2021.120667.

Wolf, A. A., Yáñez, A., Barman, P. K. and Goodridge, H. S. (2019) 'The ontogeny of monocyte subsets', *Frontiers in Immunology*, 10(JULY). doi: 10.3389/fimmu.2019.01642.Wong, W. Y., Lee, M. M. L., Chan, B. D., Kam, R. K. T., Zhang, G., Lu, A. P. and Tai, W. C. S. (2016) 'Proteomic profiling of dextran sulfate sodium induced acute ulcerative colitis mice serum exosomes and their immunomodulatory impact on macrophages', *Proteomics*, 16(7), pp. 1131–1145. doi: 10.1002/pmic.201500174.

Wynn, T. A. and Barron, L. (2010) 'Macrophages: Master regulators of inflammation and fibrosis', *Seminars in Liver Disease*, 30(3), pp. 245–257. doi: 10.1055/s-0030-1255354.

Xie, Z., Wang, Y., Yang, G., Han, J., Zhu, L., Li, L. and Zhang, S. (2021) 'The role of the Hippo pathway in the pathogenesis of inflammatory bowel disease', *Cell Death and Disease*, 12(1). doi: 10.1038/s41419-021-03395-3.

Xie, S., Liu, B., Fu, S., Wang, W., Yin, Y., Li, N., Chen, W., Liu, J. and Liu, D. (2014) 'GLP-2 suppresses LPS-induced inflammation in macrophages by inhibiting erk phosphorylation and NF-κB activation', Cellular Physiology and Biochemistry, 34(2), pp. 590–602. doi: 10.1159/000363025.

Yan, K. S., Chia, L. A., Li, X., Ootani, A., Su, J., Lee, J. Y., Su, N., Luo, Y., Heilshorn, S. C., Amieva, M. R., Sangiorgi, E., Capecchi, M. R. and Kuo, C. J. (2012) 'The intestinal stem cell markers Bmi1 and Lgr5 identify two functionally distinct populations', *Proceedings of the National Academy of Sciences of the United States of America*, 109(2), pp. 466–471. doi: 10.1073/pnas.1118857109.

Yang, F. C., Chiu, P. Y., Chen, Y., Mak, T. W. and Chen, N. J. (2019) 'TREM-1-dependent M1 macrophage polarization restores intestinal epithelium damaged by DSS-induced colitis by activating IL-22-producing innate lymphoid cells', *Journal of Biomedical Science*, 26(1), pp. 1–14. doi: 10.1186/s12929-019-0539-4.

Yang, M., Liu, J., Piao, C., Shao, J. and Du, J. (2015) 'ICAM-1 suppresses tumor metastasis by inhibiting macrophage M2 polarization through blockade of efferocytosis', *Cell Death and Disease*, 6(6), pp. 1–12. doi: 10.1038/cddis.2015.144.

Yang, R., Bie, W., Haegebarth, A. and Tyner, A. L. (2006) 'Differential regulation of D-type cyclins in the mouse intestine', *Cell Cycle*, 5(2), pp. 180–183. doi: 10.4161/cc.5.2.2306.

Yimlamai, D., Christodoulou, C., Galli, G. G., Yanger, K., Pepe-Mooney, B., Gurung, B., Shrestha, K., Cahan, P., Stanger, B. Z. and Camargo, F. D. (2014) 'Hippo Pathway Activity Influences Liver Cell Fate', *Cell*, 157(6), pp. 1324–1338. doi: 10.1016/j.cell.2014.03.060.

Ying, W., Cheruku, P. S., Bazer, F. W., Safe, S. H. and Zhou, B. (2013) 'Investigation of macrophage polarization using bone marrow derived macrophages', *Journal of visualized experiments : JoVE*, (76), pp. 1–8. doi: 10.3791/50323.

Yu, F. X., Zhao, B. and Guan, K. L. (2015) 'Hippo Pathway in Organ Size Control, Tissue Homeostasis, and Cancer', *Cell*, 163(4), pp. 811–828. doi: 10.1016/j.cell.2015.10.044.

Zanganeh, S., Hutter, G., Spitler, R., Lenkov, O., Mahmoudi, M., Shaw, A., Pajarinen, J. S., Nejadnik, H., Goodman, S., Moseley, M., Coussens, L. M. and Daldrup-Link, H. E. (2016) 'Iron oxide nanoparticles inhibit tumour growth by inducing pro-inflammatory macrophage polarization in tumour tissues', *Nature Nanotechnology*, 11(11), pp. 986–994. doi: 10.1038/nnano.2016.168.

Zarubin, T. and Han, J. (2005) 'Activation and signaling of the p38 MAP kinase pathway', *Cell Research*, 15(1), pp. 11–18. doi: 10.1038/sj.cr.7290257.

Zebisch, M., Xu, Y., Krastev, C., Macdonald, B. T., Chen, M., Gilbert, R. J. C., He, X. and Jones, E. Y. (2013) 'Structural and molecular basis of ZNRF3/RNF43 transmembrane ubiquitin ligase inhibition by the Wnt agonist R-spondin', *Nature Communications*, 4. doi: 10.1038/ncomms3787.

Zecchini, V., Domaschenz, R., Winton, D. and Jones, P. (2005) 'Notch signaling regulates the differentiation of post-mitotic intestinal epithelial cells', pp. 1686–1691. doi: 10.1101/gad.341705.1686.

Zhang, F., Wang, Hongsheng, Wang, X., Jiang, G., Liu, H., Zhang, G., Wang, Hao, Fang, R., Bu, X., Cai, S. and Du, J. (2016) 'TGF-β induces M2-like macrophage polarization via SNAIL-mediated suppression of a pro-inflammatory phenotype.', *Oncotarget*, 7(32), pp. 52294–52306. doi: 10.18632/oncotarget.10561.

Zhang, Y. H., He, M., Wang, Y. and Liao, A. H. (2017) 'Modulators of the balance between M1 and M2 macrophages during pregnancy', *Frontiers in Immunology*, 8(FEB), pp. 1–12. doi: 10.3389/fimmu.2017.00120.

Zhang, Y. et al. (2020) 'ECM1 is an essential factor for the determination of M1 macrophage polarization in IBD in response to LPS stimulation', *Proceedings of the National Academy of Sciences of the United States of America*, 117(6), pp. 3083–3092. doi: 10.1073/pnas.1912774117.

Zheng, X., Tsuchiya, K., Okamoto, R., Iwasaki, M., Kano, Y., Sakamoto, N., Nakamura, T. and Watanabe, M. (2011) 'Suppression of hath1 gene expression directly regulated by hes1 via notch signaling is associated with goblet cell depletion in ulcerative colitis', *Inflammatory Bowel Diseases*, 17(11), pp. 2251–2260. doi: 10.1002/ibd.21611.

Zhou, H., Coveney, A. P., Wu, M., Huang, J., Blankson, S., Zhao, H., O'Leary, D. P., Bai, Z., Li, Y., Redmond, H. P., Wang, J. H. and Wang, J. (2019) 'Activation of both TLR and NOD signaling confers host innate immunity-mediated protection against microbial infection', *Frontiers in Immunology*, 10(JAN), pp. 1–15. doi: 10.3389/fimmu.2018.03082.

Zhu, L., Fu, X., Chen, X., Han, X. and Dong, P. (2017) 'M2 macrophages induce EMT through the TGF-β/Smad2 signaling pathway', *Cell Biology International*, 41(9), pp. 960–968. doi: 10.1002/cbin.10788.

Zigmond, E., Bernshtein, B., Friedlander, G., Walker, C. R., Yona, S., Kim, K. W., Brenner, O., Krauthgamer, R., Varol, C., Müller, W. and Jung, S. (2014) 'Macrophage-restricted interleukin-10 receptor deficiency, but not IL-10 deficiency, causes severe spontaneous colitis', *Immunity*, 40(5), pp. 720–733. doi: 10.1016/j.immuni.2014.03.012.

Zigmond, E., Varol, C., Farache, J., Elmaliah, E., Satpathy, A. T., Friedlander, G., Mack, M., Shpigel, N., Boneca, I. G., Murphy, K. M., Shakhar, G., Halpern, Z. and Jung, S. (2012) 'Ly6Chi Monocytes in the Inflamed Colon Give Rise to Proinflammatory Effector Cells and Migratory Antigen-Presenting Cells', *Immunity*, 37(6), pp. 1076–1090. doi: 10.1016/j.immuni.2012.08.026.

Zissimopoulos, A., Vradelis, S., Konialis, M., Chadolias, D., Bampali, A., Constantinidis, T., Efremidou, E. and Kouklakis, G. (2014) 'Chromogranin A as a biomarker of disease activity and biologic therapy in inflammatory bowel disease: A prospective observational study',

Scandinavian Journal of Gastroenterology, 49(8), pp. 942–949. doi: 10.3109/00365521.2014.920910.

Zizzo, G., Hilliard, B. A., Monestier, M. and Cohen, P. L. (2012) 'Efficient Clearance of Early Apoptotic Cells by Human Macrophages Requires M2c Polarization and MerTK Induction', *The Journal of Immunology*, 189(7), pp. 3508–3520. doi: 10.4049/jimmunol.1200662.

APPENDIX A. Organoid budding efficiency in the presence of M1 macrophages

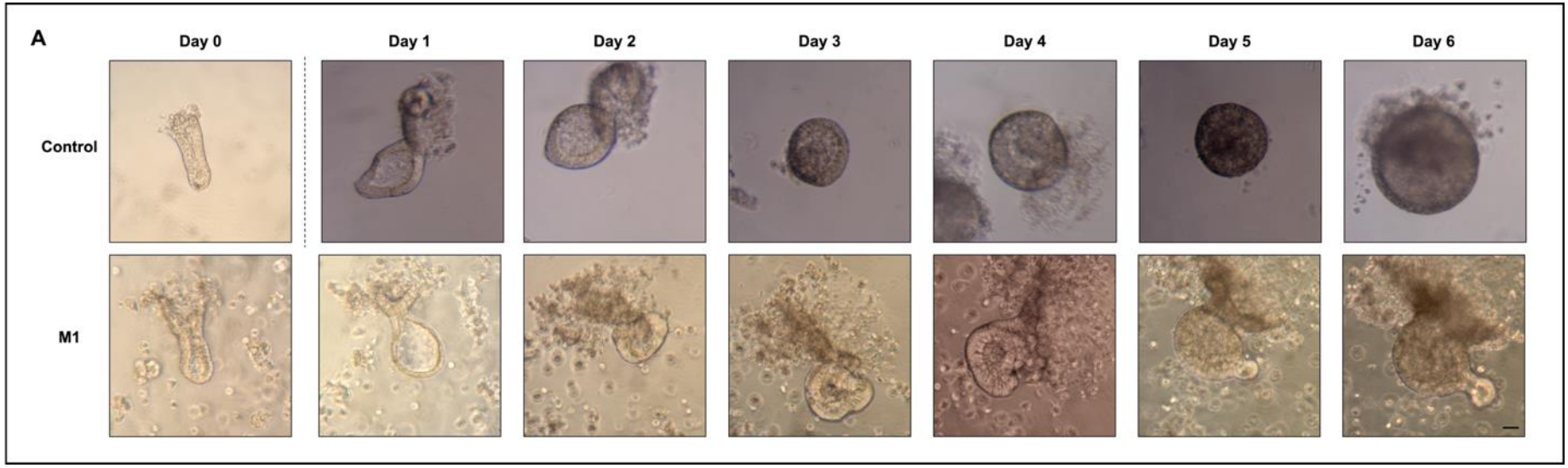

Figure A.1: Organoid budding efficiency and survival in long-term culture.

A) Representative white light images (x10) of colonic crypts on Day 0 and Day 6 in the presence and absence of M1 macrophages. Scale bar at 25µm.